DOCTORAL THESIS

Analysis of heat and mass transfer in membrane-based absorbers with new working fluid mixtures for absorption cooling systems

Faisal Asfand

Supervisor: Dr. Mahmoud Bourouis

Department of Mechanical Engineering

UNIVERSITAT ROVIRA I VIRGILI

Tarragona, 2016

UNIVERSITAT
ROVIRA I VIRGILI
DEPARTAMENT D´ENGINYERIA MECÀNICA
Escola Técnica Superior d´Enginyeria Química (ETSEQ)
Av. Països Catalans 26, 43007 Tarragona (Spain)

I STATE that the present study, entitled "*Analysis of heat and mass transfer in membrane-based absorbers with new working fluid mixtures for absorption cooling systems*", presented by **Mr. Faisal Asfand** for the award of the degree of Doctor, has been carried out under my supervision at the Department of Mechanical Engineering of this university, and that it fulfils all the requirements to be eligible for the International Doctorate.

Tarragona, March 2016

Doctoral Thesis Supervisor

Dr. Mahmoud Bourouis

Dedicated to my parents

Acknowledgement

All praise and thanks be to **ALLAH**, the almighty, the most gracious, the most merciful, for all the blessings and mercies He has bestowed upon me and peace be upon His Prophets.

I am thankful to the 'Universitat Rovira i Virgili' for granting me the Martí-Franquès research fellowship 2012 (ref. 2012BPURV-50) to pursue the doctorate degree, as well as providing me financial support to stay at the Université de Pau et des Pays de l'Adour, Pau (France) through a grant (ref. 2013AEE-06). The financial support of the FEDER and Spanish Ministry of Ministry of Economy and Competitiveness (ref. DPI2012-38841-C02-01) is also acknowledged.

I am deeply indebted to my supervisor Dr. Mahmoud Bourouis, whose help, stimulating suggestions, expertise, understanding, patience and encouragement helped me in all the time of research for and writing of this thesis. I appreciate his vast knowledge and skill in many areas. I would like to thank to Dr. Youssef Stiriba for his assistance and encouragement during the course of this work. I would like to express my gratitude to Dr. Jean-Michel Reneaume and Dr. Sylvain Serra for their help, discussions and valuable comments during my research stay in their group LaTEP (Laboratoire de Thermique Energétique et Procédés) at the Université de Pau et des Pays de l'Adour, France.

I would like to thank to the rest of professors of the CREVER group as well as the secretary of Mechanical Engineering Department for their support and help. I offer my regards and blessings to all the current and previous members of CREVER group and all of those who supported me in any respect during the completion of the project.

Finally, I would also like to thank my family for the support they provided me throughout my entire life and in particular their encouragement in this course of study.

Contribution by the Author

Articles published in peer-reviewed scientific journals

[1] Asfand F, Bourouis M. A review of membrane contactors applied in absorption refrigeration systems. **Renewable and Sustainable Energy Reviews**. 2015; 45:173–91.

[2] Asfand F, Stiriba Y, Bourouis M. CFD simulation to investigate heat and mass transfer in a membrane-based absorber for absorption refrigeration systems. **Energy**. 2015; 91:517–30.

[3] Asfand F, Stiriba Y, Bourouis M. Performance evaluation of membrane-based absorbers employing H_2O/(LiBr+LiI+$LiNO_3$+LiCl) and H_2O/($LiNO_3$+KNO_3+$NaNO_3$) as working pairs in absorption cooling systems. **Energy**. 2016; 115:781–90.

[4] Asfand F, Stiriba Y, Bourouis M. Impact of the solution channel thickness while investigating the effect of membrane characteristics and operating conditions on the absorption performance of a membrane-based absorber. **Applied Thermal Engineering**. 2016; 108:866–77.

[5] Asfand F, Bourouis M. Estimation of differential heat of dilution for aqueous lithium (bromide, iodide, nitrate, chloride) solution and aqueous (lithium, potassium, sodium) nitrate solution used in absorption refrigeration systems. **International Journal of Refrigeration**. 2016; 71:18–25.

Research work presented at international conferences

[1] Asfand F, Stiriba Y, Bourouis M. Effect of membrane contactor characteristics on heat and mass transfer in the plate-and-frame membrane absorber of an absorption refrigeration system. International Conference on Clean Cooling Technologies in the MENA Regions. Algeria. October 2015.

[2] Asfand F, Stiriba Y, Bourouis M. Heat and mass transfer analysis of a membrane-based absorber for absorption refrigeration systems. VII Congreso Ibérico de Ciencias y Técnicas del Frío. Tarragona, Spain. June 2014.

[3] Asfand F, Bourouis M. Experience and prospects of membrane contactors in absorption refrigeration systems. International Workshop on New Working Fluids for Absorption Heat Pumps and Refrigeration Systems. Tarragona, Spain. July 2013.

Abstract

Absorption refrigeration technology, which has the ability to utilize heat directly for cooling purposes, has been one of the most widely used technologies for refrigeration and cooling applications since the early stages of refrigeration technology. Working fluid mixtures employed in the absorption cooling systems are environmental friendly and do not contribute in greenhouse gas emission when compared to vapour compression systems which also use costly mechanical energy input. However, high initial costs and bigger size are some of the main obstacles that impede their wide use in small scale residential buildings and transport sector. In order to overcome these obstacles, design and configuration of the system and its components need to be investigated in order to achieve compact components and reduce the size of the system. Absorber is an important component of the absorption refrigeration system and plays a critical role in the overall performance, size, and capital cost of the system. Both heat and mass transfer take place simultaneously in the absorber. The design and configuration of the absorber significantly influence its performance. Absorber of an absorption cooling system employing water as a refrigerant works under vacuum conditions and therefore the size of the equipment is usually very big. It is the focus of this thesis to investigate advanced absorbers with new working fluid mixtures in order to enhance the heat and mass transfer processes and reduce the size of the equipment. Use of membrane contactors in the form of hollow fibre membrane modules or plate-and-frame membrane modules is one of the alternatives to achieve compact absorbers. The performance of heat and mass transfer in the components is significantly enhanced as a result of higher area to volume ratio available. In this research, a plate-and-frame membrane-based absorber was selected to investigate in detail the heat and mass transfer mechanism and fluid dynamics behaviour employing working fluid mixtures that contain water as a refrigerant. This work will provide a sound foundation to better understand the absorption process in membrane based absorbers. The performance of membrane based absorbers depends on many parameters such as the thermodynamic and transport properties of the working fluid mixture, the operating conditions, the design parameters (such as the channel thickness, membrane material characteristics) etc. Most of the research in this area is done using the conventional working fluid mixtures, water/LiBr and ammonia/water with water as a cooling medium. Moreover,

there is a growing interest for air-cooled absorption chillers, for which water/(LiBr+LiI+$LiNO_3$+LiCl) mixture is proposed as a working fluid due to its larger range of solubility. In addition, for high temperature heat sources, aqueous solution of alkitrate salts ($LiNO_3$+KNO_3+$NaNO_3$) has been proposed as an attractive alternative to effectively utilize the high temperature in the third stage of a triple effect absorption cooling cycle. However, there is very scarce information in the literature about the absorption process with these non-conventional working fluid mixtures. In this research, numerical analyses were performed to evaluate the performance of a plate-and-frame membrane-based absorber employing water/(LiBr+LiI+$LiNO_3$+LiCl) and water/($LiNO_3$+KNO_3+$NaNO_3$) working fluid mixtures. CFD tool ANSYS/FLUENT 14.0 was used to perform the simulation and investigate in detail the heat and mass transfer mechanisms and fluid dynamics behaviour at local levels in the channels. The simulation tool was very useful to perform detailed analyses and was able to predict absorption rate, concentration and temperature profiles of the solution at local levels. Results showed that absorption rate can be significantly enhanced if the solution is confined in a thinner channel with higher mass flow Reynolds numbers. Although the solution channel thickness and solution mass flow rate can be independently controlled in a plate-and-frame membrane-based absorber however it was observed that the pressure drop increases exponentially with a decrease in the solution channel thickness, while it increases linearly with an increase in the solution velocity. In this study, an optimal value of 0.5 mm for the solution film thickness and a solution velocity in the range 0.003 – 0.005 m/s are recommended to achieve higher absorption rates with a minimum pressure drop. In addition, it was observed that the percent pressure drop in case of water/($LiNO_3$+KNO_3+$NaNO_3$) working fluid mixture was significantly lower when compared to the water/LiBr and water/(LiBr+LiI+$LiNO_3$+LiCl) working fluid mixtures because of the higher operating pressure. Therefore, the use of water/($LiNO_3$+KNO_3+$NaNO_3$) working fluid mixture in a plate-and-frame membrane-based absorber which operates at higher pressures cannot only allows higher solution mass flow rate but can also allows the reduction of the solution channel thickness to achieve a compact absorber and a higher absorption rate. Moreover, MATLAB code was used to investigate the effect of membrane material characteristics and operating conditions on the absorption performance of the absorber. In this study, appropriate operating and design parameters were recommended to effectively utilize membrane-based absorbers in absorption cooling systems.

Contents

List of Figures

Chapter 1

Introduction

Energy can be considered as prerequisite for both economic growth and a higher standard of living. Increase in the consumption of electricity in public and private sectors has given rise to the energy crisis in the developing countries. The gap between demand and supply of energy has drastically increased which is adversely affecting many fields of economy. Power shortages have had a strongly negative impact on economic growth especially in the industrial sector. Over-exploitation of important natural resources such as fossil fuels due to increase in the energy consumption as a result of the large increment of the population and global energy consumption has caused excessive pollution which at the same time has resulted in the depletion of ozone layer and imbalances in the environment because of global warming and climate changes.

Energy consumers sectors include the buildings, industry and transport. The most significant reductions in energy consumption can be achieved in the buildings and transport sectors. Building sector which involves both the residential and commercial buildings account for a 20–40% of the total final energy consumption [1]. Moreover, a significant part of the buildings consumption is for heating, ventilation, cooling and lighting. It means that large amount of the energy demand of buildings is for air-conditioning of spaces. Air-conditioning systems such as mechanical compression technologies need high electrical power and a suitable refrigerant for their operation. Both of these requirements can have high environmental impacts and contribute to global warming. Many ozone-depleting substances (ODS) such as chlorofluorocarbons (CFCs) and the fluorocarbon gases such as hydrofluorocarbons (HFCs) used to replace CFCs are potent greenhouse gases and are more powerful than CO_2 in causing climate changes.

With an increasing awareness of the environmental impacts and according to our current needs due to the climate change and economic crisis, use of absorption cooling systems would imply an important impact on environment if they are driven by residual heat or

solar thermal energy. In addition, absorption air-conditioning technologies can potentially contribute in energy saving due to the fact that they can be thermally driven to produce cooling or heating in comparison with conventional electrically driven mechanical compression technologies. Working fluid mixtures employed in the absorption cooling systems are environmental friendly and do not contribute in greenhouse gas emission when compared to the vapour compression systems which also use costly mechanical energy input. This shows a great opportunity to significantly reduce greenhouse gases emissions in both developed and developing countries.

Although absorption refrigeration technology has been one of the most widely used technologies for refrigeration and cooling applications since the early stages of refrigeration technology, however, in small scale applications (small residential buildings) and transport sector thermally driven absorption technologies are still in the early periods of market development. High initial costs and bigger size are some of the main obstacles that impede their wide use. In order to overcome these obstacles, design and configuration of the system and its components are investigated in order to achieve compact components and reduce the size of the system.

1.1 Justification

Absorber is an important component of the absorption refrigeration system and plays a critical role in the overall performance, size, and capital cost of the system. Both heat and mass transfer take place simultaneously in the absorber. The design and configuration of the absorber significantly influence its performance. Poor performance of the absorber leads to a lower value of the coefficient of performance of the vapour absorption cycle. There is a growing concern to enhance heat and mass transfer processes and to improve the design and configuration of the absorber in order to achieve compact absorbers with improved performance and thermal efficiency. Reduction in the size of the absorber mean that the overall size of the system can be reduced which can allow the use of absorption cooling systems in small scale residential buildings and transport sector. Use of membrane contactors in the form of hollow fibre membrane modules or plate-and-frame membrane modules is one of the alternatives to achieve compact absorbers. Absorption cooling systems employing membrane based components provide an interesting opportunity to use the technology for small scale applications. This works aims to perform detailed analyses of a plate-and-frame

membrane-based absorber to predict the detail behaviour of heat and mass transfer processes and to evaluate its performance with water/(LiBr+LiI+$LiNO_3$+LiCl) and water/($LiNO_3$+KNO_3+$NaNO_3$) working fluid mixtures for air cooled absorption cooling systems and multi-stage high temperature heat sources applications, respectively. The study is indented to perform numerical simulations to achieve compact absorbers with enhanced heat and mass transfer.

1.2 Aims and objectives

The main objective of this work was to perform heat and mass transfer analyses of new working fluid mixtures in a membrane-based absorber for absorption cooling systems. Following objectives were accomplished in this work.

1. Literature survey to study the applications of membrane contactors in absorption cooling system and to select an appropriate membrane module for the absorption process.
2. Developing a steady-state numerical model using CFD solver based on the Navier-Stokes equations to investigate in detail the heat and mass transfer processes in a plate-and-frame membrane-based absorber employing water as a refrigerant and salt(s) as an absorbent. To study in detail the effect of solution flow and channel configuration on absorption performance as well as fluid dynamics behaviour using water/LiBr working fluid mixture. To validate the numerical model and support the obtained results, validation of the numerical model will be performed using the available literature data of a membrane-based absorber using water/LiBr working fluid mixture.
3. Performing numerical simulations using CFD approach to investigate the fluid dynamics behaviour, absorption performance and thermal efficiency of a plate-and-frame membrane-based absorber using water/(LiBr+LiI+$LiNO_3$+LiCl) and water/($LiNO_3$+KNO_3+$NaNO_3$) working fluid mixtures. This work will focus on the performance of water/(LiBr+LiI+$LiNO_3$+LiCl) working fluid mixture in a plate-and-frame membrane-based absorber at air-cooled thermal conditions and a comparison will be made with the conventional fluid mixture water/LiBr. Further, water/($LiNO_3$+KNO_3+$NaNO_3$) working fluid mixture will be investigated for high temperature heat sources (up to a temperatures of 260 °C)

and its performance will be evaluated to use it in the last stage of a triple-effect absorption cooling system.

4. Estimation of thermophysical properties of the examined working fluid mixtures which are not available in the open literature. Vapour liquid equilibria data of the examined mixtures will be used to develop correlations to predict the differential heat of dilution as a function of temperature and solution concentration.

5. Developing a steady-state simple 1D mathematical model in MATLAB to investigate the effect of different operating and design parameters on the absorption performance. Membrane material characteristics and effect of important parameters like temperature, flow rates and vapour pressure on the absorption performance of membrane-based absorbers will be studied in detail.

1.3 Methodology

Literature survey was carried out to investigate different membrane modules that can be used to effectively replace the conventional absorber of an absorption cooling system. Further, a thorough review of potential working fluid mixtures was performed and appropriate working fluid mixtures were selected for investigation in this study. In addition, thermophysical properties of the selected working fluids were collected from the available literature.

A CFD based solver was used to carry out a detailed heat and mass transfer analysis. For this, a 2-D numerical model was developed. The governing equations of continuity, momentum, energy and species transport were used to perform a steady-state numerical analysis of combined heat and mass transfer in the absorber. User defined functions were used to incorporate the source terms in the equations and use the numerical model accordingly. Similarly, user defined functions were developed to create and update the thermophysical properties of the working fluid mixtures. The flow in each channel is a homogeneous single phase flow and the species in the solution are well mixed, which mean the relative velocity between the species is negligible. In the absence of relative motion the governing mass and momentum conservation equations for homogeneous flow are reduced to the single-phase form. Therefore, instead of a mixture model, single phase equations were used to perform the simulation with less computational effort. The

computational domain was simplified and symmetrical boundary conditions were considered wherever appropriate to achieve the convergence quickly with less CPU time and memory requirements. The simulation tool was validated with experimental data in the literature for the conventional water/LiBr working fluid mixture. Numerical simulations of a plate-and-frame membrane-based absorber were performed using water/(LiBr+LiI+$LiNO_3$+LiCl) and water/($LiNO_3$+KNO_3+$NaNO_3$) working fluid mixtures for air cooled absorption cooling systems and multi-stage high temperature heat sources applications, respectively. Thermophysical properties of the examined mixtures were estimated using the available correlations in the open literature. Properties which were not available in the open literature were calculated using analytical procedure as a function of solution concentration and temperature. Clausius-Clapeyron equation was used to derive the Duhring equation and using the vapour pressure data of the examined mixtures, the differential heat of dilution data was estimated from the Duhrings diagrams. The obtained differential heat of dilution data was correlated with simple polynomial equation for the three working fluids as a function of the solution concentration and temperature.

A steady-state simple 1-D model was developed in MATLAB to investigate the effect of different operating and design parameters on the absorption performance. The mathematical model was based on energy and mass balance equations, yielding coupled heat and mass transfer model in which both the non-linear and differential equations were solved simultaneously in each cell using the Newton-Raphson method and Runge–Kutta method, respectively.

1.4 Thesis structure

This thesis is distributed into five chapters and an appendix. Apart of the present chapter, in which a brief introduction, research objectives, research approach and justification of the thesis are given, the rest of the chapters are briefly described in the following lines.

Chapter 2 includes an overview of absorption cooling systems and the absorption process. Different configurations of absorbers have been reviewed. Also, intensification techniques to improve the heat and mass transfer processes are discussed. A comprehensive review on the use of membrane contactors in absorption cooling systems

is also performed. In the literature review, the applications of membrane contactors in the field of absorption cooling systems were covered. Membrane contactor modules, components employing membrane contactors, cycle configurations, membrane material characteristics and the working fluid mixtures for the membrane contactor based absorption refrigeration systems were discussed in detail.

In Chapter 3, information about the working fluid mixtures and the thermophysical properties is given. References are given about the correlations used to predict the thermophysical properties of both the conventional working fluid pair, water/LiBr and non-conventional working fluid mixtures, water/(LiBr+LiI+$LiNO_3$+LiCl) and water/($LiNO_3$+KNO_3+$NaNO_3$). In addition, method of estimating the differential heat of dilution is discussed.

Chapter 4 is devoted to results and discussion of the numerical analyses. This chapter presents an in-depth analysis of heat and mass transfer mechanisms in a membrane-based absorber using CFD approach. A plate-and-frame membrane-based absorber with water/LiBr working fluid mixture was used to investigate the heat and mass transfer mechanisms and fluid dynamics behaviour at local levels in the channels. Moreover, water/(LiBr+LiI+$LiNO_3$+LiCl) and water/($LiNO_3$+KNO_3+$NaNO_3$) working fluid mixtures were investigated for air cooled absorption cooling systems and multi-stage high temperature heat sources applications, respectively. In addition, numerical description and simulation results of a one-dimensional mathematical model developed in MATLAB are also given in this chapter. Parametric study is performed and the impact of solution channel thickness while investigating the effect of membrane material characteristics and operating conditions has been critically evaluated.

Finally, Chapter 5 gives the conclusions about the work done in the present thesis and some comments about the future work.

The appendix section comprises of research articles which have been published in international peer-reviewed journals. Research articles which are submitted for publication are also attached.

Chapter 2

State-of-the-Art

This chapter includes an overview of absorption refrigeration systems and the absorption process. Different configurations of absorbers have been reviewed. In addition, intensification techniques to improve the heat and mass transfer processes are discussed.

2.1 Absorption Cooling Systems

Similar to the compression cycle, an absorption cycle is based on the cooling and heating processes associated with phase changes in evaporation and condensation of a refrigerant fluid at different temperatures and pressures. The working fluid mixture consists of a refrigerant and an absorbent, so that the boiling temperature can be modified by changing the pressure or composition of the mixture. The main components in the absorption refrigeration system are absorber, generator, condenser, evaporator solution heat exchanger and solution pump. Figure 2.1 shows the schematic illustration of an absorption cooling system.

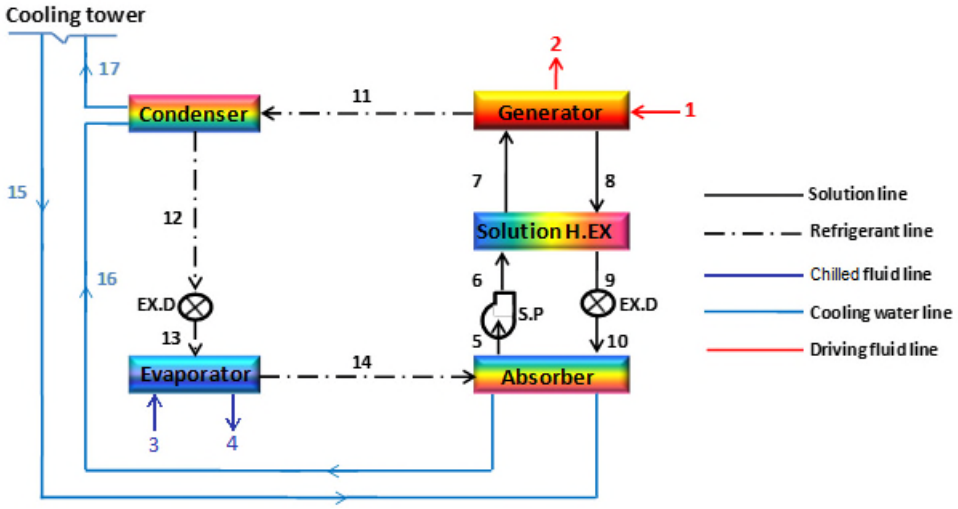

Figure 2.1: Schematic diagram of an absorption cooling system

Absorption cooling unit is partially similar to mechanical vapour compression systems in terms of operation as shown in Figure 2.2. In both the cases, system operates under two pressure levels in which the refrigerant vapour at high temperature and pressure is condensed and throttled to a very low temperature and pressure toward an evaporator where it is evaporated to provide cooling. The major difference between these systems lies in the way how refrigerant vapour is compressed from a low pressure to a high pressure. In the case of the absorption refrigeration system with respect to the vapour compression system, a thermal compressor replaces the mechanical compressor. Thermal compressor of an absorption cooling system consists mainly of an absorber, a generator, a solution pump, a solution heat exchanger and an expansion valve. In the absorber, refrigerant vapour coming from the evaporator is absorbed by a solution mixture weak in refrigerant. The solution mixture composed of refrigerant and absorbent has high affinity for the refrigerant. In the absorption process heat is released which is dissipated by the cooling medium in order to maintain the absorption potential. The solution strong in refrigerant leaving the absorber is then pumped to a high pressure generator where the absorbed refrigerant is again evaporated and separated from the solution mixture by applying heat. As the refrigerant used in absorption cooling systems is volatile compared to absorbent therefore with the application of high temperature heat source, which drives the cycle, the refrigerant vapour is separated from the absorbent and is sent to the condenser. The remaining solution mixture weak in refrigerant is sent to the absorber via solution expansion valve and the cycle repeats.

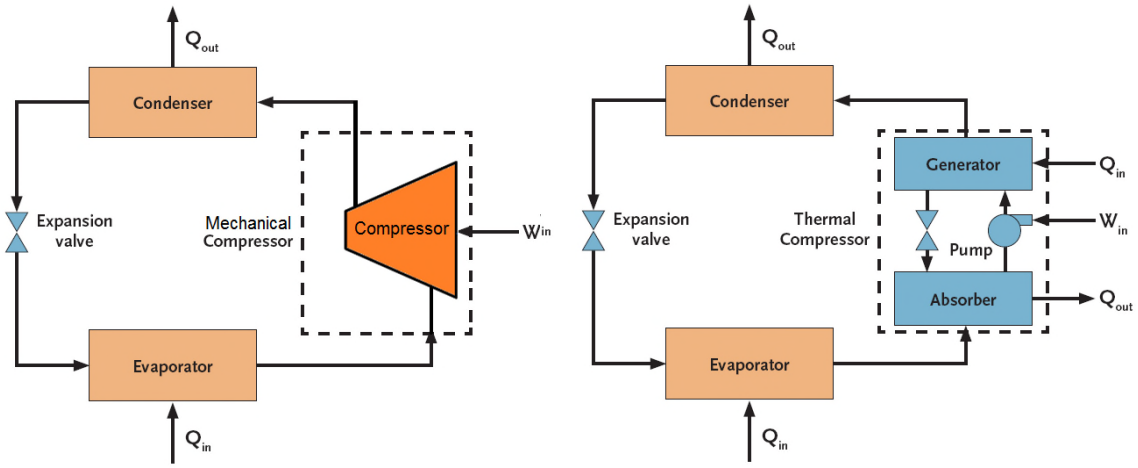

Figure 2.2: Compression and absorption refrigeration cycles

In absorption cooling systems, the main performance indicator is the COP (Coefficient Of Performance) which is defined as the ratio of the cooling capacity and the amount of heat input plus the pump consumption. Since in water/LiBr based absorption cooling systems, the pump energy consumption is relatively small in comparison with the heat input in the generator, therefore, this parameter is often neglected.

2.1.1 Classification of Absorption Refrigeration Systems

As shown in Figure 2.3, absorption systems can be classified based on several criteria: main function, firing method, number of effects and stages, condensing method, working fluids, application, working mode and capacity. However, they can be mainly distinguished in terms of working fluid mixture and number of effects/stages. Depending on the working fluid mixture used, absorption refrigeration systems are broadly classified into ammonia/water (NH_3/H_2O) and water/lithium bromide (H_2O/LiBr) systems. The basic components of both types of refrigeration systems are the absorber, desorber, condenser, evaporator and solution heat exchanger. However, in the case of NH_3/H_2O absorption refrigeration systems, a rectifier is also used at the exit of the desorber to purify the ammonia vapour by condensing the water vapour from the refrigerant vapour. As ammonia and water are both volatile, the refrigerant vapour may contain significant amount of water vapour that has a negative effect on the system performance. Therefore, a rectification process is required for the NH_3/H_2O absorption refrigeration systems. NH_3/H_2O absorption refrigeration systems operate at higher pressures and are commonly used for low temperature (-40 °C to +5 °C) cooling applications. H_2O/LiBr absorption refrigeration systems operate under vacuum conditions and are used in air-conditioning applications where the cooling temperature requirement is above 7 °C. In order to increase the efficiency, one or more additional components at different pressures or concentrations can be added to the basic absorption cycle. With respect to the number and type of additional components, absorption machines can be categorized by the number of effects or by the number of stages. The term effect refers to the number of generators used to thermally drive the absorption cycle. In this way, absorption cooling system can be single-effect, double-effect or a triple-effect system. Similarly, multistage absorption systems (single-stage, double-stage or triple-stage) differ by the number of basic cycles that are combined; where the number of evaporator-absorber pairs at different temperatures in absorption machines determines the number of stages.

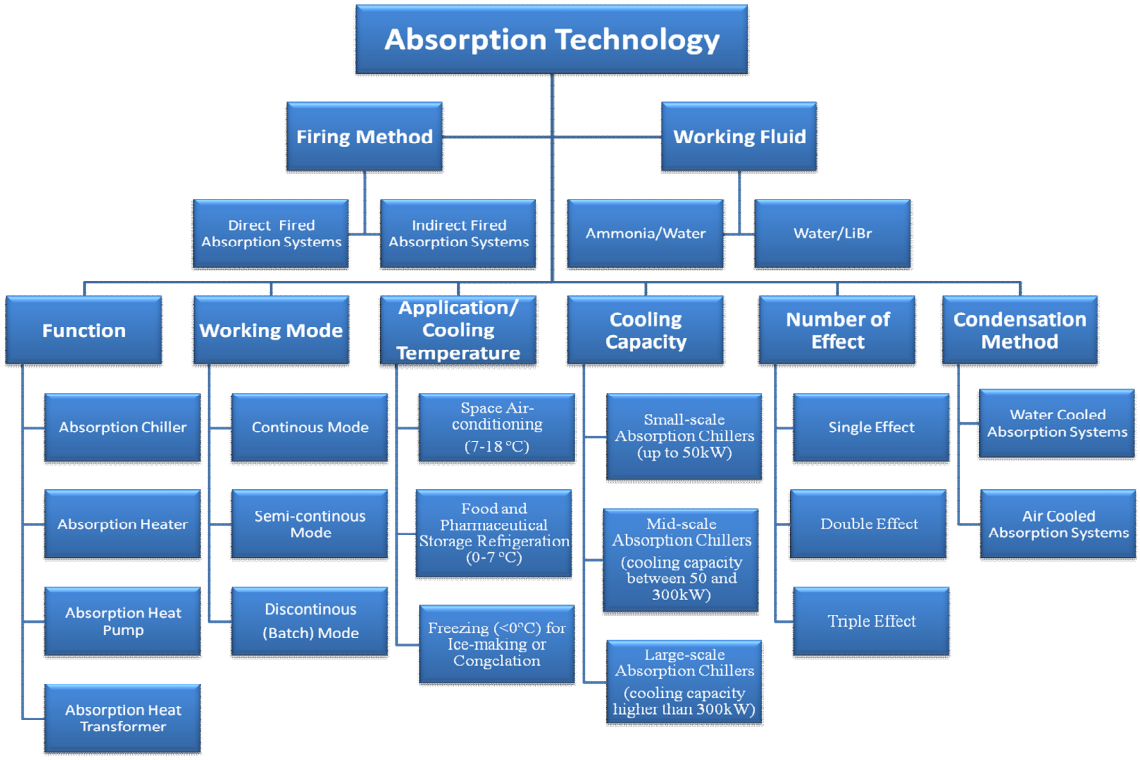

Figure 2.3: Classification of absorption cooling systems

2.2 Absorption Process

Absorption cooling systems can utilize heat directly for cooling which make them an attractive method for produce cooling against the conventional vapour compression systems which consume costly mechanical energy. Absorption cooling systems have few moving parts (only a small liquid pump) leading to low noise and very low vibration levels. In addition, the electricity consumption by the solution pump is very low. Cycle activation by thermal energy and use of natural refrigerants, which do not contribute in ozone depletion as well as global warming, make absorption cooling systems a better choice. Despite these advantages, absorption cooling systems are not yet competitive with mechanical vapour compression systems in terms of efficiency, size and cost. Improvements in the design and configuration of the absorption refrigeration system and its components can provide an opportunity to compete in the global market. The present thesis is focused on the absorber in which both heat and mass transfer processes take place simultaneously. Absorber is one of the main components which can greatly affect the performance, cost and size of the whole absorption system. Operating conditions, geometry of the heat exchanger and thermophysical properties of the working fluid mixture greatly influence the heat and

mass transfer mechanisms in absorber. Extensive research work has been carried out to improve the design and configuration of absorbers. Conventional absorbers are mainly classified into falling film absorber, adiabatic absorber and bubble absorber. The absorption operation varies in these absorbers depending on the mode, in which the refrigerant vapour coming from the evaporator is introduced into the absorber and brought together in contact with the solution. Beside the conventional absorbers, recently a novel absorber design has been proposed utilizing membrane contactors in the form of plate-and-frame membrane module and hollow fibre membrane module. A brief overview of the different configuration and design of absorber is given below.

2.2.1 Falling film absorbers

The falling film configuration of the absorber is the most common type used in commercial cooling absorption machines. Thin falling film heat transfer mode provides a high heat transfer coefficient which in turn enhances heat and mass transfer during the absorption process. Falling film absorbers are further classified into horizontal tube falling film absorbers and vertical tube falling film absorbers. A distributor located in the upper section of the absorber is used to introduce the solution that falls in the form pendent droplet between the coolant tubes and flow over the coolant tubes in the form of thin film. Beside the horizontal tubes, the rest of the space in the absorber is occupied by refrigerant vapours. The solution leaving the distributor is in direct contact with the saturated vapour phase of refrigerant. The falling film vertical tube configuration consists of two concentric tubes aligned vertically. On one side of the tube coolant is flowing whereas on the other side solution flows in the form of film which is in direct contact with the saturated refrigerant vapour coming from the evaporator. The weak solution flows downward through the outer space of the vertical tubes whereas cooling water usually flows upward through the tubes. In both configurations, the heat of absorption is dissipated by the coolant flowing inside the tubes. The strong solution in refrigerant leaves the absorber through the lower section. Horizontal falling film configuration is most commonly used in commercial absorption machines because of a lower pressure drop however its design is complicated due to solution distribution limitations and wettability problem which deteriorate the absorption performance. Figure 2.4 shows the configuration of both horizontal and vertical falling film absorbers.

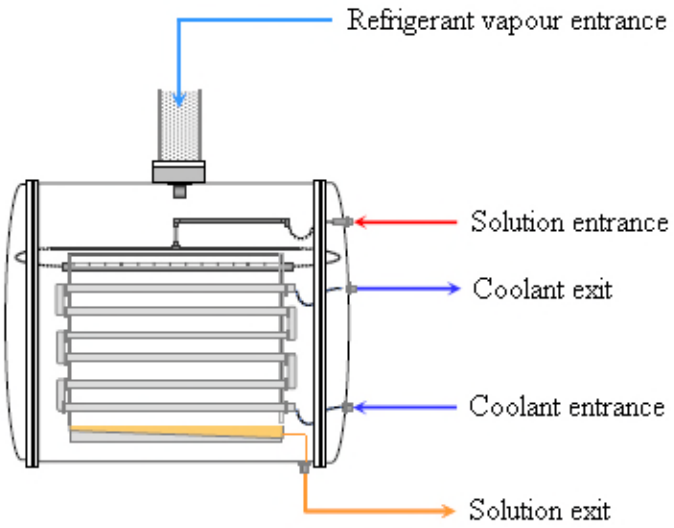

(a) Horizontal tube absorber

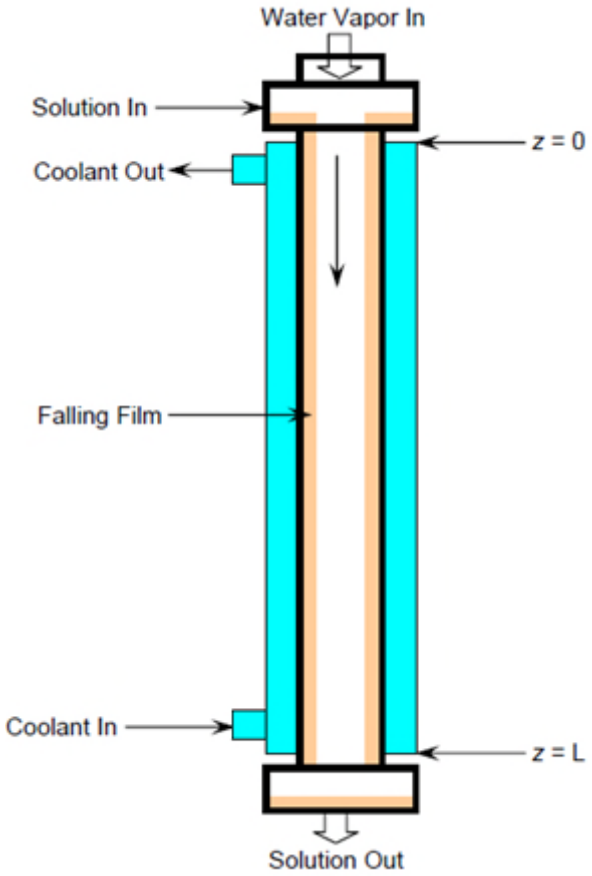

(b) Vertical tube absorber

Figure 2.4: Schematic diagram of falling film absorber

2.2.2 Adiabatic absorbers

Adiabatic absorbers consist of an adiabatic chamber and solution sprayer as shown in Figure 2.5. A separate external conventional single-phase heat exchanger is used to sub-cool the absorbent solution. Thus, the heat and mass transfer processes do not take place simultaneously. The solution weak in refrigerant is introduced into the adiabatic chamber in a fine spray mode where it gets in contact with the refrigerant vapour coming from the evaporator. The solution strong in refrigerant is collected in the lower section of the adiabatic chamber. The solution sprayer disperses the solution into the chamber in very fine drops which helps to improve the absorption potential. This configuration allows reduction in size and cost. To increase the absorption capacity and get close to the solution equilibrium conditions, it is necessary to circulate part of the strong solution through the adiabatic absorber.

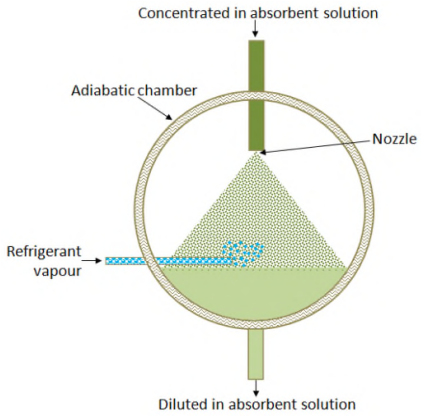

Figure 2.5: Schematic diagram of an adiabatic absorber [2]

2.2.3 Bubble absorbers

Bubble absorbers consist of a vertical tube in which the solution weak in refrigerant flows in the upward direction. Saturated refrigerant vapour coming from the evaporator is injected at the bottom of the channel in bubble mode and is absorbed as it goes up. Cooling fluid is circulated on the outside of the solution channel to dissipate the heat of absorption. Bubble absorption mode allows a good mixing between the liquid and the vapour which in turn enhance the heat and mass transfer coefficients. In case of low solution flow rates, bubble absorber is generally more efficient than falling-film absorbers. Figure 2.6 shows the bubble absorber configuration.

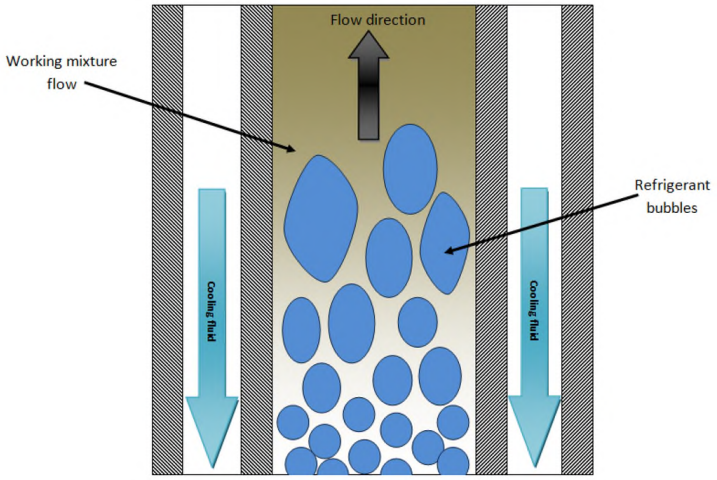

Figure 2.6: Schematic diagram of a bubble absorber [2]

2.2.4 Membrane-based absorbers

Recent research shows that membrane contactors can be employed in the components of absorption cooling systems in order to enhance the heat and mass transfer processes and achieve compact absorbers. There are mainly two configurations, plate-and-frame membrane absorber and hollow fibre membrane absorber in which the membrane contactors can be incorporated in the absorbers. Due to the parallel plates/flat sheets in the plate-and-frame membrane module the pressure drop is small, it is therefore considered as a better option for the water/salt(s) based absorption refrigeration systems. Nevertheless, the hollow fibre module allows more efficient mass transfer due to external transverse flow and is considered an appropriate choice for the ammonia/water based absorption refrigeration systems. The configuration of the plate-and-frame absorber is set as such that the solution, coolant and vapour flow in individual flow channels (Figure 2.7). Each coolant channel serves two solution channels and is fed in the counter flow direction. The first and last cells of the module have half width coolant channels. Similarly, each vapour channel serves two solution channels and can be in a counter flow or co-current flow. The coolant and solution are separated using a metallic plate across which heat transfer takes place whereas a microporous hydrophobic membrane sheet is placed at the aqueous solution–water vapour interface in the form of parallel sheet along the metallic plate. Both heat and mass transfer processes take place across the membrane sheet. Both solution mass flow rate and solution film thickness can be independently controlled in plate-and-frame absorbers.

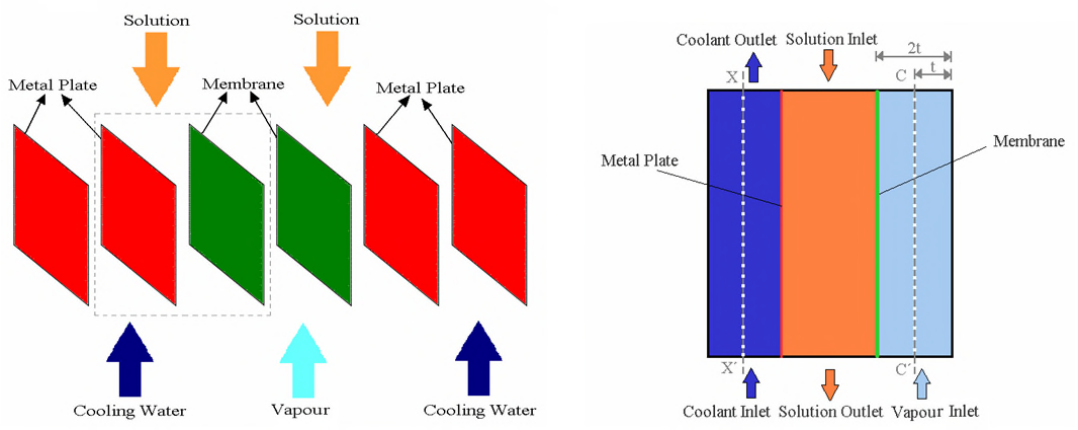

(a) Flow channel configuration (b) 2D sectional view of a single unit

Figure 2.7: Configuration of a plate-and-frame membrane absorber

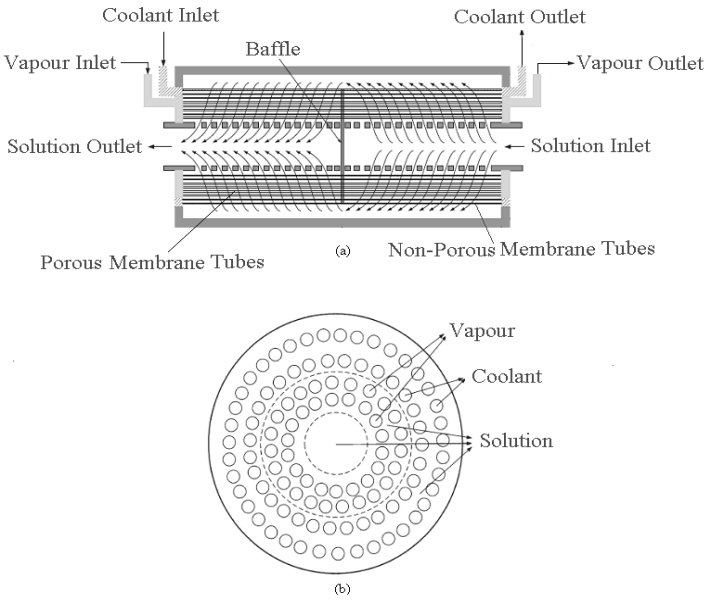

Figure 2.8: Hollow fiber membrane absorber [3]

The hollow fibre membrane absorber (Figure 2.8) consists of hundreds of both microporous hydrophobic membrane fibres and non-porous membrane fibres, assembled and made into a shell-and-tube module. The refrigerant-absorbent solution flows into the shell side of the hollow fibre module. The refrigerant vapours to be absorbed flow into the microporous hollow fibres while the cooling fluid flows into the non-porous hollow fibres of the module.

A comprehensive literature review is carried out on the applications of membrane contactors in absorption refrigeration systems and has been published in international peer-reviewed journal of Renewable and Sustainable Energy Reviews. The article is attached in appendix A1. In this review article, membrane contactors modules which replace the conventional components of absorption refrigeration systems are discussed. The principle of the operation of membrane contactor modules and its applications in the components of absorption refrigeration systems is described. Characteristics of membrane contactor materials employed in absorption refrigeration systems are overviewed. Information is collected on the choice of the working fluid mixture to be used in absorption refrigeration systems that use membrane based components and the compatibility of working fluid mixtures with the membrane contactor material is discussed. Experimental and numerical analyses reported in the open literature to investigate membrane-based components, including absorber, desorber and solution heat exchanger are reviewed and their performance is evaluated with reference to conventional components of absorption refrigeration systems. Different configurations of absorption refrigeration systems utilizing membrane modules in the components are reviewed. The principle of the operation of membrane contactor modules and its effect on the absorption refrigeration cycle configuration is described.

2.3 Intensification of the heat and mass transfer processes

Numerous investigations have been carried out in order to intensify the heat and mass transfer processes taking place in the absorber. Both active and passive techniques have been investigated for enhancing the absorption rate in the absorbers of absorption refrigeration systems. Among these mechanical treatment, chemical treatment, and nanotechnology techniques can be effective to achieve the intensification of heat and mass transfer processes. Resistance to heat and mass transfer processes is more dominant on the solution side therefore the intensification techniques are usually applied in this side to enhance the interaction of both liquid and vapour phases and their heat and mass transfer. The intensification of heat and mass transfer coefficients in the absorber would not only allow reduction in the size of absorber but can also reduce the cycle driving temperature and allow a higher heat sink temperature for the heat dissipation in the absorber and condenser. It means that

the intensification process can help in avoiding the use of humid cooling towers and can enhance the efficiency of solar cooling applications effectively.

A brief description of the different intensification techniques to enhance the absorption process is presented as follows.

2.3.1 Use of mechanical treatment

In mechanical treatments, internal micro-finned tubes, scratched and corrugated surfaces are produced to enhance the heat and mass transfer coefficients. The heat and mass transfer coefficients are enhanced by causing interfacial turbulence. In falling film mode absorbers, mechanical treatment includes both scratching the tube surface to increase the surface roughness as well as the use of advanced surface tubes such as constant curvature tubes, fluted tubes or micro-finned tubes. In bubble mode absorbers, mechanical treatment includes the use of internal micro-finned area for tubular absorbers and the use of corrugated surfaces for plate absorbers. Absorption rates can increase by a factor of 2 or more if finned structures are used [4].

2.3.2 Use of chemical treatment

In chemical treatments, the addition of small quantities of additives (surfactants) has been extensively investigated to induce surface tension gradients in the solution in order to cause Marangoni effect (interfacial turbulence) and lead to higher heat and mass transfer coefficients. The surface tension can considerably affect the flow patterns and is more significant in the bubble mode absorption process. The interfacial area between the liquid and vapour phase is significantly affected by the surface tension of the liquid. Higher surface tension of the liquid leads to a lower interfacial area for mass transfer. In addition, higher surface tension lowers the wettability of the tubes which can significantly affect the heat and mass transfer in a falling film absorption mode. An enhancement of about 2 to 4 times is achievable in presence of the surfactant compared with the absorption rate without additives [4].

2.3.3 Use of nanotechnology

Recent advances in the area of nanotechnology have shown that this technology can be effectively utilized in the absorption cooling systems for enhancing heat and mass

transfer processes. Nanoparticles can enhance not only the effective thermal conductivity of the base fluid but also affect directly the heat and mass transfer characteristics of the fluid. In absorption cooling systems, nanoparticles are added to the working fluid mixture, forming a binary nanofluid mixture with evenly suspended nano-sized particles (d_p < 100 nm) to enhance the heat and mass transfer [5]. Thermal conductivity and convective heat transfer coefficient of binary nanofluids increase with respect to the base fluid which enhance the heat and mass transfer processes. For instance, an average enhancement factor of 2 to 3 times is possible if carbon nanotubes (CNTs) with a concentration of 0.1 wt% are used [6].

Chapter 3

Working Fluid Mixtures

In the following sections, characteristics of ideal working fluid mixtures have been described and the significance of proposed working fluid mixtures is discussed. Information about the working fluid mixtures and the thermophysical properties is given. References are given about the correlations used to predict the thermophysical properties of both the conventional and non-conventional working fluid mixtures. In addition, method of estimating the differential heat of dilution is discussed.

3.1 Working fluid mixture characteristics

Working fluid mixtures significantly influence the performance of absorption cooling systems. Choice of the working fluid is critically dependent on the chemical and thermodynamic properties and the thermodynamic cycle working conditions. The fundamental requirements of the working fluid mixture are that the mixture has a margin of miscibility within the operating temperature range of the cycle and that the transport properties that influence heat and mass transfer, e.g., viscosity, thermal conductivity, and diffusion coefficient should be favourable. Beside this, the mixture should be low-cost, environmental friendly, chemically stable, non-corrosive, non-toxic, and non-explosive. In addition, it is required that the refrigerant has high latent heat of vaporization and that the absorbent is non-volatile in nature.

In this section the characteristics of working fluid mixture in reference to membrane-based absorbers are discussed. For those absorption refrigeration systems utilizing membrane contactors, the properties and requirements of the absorbent/refrigerant combination should be compatible with the membrane contactor characteristics and materials. For instance, a hydrophobic membrane material should be used when the absorbent solution contains water as a mixture component so that the liquid solution molecules do not pass through the membrane pores in case of non-selective membrane contactors. Water can be employed in the absorbent solution either as a

refrigerant or an absorbent and can be used as an additional component to enhance the transport properties of a binary working fluid. For selective microporous membrane contactors, the working fluid pair should be carefully selected in accordance with the membrane properties so that refrigerant molecules observe less transport resistance than the absorbent molecules and hence only the refrigerant molecules pass through the pores. Griesheim and Rodenbach [7] reported that for a dissolution diffusion membrane, the refrigerant should have the characteristic properties of dissolving in the membrane material and diffusing through the membrane, whereas the absorbent should be insoluble in the membrane material. However, for a microporous membrane, a working fluid pair should be selected such that it does not cause wetting of the microporous membrane. If the driving force across the membrane contactor is the difference in vapour pressure, then the working fluid pair should be selected such that the vapour pressure of the absorbent is much lower than the vapour pressure of the refrigerant. Griesheim and Rodenbach [7] reported that in an absorption refrigeration machine utilizing semi-permeable membrane, the vapour pressure of the sorption medium should be a factor of more than 10,000 lower than the refrigerant vapour pressure.

3.2 Working fluid mixtures

Ammonia/water and water/lithium bromide are the most commonly used working fluid pairs analysed both analytically and experimentally to investigate the performance of membrane-based components of absorption cooling systems. One of the key advantages of these working fluid pairs is that the thermophysical properties are well known and established. However, other working fluids such as ammonia/(lithium nitate+water), water/multicomponent salt mixtures and ionic liquid based absorbent solutions can also be effectively utilized in membrane-based absorption refrigeration systems.

3.2.1 Ammonia/water working pair

Ammonia/water working fluid pair is used in the industrial and commercial applications where the cooling temperature requirement is in the range of -40 °C to +5 °C. NH_3/H_2O based absorption refrigeration systems do not have crystallization problems and the system normally operates at a higher pressure (above atmospheric

pressure), hence no vacuum is required. As the working fluid pair contains water as an absorbent, therefore a non-selective membrane contactor with hydrophobic surface can be used in the membrane based components. Despite the high thermal stability of the NH_3/H_2O working pair, the high latent heat of vaporization of NH_3 and the feasibility of using NH_3 as refrigerant for low temperature cooling applications there is still a drawback in that both NH_3 and water are volatile, and thus a rectifier is required to strip away water that normally evaporates with NH_3. The rectification process has a negative effect on the cycle performance and also increases the cost of the absorption refrigeration system. Other disadvantages include the toxicity and corrosive action to copper and copper alloy.

3.2.2 Water/LiBr working pair

Water/lithium bromide working fluid pair is used in those absorption refrigeration applications where the cooling temperature requirement is above 7 °C. H_2O/LiBr based absorption refrigeration systems operate under vacuum conditions. The use of H_2O/LiBr for absorption refrigeration systems offers outstanding features such as the non-volatility of LiBr absorbent (the need for a rectifier is eliminated) and high heat of vaporization of water (refrigerant). However, using water as a refrigerant eliminates the applications for which low cooling temperatures are required and the system must be operated under vacuum conditions. H_2O/LiBr based absorption refrigeration systems also suffer from corrosion problems. In addition, at high cooling-water temperatures and high concentrations the solution is prone to crystallization.

3.2.3 Ionic liquid based working fluid pair

In recent years, intensive research work has been carried out regarding the use of ionic liquids as an absorbent in absorption refrigeration cycles. Advantages of ionic liquids as an absorbent are the low volatility, low melting point, metal-compatibility, high thermal stability and that they are environment friendly and not prone to crystallization problem [8–10]. Ionic liquids have an almost zero vapour pressure, so can be considered a better choice for membrane based absorbers and desorbers. The issue of the high viscosity of ionic liquids can be overcome by adding a small fraction of a ternary component such as water to the ionic liquid based mixtures. A number of

refrigerants in combination with ionic liquids have been recommended for the use in absorption refrigeration systems. Among these, carbon dioxide, water and ammonia are the most prominent refrigerants.

3.3 Proposed working fluid mixtures

In this study, the aim was to investigate the performance of a plate-and-frame membrane-based absorber at air-cooled thermal conditions and for high temperature heat sources applications. Water/(LiBr+LiI+$LiNO_3$+LiCl) and water/($LiNO_3$+KNO_3+$NaNO_3$) working fluid mixtures were investigated for air-cooled absorption cooling systems and multi-stage high temperature heat sources applications, respectively. The significance of these working fluid mixtures are described in the subsequent sections.

3.3.1 Water/(LiBr+LiI+$LiNO_3$+LiCl) working fluid mixture

There is a growing interest for air-cooled absorption chillers in which the heat rejected in the absorber and condenser is directly dissipated to ambient air instead of employing cooling towers. Further, it will not only reduce the investment cost of the installation but also the maintenance cost of cooling towers will be eliminated. In addition, the system size can be reduced which can favour the use of absorption systems in small scale applications. However, the absorber and condenser must operate at higher temperatures to effectively dissipate the heat of rejection into the ambient air which in turn can increase the risk of crystallization of the solution. Water/LiBr solution has limited range of solubility which restricts the range of feasible temperatures in the air-cooled absorbers and hinders in the development of an air-cooled absorption system for cooling applications. Recent research has shown that addition of other salts to LiBr aqueous solutions can significantly improve the solubility of the solution. However, the criteria for selecting an appropriate salt mixture should not only include the increase in the solubility range but also other aspects of the machine operation such as vapour pressure, viscosity, corrosivity, thermal and chemical stability. Bourouis et al. [11, 12] and Medrano et al. [13] experimentally and numerically investigated aqueous solution of the quaternary salt system (LiBr+LiI+$LiNO_3$+LiCl) for air-cooled absorption systems and reported that the aqueous solution of quaternary salt system is less corrosive and its crystallization

temperature is about 35 K lower than that of water/LiBr. The presence of lithium chloride decreases the vapour pressure, lithium iodide and lithium nitrate improve the solubility and lithium nitrate reduces corrosion in the system. Thus the use of multi-salt mixture can overcome the crystallization problem and allows the development of an air-cooled absorption system with membrane contactor based components for small scale applications. As water is used as refrigerant, microporous non-selective hydrophobic membranes can be employed in the membrane based components to achieve efficient performance.

3.3.2 Water/($LiNO_3$+KNO_3+$NaNO_3$) working fluid mixture

In order to improve the thermal utilization of the high temperature heat sources and improve the efficiency of absorption cooling systems, different triple-effect absorption cycles have been proposed. The triple-effect absorption cooling cycles are intended not only to improve the COP but also to miniaturize the size of the equipment for small scale applications. However, the thermal stability, corrosion and crystallization problems of H_2O/LiBr at high temperatures restrict the development of H_2O/LiBr triple-effect cycles for efficient thermal utilization of high temperature heat sources. The conventional H_2O/LiBr working fluid mixture suffers from serious problems of corrosion and thermal decomposition at temperatures of over 180 °C.

Davidson and Erickson [14] proposed the use of aqueous solution of three alkali-metal nitrate salts ($LiNO_3$+KNO_3+$NaNO_3$), called Alkitrates, to extend the upper temperature limit of absorption systems to 260 °C or above. Although the working fluid mixture is compatible with austenitic stainless steel materials at high temperatures, however, Howe and Erickson [15] reported that this working fluid mixture does not exhibit a wide range of solubility, and consequently its use at low temperatures is limited due to crystallization problems. Therefore, Erickson et al. [16] suggested that Alkitrate could be used in the high temperature components of triple-effect absorption cooling cycles, while the conventional working fluid H_2O/LiBr could be used in the low temperature components. The working fluid mixture composed of H_2O and alkitrates is potentially useful to operate at high temperature in the last stage of a triple-effect cycle because of its non-corrosive nature and high thermal stability up to temperatures of about 260 °C [17]. Moreover, aqueous solution

of Alkitrates contain water as a refrigerant therefore a membrane based absorber employing microporous hydrophobic membrane contactor can be effectively utilized to improve the heat and mass transfer processes and reduce the size of the system.

3.4 Thermophysical properties of the working fluid pairs

Thermophysical properties of the working fluid mixture critically influence the overall performance of absorption cooling systems. In this study, the quaternary salt system ($LiBr+LiI+LiNO_3+LiCl$) and the ternary mixture of alkali nitrates ($LiNO_3+KNO_3+NaNO_3$) were used as absorbents with water as a refrigerant. Conventional water/LiBr working fluid mixture was investigated in order to compare the results and perform a parametric study. The thermophysical properties of these systems were taken from the available literature. Those properties of the working fluid mixtures which were not available in the open literature were estimated by developing a correlation or from available equations. Further the procedure to estimate these properties was validated using known properties. To perform the simulations, densities, viscosities, thermal conductivity, specific heat capacity and diffusion coefficient of the aqueous solution of the examined working fluid mixtures were calculated as a function of solution concentration and temperature.

3.4.1 Vapour liquid equilibria

The correlation developed by Uemura and Hasaba [18] was used to calculate the vapour pressure of the water/LiBr solution. The vapour pressure data of Koo et al. [19] and the correlation developed by the research group from Rovira i Virgili University [20] were used to calculate the vapour pressure of the quaternary salt working fluid mixture. To calculate the vapour pressure of aqueous solution of alkitrate, the correlation developed by Álvarez et al. [21] was used.

3.4.2 Density and viscosity

The density and viscosity of the aqueous solution of lithium bromide were calculated using the correlation developed by Lee et al. [22]. The correlation developed by the research group from Rovira i Virgili University [20] was used to calculate the density and viscosity of the quaternary salt working fluid mixture. To calculate the density

and viscosity of the aqueous solution of alkitrate, the correlation developed by Álvarez et al. [23] was used.

3.4.3 Specific heat capacity

The correlation reported in Kaita [24] was used to calculate the specific heat capacity of the water/LiBr mixture. The correlations reported in Salavera et al. [25] and Koo et al. [19] were used to calculate the specific heat capacity of the quaternary salt working fluid mixture. Whereas, the procedure reported by Laliberté [26] was used to calculate the specific heat capacity of the aqueous solution of alkitrate.

3.4.4 Thermal conductivity

The thermal conductivity of the water/LiBr mixture was calculated using the correlation of DiGuilio et al. [27]. The correlation developed by the research group from Rovira i Virgili University [20] was used to calculate the thermal conductivity of the quaternary salt working fluid mixture. To calculate the thermal conductivity of the aqueous solution of alkitrate, the method of Aseyev [28] was used.

3.4.5 Diffusion Coefficient

The diffusion coefficient of water in the aqueous lithium bromide solution was calculated from the experimental data of Gierow and Jernqvist [29] which was determined at constant temperature and different concentrations. However, at other temperatures the diffusion coefficient was estimated using the equation given below.

$$\frac{D_1 \mu_1}{T_1} = \frac{D_2 \mu_2}{T_2} \qquad (1)$$

where D is the diffusion coefficient, μ is the dynamic viscosity and T is the absolute temperature. State 1 refers to the values calculated at 25 °C whereas sate 2 refers to the values calculated at any other temperature.

Mass diffusivity coefficient of the aqueous solution of alkitrate and quaternary salt working fluid mixtures were estimated using the Stokes-Einstein equation reported in Bird [30]. The method was validated against the known diffusion coefficient of water/LiBr working fluid mixture.

3.4.5 Enthalpy

The enthalpy of water vapour was calculated using the correlation reported in Florides et al. [31]. The specific enthalpies of aqueous solutions of LiBr, quaternary salt system and the ternary mixture of alkali nitrates were calculated using the correlations reported in [24], [20], and [32], respectively.

The differential heat of dilution, which contributes in the heat released during the absorption process, was required in the numerical simulation to analyse the heat and mass transfer phenomena. The differential heat of dilution of water/(lithium bromide+lithium iodide+lithium nitrare+lithium chloride) with mass compositions in salts of 60.16%, 9.55%, 18.54% and 11.75%, respectively, and water/(lithium nitrate+potassium nitrate+sodium nitrate) with mass compositions in salts of 53%, 28% and 19%, respectively, was not available in the open literature and an analytically procedure was used to estimate these values at different solution concentrations and temperatures. The Clausius-Clapeyron equation was used to derive the Duhring equation and using the vapour pressure data of the examined mixtures, the differential heat of dilution data were estimated from the Duhring diagrams. The differential heat of dilution data obtained were correlated with simple polynomial equations for the three working fluids as a function of the solution concentration and temperature. The correlation is able to predict the differential heat of dilution with a mean absolute percentage error of 0.54%, 0.70% and 1.66% for water/LiBr, water/(LiBr+LiI+$LiNO_3$+LiCl) and water/($LiNO_3$+KNO_3+$NaNO_3$), respectively. The procedure to calculate the differential heat of dilution is reported in Appendix A2.

Chapter 4

Results and Discussion

This chapter presents an in-depth analysis of heat and mass transfer mechanisms in a membrane-based absorber using CFD approach. Plate-and-frame membrane-based absorber with water/LiBr working fluid mixture is used to investigate the heat and mass transfer mechanisms and fluid dynamics behaviour at local levels in the channels. Moreover, water/(LiBr+LiI+$LiNO_3$+LiCl) and water/($LiNO_3$+KNO_3+$NaNO_3$) working fluid mixtures are investigated for air-cooled absorption cooling systems and multi-stage high temperature heat sources applications, respectively. In addition, numerical description and simulation results of a one-dimensional mathematical model developed in MATLAB are also given in this chapter. A parametric study is performed and the impact of solution channel thickness while investigating the effect of membrane material characteristics and operating conditions has been critically evaluated.

4.1 CFD analysis of heat and mass transfer

Absorber of an absorption cooling system employing water as a refrigerant operates under vacuum conditions and therefore high pressure drop in the absorber can influence its performance and hinder the normal operation. Literature review reveals that plate-and-frame membrane module offers minimum pressure drop and could be an interesting choice for water-based working fluid mixtures employing water as refrigerant. Therefore, in this study a plate-and-frame absorber module incorporating a membrane contactor at the solution-vapour interface is selected for the analysis. The structural unit of the absorber configuration with a membrane contactor is described in section 2.2.4 of Chapter 2. Experimental and analytical analyses have been carried out to investigate the performance of the membrane based absorbers, however, detailed behaviour of the heat and mass transfer mechanisms at local levels in the channels and the fluid dynamic behaviour need to be investigated to better understand

the phenomenon and the effect of flow parameters. In this work, numerical analyses of heat and mass transfer in a plate-and-frame membrane-based absorber are performed using CFD approach. Both conventional working fluid mixture water/LiBr and non-conventional working fluid mixtures, water/(LiBr+LiI+$LiNO_3$+LiCl) and water/($LiNO_3$+KNO_3+$NaNO_3$) are investigated in detail. Commercial CFD solver ANSYS/FLUENT 14.0, which is based on Navier-Stokes equations that are solved using finite volume method, is used to simulate the mass transfer across the membrane and the heat transfer between the solution and coolant in the absorber. Navier-Stokes equations are capable of solving both transient (time-dependent) and steady-state equations. As in this study a steady-state analysis is performed therefore CFD solver based on the Navier-Stokes equation was selected as a favourable option.

4.1.1 CFD simulation approach

A two-dimensional model was developed to simulate the flow, heat and mass transfer phenomena in a single unit of the plate-and-frame membrane module. The governing equations of continuity, momentum, energy and species transport were used to perform steady-state numerical analysis of combined heat and mass transfer in the absorber. User defined functions were used to incorporate the source terms in the equations and use the numerical model accordingly. Similarly, user defined functions were developed to create and update the thermophysical properties of the working fluid mixtures. The flow in each channel is a homogeneous single phase flow and the species in the solution are well mixed, which mean that the relative velocity between the species is negligible. In the absence of relative motion the governing mass and momentum conservation equations for homogeneous flow are reduced to the single-phase form. Therefore, instead of a mixture model, single phase equations were used to perform the simulation with less computational effort. The computational domain was simplified and symmetrical boundary conditions were considered wherever appropriate to achieve the convergence quickly with less CPU time and memory requirements.

As the solution flow Reynolds numbers are low (in the range of 0.5 to 8), a laminar model is selected for the analysis. The calculations were performed by a combination of the SIMPLE (Semi-Implicit Method for Pressure Linked Equations) algorithm for pressure-velocity coupling and the first-order accurate implicit scheme for the

linearized discretized equation in the segregated solver. A second-order upwind discretization scheme was used to compute advection terms. For the energy and specie transport equation, a second-order discretization scheme was used. In the present work, the numerical computation is considered to have converged when the scaled residuals of the different variables (continuity, momentum, species and energy equations) are lowered by tenth orders of magnitude and the steady state results are analysed.

4.1.2 CFD results

A parametric study has been performed to investigate the effect on the absorption rate of the solution channel thickness, solution flow rate and coolant wall temperature. The effect of solution channel thickness and solution mass flow rate on the solution pressure drop along the channel length, which is an important parameter of concern in absorbers operating under vacuum condition with water as a refrigerant, is critically investigated which was not previously reported. Further, the fluid dynamics behaviour of the water/LiBr solution is investigated and the effect of thermophysical properties on the solution flow profile is investigated as well. In addition, a case study is selected to analyse the boundary layers at the solution membrane interface and the local profiles of velocity, temperature and concentration of the working fluid in order to better understand heat and mass transfer phenomena.

The simulation results show that an absorption rate can be increased by a factor of 2.5 when the solution inlet velocity is increased from 0.00118 m/s to 0.00472 m/s. Moreover, it was observed that the absorption rate increased by a factor of 3 when the solution channel thickness was reduced from 2 mm to 0.5 mm. However, it was observed that the pressure drop increases exponentially with a decrease in the solution film thickness, while it increases linearly with an increase in the solution velocity. Therefore to design a compact and efficient plate-and-frame membrane-based absorber with water as a refrigerant, the solution channel thickness and solution mass flow rate should be selected in a manner to achieve high absorption rates with acceptable pressure drop along the solution channel. The solution film thickness and velocity can be independently controlled in plate-and-frame membrane-based absorbers, therefore, to avoid high pressure drop along the solution channel, which

operate under vacuum condition, an optimal value of 0.5 mm for the solution film thickness is suggested and a solution velocity of about 0.003 – 0.005 m/s is recommended in this study based on the CFD simulation. The local absorption rate decreases slightly along the length of the channel which affects the performance of the absorber. In addition, the pressure drop down the channel length is more significant in thinner channels therefore an absorber length of 100 – 200 mm is recommended for a plate and frame membrane-based absorber to obtain a higher absorption rate with a minimum pressure drop. Further, from a comparison of the bulk solution concentration along the 0.5 mm and 2 mm solution channels, it was observed that reducing the solution channel thickness enhances the mass transfer rate and as a result the exit bulk solution concentration achieved in case of a 2 mm solution channel can be achieved at a length of about 0.115 m in case of 0.5 mm solution channel. Thus, decreasing the channel thickness from 2 mm to 0.5 mm and reducing the absorber length from 400 mm to 100 mm can decrease the solution space requirement by a factor of 16, whereas the absorber size can be reduced by a factor of about 5.5 keeping the same thickness of 1.5 mm and 1 mm for the coolant and vapour channels, respectively. Further, for smaller channel length a lower pressure drop will be observed. Thus, considering a thinner channel with reduced length can both allow higher absorption rates and lower pressure drops along the channel. Therefore, reducing the channel thickness and length can allow for the design of highly compact membrane absorbers. Detail about simulation approach, governing equations, numerical scheme and results are given in the research article published in peer-reviewed journal of Energy attached as appendix A3 in this thesis.

CFD analysis of heat and mass transfer mechanisms were performed to investigate the performance of a plate-and-frame membrane based absorber employing water/(LiBr+LiI+$LiNO_3$+LiCl) and water/($LiNO_3$+KNO_3+$NaNO_3$) working fluid mixtures for air-cooled absorption cooling systems and multi-stage high temperature heat sources applications, respectively. Absorption rate, local temperature and concentration profiles as well as pressure drop along the solution channel are analysed in detail. Results shows that a 25% increase in the absorption rate can be achieved utilizing water/(LiBr+LiI+$LiNO_3$+LiCl) when compared to water/LiBr at air-cooled conditions without crystallization problem. Further, absorption rate as higher as 0.00523 kg/m^2.s can be achieved when water/($LiNO_3$+KNO_3+$NaNO_3$) working fluid

mixture is utilized in the membrane-based absorber of the third stage of a triple effect cycle. In addition, it was observed that the percent pressure drop in case of water/($LiNO_3$+KNO_3+$NaNO_3$) working fluid mixture is significantly lower when compared to the water/LiBr and water/(LiBr+LiI+$LiNO_3$+LiCl) working fluid mixtures because of the higher operating pressure. Therefore, the use of water/($LiNO_3$+KNO_3+$NaNO_3$) working fluid mixture in a plate-and-frame membrane absorber which operates at higher pressures cannot only allows higher solution mass flow rate but can also allow the reduction of the solution channel thickness to achieve compact absorber. This means that a narrow solution channel (less than 0.5 mm) with a higher solution mass flow rate can be adopted in case of water/($LiNO_3$+KNO_3+$NaNO_3$) working fluid mixture to achieve a much higher absorption rate. Detail about simulation results are given in the research article submitted to peer-reviewed journal of Energy and is attached in appendix A4 of this thesis.

The calculations preformed using CFD approach were carried out in a workstation cluster of 24 AMD opteron 248 dual core processors (64 bits) and 7 Intel 3 Ghz processors, with 3 Terabytes of Disk, linked with a Giga ethernet in a Linux environment. Simulations were performed in parallel using four processors and each case simulated took approximately 6 days to achieve a steady-state condition. In order to investigate the membrane material characteristics and operating condition of a membrane-based absorber it was time consuming to perform the simulation using CFD tool. In this regard a simple global model was developed in MATLAB code to investigate the membrane material characteristics and operating conditions. It is noteworthy that the same CFD case was simulated using the global model developed in MATLAB and a desktop computer with a 3.0 MHz processor was used to perform the simulation. In this case, steady-state results were obtained within approximately 3 minutes in case of coolant flowing in counter flow direction whereas when the coolant flow was considered in the co-current direction, steady-state results were obtained in less than 20 seconds.

4.2 Membrane material characteristics and operating conditions

The concentration and thermal boundary layers thickness decrease when the solution channel thickness is decreased therefore the absorption potential varies for different solution channel thickness. Further, the resistance to the refrigerant mass transfer also differs which means that the impact of membrane mass transfer resistance and solution mass transfer resistance varies and the relative contribution of each resistance can change. Therefore, a steady-state numerical analysis using simplified 1D mathematical model is performed to critically evaluate the impact of solution channel thickness while investigating the effect of membrane characteristics. The membrane properties such as porosity, membrane thickness and membrane mean pore size are varied over a range to investigate their effect on the absorption performance. In addition, a parametric study is performed to study the effect of operating conditions on the absorption rate in a plate-and-frame absorber to select optimal operating conditions for efficient performance.

4.2.1 Methodology

A mathematical code is developed in MATLAB using simplified one dimensional heat and mass transfer equations which can perform steady-state analysis with less computation efforts and CPU time. The mathematical model is based on energy and mass balance equations in an infinitesimal area along the channel, yielding coupled heat and mass transfer model in which both the governing non-linear and differential equations are solved simultaneously in each cell using the Newton-Raphson method and Runge–Kutta method, respectively.

4.2.2 Results

Results show that the absorption rate increases logarithmically with the increase in the membrane mean pore size. An increase of about 75%, 55%, 40% and 25% in the absorption rate is achievable when the membrane pore diameter is increased from 0.25 μm to 1 μm in the case of 0.1 mm, 0.25 mm, 0.5 mm and 1 mm solution channel, respectively. Moreover, further increasing the pore diameter from 1 μm to 5 μm results in an increase of about 22%, 16%, 11% and 7% in the absorption rate in the

case of 0.1 mm, 0.25 mm, 0.5 mm and 1 mm solution channel, respectively. Increasing the membrane pore diameter reduces the resistance to the vapour transport through the pore which helps in enhancing the absorption rate, however, the mechanical strength of the membrane decreases with the increase in membrane pore size. Therefore, it is crucial to select a membrane with suitable pore diameter that will not only allow a higher absorption rate but will also augment the mechanical strength of the membrane.

Similarly, absorption rate increases almost linearly if the porosity of the membrane contactor is increased from 50% to 85%. Again, the increase in the absorption rate is lower in thicker solution channels when the membrane porosity is increased. An increase of about 68%, 49%, 35% and 23% in the absorption rate is achievable when the membrane porosity is increased from 50% to 85% μm in the case of 0.1 mm, 0.25 mm, 0.5 mm and 1 mm solution channel, respectively. Highly porous membranes exhibit less resistance to the mass transfer flux; however the mechanical strength of the membrane decreases with an increase in porosity. A linear decrease in the absorption rate is observed when the membrane contactor thickness is increased from 20 μm to 100 μm. It can be seen from the results that the decrease in the absorption rate is not significant in thicker solution channels when the membrane contactor thickness is increased. A decrease of about 35%, 28%, 21% and 15% in the absorption rate is observed when the membrane contactor thickness is increased from 20 μm to 100 μm in the case of 0.1 mm, 0.25 mm, 0.5 mm and 1 mm solution channel, respectively. Mass transfer resistance increases with an increase in thickness of the membrane contactor which reduces the mass transfer across the membrane. However, the mechanical strength of the membrane contactor increases with an increase in thickness of the membrane.

The analysis shows that membrane contactor characteristics have a less prominent effect on the absorption rate in the case of thicker solution channels and that the solution resistance is the dominant resistance to the mass transfer of refrigerant molecules in the solution. Moreover, it can be concluded that the membrane mass transfer resistance is dominant only when the solution channel thickness is in the range of 0.1 mm. The thickness of the concentration and thermal boundary layers in thinner solution channels is smaller and the heat is well dissipated to the coolant

because of the decrease in thickness. Therefore, in this case the effect of the membrane mass transfer coefficient is more pronounced.

A parametric study was performed to study the effect of vapour pressure, solution inlet concentration and cooling water temperature on the absorption performance considering different solution channel thickness. It was observed that about 50% increase in the absorption rate is achievable at the same operating conditions when the solution channel thickness is reduced by half from 1 mm to 0.5 mm. Further, the absorption rate increases by approximately 10% when the vapour pressure is increased by 7% and the same mass flow rate is kept in each solution channel, whereas increasing the coolant water inlet temperature from 25 °C to 35 °C results in about a 35% decrease in the absorption rate. Similarly, a higher absorption rate can be achieved if the solution inlet concentration is around 60% for water/LiBr. Selection of suitable operating conditions is important to achieve higher absorption rate without crystallization problem and other limitations. It is recommended that a vapor pressure of about 1.3 kPa, a solution inlet concentration of 60% for water/LiBr and a cooling water inlet temperature of 30 °C should be adopted for water/LiBr membrane-based absorbers of absorption cooling systems. Detail about the mathematical model, governing equations and results are given in the research article published in the peer-reviewed journal of Applied Thermal Engineering and is attached in appendix A5 of this thesis.

Chapter 5

Conclusion

Absorption cooling is an attractive technology since the early stages of cooling technology because of its ability to utilize heat directly for cooling purposes. Continued improvements in the design and configuration of the components of absorption cooling systems have been suggested and implemented commercially to improve the performance. In this work, the application of membrane contactors in the absorber of an absorption cooling system has been investigated in detail. A comprehensive review on the use of membrane contactors in absorption cooling systems has been performed. Heat and mass transfer analyses of a plate-and-frame membrane-based absorber were carried out using CFD approach. In addition, 1D numerical model was developed in MATLAB code to study the performance of a plate-and-frame membrane-based absorber at different operating conditions and membrane material characteristics. Detailed analysis using CFD simulation was carried out with the conventional water/LiBr working fluid mixture to investigate the heat and mass transfer, and fluid dynamics behaviour at local level to better understand the phenomena and identify a suitable geometry and working conditions of a membrane-based absorber. Further, non-conventional working fluid mixtures, water/(LiBr+LiI+$LiNO_3$+LiCl) and water/($LiNO_3$+KNO_3+$NaNO_3$) were investigated in a plate-and-frame membrane-based absorber for air-cooled and high temperature heat source applications, respectively. Effect of membrane material characteristics and operating conditions on the absorption performance was studied using the 1D mathematical code considering water/LiBr working fluid mixture. This work presents an in-depth knowledge to understand and design membrane-based absorbers for absorption cooling systems.

In the literature review, the applications of membrane contactors in the field of absorption cooling systems were covered. Membrane contactor modules, components employing membrane contactors, cycle configurations, membrane material characteristics and the working fluid mixtures for the membrane contactor based absorption refrigeration systems were discussed in detail. From the literature survey it

is concluded that the use of light weight polymeric hydrophobic microporous membrane contactors can provide a larger interfacial area for heat and mass transfer processes, which in turn not only can reduce the size and weight of the components but also can enhance the performance of the system. Membrane modules are smaller in size and weight than the conventional components because polymeric fibres/membrane sheets replace the heavy metallic tubes/plates. Thus, the size of the absorption refrigeration system utilizing membrane-based components can be reduced significantly, allowing its use in transport and small scale applications.

Both the plate-and-frame membrane module and hollow fibre membrane module are promising alternatives to the conventional components of absorption refrigeration systems and can be used with water and ammonia based refrigerants, respectively. Plate-and-frame module is generally selected when the aqueous solution of H_2O/LiBr is used as a working fluid mixture in absorption refrigeration systems whereas hollow fibre module is usually selected for the ammonia/water based absorption refrigeration systems. Due to the parallel plates/flat sheets in the plate-and-frame membrane module the pressure drop is small, it is therefore considered as a better option for the water/lithium bromide based absorption refrigeration systems which operate under vacuum condition. The hollow fibre module allows more efficient mass transfer due to external transverse flow and is considered an appropriate choice for the ammonia/water based absorption refrigeration systems. Hybrid hollow fibre membrane module can be an interesting replacement of the conventional absorbers as compared to ordinary hollow fibre membrane module as in this type of module non-porous membrane fibres are incorporated within the module for coolant flow to dissipate the heat of absorption from the solution and therefore can enhance the absorption performance of the absorber. The driving force for the refrigerant mass transfer in the case of ammonia/water and water/LiBr solutions is considered to be the difference in concentration and water vapour partial pressure, respectively. The use of a porous hydrophobic membrane contactor to constrain the solution film in narrow micro-channels can allow the design of a compact membrane-based absorber utilizing water as a refrigerant under vacuum conditions. In a plate-and-frame membrane-based component, both the solution film thickness and solution mass flow rate can be independently controlled. It is worth to note that a higher absorption rate can be achieved if the solution film thickness is around 100 μm. However, an optimal

solution film thickness and solution mass flow rate is important to avoid higher pressure drop along the channel which can significantly affect the operation of absorber working under vacuum condition. Also the use of micro-scale features on the flow channels surface in a plate-and-frame can significantly improve the absorption rate by producing vortices within the solution which continuously bring the concentrated solution to the solution vapour interface. However, the ease and economic viability to manufacture a surface with micro-scale features for membrane based absorbers need to be investigated for the commercial use of such plate-and-frame membrane absorber.

A membrane-based absorber or solution heat exchanger do not affect the cycle configuration, however, membrane-based desorbers can alter the configuration of absorption cooling cycles and the cycle components can be reduced in some cases. In addition, absorption refrigeration systems utilizing membrane-based desorbers can operate at lower desorber temperatures which can extend the use of low grade heat sources effectively in absorption refrigeration systems. In membrane-based desorbers, desorption rate can be enhanced by direct diffusion at low desorber temperatures. Adequate permeation flux is possible across the membrane without the need for the hot feed to reach boiling point. Heating of the aqueous solution to the boiling point is not needed as long as the temperature difference exists between the two sides of the membrane pores. Due to the temperature difference across the membrane, a pressure difference arises and acts as the driving force for the mass transfer across the membrane pores. Consequently, the membrane based desorber can operate at a lower temperature than conventional desorbers where the solution must be heated to boiling point to achieve the separation of the refrigerant from the solution. This means that low grade heat sources can be efficient if membrane module desorbers are used in absorption refrigeration systems.

The absorber is one of the major components in absorption cooling systems and has a direct effect on the size and performance of this equipment. Introducing polymeric hydrophobic microporous membranes into the absorber design can be one of the alternatives for achieving highly compact absorbers with enhanced heat and mass transfer. Solution flow rate, temperature and solution film thickness are crucial parameters for the plat-and-frame absorbers and a suitable value should be selected to

achieve high absorption rate. CFD approach to investigate the heat and mass transfer mechanisms and fluid dynamics behaviour at local levels in the channels, show interesting results to better understand the phenomena. The effect of important parameters like solution film thickness, solution flow velocity and coolant temperature on the performance of membrane based absorbers was studied. The results of CFD simulation are useful and can play an important role in the design of membrane based absorbers that use water as a refrigerant. Steady-state CFD analysis of heat and mass transfer mechanism in a plate-and-frame membrane-based absorber, using water/LiBr working fluid mixture, show that the solution film thickness and solution flow rate are important parameters which significantly affects the mass transfer processes. The solution film thickness and velocity can be independently controlled in plate-and-frame membrane-based absorbers however CFD results showed that the solution pressure drop increases exponentially with a decrease in the solution channel thickness. Moreover, a linear increase in the pressure drop occurs while increasing the solution mass flow rate. Therefore to design a compact and efficient plate-and-frame membrane-based absorber with water as a refrigerant, the solution channel thickness and solution mass flow rate should be selected in a manner to achieve high absorption rates with acceptable pressure drop along the solution channel. Further, it was observed that decreasing the channel thickness and reducing the absorber length cannot only decrease the solution space requirement but also the overall pressure drop along the solution channel can be lowered. Thus, considering a thinner channel with reduced length can allow design of highly compact membrane-based absorbers with higher absorption rates.

Ammonia/water and water/lithium bromide are the most commonly used working fluid pairs analysed both analytically and experimentally to investigate the performance of membrane based components of absorption refrigeration systems. One of the key advantages of these working fluid pairs is that the thermophysical properties are well known and established. However, other working fluids such as ammonia/(lithium nitate+water), water/multicomponent salt mixtures and ionic liquid based absorbent solutions can also be effectively utilized in membrane based absorption refrigeration systems. In this study, water/(LiBr+LiI+$LiNO_3$+LiCl) and water/($LiNO_3$+KNO_3+$NaNO_3$) working fluid mixtures were investigated for air-cooled absorption cooling systems and multi-stage high temperature heat sources

applications, respectively. Results showed that a higher absorption rate can be achieved utilizing water/(LiBr+LiI+$LiNO_3$+LiCl) when compared to water/LiBr working fluid mixture at air-cooled conditions. Further, absorption rate as higher as 0.00523 kg/m^2.s is achieved when water/($LiNO_3$+KNO_3+$NaNO_3$) working fluid mixture is utilized in the membrane-based absorber of the third stage of a triple effect cycle operating with high temperature heat sources. Because of the higher operating pressure the percent pressure drop in case of water/($LiNO_3$+KNO_3+$NaNO_3$) working fluid mixture is significantly lower which allows the use of narrow solution channel with a higher solution mass flow rate to achieve compact absorber design with higher absorption rate.

For those absorption refrigeration systems utilizing membrane contactors, the properties and requirements of the absorbent/refrigerant combination should be compatible with the membrane contactor characteristics and materials. Therefore, selection of appropriate membrane contactor material with suitable characteristics, such as porosity, pore size, thickness, tortuosity etc. is crucial while designing a membrane based component. Moreover, the mechanical strength of the membrane contactor is also dependent on the above mentioned characteristics. In this study, a numerical analysis was carried out using 1D mathematical model in MATLAB code to investigate the effect of membrane contactor characteristics and operating conditions on the absorption performance in a plate-and-frame membrane based absorber for absorption cooling systems. Results showed that the membrane contactor characteristics do not significantly affect the absorption rate and that the solution mass transfer resistance is the dominant resistance to the vapour absorption. Moreover, it was observed that the influence of solution channel thickness in a plate-and-frame membrane-based absorber is significant while investigating the effect of membrane characteristics on the absorption performance. It is concluded that the selection of appropriate membrane characteristics should be made keeping in mind the solution channel thickness. Although solution channel thickness of the order 0.1 mm can allow a higher absorption rate however the higher pressure drop along the channel can hinder the performance of the membrane based absorber working under vacuum condition. Solution channel thickness of about 0.5 mm is considered appropriate to avoid higher pressure drop in the solution channel. Analytical analysis performed in this study shows that the effect of membrane characteristics is insignificant when the

solution channel thickness is in the range of 0.5 mm. Therefore, it is recommended to select a membrane contactor with a pore size and thickness such that it does not affect the mechanical strength of the membrane material. In this way the additional support layer of the membrane can be avoided which is an additional resistance to the membrane mass transfer resistance. Further, emphases should be given on the selection of a membrane contactor with appropriate surface properties such as hydrophobicity of the material which is important to limit the solution to pass through the pores that can hinder the performance of the membrane based absorber. Selection of suitable operating conditions is important to achieve higher absorption rate without crystallization problem and other limitations. Based on the parametric study performed in this work, it is recommended that a vapor pressure of about 1.3 kPa, a solution inlet concentration of 60% for water/LiBr and a cooling water inlet temperature of 30 °C should be adopted for water-LiBr membrane-based absorption air-conditioning systems.

5.1 Future Work

This work reveals that the application of membrane contactors is an emerging technique in the field of absorption cooling systems, however, a commercial plant has not yet been designed to explore the long term operation of membrane contactor based components in absorption refrigeration systems. Further research is needed to explore the long term operation consequences of membrane contactors in absorption and desorption processes. One of the prominent areas for future investigation is the use of non-conventional working fluid mixtures in membrane contactor components. Potential research could be carried out on the use of ionic liquid as an absorbent in absorption refrigeration systems employing membrane based components. Membrane contactor modules are available in different types hence, membrane modules other than plate-and-frame membrane module and hollow fibre module should also be investigated. Membrane contactor surface properties need to be studied further for more efficient use in absorption refrigeration components. In this regard, further research work is required to improve the hydrophobic character of membrane material, enhance the mechanical strength and to improve the compatibility of the membrane material with the working fluid mixtures. Membrane contactors do not suffer corrosion problems as it occurs in conventional absorption refrigeration

components. However, fouling of membrane contactors means that more need for research is necessary with regard to absorption refrigeration components employing membrane contactors, so that durability and life span cost of the absorption refrigeration system can be evaluated more precisely. Although experimental analyses have been carried out to investigate the performance of the membrane based desorber, however, detailed behaviour of the heat and mass transfer mechanisms at local levels and the fluid dynamic behaviour need to be investigated to better understand the phenomenon and the effect of flow parameters both in direct diffusion mode and boiling mode. Membrane module desorbers should be tested and analysed at higher operating temperatures to investigate the effect of high temperatures on membrane materials and performance.

References

1. Perez-Lombard L, Ortiz J, Pout C. A review on buildings energy consumption information. Energy and Buildings. 2008; 40:394–8.

2. Ibarra-Bahena J, Romero JR. Performance of Different Experimental Absorber Designs in Absorption Heat Pump Cycle Technologies: A Review. Energies. 2014; 7:751–66.

3. Chen J, Chang H, Chen S. Simulation study of a hybrid absorber–heat exchanger using hollow fiber membrane module for the ammonia–water absorption cycle. International Journal of Refrigeration. 2006; 29:1043–52.

4. Carlos AC. Intensification of NH_3 Bubble Absorption Process using Advanced Surfaces and Carbon Nanotubes for $NH_3/LiNO_3$ Absorption Chillers. PhD Thesis. Rovira i Virgili University. 2013. Spain.

5. Choi SUS, Eastman JA. Enhancing thermal conductivity of fluids with nanoparticles. ASME International mechanical engineering congress and exhibition. 1995; 231:99–105.

6. Y.T. Kang, H.J. Kim, K.I. Lee Heat and mass transfer enhancement of binary nanofluids for H_2O/LiBr falling film absorption process. International Journal of Refrigeration. 2008; 31:850–6.

7. Griesheim MS, Rodenbach BG. Absorption refrigeration machine. US Patent No 2010 / 0326126 A1, 2010.

8. Marsh KN, Boxall JA, Lichtenthaler R. Room temperature ionic liquids and their mixtures - a review. Fluid Phase Equilibria. 2004; 219:93–8.

9. Valkenburg MEV, Vaughn RL, Williams M, Wilkes JS. Thermochemistry of ionic liquid heat-transfer fluids. Thermochim Acta. 2005; 425:181–8.

10. Khamooshi M, Parham K, Atikol U. Overview of ionic liquids used as working fluids in absorption cycles. Advances in Mechanical Engineering. 2013. http://dx.doi.org/10.1155/2013/620592

11. Bourouis M, Vallès M, Medrano M, Coronas A. Performance of air-cooled absorption air conditioning systems working with water-(LiBr+LiI+$LiNO_3$+LiCl). Journal of Process Mechanical Engineering. 2005; 219:205–12.

12. Bourouis M, Vallès M, Medrano M, Coronas A. Absorption of water vapour in the falling film of water-(LiBr+LiI+$LiNO_3$+LiCl) in a vertical tube at air-cooling thermal conditions. International Journal of Thermal Sciences. 2005; 44:491–98.

13. Medrano M, Bourouis M, Coronas A. Absorption of water vapour in the falling film of water-lithium bromide inside a vertical tube at air-cooling thermal conditions. International Journal of Thermal Science. 2002; 41:891 – 8.

14. Davidson W, Erickson D. 260 °C Aqueous absorption working pair under development. Newsl. IEA Heat Pump Cent. 1986; 4:29–31.

15. Howe L, Erickson D. Proof-of-Concept Testing of Alkitrate. Phase III. Final Report- Energy Concepts Co. 1990. USA.

16. Erickson D, Potnis SV, Tang J. Triple Effect Absorption Cycles. Energy Conversion Engineering Conference IECEC 96. Proceedings of The 31st Intersociety. 1996; 1072–7.

17. Álvarez M, Esteve X, Bourouis M. Performance analysis of a triple-effect absorption cooling cycle using aqueous (lithium, potassium, sodium) nitrate solution as a working pair. Applied Thermal Engineering. 2015; 79:27–36.

18. Uemura T, Hasaba S. Studies on the lithium bromide-water absorption refrigeration machine. Technology Reports of Kansai University. 1964; 6:31–55.

19. Koo KK, Lee HR, Jeong S, Oh YS, Park DR, Baek YS. Solubilities, Vapor Pressures, and Heat Capacities of the Water + Lithium Bromide + Lithium Nitrate + Lithium Iodide + Lithium Chloride System. International Journal of Thermophysics. 1999; 20:589–600.

20. Confidential Report. Thermophysical properties of the fluid mixture water/(LiBr+LiI+$LiNO_3$+LiCl). Universitat Rovira i Virgili. 2012.

21. Álvarez M, Bourouis M, Esteve X. Vapor-liquid equilibrium of aqueous alkaline nitrate and nitrite solutions for absorption refrigeration cycles with high temperature driving heat. Journal of Chemical & Engineering Data. 2011; 56:491–6.

22. Lee RJ, DiGuilio RM, Jeter SM, Teja AS. Properties of lithium bromide-water solutions at high temperatures and concentrations - II Density and viscosity. ASHRAE Transactions. 1990; Paper 3381. RP-527:709–14.

23. Álvarez ME. Theoretical and experimental study of the aqueous solution of lithium, sodium and potassium nitrates as a working fluid in absorption chillers driven by high temperature heat sources. PhD Thesis. Rovira i Virgili University. 2013. Spain.

24. Kaita Y. Thermodynamic properties of lithium bromide–water solutions at high temperatures. International Journal of Refrigeration. 2001; 24:374–90.

25. Salavera D, Esteve X, Patil KR, Mainar AM, Coronas A. Solubility, heat capacity, and density of lithium bromide+lithium iodide+lithium nitrate+lithium chloride aqueous solutions al several compositionss and temperature. J. Chem. Eng. Data, 2004, 49, 613-619.

26. Laliberté M. A model for calculating the heat capacity of aqueous solutions, with updated density and viscosity data. Journal of Chemical and Engineering Data. 2009; 54:1725–60.

27. DiGuilio RM, Lee RJ, Jeter SM, Teja AS. Properties of lithium bromide-water solutions at high temperatures and concentrations - I Thermal conductivity. ASHRAE Transactions. 1990; Paper 3380. RP-527:702–8.

28. Aseyev G. Electrolytes - Properties of solutions methods for calculation of multicomponent systems, and experimental data on thermal conductivity and surface tension. Begell House Publishers. New York. 1998.

29. Gierow M, Jernqvist A. Measurement of mass diffusivity with holographic interferometry for H_2O/NaOH and H_2O/LiBr working pairs. International Absorption Heat Pump Conference. 1993; 31:525–32.

30. Bird R, Stewart W, Lightfoot E. Transport Phenomena. 2nd ed. OUP. 2001.

31. Florides GA, Kalogirou SA, Tassou SA, Wrobel LC. Design and construction of a LiBr–water absorption machine. Energy Conversion and Management. 2003; 44:2483–508.

32. Ally M. Thermodynamic properties of aqueous ternary solutions relevant to chemical heat pumps. Final Report. ORNL/TM-10258. Oak Ridge National Laboratory. 1987.

Appendix A

Research Articles

A.1 A Review of Membrane Contactors Applied in Absorption Refrigeration Systems.

Renewable and Sustainable Energy Reviews 45 (2015) 173–191

Contents lists available at ScienceDirect

Renewable and Sustainable Energy Reviews

journal homepage: www.elsevier.com/locate/rser

A review of membrane contactors applied in absorption refrigeration systems

Faisal Asfand, Mahmoud Bourouis *

Department of Mechanical Engineering—Universitat Rovira i Virgili, Av. Països Catalans No. 26, 43007 Tarragona, Spain

ARTICLE INFO

Article history:
Received 11 June 2014
Received in revised form
8 January 2015
Accepted 12 January 2015
Available online 7 February 2015

Keywords:
Membrane contactors
Absorption refrigeration
Hydrophobic microporous membrane
Hollow fiber membrane module
Plate-and-frame membrane module

ABSTRACT

The use of membrane contactor technology is well-known in the process industry and can be employed in many important fields; such as separation and absorption processes, membrane distillation, pervaporation, biotechnology, food industries etc. In recent years, research has been carried out regarding the use of membrane contactors in the components of absorption refrigeration systems. The use of membrane contactors makes it realizable to design compact components with improved heat and mass transfer. Heat and mass transfer performance of the components is significantly enhanced due to the higher area to volume ratio available. Membrane based absorber and desorber allow the reduction in size of the absorption refrigeration systems to a great extent and thus absorption refrigeration technology can be used in transport and small scale applications. In this paper, the applications of membrane contactors in absorption refrigeration systems are reviewed. The application of membrane contactors in the components of absorption refrigeration systems, the configurations of refrigeration cycles that employ membrane contactors and the characteristics of the membrane contactors used in absorption refrigeration systems are all reviewed in detail. Information is collected on the choice of working fluid mixture to be used in absorption refrigeration systems that use membrane based components and the compatibility of working fluid mixtures with the membrane contactor material is discussed. The significance and limitations of using membrane contactors in absorption refrigeration systems is included in this paper.

Contents

* Corresponding author. Tel.: +34 977 55 86 13; fax: +34 977 55 96 91.
E-mail address: mahmoud.bourouis@urv.cat (M. Bourouis).

http://dx.doi.org/10.1016/j.rser.2015.01.054
1364-0321/

1. Introduction

The application of membranes in the process industry is growing. This is due to the relative simplicity, reliability, high parameters of separation, large interfacial area and lower energy consumption with improved heat and mass transfer. The cost of the membrane based components is also lower under short time of capital recurring and suffers negligible corrosion. Membrane contactors can be utilized in many important fields. These include separation and absorption processes, membrane distillation, pervaporation, biotechnology and food industries among others. Hydrophobic porous membranes are extensively utilized in the field of distillation technology and in air-conditioning systems to remove excess moisture, carbon dioxide and organics. Air moisture content and carbon dioxide concentration can be independently and simultaneously controlled efficiently with the help of membrane contactors. One of the emerging applications of membrane contactors lies in the field of absorption refrigeration systems.

Absorption refrigeration technology, which has the ability to utilize heat directly for cooling purposes, has been one of the most widely used technologies for refrigeration and cooling applications since the early stages of refrigeration technology. Vapour compression systems can achieve high values of the coefficient of performance (COP) but at a cost of very high mechanical energy input. However, absorption refrigeration systems can efficiently utilize the renewable energy sources, such as solar energy and low grade thermal energy (i.e. waste heat energy) as a source of energy input instead of using costly mechanical energy. Moreover, the refrigerants used in conventional vapour compression refrigeration systems are not environmental friendly and can contribute to ozone depletion and greenhouse effects, whereas in the absorption refrigeration systems the working fluid mixtures are environmental friendly. Currently, the world is facing an energy shortage problem and it is predicted that the interest in absorption refrigeration systems will increase in the future due to the fact that they can use renewable energy sources and refrigerants that are environmental friendly and do not contribute to Ozone depletion. Absorption refrigeration systems have a high capital cost when compared to vapour compression systems, but for large scale applications the lifecycle cost is very low. However, the absorption refrigeration technology is still relatively little used for cooling applications. In particular, in the sector of mobile refrigeration/air-conditioning, absorption refrigeration has not yet gained much interest. The main drawback of absorption refrigeration systems is the large volume per unit of cooling capacity which has limited their use in mobile applications and small commercial and residential buildings. There is a growing need to design an absorption refrigeration system which has a smaller space requirement for small scale applications. Drost et al. [1] reported that the development of compact absorbers could permit the use of absorption refrigeration systems in small scale heating and cooling applications, heat-actuated automotive air conditioning, and portable cooling. Thus, the success of absorption technology mainly depends on reducing the cost of investment and the size of the components.

Depending on the working fluid mixture used, absorption refrigeration systems are broadly classified into ammonia/water (NH_3/H_2O) and water/lithium bromide (H_2O/LiBr) systems. The basic components of both types of refrigeration systems are the absorber, desorber, condenser, evaporator and solution heat exchanger. However, in the case of NH_3/H_2O absorption refrigeration systems, a rectifier is also used at the exit of the desorber to purify the ammonia vapour by condensing the water vapour from the refrigerant vapour. As ammonia and water are both volatile, the refrigerant vapour may contain significant amount of water vapour that has a negative effect on the system performance. Therefore, a rectification process is required for the NH_3/H_2O absorption refrigeration systems. NH_3/H_2O absorption refrigeration systems operate at higher pressures and are commonly used for low temperature (-40 °C to $+5$ °C) cooling applications. H_2O/LiBr absorption refrigeration systems operate under vacuum conditions and are used in air-conditioning applications where the cooling temperature requirement is above 7 °C. The basic single-stage cycle configurations of both H_2O/LiBr and NH_3/H_2O absorption refrigeration systems are shown in Fig. 1.

The performance of absorption refrigeration systems is primarily dependent on the absorber and desorber which are the major components of this kind of refrigeration system. The design of these components is crucial for efficient performance of the absorption refrigeration system. Both the absorber and desorber used in absorption technology are relatively expensive and are large in size. In the case of H_2O/LiBr absorption refrigeration systems the absorber operates under static vacuum pressure accompanied by a high

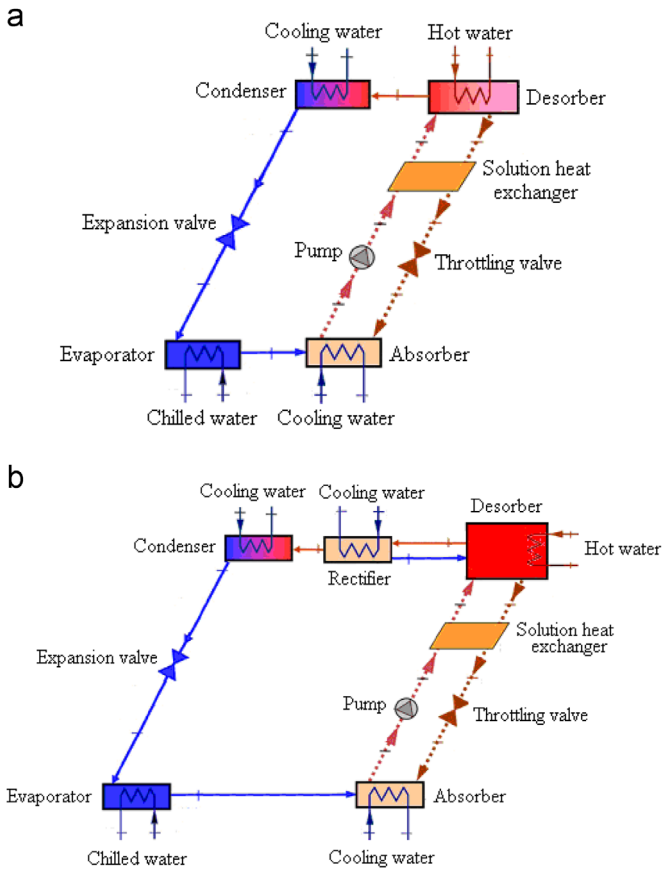

Fig. 1. Basic absorption refrigeration cycle configuration. (a) H_2O/LiBr (b) NH_3/H_2O.

Nomenclature

A	area (m^2)
B	pore geometric factor (–)
d	diameter (m, μm)
k	thermal conductivity (W/m-K)
p	vapour pressure (mbar, Pa)
P	pressure (Pa)
R	general gas constant (J/mol-K)
T	temperature (°C, K)
V	molar volume (cm^3/mol)

Greek letters

ε	membrane porosity (–)
θ	contact angle (°)
ρ	density (kg/m^3)
σ	liquid surface tension (N/m)
τ	membrane tortuosity (–)

Superscripts

0	equilibrium state
c	critical

Subscripts

g	gas
i	component index
max	maximum
mem	membrane
P	permeate
p	pore
pol	polymer
s	solid

Abbreviations

COP	coefficient of performance
CFI	cold fluid inlet
HFI	hot fluid inlet
LEP	liquid entry pressure
NA	not available
PE	polyethylene
PP	polypropylene
PTFE	polytetrafluoroethylene/Teflon
PVDF	polyvinylidene fluoride
sqm	square meter
SS	strong solution
UV	ultraviolet
WS	weak Solution

Chemical formulas

H_2O	water
LiBr	lithium bromide
LiCl	lithium chloride
LiI	lithium iodide
$LiNO_3$	lithium nitrate
NH_3	ammonia

specific volume of water vapour. It therefore has a direct effect on the size, weight and space requirement of absorption refrigeration systems. Research is currently being carried out to design compact absorbers and desorbers for absorption refrigeration systems. Recently, research has shown that membrane contactor technology can be utilized in absorption refrigeration systems, especially in the case of the absorber and desorber, so as to reduce the size, weight and cost of the system and also significantly enhance the heat and mass transport processes taking place in the systems. The use of polymeric hydrophobic microporous membrane contactors in both the absorber and desorber could mean a reduction in manufacturing costs. To be attractive for usage in small scale applications, the absorption chiller size must be compact, lightweight and resistant to mechanical shocks. Thus, utilizing polymeric hydrophobic microporous membrane contactors in the absorber and desorber of an absorption refrigeration system could reduce both the size and weight of the components and open the use of the system to the sector of transport refrigeration and air-conditioning. The driving force for the refrigerant mass transfer in the case of ammonia/water and water/LiBr solutions is considered to be the difference in concentration and water vapour partial pressure, respectively. A membrane based desorber could operate at a lower temperature than a conventional desorber and would not require heating the solution to its boiling point to achieve the separation of the refrigerant from the solution. Therefore, low grade heat sources could be efficient if membrane module desorbers were used in absorption refrigeration systems.

In this paper the applications and significance of membrane contactors in absorption refrigeration systems are reviewed in detail and different types of membrane modules used in components of absorption refrigeration systems are illustrated. Characteristics of membrane contactors employed in the components of absorption refrigeration systems are overviewed. Working fluid mixtures employed in membrane based absorption refrigeration systems are analysed and the compatibility of working fluid mixtures with membrane contactor characteristics and materials are discussed. The principle of the operation of membrane contactor modules and its effect on the absorption refrigeration cycle configuration is described. Different configurations of absorption refrigeration systems utilizing membrane modules in the components are reviewed.

2. Membrane contactor materials and characteristics

Membrane acts as a semi-permeable barrier to separate components of the feed solution into a retentate and a permeate, by controlling the movement of molecules across the membrane. In addition, membrane can be used as a contactor between two components to enhance the absorption of a gas or vapour molecules in the absorbent. In the open literature, membrane materials are broadly classified into two categories based on the membrane structure. These include microporous membranes and dense membranes. Microporous membranes have interconnected pores which allow one of the components of the solution mixture to pass through it while restrict the other components depending on the pore size. If the relative pore size of the microporous membrane is big then the selectivity of the membrane contactor decreases, however, the mass transfer flux increases with bigger pore size. Dense membranes are nonporous solid membranes which are used for separation of small molecules from the mixture. The mechanism of the separation process involves diffusion of the molecules to the surface of the membrane, dissolving

into the membrane material, diffusing through the solid and desorbing at the downstream interface. Though dense membranes have very high selectivity but due to their low permeability they have limited applications in the industry. The compatibility of the dense membrane with the working fluid mixture is very important as the separation process depends on both the solubility and the diffusivity of the permeate.

On the basis of material, membranes are generally categorized into organic and inorganic membranes. Inorganic membranes are made of materials such as ceramic, carbon, silica, etc. and metals such as palladium, silver and their alloys. Organic membranes are made of polymeric microporous materials. Currently, the microporous polymeric membranes are widely used in the industrial application because of competitive performance and low cost. Inorganic membranes are generally more expensive than organic polymeric membranes. However they have the advantage to withstand high temperature and pressure as well as possess high stability. In absorption refrigeration systems, polymeric microporous membranes are mostly used for the separation of refrigerant from the solution and also as a contactor between the refrigerant and absorbent to enhance the absorption performance.

The literature survey regarding the use of membrane contactors in absorption refrigeration systems reveals that various types of membranes with different characteristics and properties were experimentally investigated. Yu et al. [2] used a cellulose triacetate membrane, Riffat et al. [3] used dense membrane and silicon porous membrane, Schaal et al. [4], Thorud et al. [5], Wang et al. [6], Ali and Schwerdt [7] used hydrophobic porous membrane, Isfahani et al. [8,9], Isfahani and Moghaddam [10] and Bigham et al. [11,12] used superhydrophobic nanofibrous membrane, Drost et al. [1] used a woven membrane and a laser-machined membrane. The laser-machined membranes have higher water vapour permeability as compared to commercially available hydrophobic porous membranes, albeit with a high cost. Deerberg and Gehrke [13] reported that the specific price of 1 sqm of laser machined membrane with an average pore diameter of 1 to 10 μm is about 1000€ and the price could be more than triple if the pore diameter is less than 1 μm. The common commercially microporous hydrophobic membranes are available in capillary or flat sheet shape and are made of polyethylene (PE), polypropylene (PP), polyvinylidene fluoride (PVDF) and polytetrafluoroethylene (PTFE, Teflon), with a high porosity (70–80%), a membrane thickness of 10–300 μm and provide microfiltration properties with pore sizes from 0.1 to 1.0 μm.

It is essential to know the transport phenomena across the membrane contactor in order to use a suitable membrane contactor. Selection of membrane material and characteristics also depend on the process and properties of the working fluid pair. Care must be taken while selecting a microporous membrane for use in membrane contactors. Schaal et al. [4] suggested the use of porous non-selective membrane because of the low transport resistance. They mentioned that although all components can pass through a non-selective membrane, this issue can be overcome by appropriately selecting the surface properties of the membranes and the difference in vapour pressure between the two phases. In absorption refrigeration systems, the literature review considers that the surface of the membrane contactors used in the cases of ammonia/water and water/LiBr working mixtures should be hydrophobic in nature to allow only the vapours to enter and pass through the membrane pores. This is because due to the hydrophobic nature of the membrane material, the aqueous solution does not penetrate into the membrane pores.

Mass transfer is the most important phenomenon of concern taking place across the membrane contactor. The driving force could be the vapour pressure difference or the concentration difference. The mass transfer across the membrane should be such that only refrigerant is allowed to pass through the membrane. The overall mass transfer across the membrane is significantly affected by the membrane properties. The selection of a suitable membrane for the desired process is of critical importance for optimal performance, as the membrane contactor adds resistance to mass transfer when compared with direct contactors. The characteristics of a membrane contactor have a huge impact on the performance and both the capital and operating costs. Microporous membranes are commonly characterised by measuring the hydraulic permeability, porosity, tortuosity, mean pore size, thickness, thermal conductivity, and liquid entry pressure. Ali and Schwerdt [7] analysed the characteristics of commercially available microporous hydrophobic membranes for use in a compact absorber for water/LiBr based absorption refrigeration systems. They investigated experimentally and analytically the properties that influence the water vapour mass transfer flux into a thin film of water/LiBr solution and defined the criteria for utilizing membranes in the design of a compact absorber for absorption refrigeration systems. Iversen et al. [14] have characterized a wide variety of potential microporous membranes and reported that the performance of microporous membranes in membrane contactors depends on the porosity, thickness, average pore radius and geometry and the manufacturing method.

The characteristics of the membrane contactors reported in the investigations reviewed in this work are summarized in Table 1. It can be seen from Table 1 that hydrophobic membranes are being used by the researchers as they play a critical role in limiting the mass transfer of the absorbent solution across the membrane due to their surface properties. Similarly most of the researchers have chosen highly porous membranes (0.7–0.85) because membrane with higher value of porosity can significantly increase the mass transfer process. However, an optimized value of porosity should be selected to avoid the adverse effect of porosity on the mechanical strength of the membrane contactor. It can be noticed that the nominal thickness of membrane contactors used in the components of absorption refrigeration systems lies in the range of micrometers. Although mass transfer resistance increases with increase in thickness however for high mechanical strength a

Table 1
Characteristics of membrane contactors reported in the investigations reviewed in this work.

Reference	Membrane material	Porosity	Pore size (μm)	Thickness (μm)	Membrane type
Schaal et al. [4]	Polypropylene	NA	0.04	40	Hydrophobic
Wang et al. [6]	Polyvinylidene Fluoride	0.85	0.16	150	Hydrophobic
Ali and Schwerdt [7,15]	Polytetrafluoroethylene	0.64–0.75	0.20–0.45	65–175	Hydrophobic
Isfahani et al. [9]	Polytetrafluoroethylene	NA	0.45	50	Hydrophobic
Isfahani and Moghaddam [10]	NA	0.80	1.0	NA	Hydrophobic
Bigham et al. [11]	Polytetrafluoroethylene	0.60	1.0	20	Hydrophobic
Yu et al. [16]	NA	0.50–0.80	0.40–6.00	20–100	Hydrophobic
Ali [49]	Polytetrafluoroethylene	0.75	0.45	60	Hydrophobic
Chen et al. [53]	NA	0.40	0.03	30	Hydrophobic

nominal thickness of membrane contactor should be selected. It can be seen from the literature data that the mean pore size of the membrane selected in case of ammonia/water is smaller (0.03–0.04 μm) when compared to water/lithium bromide (0.16–6 μm). This could be because of the difference in relative size of the absorbent and refrigerant molecules in both cases.

The description of the characteristics of membrane contactors and the corresponding mathematical equations are presented in the following sections.

2.1. Membrane porosity

Porosity is the measure of void spaces in the membrane material. It is the fraction of volume of voids in the total volume of the membrane contactor. Mass transfer flux across the membrane contactor is directly related to the porosity of the membrane. Highly porous membranes exhibit less resistance to the mass transfer flux; however the mechanical strength of the membrane decreases with an increase in porosity. A membrane should have enough mechanical strength to withstand the absorption refrigeration system operating conditions. Ali and Schwerdt [7,15] recommended membrane porosity in the range of 0.7–0.8 for the membrane contactors employed in the absorber of an absorption refrigeration system. Their results show that the membrane mass transfer flux increases with an increase in porosity, regardless of the membrane pore diameter. However, the results reported by Yu et al. [16] illustrate that the effect of membrane porosity on the mass transfer flux is less prominent in membranes with bigger pore sizes, while the mass transfer flux increases with an increase in porosity of membranes with small pore sizes. It is concluded that membrane mass transfer resistance is more dominant in membranes with small pore sizes while membrane mass transfer resistance decreases and diffusion resistance into the solution becomes a dominant factor in membranes with larger pore sizes. Smolder–Franken equation [17] can be used to calculate the porosity of a membrane contactor.

$$\varepsilon = 1 - \left(\frac{\rho_{mem}}{\rho_{pol}}\right) \tag{1}$$

where ε is the porosity, ρ_{mem} is the density of the membrane in kg/m^3 and ρ_{pol} is the density of the polymer material in kg/m^3.

2.2. Mean pore size

Mean pore size refers to the average diameter of the pores in the membrane contactor and is usually in the range of μm. Pore size can vary in the membrane contactor and sometimes the pore size distribution can also be used in characterizing a membrane contactor. Ali and Schwerdt [7] recommended a pore size of 0.45–1.0 μm to obtain a high mass transfer flux across the membrane. Ali and Schwerdt [15] reported that the membrane mass transfer flux increases linearly with an increase in the membrane mean pore size from 0.2 to 1 μm. In addition, their results show that the increase in membrane mass transfer flux with increase in pore size is more prominent for high porous membrane. Yu et al. [16] obtained an exponential increase in the membrane mass transfer flux with increase in the membrane mean pore size from 0.5 to 6 μm. They reported that the membrane mass transfer flux initially increases significantly with an increase in the membrane pore size from 0.5 to 4 μm because the effect of membrane mass transfer resistance is more dominant in membranes with small pore size and the mass transfer resistance decreases with an increase in the membrane mean pore size. However, further increase in the mean pore size has almost no effect on the mass transfer flux because in membranes with larger pore size the diffusion resistance into the solution is a more dominant factor instead of the membrane mass transfer resistance.

2.3. Membrane thickness

Membrane contactor thickness is an important characteristic which is inversely related to the mass transfer flux and it has a significant effect on both heat and mass transfer processes. Mass transfer resistance increases with an increase in thickness of the membrane contactor which reduces the mass transfer across the membrane. However, the mechanical strength of the membrane contactor increases with an increase in thickness of the membrane. Yu et al. [16] performed an analysis to investigate the effect of membrane thickness on mass transfer flux. Their results show that the mass transfer flux decreases almost linearly with an increase in the membrane contactor thickness. However, results reported by Ali and Schwerdt [7,15] reveal that the membrane mass transfer resistance increases exponentially with an increase in the membrane thickness. Mass transfer flux decreases more rapidly initially with an increase in membrane thickness while at higher values of thickness the change in mass transfer flux is less prominent. Ali and Schwerdt [7,15] suggested that the active membrane layer thickness should be up to 60 μm so that optimum mechanical stability and low resistance to water vapour flux is achieved. They also reported that an additional highly porous support layer on the vapour side of the membrane can significantly increase mechanical stability without degrading the vapour flux since the mass flux is not disturbed if the supporting layer is placed on the vapour side.

2.4. Membrane tortuosity

Tortuosity represents the average length of the pore as compared with membrane thickness. Membranes with pores which are perpendicular to the membrane surface are more favourable, as in such cases the tortuosity of the membrane pore is considered equal to one. Martınez and Rodrıguez-Maroto [18] reported that generally the tortuosity is in the range of 1.5–2.5 as typically membranes have a more meandering pore pathway. The tortuosity of a membrane is inversely related to its porosity. Different empirical correlations have been reported to calculate the tortuosity value from the membrane porosity. Iversen et al. [14] compared the empirical correlations and the experimental values of tortuosity. They concluded that the empirical correlation developed by Mackie and Meares [19] best describes the tortuosity of a membrane that is spongier, similar to the interstices between closed packed spheres, and is given as:

$$\tau = \frac{(2-\varepsilon)^2}{\varepsilon} \tag{2}$$

where τ is the tortuosity and ε the porosity of the membrane.

Iversen et al. [14] reported that the fractal theories of random walks can be used to predict the tortuosity of membrane material with random clusters, similar to loose packed spheres, and is given as:

$$\tau = \frac{1}{\varepsilon} \tag{3}$$

2.5. Wettability and liquid entry pressure

The non-wetting characteristic of membrane contactors is also important as the aqueous solution can enter the larger pores of the membrane by breaking the surface tension at the interface between the aqueous solution and the water vapour at the entrance to the membrane pores, thus affecting the mass transfer. Alkhudhiri et al. [20] reported that the maximum pore size which

would prevent wetting should be in the range 0.1–0.6 μm. LEP (liquid entry pressure) is the minimum hydrostatic pressure that must be applied around the membrane so that the aqueous solution does not overcome the hydrophobic forces and penetrate into the membrane pores. Alkhudhiri et al. [20] reported that the increase in feed concentration and the presence of organic solutes can reduce the LEP. They reported that LEP mainly depends on the maximum pore size and the hydrophobicity of the membrane. Gabino et al. [21] reported the Laplace (Cantor) equation for relating the maximum pore size and the liquid entry pressure which is given as,

$$\Delta P = \frac{4 \times B \times \sigma \times \cos\theta}{d_{p,(\max)}} \tag{4}$$

where B is the pore geometric factor which is 1 for cylindrical pores, σ is the solution surface tension in N/m, θ is the contact angle and $d_{p,(\max)}$ is the maximum pore diameter in meters. Thus for a high value of LEP, a membrane should have a high contact angle, small pore size and a higher value of surface tension for the solution. Ali and Schwerdt [7] mentioned the importance of liquid entry pressure and suggested that a membrane should have high LEP and the pore size should be in a range of 0.45–1.0 μm to avoid wettability of the membrane pores by the aqueous solution. Zidu [22] reported that the polymeric membrane material that is used in the membrane based components should have a surface energy of at least 10 dyn/cm less than the lowest among the weak absorbent solution surface tension or the refrigerant surface tension.

2.6. Thermal conductivity

Thermal conductivity is the ability of the membrane material to transfer heat energy. The thermal conductivity of membrane contactors made of polymeric material is usually low as compared to metals; however, the large specific heat transfer area provided by membrane contactors can overcome the heat transfer resistance of the membrane material. The thermal conductivity measurement of a membrane contactor depends on both the thermal conductivity of the membrane material and the gas inside the voids of the membrane contactor. The thermal conductivity of PTFE can be estimated using the correlation given by Sperati et al. [23].

$$k_s = (4.86 \times 10^{-4} \times T) + 0.253 \tag{5}$$

where T is the temperature in °C and k_s is the thermal conductivity in W/m-K.

If the gas inside the membrane voids is air or water vapour then the thermal conductivity of gas can be estimated by the correlation of Jönsson et al. [24].

$$k_g = \left(1.5 \times 10^{-3}\right) \times \sqrt{T} \tag{6}$$

where T is the absolute temperature in Kelvin and k_g is the thermal conductivity in W/m-K.

The correlation can be used either for air or water vapours as both have a thermal conductivity of the same order at a temperature of around 40 °C.

The thermal conductivity of the membrane is estimated as a volume average of both the conductivities k_s and k_g, as given by Martınez and Rodrıguez-Maroto [18].

$$k_{\text{mem}} = \varepsilon \times k_g + (1-\varepsilon) \times k_s \tag{7}$$

2.7. Hydraulic permeability

Hydraulic permeability is the ability of a membrane to transfer a fluid across the membrane. It is the inverse of resistance to flow across the membrane. Ideally, the membrane should have minimum resistance to the refrigerant mass transfer which depends on the size and tortuosity of the membrane pores and on the porosity and thickness of the membrane. Martinez et al. [25] modelled and evaluated the water vapour permeability in hydrophobic membranes. They used three commercial hydrophobic membranes TF1000, TF450 and TF200 with pore sizes of 1.00, 0.45 and 0.20 μm, respectively and a porosity of 0.8. The authors concluded that for applications in which no viscous flux is present, the Knudsen and molecular diffusion resistances are important to be analyzed, while in applications including diffusive and viscous transport mechanisms, the contribution of both mechanisms is important enough to be analyzed. However, at low water vapour pressures the viscous contribution is low for the membranes with smaller pores. They also concluded from their study that the membranes have narrow pore size distributions and the values of the average pore sizes are slightly different from those given by the manufacturer. They mentioned that the capillary diameter of the membrane provided by the manufacturer is not sufficient to perform the transport model calculation. Albrecht et al. [26] determined the water vapour permeability of different structured hollow fiber membranes with ultrafiltration separation profiles. They concluded that membranes with ultrafiltration separation profiles are beneficial alternatives for the preparation of coated membranes and are suitable for the preparation of effective membrane contactors. Ali and Schwerdt [7] reported that to obtain a higher water vapour flux, the membrane pore sizes should range from 0.45 to 1.0 μm, and have a porosity of up to 0.8 for high permeability to water vapour.

2.8. Capillary condensation

One of the desired characteristics of the membrane contactor is for it to prevent capillary condensation of refrigerant vapour inside the membrane pores which can result in blockage of the pore. Rautenbach and Albrecht [27] reported that as well as the membrane active layer surface, the inner surface of the capillary is also involved in the desorption/evaporation process. They pointed out the significance of the capillary condensation and reported that the membrane effectiveness can decrease if vapours condense inside the membrane pores. By using the Kelvin equation, they proposed an equation which can be used to calculate the critical water vapour pressure at which condensation can occur in large pores, and it is given as:

$$p_i^c = p_i^0 \times \exp\left(-\frac{4 \times \sigma_P \times V_i}{d_p \times R \times T}\right) \tag{8}$$

where p_i^c is the critical water vapour pressure in mbar, p_i^0 is the equilibrium state pressure in mbar, σ_P is the surface tension of the permeate in N/m, V_i is the molar volume in cm^3/mol, d_p is the pore size (diameter) in m, R is the universal gas constant which is 8.314 J/mol-K and T is the temperature in K.

Ali and Schwerdt [7] recommended that the membrane pore size should be as small as possible to avoid capillary condensation of water vapours. They recommended a pore size of 0.45 μm to limit the capillary condensation in the membrane based absorber of an absorption refrigeration system.

2.9. Fouling of membrane contactors

Membrane materials are non-corrosive and are compatible with most of the materials and working fluids. Fouling of the membrane contactor material is less prominent compared with that of metallic contactors. However, membrane contactors are prone to pore clogging with inorganic salt and biological fouling. Biological fouling is mainly caused by bacteria and algae. Lawson and Lloyd [28] reported that biological fouling can be avoided by

adding certain appropriate chemicals to the solution or by UV treatment. They also pointed out that fouling is less significant in membranes with relatively larger pore sizes such as the membranes used in distillation processes. Membrane mass transfer resistance increases due to the fouling phenomenon. In membrane contactors, the mass transfer flux may decrease if the accumulation of crystallized inorganic salt or deposition of any other particulate material occurs at the membrane surface and in the pores of the membranes. However, membrane contactors have the advantage that they can be cleaned easily and thus the reduction of mass transfer flux across the membrane due to membrane fouling can be recovered. The decrease in mass transfer flux across the membrane with time, usually termed as flux decay and which occurs due to membrane fouling, can be classified into reversible and irreversible fouling. Flux decay due to reversible fouling in porous membranes can be recovered by backflushing the membrane contactors, while in the case of irreversible fouling, the membrane contactor either has to be replaced or cleaned with chemical reagents. Riffat et al. [3] investigated two membrane modules, sheet polymer membranes and tubular silicon membranes for use in the pervaporation absorption refrigerator. They observed that the permeate flux of the silicon membrane module decreased with time due to pores being blocked by the salt. However, they were able to restore the original permeate flux by cleaning the membrane module with fresh water. Pre-treatment of the membrane can also be done to control the fouling. Alklaibi and Lior [29] pointed out the importance of pre-treatment and concluded from their investigations that the permeate flux can be increased by 25% with the pre-treatment process. Shirazi et al. [30] reported that membrane fouling is mainly dependent on the module configuration, solution characteristics and hydrodynamic conditions. They pointed out that the high concentration of inorganic salts in the solution can lead to fouling of the membrane contactor. They reported that the scale formation on the membrane surface is mainly because of the crystallization of the solution and the particulate fouling, both of which occur due to the decrease of salt solubility or the existence of particulates in the solution. In crystallization, precipitation of ions occurs at the surface of membrane, while in particulate fouling, particulate matter from the bulk solution deposits on the membrane surface as a result of convective transportation. For porous membranes, if the particulate matters are smaller than the membrane pore size then pore plugging can also occur in addition to the formation of cake on the membrane surface. Gryta [31] reported that partial wetting of the membrane pores can result in scale formation on the membrane surface, as the adjacent pores are being filled with the feed solution. The author pointed out that an additional thermal resistance is created by the deposits of inorganic salts and particulates on the membrane surface. Controlled hydrodynamic and thermal conditions can also limit the fouling phenomenon. Gryta [32] reported that fouling can be minimized by lowering the feed temperature and increasing the feed flow rate.

3. Working fluid mixtures

Ammonia/water and water/lithium bromide are the most commonly used working fluid pairs analysed both analytically and experimentally to investigate the performance of membrane based components of absorption refrigeration systems. One of the key advantages of these working fluid pairs is that the thermophysical properties are well known and established. However, other working fluids such as ammonia/(lithium nitate + water), water-multicomponent salt mixtures and ionic liquid based absorbent solutions can also be effectively utilized in membrane based absorption refrigeration systems. For those absorption refrigeration systems utilizing membrane contactors, the properties and requirements of the absorbent/refrigerant combination should be compatible with the membrane contactor characteristics and materials. For instance, a hydrophobic membrane material should be used when the absorbent solution contains water as a mixture component so that the liquid solution molecules do not pass through the membrane pores in case of non selective membrane contactors. Water can be employed in the absorbent solution either as a refrigerant or an absorbent and can be used as an additional component to enhance the transport properties of a binary working fluid. For selective microporous membrane contactors, the working fluid pair should be carefully selected in accordance with the membrane properties so that refrigerant molecules observe less transport resistance than the absorbent molecules and hence only the refrigerant molecules pass through the pore. Griesheim and Rodenbach [33] reported that for a dissolution diffusion membrane, the refrigerant should have the characteristic properties of dissolving in the membrane material and diffusing through the membrane, whereas the absorbent should be insoluble in the membrane material. However, for a microporous membrane, a working fluid pair should be selected such that it does not cause wetting of the microporous membrane. If the driving force across the membrane contactor is the difference in vapour pressure, then the working fluid pair should be selected such that the vapour pressure of the absorbent is much lower than the vapour pressure of the refrigerant. Griesheim and Rodenbach [33] reported that in an absorption refrigeration machine utilizing semi-permeable membrane, the vapour pressure of the sorption medium should be a factor of more than 10,000 lower than the refrigerant vapour pressure. They suggested that ionic liquids could be used as an absorbent as they have a vapour pressure of almost 0.

Ammonia/water working fluid pair is used in the industrial and commercial applications where the cooling temperature requirement is in the range of $-40\ ^{\circ}C$ to $+5\ ^{\circ}C$. NH_3/H_2O based absorption refrigeration systems do not have crystallization problems and the system normally operates at a higher pressure (above atmospheric pressure), hence no vacuum is required. As the working fluid pair contains water as an absorbent, therefore a non-selective membrane contactor with hydrophobic surface can be used in the membrane based components. Despite the high thermal stability of the NH_3/H_2O working pair, the high latent heat of vaporization of NH_3 and the feasibility of using NH_3 as refrigerant for low temperature cooling applications there is still a drawback in that both NH_3 and water are volatile, and thus a rectifier is required to strip away water that normally evaporates with NH_3. The rectification process has a negative effect on the cycle performance and also increases the cost of the absorption refrigeration system. Other disadvantages include the toxicity and corrosive action to copper and copper alloy. To overcome these problems, Oronel et al. [34] investigated absorption refrigeration systems that use $NH_3/LiNO_3$ and $NH_3/(LiNO_3+H_2O)$ as working fluid mixtures. They suggested that $NH_3/LiNO_3$ would be a good alternative to the ammonia based conventional working fluid pair. $NH_3/LiNO_3$ working fluid pair has an advantage that a rectification process is not needed and it can be used at a lower temperature in the desorber. However, the viscosity of $NH_3/LiNO_3$ is very high and can significantly reduce the absorber performance and consequently the performance of the whole absorption refrigeration system. For membrane contactor based components, the compatibility of $NH_3/LiNO_3$ with the membrane contactor has to be investigated. As $NH_3/LiNO_3$ working fluid pair does not contain water either as a refrigerant or as an absorbent, the hydrophobic surface of the membrane may not be useful in restricting the mass transfer of the solution across the membrane. The high viscosity of the binary working fluid can be overcome by adding water to the binary mixture as reported by Oronel et al. [34]. Thus, the addition of water to the $NH_3/LiNO_3$ solution not only decreases the viscosity

of the mixture but also makes it possible to utilize microporous non-selective hydrophobic membranes.

Water/lithium bromide working fluid pair is used in those absorption refrigeration applications where the cooling temperature requirement is above 7 °C. H_2O/LiBr based absorption refrigeration systems operate under vacuum conditions. The use of H_2O/LiBr for absorption refrigeration systems offers outstanding features such as the non-volatility of LiBr absorbent (the need for a rectifier is eliminated) and high heat of vaporization of water (refrigerant). However, using water as a refrigerant eliminates the applications for which low cooling temperature is required and the system must be operated under vacuum conditions. H_2O/LiBr based absorption refrigeration systems also suffer from corrosion problems. At high cooling-water temperatures and high concentrations the solution is prone to crystallization. The addition of other salts to the conventional working fluid pair can improve the solubility of the solution. Bourouis et al. [35,36] investigated the use of a multi-component salt solution ($LiBr+LiI+LiNO_3+LiCl$) as an absorbent with water as a refrigerant. They reported that the multi-component salt solution has higher solubility and is less corrosive. The safety margin for crystallization of the strong solution leaving the solution heat exchanger is much higher. Mesones [37] performed experimental and theoretical study on the solubility of new absorbents in natural refrigerants. He reported that the solubility of the multi-component salt can be further improved if the mixture of only three components ($LiBr+LiI+LiNO_3$) is used as an absorbent with water as a refrigerant. As water is used as refrigerant, microporous non-selective hydrophobic membranes can be employed in the membrane based components to achieve efficient performance.

In recent years, intensive research work has been carried out regarding the use of ionic liquids as an absorbent in absorption refrigeration cycles. Advantages of ionic liquids as an absorbent are the low volatility, low melting point, metal-compatibility, high thermal stability and that they are environment friendly and not prone to crystallization problem [38–40]. Ionic liquids have an almost zero vapour pressure, so can be considered a better choice for membrane based absorbers and desorbers. The issue of the high viscosity of ionic liquids can be overcome by adding a small fraction of a ternary component such as water to the ionic liquid based mixtures. A number of refrigerants in combination with ionic liquids have been recommended for the use in absorption refrigeration systems. Among these, carbon dioxide, water and ammonia are the most prominent refrigerants. Water as a refrigerant can be a better choice for absorption refrigeration systems employing hydrophobic microporous membrane contactors in the membrane based components. Yokozeki and Shiflett [41–43] analytically investigated a number of ionic liquids as absorbents with ammonia and water as refrigerants in absorption refrigeration systems. They achieved favourable results with NH_3/[DMEA][Ac] (ammonia/N,N-dimethylethanolammonium acetate) and H_2O/[emim][$(CH_3)_2PO_4$] (water/1-ethyl-3-methylimidazolium dimethylphosphate) as working fluid pairs in a single-stage absorption refrigeration system. Martin and Bermejo [44] performed thermodynamic analysis of absorption refrigeration cycles to investigate the application of ionic liquids as absorbents with supercritical carbon dioxide as a refrigerant. They recommended CO_2/[bmpyrr][Tf_2N] (carbon dioxide/1-butyl-1-methyl-pyrrolidinium) as a favourable working fluid mixture for absorption refrigeration systems. Kim et al. [45] numerically investigated the feasibility of several refrigerant/ionic liquid mixtures and recommended H_2O/[emim][BF_4] (water/1-ethyl-3-methylimidazolium tetrafluoroborate) as a promising working fluid mixture in absorption refrigeration systems for electronic cooling. Absorption refrigeration systems employing ionic liquid as an absorbent and water as a refrigerant could be a better option for membrane based components employing hydrophobic membranes. NH_3 or CO_2 can also be used as a refrigerant with an ionic liquid as an absorbent, however, it is important to select an appropriate membrane contactor with suitable surface properties to limit the solution from crossing the membrane pores. The literature reviewed in this study regarding the use of ionic liquids as an absorbent shows that ionic liquids based absorption refrigeration systems have high solution circulation ratio and thus further investigations are needed for the feasibility of such systems.

Operating conditions and the crystallization behavior of working fluid mixtures discussed in this section are summarized in Table 2. It can be seen that inorganic salt based absorbent solutions exhibit crystallization behavior however ionic liquid based absorbent solutions are not prone to crystallization phenomenon in the working range of absorption refrigeration cycles, as many of the ionic liquids have melting points below the lowest solution temperature in the absorption systems [38–40]. Also it can be seen that absorption refrigeration cycles using ammonia as a refrigerant operate at above atmospheric pressure whereas absorption refrigeration cycles employing water as a refrigerant operate under vacuum pressure.

4. Membrane modules

Different kinds of membrane modules are being used in the process industry for separation processes and distillation applications. Among these membrane modules, the hollow fiber membrane module, spiral membrane module, plate-and-frame/flat sheet membrane module, tubular membrane module and capillary membrane module are the most widely used. However, hollow fiber membrane module and plate-and-frame/flat sheet membrane modules are the types mostly investigated as membrane based components in the absorption refrigeration systems. In the open literature, the plate-and-frame module is generally selected when the aqueous solution of H_2O/LiBr is used as a working fluid mixture in absorption refrigeration systems whereas hollow fibre module is usually selected for the ammonia/water based absorption refrigeration systems. Due to the parallel plates/flat sheets in the plate-and-frame membrane module the pressure drop is small, it is therefore considered as a better option for the water/lithium bromide based

Table 2
Operating conditions and crystallization limit of the working fluid mixtures reported in the investigations reviewed in this work.

Working fluid mixture	Crystallization limit	Operating pressure	Cooling temperature requirment
NH_3/H_2O	No	Above atmospheric pressure	−40 °C to +5 °C
NH_3/ionic liquid [38–40]	No	Above atmospheric pressure	−40 °C to +5 °C
$NH_3/LiNO_3$ [37,46]	Above 0.72 mass fraction of $LiNO_3$ at 50 °C	Above atmospheric pressure	−40 °C to +5 °C
$NH_3/(LiNO_3+H_2O)$	Crystalization risk is lower than $NH_3/LiNO_3$ for same absorbent composition at 50 °C	Above atmospheric pressure	−40 °C to +5 °C
H_2O/LiBr [47]	Above 0.65 mass fraction of LiBr at 50 °C	Under vacuum condition	Above 7 °C
$H_2O/(LiBr+LiI+LiNO_3+LiCl)$ [48]	Above 0.68 mass fraction of $(LiBr+LiI+LiNO_3+LiCl)$ at 50 °C	Under vacuum condition	Above 7 °C
$H_2O/(LiBr+LiI+LiNO_3)$ [37]	Above 0.69 mass fraction of $(LiBr+LiI+LiNO_3)$ at 36.65 °C	Under vacuum condition	Above 7 °C
H_2O/ionic liquid [38–40]	No	Under vacuum condition	Above 7 °C

absorption refrigeration systems. Nevertheless, the hollow fibre module allows more efficient mass transfer due to external transverse flow and is considered an appropriate choice for the ammonia/water based absorption refrigeration systems. It is also important to select a membrane with adequate properties which uses the mass transfer potential more efficiently for such modules. A brief illustration of these membrane modules is described and discussed in the following sub-sections.

4.1. Plate-and-frame membrane module

The plate-and-frame membrane module is currently being widely investigated as a heat and mass transfer device for use in the absorption refrigeration systems. Thorud et al. [5], Isfahani et al. [8,9] and Bigham et al. [12] used the concept of the plate-and-frame heat exchanger and manufactured a laboratory scale desorber to investigate the performance of a plate-and-frame membrane module. Ali [49,50], Ali and Schwerdt [7,15], Yu et al. [16], Isfahani et al. [8], Isfahani and Moghaddam [10] and Bigham et al. [11] used the plate-and-frame membrane module for investigating the application of membrane contactors in the absorber. Due to the ease of use and availability of membrane in flat sheets, the plate-and-frame membrane module is widely used in laboratories to perform experimental analyses. These modules are easy to clean and replace. However, the flat sheets of membrane in the plate-and-frame membrane module have poor mechanical strength and thus a support is usually required.

The driving force for the vapour transfer into the aqueous solution in a H_2O/LiBr absorber is the difference in water vapour partial pressure. In the conventional falling film absorber, the water vapour pressure difference is usually small. To get a higher mass transfer rate across the membrane contactor there should be minimum pressure drop in the membrane configuration. Baker [51] reported that the plate-and-frame membrane module offers minimum pressure drop among the different membrane configurations. Therefore, to design an efficient and compact absorber with H_2O/LiBr as a working fluid mixture, the plate-and-frame absorber with a non-selective hydrophobic microporous membrane at aqueous solution–water vapour interface is a better alternative. The plate-and-frame membrane module has the potential to enhance the mass transfer flux as a result of narrow confined flow channels formed by the membrane contactor.

The structural unit of a plate-and-frame absorber with a membrane contactor at the solution–vapour interface is shown in Fig. 2(a). The configuration of the plate-and-frame membrane module is set so that the lattice cell consists of a metallic plate for heat transfer and membrane sheets for both the heat and mass transfer. The membrane contactors are placed at the aqueous solution and water vapour interface in the form of parallel sheets, while the metallic plates are placed along the solution and coolant interface. The membrane sheets and the metallic plates are arranged in such a manner as to create individual flow channels for solution, coolant and refrigerant. Each refrigerant channel serves two absorbent solution channels at each side as shown in Fig. 2(b). Similarly the coolant channels also serve two aqueous solution channels. The first and last units of the module have half width coolant channels. The coolant flows along the metallic plate to dissipate the heat of absorption from the solution. The refrigerant and the absorbent solution are brought into contact with each other using the microporous membrane contactor. The refrigerant enters the membrane pores and is absorbed into the solution on the other side of the membrane sheet. If water is present in the working fluid mixture either as a refrigerant, an absorbent or as a third component, then a hydrophobic membrane contactor can be utilized so that the aqueous solution does not penetrate the membrane pores as a result of the hydrophobic

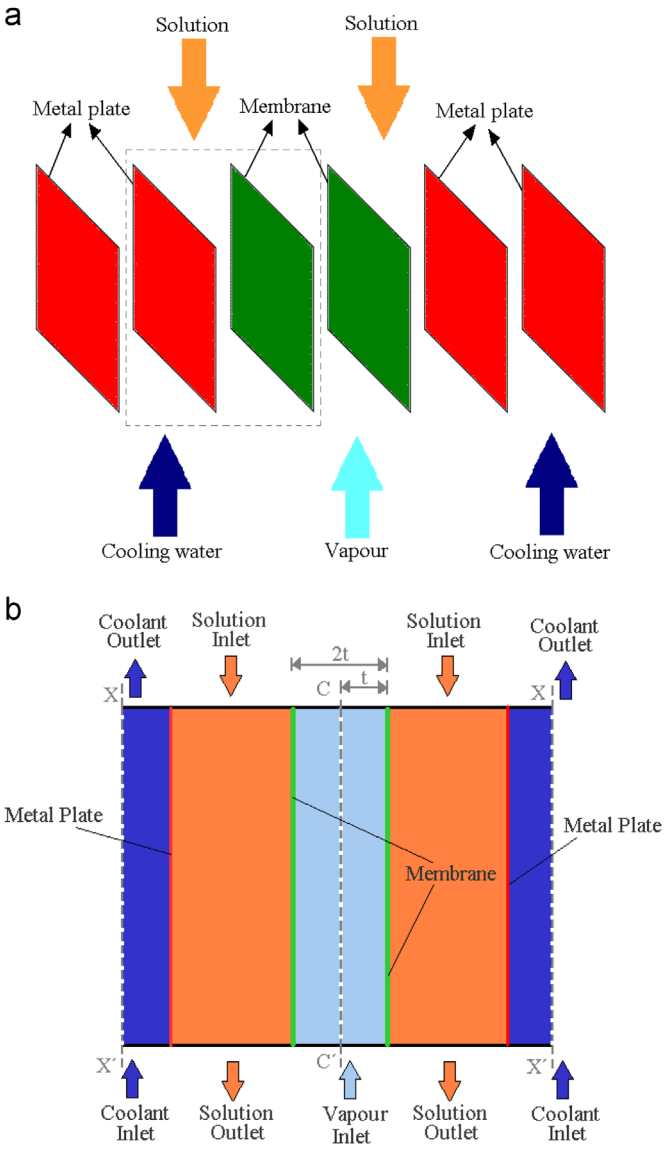

Fig. 2. Plate-and-frame membrane module.

nature of the membrane material and that only refrigerant passes through the membrane. The thin channel of refrigerant has no exit so all the refrigerant has to be absorbed by the aqueous solution through the membrane contactor. As the refrigerant vapour pressure is higher than the partial pressure of the refrigerant vapour inside the solution, the refrigerant is absorbed at the liquid–vapour interface and diffuses into the solution film. The flow configuration in this module can be co-current flow or counter current flow. However, counter current flow direction of the coolant and absorbent is more advantageous, while the absorbent solution and refrigerant flow can be either counter current or co-current.

Geometric dimensions and parameters of the plate-and-frame membrane modules reviewed in this work are listed in Table 3.

4.2. Hollow fiber membrane module

Hollow fiber membrane modules have been widely investigated for heat and mass transfer enhancement. The vast interfacial area provided by the polymeric hollow fiber membranes significantly improves heat and mass transfer processes. However, the mechanical strength of the polymeric membrane limits the

Table 3
Geometric dimensions and parameters of the plate-and-frame membrane modules reported in the investigations reviewed in this work.

Reference	Length (mm)	Width (mm)	Depth (mm)	Solution channel thickness (mm)	Wall thickness (mm)	No. of channels
Thorud et al. [5]	58	29	NA	0.170–0.745	NA	NA
Isfahani et al. [8,10]	38	203	1	0.160	NA	NA
Yu et al. [16]	20	NA	NA	0.05–0.20	NA	NA
Ali [49]	400	388	300	2.0	1	50
Kim et al. [62]	100	100.3	0.3	0.5	0.3	125

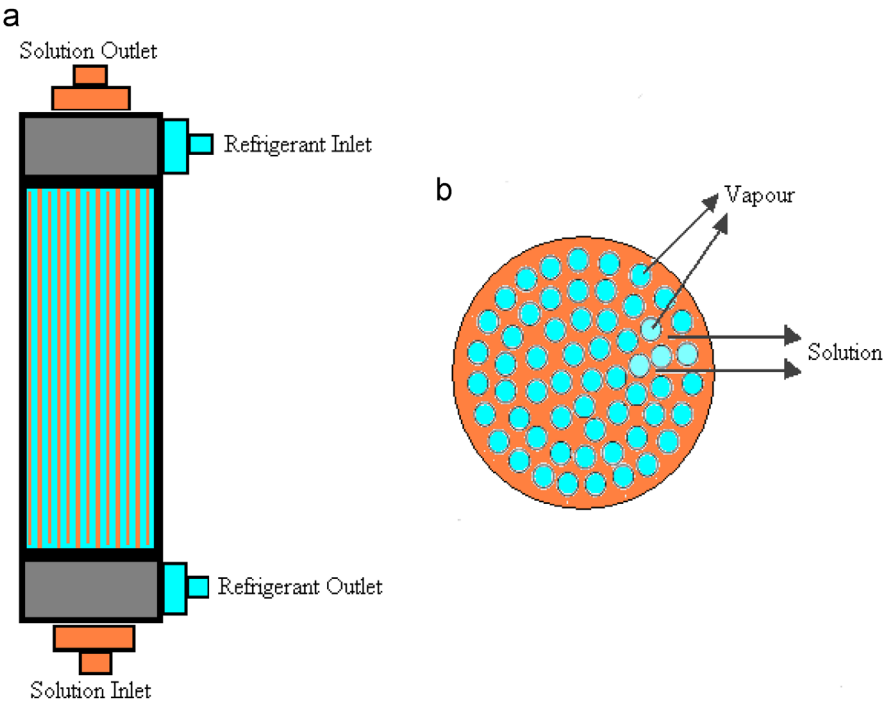

Fig. 3. Hollow fiber membrane module [6].

application of polymeric hollow fiber membranes at elevated temperatures and high pressure. Zarkadas and Sirkar [52] proposed a polymeric hollow-fiber membrane heat exchanger for low temperature (up to 150–200 °C) applications. Their investigation showed that the large specific interfacial area makes polymeric hollow fiber heat exchangers more efficient than metal heat exchangers for lower heat source temperature applications. Hollow fiber membrane contactors made of non-selective, microporous membranes have been widely accepted as effective gas–liquid or liquid–liquid devices because of the independent gas and liquid velocities which prevent flooding, loading and turn down ratio problems from two-phase flows. Experimental and analytical analyses were performed by Schaal et al. [4] and Chen et al. [53], respectively, in order to investigate the performance of a hollow fiber membrane module as an absorber unit in the absorption refrigeration system. Wang et al. [6,54] used the concept of vacuum distillation to separate the refrigerant from feed solution and investigated the use of the hollow fiber module as a desorber in the absorption refrigeration system. Wang et al. [55,56] and Wang et al. [57] investigated and proposed the hollow fiber module as an alternative to the solution heat exchanger of the H_2O/LiBr absorption refrigeration system. Hollow fiber membrane modules used in the absorption refrigeration systems can be classified into two types; an ordinary hollow fiber membrane module which is usually utilized as a desorber and a hybrid hollow fiber membrane module which is utilized as an absorber.

The ordinary hollow fiber membrane module consists of hundreds of microporous hydrophobic membrane fibers/tubes, assembled and made into a shell-and-tube module as shown in Fig. 3. The microporous hydrophobic membrane fibers in the module allow both heat and mass transfer between the absorbent solution and the refrigerant vapours. Hollow fiber membrane module can be specifically used as a desorber or as a solution heat exchanger in the absorption refrigeration systems. The feed solution, which is preheated before entering the module, flows inside the microporous hollow fibers of the module. In the case of vacuum membrane separation processes, vacuum pressure is kept inside the shell for efficient performance of the module. The refrigerant in the feed solution vaporizes and passes through the pores of the membrane and is collected inside the shell and then condensed in the condenser under vacuum conditions.

The hybrid hollow fiber membrane module consists of hundreds of both microporous hydrophobic membranes fibers and non-porous membrane fibers, assembled and made into a shell-and-tube module. The hybrid hollow fiber membrane module is used as an absorber in the absorption refrigeration systems. The refrigerant–absorbent solution flows into the shell side of the hollow fiber module. The refrigerant vapours to be absorbed flow into the microporous hollow fibers while the cooling fluid flows into the non-porous hollow fibers of the module. The non-porous membrane fibers for the cooling fluid are arranged in concentric order at the outer periphery of the shell, while the porous

membrane fibers are arranged concentrically in the central portion of the shell. The hollow fiber membrane module contains a central baffle that deflects the solution flow on the shell side in the module but not the flows on the lumen side of the fibers. The absorbent solution enters in the shell through the center tube in the upstream half of the module, flows through the gap between the baffle and the module housing and then exits from the shell through the center tube in the downstream half of the module. The solution hence forms cross-flow to the fibers in both upstream half and downstream half of the module. The configuration of a hybrid hollow fiber membrane module is shown in Fig. 4. It is reported that the heat transfer process can be enhanced if the cooling fluid and the absorbent solution flow in the counter-current direction, however, the vapour and the absorbent solution flow direction has no significant effect on the heat and mass transfer and so can be co-current or counter-current.

Geometric dimensions and parameters of the hollow fiber membrane module reviewed in this work are listed in Table 4.

5. Membrane contactors in components of absorption refrigeration systems

Analytical and experimental investigations are being carried out on the use of membrane contactors in the absorber, desorber and solution heat exchanger of absorption refrigeration systems. The utilization of microporous membrane contactors in these components can provide a high specific surface area and therefore higher volumetric mass transfer rates can be achieved compared to conventional absorbers and desorbers. Schaal et al. [4] reported that membrane contactors can provide up to 30,000 m^2/m^3 specific area. Due to the high specific interfacial area provided by the membrane contactor, it is possible to manufacture compact components for use in small cooling capacity absorption chillers. In this section, the use of membrane contactors in the components of absorption refrigeration systems is reviewed.

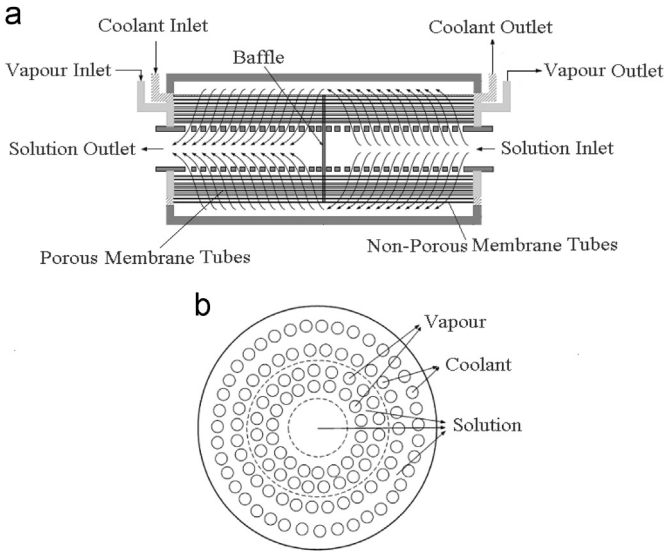

Fig. 4. Hybrid hollow fiber membrane module [53].

5.1. Absorber

Absorber is one of the major components in absorption chillers and has a direct effect on the size of the absorption refrigeration system. Introducing polymeric hydrophobic microporous membranes in the absorber design could provide one of the alternatives for achieving highly compact absorbers since microporous membrane contactors can provide a high specific surface area. The absorption rate of the conventional absorbers normally depends upon the working fluid mixture, the corrugated or smooth surface, absorber configuration, operating conditions etc. Different absorber configurations have been investigated and adopted to enhance the absorption rate. In this section, the membrane based absorbers investigated in the literature are discussed and evaluated. As discussed earlier, the membrane based absorbers investigated in the literature are broadly divided into two categories, namely plate-and-frame membrane absorber and hollow fiber membrane absorber.

Chen et al. [53] performed numerical simulations to study and evaluate the performance of an innovative hybrid hollow fiber membrane absorber. The proposed hybrid hollow fiber membrane absorber was designed for an ammonia/water absorption cycle and was made up of both microporous and nonporous fibers for refrigerant and coolant flows, respectively. They reported that, for the same absorption rate, the volume of hollow fiber membrane absorber was only 31% of that of a plate heat exchanger falling film absorber, while the mass transfer interfacial area was 4.3 times of that of plate heat exchanger falling film absorber. From their results it was observed that the COP of a typical ammonia/water absorption system utilizing hollow fiber membrane absorber could be increased by 14.8% and a 26.7% reduction in the overall system exergy loss could be achieved. The solution flow rate reduction obtained in the analysis was 43% for the same cooling effect. They reported that the solution side mass transfer coefficient is the most dominating factor affecting the absorption process in the hollow fiber membrane absorber.

Schaal et al. [4] investigated experimentally and performed simulation of an absorption refrigeration system with a single hollow fiber microporous membrane module absorber in which ammonia/water was used as a working fluid mixture with integrated cooling. Their results showed a higher mass transfer rate for the membrane absorber compared with the plate absorber. A linear increase in the absorption rate was observed with an increase in the driving force, which is the difference of the ammonia mole fraction at the saturation state and the actual ammonia fraction at the inlet of the membrane module. In addition, increase in the mass transfer flux with an increased driving force was more significant for the membrane absorber than for the plate absorber. Their results also showed that the ammonia mass transfer rate increases with the increase in gas pressure. However, a decrease in the ammonia mass transfer flux was observed with higher ammonia mole fractions in the solution. From the experimental and simulation results, they concluded that

Table 4
Geometric dimensions and parameters of the hollow fiber membrane modules reported in the investigations reviewed in this work.

Reference	Outer diameter (μm)	Inner diameter (μm)	Wall thickness (μm)	Shell Inside diameter (cm)	Effective fiber length (cm)	No. of fibers
Schaal et al. [4]	NA	170	40	2.0–2.2	11	2100
Wang et al. [6]	NA	800	150	4.2	40	300
Chen et al. [53]	300	240	30	5.55	20	5000
Wang et al. [57]	1100	800	150	4.2	80	600

the size of the absorber can be reduced up to 10 times as compared to plate absorbers by utilizing the micro-porous hollow fiber membrane module.

Ali [49] performed an analytical analysis to design a compact plate-and-frame absorber possessing a hydrophobic microporous membrane contactor at the aqueous solution–water vapour interface. The author pointed out that the most important factor affecting the absorption rate was the solution film thickness. His results showed that the aqueous solution channel thickness greatly influences the absorber size compactness. Increasing the solution channel thickness from 1.0 to 2.5 mm while keeping the other parameters constant resulted in an increase in the required net membrane contactor area from 5.2 to 6.53 m^2. In addition a decrease from 238.54 to 139.2 m^2/m^3 is obtained in the ratio of mass transfer area to net volume. In the experimental study performed by Ali and Schwerdt [7], a solution film thickness of 4 mm was used and a differential pressure of nearly three times the available pressure in a typical absorber was applied. However, the absorption rate was approximately half that of the conventional absorbers. In a conventional absorber, the solution thickness flowing over a tube bundle varies from 0.1 to 1.0 mm. Ali [49] observed that reducing the solution film thickness from 2.5 to 1.0 mm can result in a higher absorption rate of about 20%. Thus, the low absorption rate obtained in the Ali and Schwerdt [7] analysis could be due to the higher values of the solution film thickness. Also they did not observe a change in the absorption rate when the vapour pressure potential was increased. They ascribed this behavior to the dominant mass transfer resistance of their membrane. However, recent studies [8,10] suggest that vapour pressure potential has a direct effect on the vapour mass transfer flux across the membrane and that the mass transfer through the solution is the dominant resistance as compared to the membrane mass transfer resistance. Ali and Schwerdt [15] experimentally and analytically analysed the factors that affect the water vapour transfer flux when using a membrane contactor at water/LiBr solution and water vapour interface. They reported that at high solution flow rates, the mass transfer coefficient between the interface boundary layer and the bulk solution is high, as a result of low hydrodynamic boundary layer resistance. They concluded from their experimental results that the water vapour transfer flux through the membrane contactor is improved at higher aqueous lithium bromide solution flow Reynolds numbers for larger pore diameters. Ali [50] analytically performed heat and mass transfer analysis of a plate-and-frame membrane based absorber as a component of a 5 kW single-effect water/lithium bromide absorption refrigeration system. He reported that for the same cooling capacity the required absorber size increased with the increase in the driving hot water temperature. However, a slight decrease in the required absorber area was observed with a decrease in the cooling water inlet temperature. The author suggested the use of plate-and-frame membrane absorbers in places where lower cooling inlet temperature is available.

Yu et al. [16] performed numerical simulation to analyze the influence of different operational and geometric parameters of a membrane based absorber. They reported that the solution film thickness and solution velocity significantly affect the absorption rate. However, in contrast to conventional absorbers, the solution film thickness and velocity can be independently controlled and adjusted to achieve an optimal performance in plate-and-frame membrane absorber. They obtained a 3-fold increase in the absorption rate when the solution film thickness was reduced from 150 μm to 50 μm. In addition, they observed a 50% increase in the average absorption rate when the solution velocity was increased from 0.009 m/s to 0.036 m/s. Also, they investigated the effect of membrane surface roughness on the absorption rate and obtained a 15% increase in the absorption rate when compared to the smooth surface. The authors concluded that the absorption rate in case of a rough membrane surface increases as a result of convective effects induced by the rough surface.

Isfahani et al. [8] experimentally investigated a membrane based absorber for the absorption of water vapour in the aqueous solution of LiBr. Their results showed that the mass transfer flux can be significantly enhanced if the solution flow velocity is increased and the solution film thickness is reduced to an order of 100 μm. They reported that decreasing the solution film thickness resulted in better cooling of the solution–vapour interface so the water vapour pressure in the solution was lowered and a high absorption rate was achieved. Similarly they observed that when the solution temperature was increased then the water vapour pressure in the solution also increased which in turn decreased the absorption rate. A linear increase in the absorption rate with an increase in the vapour pressure was observed. They reported that the absorption rate in the membrane based absorber was 2.5 times higher than that in the falling film absorbers.

Isfahani and Moghaddam [10] experimentally analyzed absorption characteristics of water vapour into a thin LiBr solution constrained by superhydrophobic nanofibrous membrane structures. They reported that the use of a superhydrophobic nanofibrous membrane at the H_2O/LiBr solution and water vapour interface could constrain the solution film thickness and that in this type of configuration the velocity and solution thickness could be independently controlled to achieve higher absorption rates. They studied the effect of water vapour pressure, cooling temperature, solution film thickness and solution mass flow rate on the absorption rate in a membrane based absorber. They achieved an absorption rate of 0.006 $kg/m^2/s$ with a solution film thickness of 100 μm and a velocity of 0.005 m/s. In contrast to Ali and Schwerdt [7], they obtained a linear increase in the absorption rate with increase in the water vapour driving potential across the membrane.

Bigham et al. [11] experimentally and numerically investigated the implementation of micro-scale features on the flow channel surface to induce vortices within the solution film. They observed that the laminar streamlines within the solution film are stretched and folded as a result of the vortices. They reported that the mass transport mode in such configuration could be changed from diffusive to advective mode. In their analysis they used a 500 μm solution film thickness and obtained an increase in the absorption rate by a factor of 2.5 from 0.0016 $kg/m^2/s$ to 0.004 $kg/m^2/s$.

It is evaluated from the literature review that utilizing the microporous hydrophobic membrane in the absorber not only reduces the size of the component but also enhances the mass transfer rate significantly. Both the plate-and-frame membrane absorber and hollow fiber membrane absorber are promising alternatives to the conventional absorbers and can be used with water and ammonia based refrigerants, respectively, in absorption refrigeration systems. Hybrid hollow fiber membrane module can be an interesting replacement of the conventional absorbers as compared to ordinary hollow fiber membrane module as in this type of module non-porous membrane fibers are incorporated within the module for coolant flow to dissipate the heat of absorption from the solution and therefore can enhance the absorption performance of the absorber. In case of the plate-and-frame membrane absorber, it is worth to note that a higher absorption rate can be achieved if the solution film thickness is around 100 μm, therefore, the use of porous membranes to constrain the solution film in narrow micro-channels can significantly enhance the heat and mass transfer performance of the absorber. In addition, constraining the solution film by a hydrophobic membrane contactor can allow design of a compact membrane based absorber utilizing water as a refrigerant under

vacuum conditions. However, it is worth to note that the pressure drop along the solution channel length may increase significantly with the decrease in the solution channel thickness and therefore further analysis is required to select an optimum value of the solution channel thickness with higher absorption rate and lower pressure drop. Also the use of micro-scale features on the flow channels surface can significantly improve the absorption rate by producing vortices within the solution which continuously bring the concentrated solution to the solution vapour interface. However, the ease and economical viability to manufacture a surface with micro-scale features for membrane based absorbers need to be investigated for the commercial use of such plate-and-frame membrane absorber. In addition, the effect of micro-scale features on the pressure drop could be significant which may also affect the performance of the absorber.

5.2. Desorber

Desorber is also one of the major components in absorption refrigeration systems and is used to separate the refrigerant from the absorbent solution. The performance of the desorber has a direct effect on the coefficient of performance (COP) of the system. The conventional desorber is usually heavier and bigger in size and thus limits the use of vapour absorption systems in small scale applications. The temperature of the driving heater in the conventional desorber is usually higher than low grade energy resources such as regenerative energy or waste heat energy. These issues can be resolved by replacing the conventional desorption process with a membrane separation process. Membrane modules are smaller in size and weight than the conventional desorbers because polymeric fibers/membrane sheets replace the heavy metallic tubes/plates. In the membrane distillation process, vapour extraction from aqueous solution is possible at a lower operating temperature than the boiling point of the solution. Due to the temperature difference across the membrane, a pressure difference arises and acts as the driving force for the mass transfer across the membrane pores. At the liquid–vapour interface of the membrane pores refrigerant molecules evaporate at the hot interface, cross through the membrane pores in vapour phase and condense on the cold side.

Mengual et al. [58] reported that the vapour permeation flux mainly relies on the vapour pressure difference between the two sides of the membrane. Qtaishat et al. [59] reported that adequate permeation flux is possible across the membrane without the need for the hot feed to reach boiling point. Heating of the aqueous solution to the boiling point is not needed as long as the temperature difference exists between the two sides of the membrane pores. Consequently, the membrane based desorber can operate at a lower temperature than conventional desorbers where the solution must be heated to boiling point to achieve the separation of the refrigerant from the solution. This means that low grade heat sources can be efficient if membrane based desorbers are used in absorption refrigeration systems.

Research is currently being carried out on the use of microporous membranes in the desorber for the separation of the refrigerant from the refrigerant–absorbent solution. Different membrane separation processes are employed for refrigerant separation in the desorber. Riffat and Su [60,61] proposed a reverse osmosis mechanism to separate the refrigerant from the mixture in the desorber. They replaced the conventional desorber by a centrifuge desorber in which a reverse osmosis membrane was utilized. The centrifuge desorber is a rotary hollow cylinder with a membrane placed around the outside periphery of the cylinder. The centrifuge desorber is rotated at a high angular velocity and as soon as the pressure difference between the two sides of the membrane exceeds the osmotic pressure of the solution, the refrigerant permeates the reverse osmosis membrane. They developed a thermodynamic model to study the osmotic pressure of the absorption solution using its density and vapour pressure. From their analysis they observed that the osmotic pressure increased with an increase in the specific latent heat of evaporation. They pointed out that a high angular speed is required to achieve a high pressure difference in order to separate the refrigerant from the solution using reverse osmosis mechanism. Furthermore, they mentioned that the high rotation speed requirement could give rise to issues related to the mechanical strength of materials and the balance of structures. However, they reported that the angular speed of the centrifuge desorber could be reduced if refrigerants with a lower latent heat of evaporation were used. They concluded that the feasibility of pressure driven absorption systems would also be dependent on the availability of suitable membranes due to the high osmotic pressure involved. Riffat et al. [3] experimentally investigated an absorption refrigeration system in which the pervaporation process replaced the conventional desorption process for vapour extraction. They used aqueous potassium formate solution and two membranes. One was a dense membrane, and the other was a silicon porous membrane. They suggested that the pervaporation membrane material should be compatible with the working fluid mixture. They achieved a permeate flux of above 0.58 kg/m^2-h when they used a mixture of potassium formate and caesium formate and was five times that of the potassium only solution. They observed that the permeate flux decreased with the solution temperature but increased with decreasing concentration. Similarly, a decrease in the permeate flux was obtained when the permeate pressure was increased. However, the decrease in the permeate flux was smaller at high solution temperature because of the high chemical potential of feed side. They achieved higher permeate flux with silicon membrane module when compared to the dense membrane due to the porous structure of the silicon membrane module.

Thorud et al. [5] experimentally tested a constrained thin film desorption scheme to determine the desorption rates of water from an aqueous solution of LiBr through a confining hydrophobic porous membrane made up of Teflon material. The assembly of the module resembled that of a plate-and-frame module in which desorption takes place in a channel created between two parallel plates with one of the walls being both heated and porous. Their experimental investigation focused on the performance of vapour extraction as a function of confined thin film thickness, pressure difference across the membrane and inlet concentration of LiBr solution. In their experiments, a constant inlet mass flow rate of 3.2 g/min was kept up at a pressure of 33.5 kPa and a membrane with surface area of 16.8 cm^2 was used for all cases. The inlet concentration of LiBr solution was varied from 31.6 wt% to 50.2 wt %, and the pressure difference across the membrane was varied from 5.83 kPa to 11.5 kPa along with two channel heights of 170 μm and 745 μm. They achieved a maximum desorption rate of 0.51 g/min at the following conditions: LiBr solution concentration of 32 wt%, differential pressure of 12.0 kPa, and channel height of 170 μm. Evaluation of the results showed that vapour extraction increases with an increase in pressure difference across the membrane, decrease in channel height and lower inlet LiBr solution concentration. The heat transfer coefficient was also studied as a function of the wall superheat temperature. Increase in the channel height required larger superheat values for a fixed desorption rate and thus had a negative influence on the heat transfer coefficient.

Kim et al. [62] analysed an absorption based miniature heat pump system and demonstrated with analytical results the feasibility of such a system for electronic cooling applications.

To miniaturize the system, they integrated the desorber and condenser as a single unit separated by a hydrophobic membrane which acted as a common interface to separate the refrigerant vapour from the absorbent solution. Their design facilitates to reduce the size of the entire heat pump system to a 150 mm × 150 mm × 100 mm envelope. The analytical results showed that a chip temperature of about 30 °C is achievable with heat removal capability of 100 W from the electronic components.

Zidu [22] proposed an absorption refrigeration cycle in which the conventional desorber was replaced with hollow fiber membrane module. The tubes of the membrane module were made up of a microporous hydrophobic membrane material with a pore size in the range of 0.1 to 0.6 μm and a porosity greater than 0.5. The author reported that a higher COP could be achieved with an improved mass transfer rate at a low desorber temperature utilizing a hollow fiber membrane desorber.

Wang et al. [6,54] demonstrated the application of vacuum membrane distillation process in absorption refrigeration systems. They experimentally investigated the desorption rate of water vapours from an aqueous solution of lithium bromide with vacuum membrane distillation process which used a hollow fiber membrane module. In such configuration a hot feed of the absorbent solution flows in the tube side, while the shell side is kept under vacuum pressure either by cooling water or by vacuum pump. They concluded from the test results that the permeation flux of water vapour increases when the feed flux of solution is increased and at high feed temperature in tube side while decreases with an increase in pressure in the shell side. Therefore, an increase in the permeation flux is achievable by decreasing the pressure on the shell side. Also, they concluded that the feed temperature had the maximum influence on the desorption rate, followed by the vacuum pressure on the shell side while the feed flux of solution had the lowest influence on the desorption rate.

Isfahani et al. [8] experimentally investigated a membrane based desorber used for the extraction of water vapour from aqueous solution of LiBr. They achieved a desorption rate of about 0.01 kg/m^2/s which is higher than the reported work of Thorud et al. [5]. They observed that the desorption of water vapour from the aqueous solution of LiBr starts at a temperature of approximately 60 °C and increases slightly with an increase in temperature, however, the increase in the desorption rate is more pronounced at temperatures over 90 °C. This is because at higher solution temperatures, the partial pressure of water vapour in the solution increases and therefore the pressure difference across the membrane increases which improves the desorption rate. In addition, they reported that the effect of vapour pressure on the desorption rate subsides as the solution superheat temperature increases and no significant change for a superheat temperature of about 25 °C was obtained. They observed that at the same operating conditions, the solution pressure had an insignificant effect on the desorption rate through direct diffusion, as the driving force for mass transfer is the vapour pressure difference. However, the solution pressure significantly affects the desorption rate with the boiling process. They also observed that the solution flow rate does not influence the desorption rate in the direct diffusion desorption mode. However, they noticed an increase of about 50% in the desorption rate in boiling mode when the solution flow rate was increased from 0.75 kg/h to 3.25 kg/h.

Isfahani et al. [9] experimentally investigated the influence of wall temperature, solution and vapour pressures and solution mass flow rate on the desorption rate of a membrane-based desorber in which the solution was constrained by a thin microporous membrane. They analyzed two mechanism of desorption based on the diffusion of refrigerant molecules across the membrane. In the first case they analyzed direct diffusion of molecules out of the solution and their subsequent flow through the membrane whereas in the second case they investigated the formation of water vapour bubbles within the solution and their venting through the membrane. They reported that the direct diffusion was the dominant desorption mode at low surface temperature in which the desorption rate was directly related to vapour pressure, solution concentration and surface temperature whereas in case of boiling desorption mechanism the solution flow pressure control the desorption mechanism. In addition, they reported that in the boiling desorption mode, at certain solution mass flow rate, some water vapour bubbles are carried out of the

Table 5
Summary of the operating conditions of membrane based components reported in the investigations reviewed in this work.

Reference	Membrane module	Working fluid	Component	Operating conditions			
				Temperature (°C)	Pressure (kPa)	Absorbent Concentration in solution (kg/kg)	Solution flow rate (kg/s)
Schaal et al. [4]	Hollow fiber	NH_3/H_2O	Absorber	20.0	534.8	0.52 mol/mol	NA
Thorud et al. [5]	Plate-and-frame	H_2O/LiBr	Desorber	Saturation Temperature (T_s)	33.5	0.316–0.502	5.33×10^{-5}
Wang et al. [6]	Hollow fiber	H_2O/LiBr	Desorber	65.0–88.0	5.0–15.0	0.500	40–120 l/h
Isfahani et al. [8]	Plate-and-frame	H_2O/LiBr	Desorber	70.0	23.0	0.500	6.94×10^{-4}
Isfahani et al. [8]	Plate-and-frame	H_2O/LiBr	Absorber	25.0	1.1	0.600	1.67×10^{-4}
Isfahani et al. [9]	Plate-and-frame	H_2O/LiBr	Desorber	50.0–125.0	13.0–30.0	0.550	2.08×10^{-4}–9.03×10^{-4}
Isfahani and Moghaddam [10]	Plate-and-frame	H_2O/LiBr	Absorber	25.0–35.0	0.8–1.8	0.540–0.600	1.67×10^{-4}–5.83×10^{-4}
Bigham et al. [11]	Plate-and-frame	H_2O/LiBr	Absorber	35.5	0.87	0.600	Solution mean velocity 0.05 m/s
Bigham et al. [12]	Plate-and-frame	H_2O/LiBr	Desorber	60.0–103.0	23.0–30.0	0.48–0.53	6.94×10^{-4}
Yu et al. [16]	Plate-and-frame	H_2O/LiBr	Absorber	55.0	0.87	0.550–0.640	Solution mean velocity 0.009–0.036 m/s
Ali [49]	Plate-and-Frame	H_2O/LiBr	Absorber	35.5	0.81	0.578	5.89×10^{-2}
Chen et al. [53]	Hollow Fiber	NH_3/H_2O	Absorber	77.9	480.0	0.733	9.78×10^{-3}
Wang et al. [57]	Hollow fiber	H_2O/LiBr	Solution heat exchanger	HFI=99.8 °C CFI=40 °C	NA	SS=0.550 WS=0.500	4.26×10^{-2}
Kim et al. [62]	Flat sheet	H_2O/LiBr	Desorber	90.0	12.34	0.403	2.96×10^{-4}

desorber through the solution micro-channels rather than passing through the membrane.

Bigham et al. [12] experimentally and numerically investigated the implementation of micro-scale features on the flow channel surface to induce vortices within the solution film to enhance the desorption rate. They observed that the laminar streamlines within the solution film were stretched and folded as a result of the vortices and therefore it was possible to limit the concentration boundary layer growth which in turn had a desirable effect on the desorption mechanism. They achieved an average desorption rate of 0.0068 kg/m^2/s which was 1.7 times more than the base case without surface features at the same surface temperature.

From the literature review on membrane based desorbers it is evident that the desorption rate can be enhanced by direct diffusion at low desorber temperatures. Thus, the absorption refrigeration systems utilizing membrane contactors can operate at lower desorber temperatures. In addition, the desorber size can also be reduced using the vast interfacial area provided by the membrane contactors. It is evaluated from this literature review that both plate-and-frame membrane desorber and hollow fiber membrane desorber are promising alternatives to the conventional desorbers and can be used with water and ammonia based refrigerants respectively in absorption refrigeration systems. Solution flow rate, temperature and solution film thickness are crucial parameters for the plat-and-frame desorber and a nominal value should be selected to achieve high desorption rate. Centrifuge desorber in which reverse osmosis mechanism is used to separate the refrigerant from the absorbent does not seem practically feasible as a higher rotation speed is required which need components with higher mechanical strength. It can be concluded that a lower desorption rate is obtained when a pervaporation membrane is used for the desorption process because of the high selectivity of the pervaporation membranes however it is suggested to select a suitable membrane with an appropriate working fluid mixture in order to effectively utilize the pervaporation process for the refrigerant separation from the solution.

5.3. *Solution heat exchanger*

Solution heat exchangers were investigated by researchers with the aim of improving the performance of the system. Shell and tube configurations are usually adopted for the solution heat exchanger in conventional absorption refrigeration systems. Wang et al. [55,56] and Wang et al. [57] proposed and analysed a hollow fiber membrane heat exchanger for water/LiBr absorption refrigeration systems. The shell side of the module contains hundreds of membrane tubes through which the hot feed solution from the desorber flows, while the cold feed solution from the absorber is passed to the desorber through the shell side. Wang et al. [57] reported that the use of hollow fiber membrane modules instead of conventional solution heat exchanger could not only enhance heat transfer as a result of the large heat transfer interfacial area provided by the small membrane tubes but that the mass transfer of the refrigerant vapour could also contribute about one third of the total heat duty. The water vapour mass transfer in the membrane based solution heat exchanger also simultaneously increases the concentration of refrigerant in the solution rich in refrigerant and further decreases the concentration of refrigerant in the solution weak in refrigerant, which helps to minimize the solution circulation ratio. They reported that the flow resistance increases in the membrane heat exchanger which may cause the solution pump to work harder than in a conventional heat exchanger, although this could be compensated by reducing the thermal load in the desorber and absorber.

Table 5 summarises the operating parameters of the components employing membrane contactors in the absorption refrigeration cycles that were reported in the investigations reviewed in this work.

6. Influence of membrane contactors on the cycle configuration

Membrane contactors can be used in different components of absorption refrigeration systems such as the absorber, desorber, solution heat exchanger etc. In this section, absorption refrigeration cycle configurations of the investigations reviewed in the present work are discussed. The principle of operation and the use of membrane contactors in the desorber of absorption refrigeration systems can alter the configuration of the cycle. However, the use of membrane contactors in the absorber and solution heat exchanger has no significant effect on the configuration of the cycle. Ali [49,50] used the plate-and-frame membrane module absorber with the same configuration as the conventional single-effect water/LiBr absorption refrigeration cycle as shown in Fig. 1 (a). Schaal et al. [4] and Chen et al. [53] used the conventional configuration of the single-effect ammonia/water absorption cycle with a hollow fiber membrane module absorber. The unconventional cycle configurations used in the investigations reviewed in this work are herein discussed.

Zerweck [63] proposed an absorption refrigeration cycle utilizing the osmotic membrane as shown in Fig. 5. The major components of the cycle are a condenser, an evaporator and an absorber–desorber unit. In this configuration the rich-refrigerant

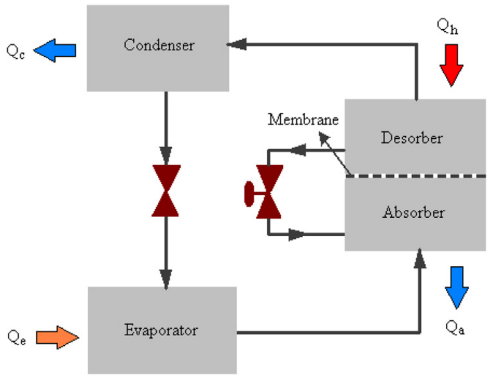

Fig. 5. Absorption refrigeration cycle proposed by Zerweck [63].

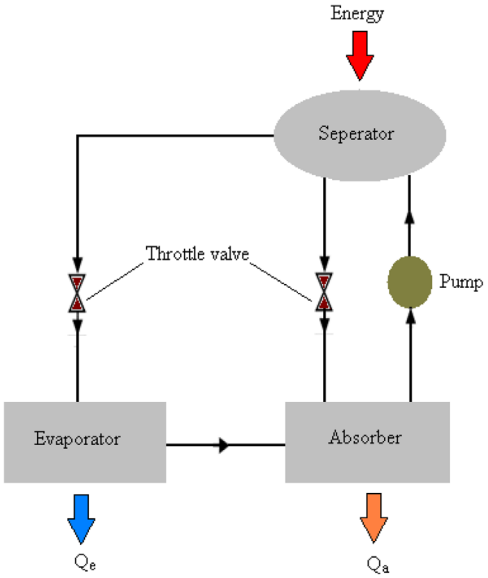

Fig. 6. Absorption refrigeration cycle proposed by Riffat and Su [60].

solution in the absorber and weak-refrigerant solution in the desorber are separated from each other by an osmotic membrane. Only the refrigerant is allowed to pass through the osmotic membrane. A solution pump is not utilised in the system as the refrigerant from the absorber is transferred to the desorber by osmotic diffusion through the membrane without the use of a mechanical pump. The pressure difference between the desorber and the absorber is dependent on the type of the membrane used. As there is usually a possibility that the absorbent from the absorber may be diffused together with the refrigerant to the desorber, a bleed valve is also used to re-strengthen the solution in the absorber.

Riffat and Su [60] proposed and investigated a centrifugal absorption refrigeration system using reverse osmosis principle as shown in Fig. 6. The major components of the cycle were an evaporator, an absorber and a membrane-integrated centrifuge. In this configuration the weak solution from the absorber is pumped to the centrifuge desorber up to the saturated pressure of the refrigerant at the given solution temperature. The centrifuge desorber is rotated at a certain angular velocity so as to achieve the required osmotic pressure of the solution. In the centrifuge desorber, the weak solution is separated into a strong solution and a pure refrigerant using a reverse osmosis membrane. At the osmotic pressure the solution components are separated such that the refrigerant passes out through the reverse osmosis membrane and is collected. As in the reverse osmosis mechanism, the refrigerant is separated from the solution in a liquid state so a condenser is not needed in the cycle. The strong solution returns to the absorber through a throttle valve while the refrigerant is supplied to the evaporator after passing through the refrigerant expansion valve. The vapour at the evaporator exit is absorbed in the absorber and the cycle repeats. Absorption refrigeration cycles using the reverse osmosis mechanism for refrigerant separation have a comparable COP to those of conventional vapour compression cycles depending on the angular speed of centrifuge. However, very high pressure energy is required to separate the refrigerant from the solution using reverse osmosis mechanism.

Riffat et al. [3] investigated an absorption refrigeration cycle utilizing a pervaporation membrane to separate the refrigerant from the solution. In this configuration a pervaporation membrane replaces the conventional desorber for concentrating the working fluid. A pervaporation membrane is used for the separation process which involves the partial vaporization of a liquid mixture through a dense membrane while the downstream side of the membrane is kept under vacuum. Components which are separated can undergo dissolution, diffusion and evaporation in the pervaporation process. In the pervaporation process the component is diffused in a liquid phase in contrast to that of the distillation process where the components pass through the membrane in a vapour phase. The basic components and the working principle of the cycle are the same as those of the conventional absorption refrigeration cycle. However, the desorber is replaced by a heater and a pervaporation membrane. The weak solution from the absorber is passed through the solution heat exchanger and is then heated in the heater. The heated solution in the liquid phase is transferred from the heater and enters into the pervaporation membrane unit where a membrane is used to separate the refrigerant from the solution. Only the refrigerant passes through the pervaporation membrane and is collected on the other side. A vacuum is created on the downstream side of the membrane. The refrigerant is condensed and throttled to the evaporator to produce cooling and then is absorbed in the absorber and the cycle repeats. The schematic diagram of this cycle is shown in Fig. 7. The COP of the cycle utilizing the pervaporation membrane process for vapour desorption is low compared with conventional absorption systems, as the pervaporation process requires a very high solution feed flow rate. The authors obtained a COP of 0.06 for their

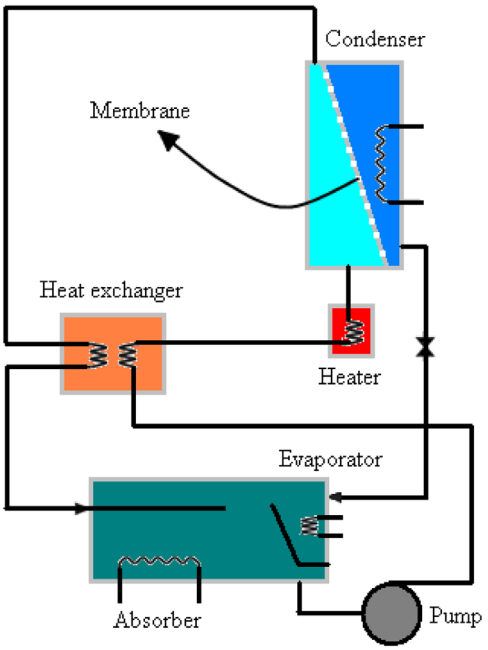

Fig. 7. Absorption refrigeration cycle proposed by Riffat et al. [3].

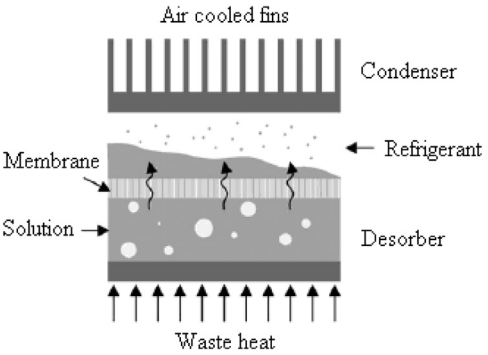

Fig. 8. Absorption refrigeration cycle proposed by Kim et al. [62].

prototype working with the pervaporation membrane principle. They argued that the low COP was due to the high circulation ratio as a high feed flow rate is required to operate such pilot membrane modules.

Kim et al. [62] proposed an absorption refrigeration system which could be fitted into a small scale envelope for electronic cooling. Conventional absorption refrigeration is too bulky for the electronic system cooling therefore the concept of a combined micro-channel condenser and desorber was proposed as shown in Fig. 8. In this configuration a hydrophobic membrane is placed between the desorber and the condenser while micro-channel heat exchangers are attached at the other ends. The condenser is air-cooled and for heat transfer enhancement, offset strip fins are installed. The overall cycle operating principle is similar to that of the conventional absorption cycle. The refrigerant inside the desorber is vaporized using a waste heat source. Only the refrigerant is allowed to pass through the hydrophobic membrane from the desorber to the condenser. The surface tension and capillary actions, upon interaction with the hydrophobic membrane, prevent the liquid solution from flowing through the membrane pores. The refrigerant vapour collected in the micro-channel condenser is cooled by dissipating the heat to the ambient with the aid of an offset strip fin array. The refrigerant is throttled through an expansion valve and is passed to the evaporator to produce cold. The refrigerant from the evaporator is absorbed in the absorber and the cycle continues. The authors

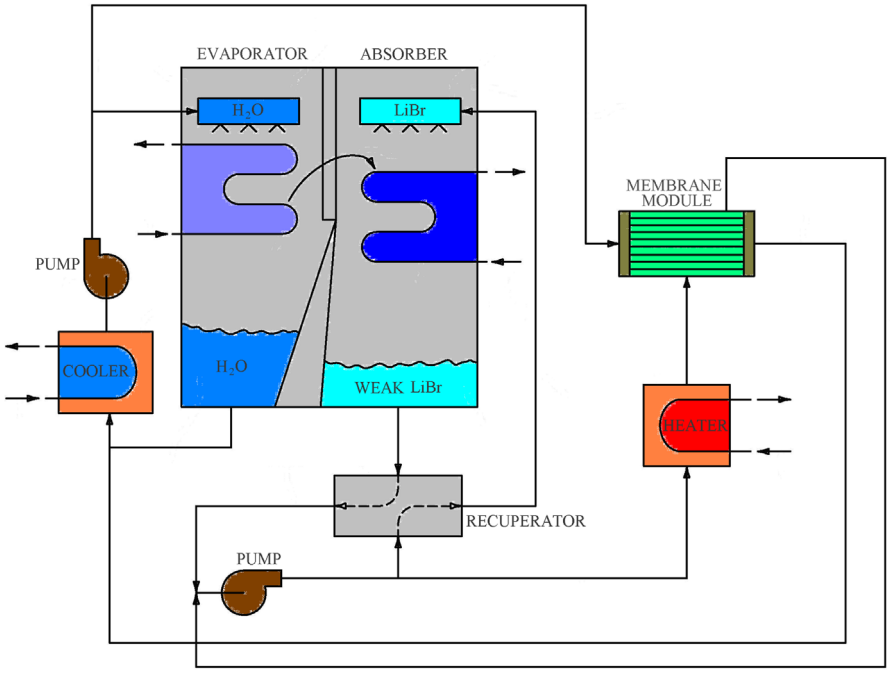

Fig. 9. Absorption refrigeration cycle proposed by Zidu [22].

reported that a COP in the range of 0.74 to 0.87 of the proposed cooling system is achievable with a cooling capacity of 100 W.

Zidu [22] proposed an absorption refrigeration cycle in which a hollow fiber membrane module was used instead of the conventional desorber to separate the refrigerant from the solution. The cycle consists of the basic absorption refrigeration system components such as the absorber, evaporator, weak solution heater, cooler, solution circulating pump, solution recuperator and a membrane distiller as shown in Fig. 9. The refrigerant in the liquid phase is circulated by a refrigerant pump and part of the refrigerant is supplied to the membrane module while the rest is supplied to the evaporator, where it is sprayed on the evaporator tubes. The refrigerant vaporizes and is collected in the absorber because of the vapour pressure difference. In the absorber, the absorbent solution with lower vapour pressure than the water vapour pressure absorbs the refrigerant vapours. The absorbent solution is sprayed from a spray tree on the outside of the cooling tubes in which a cooling medium is used to dissipate the heat of absorption. The rich solution in LiBr coming from the membrane module is passed through the recuperator to preheat the weak solution in LiBr before entering the solution heater. The solution is heated in the heater to a predefined temperature before entering the hollow fiber membrane module. The feed solution is passed through the shell side while the liquid refrigerant passes in the tubes made up of microporous hydrophobic membrane. The volatile refrigerant in the pre-heated feed solution vaporizes at the membrane interface, passes through the membrane pores in the vapour phase and is condensed on the other side. The pre-heating of the feed absorbent solution to a specified temperature generates a vapour pressure that is higher than that of the liquid refrigerant on the tube side, thus a differential vapour pressure is achieved which acts as a driving force. The strong solution in LiBr is resupplied to the absorber through the recuperator while the refrigerant is transferred to the cooler from where it is pumped back to the evaporator and the membrane module, and the cycle then repeats. In this configuration of the absorption refrigeration cycle, a condenser is not used as the refrigerant is separated and collected in liquid state. The author reported that the cycle could achieve a COP of a conventional single effect absorption

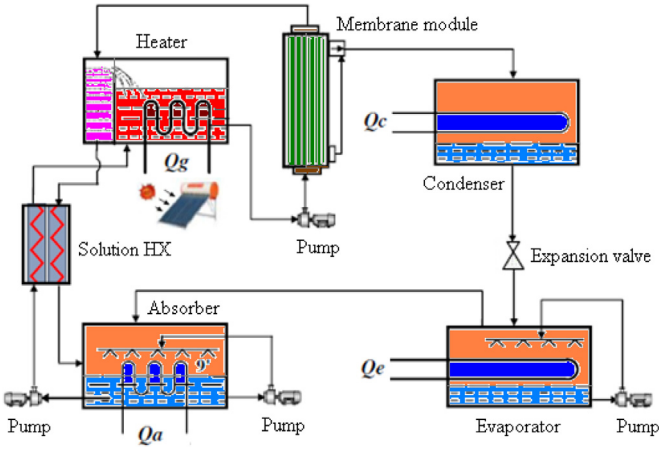

Fig. 10. Absorption refrigeration cycle proposed by Wang et al. [6].

refrigeration cycle and could be operated at a lower desorber temperature than that of the conventional cycle.

Wang et al. [6] proposed an absorption refrigeration cycle utilizing the vacuum membrane distillation process. The working principle of the cycle is similar to that of the conventional absorption refrigeration systems but the desorber is replaced by a vacuum distillation unit which comprises of a solution heater unit and a hollow fiber membrane module. In the hollow fiber membrane module, the hot feed solution flows in the membrane fibers whereas in the shell side a vacuum pressure is kept. The vacuum pressure is usually decided by the temperature of cooling water. Fig. 10 shows a schematic diagram of this cycle. The hot feed solution from the solution heater unit is transported to the hollow fiber membrane module by a pump. Using the concept of a vacuum distillation process, the refrigerant vapours are collected in the shell side and then cooled in the condenser under vacuum conditions. Strong solution in LiBr from the membrane module is transferred back to the solution heater unit which is divided into two parts for storing the strong solution and heating the weak solution. Part of the strong solution in the storage section flows to

Table 6
Operating conditions of absorption refrigeration cycles using membrane based components reported in the investigations reviewed in this work.

Reference	Operating conditions					COP
	Absorber temperature/heat duty	Desorber temperature/heat duty	Condenser temperature/heat duty	Evaporator temperature/cooling capacity	Pressure ratio (P_{High}/P_{Low})	
Riffat et al. [3]	30 °C	75 °C	30 °C	10 °C/140 W	NA	0.060
Schaal et al. [4]	20 °C/28.7 kW	78 °C/22 kW	20 °C/28.7 kW	6 °C/6.7 kW	3.32	0.305
Ali [49]	35 °C/7.1 kW	75 °C/7.35 kW	34.5 °C/5.3 kW	4 °C/5 kW	6.74	0.680
Chen et al. [53]	45 °C/10.54 kW	145 °C/10.36 kW	51.42 °C/7.16 kW	10 °C/6.18 kW	4.31	0.596
Kim et al. [62]	35 °C/110 W	87.5 °C/135 W	38.9 °C/125 W	23.6 °C/100 W	4.24	0.740

the absorber and the rest overflows into the solution heater through the overflow plate. In the solution heater, weak solution from the absorber and strong solution from the strong solution storage pool are blended and then heated by low grade energy. Finally, the hot solution is pumped into the membrane module by a pump and the process continues. Functions and operating principles of the other components such as the condenser, expansion valve, evaporator, absorber, solution heat exchanger and other auxiliary units are similar to the conventional absorption refrigeration system. This cycle configuration can improve the COP of the cycle and allow the refrigeration system to produce cooling at a low desorber temperature as the solution does not require heating to boiling point in the membrane distillation process.

Table 6 summarises the operating conditions of the absorption refrigeration cycles with membrane based components that were used in the investigations reviewed in this work.

7. Conclusion

From the literature survey it is concluded that the use of light weight polymeric hydrophobic microporous membrane contactors can provide a larger interfacial area for heat and mass transfer processes. Thus, not only the size and weight of the components can be reduced but also the system performance can be enhanced. Use of membrane contactors in the desorber can extend the use of low grade heat sources effectively in absorption refrigeration systems. It is evaluated from the literature review that membrane based desorbers can alter the configuration of absorption refrigeration cycles and the cycle components can be reduced in some cases. Despite these advantages, there are some limitations associated with membrane contactors such as the mechanical strength of membrane contactors, which is very low and the fact that they cannot operate at very high temperatures.

In this review the applications of membrane contactors in the field of absorption refrigeration systems are covered. Membrane contactor modules, components employing membrane contactors, cycle configuration, membrane material characteristics and the working fluid mixtures for the membrane contactor based absorption refrigeration systems are all discussed. This review reveals that the applications of membrane contactors for absorption and desorption is an emerging technique in the field of absorption refrigeration systems, however, a commercial plant has not yet been designed to explore the long term operation of membrane contactor based components in absorption refrigeration systems. Further research is needed to explore the long term operation consequences of membrane contactors in absorption and desorption processes. One of the prominent areas for future investigation is the use of non-conventional working fluid mixtures in membrane contactor components. Potential research could be carried out on the use of ionic liquid as an absorbent in absorption refrigeration systems employing membrane based components. Membrane contactor modules are available in different types hence, membrane modules other then plate-and-frame membrane module and hollow fiber module should also be investigated. Membrane contactor surface properties need to be studied further for more efficient use in absorption refrigeration components. In this regard, further research work is required to improve the hydrophobic character of membrane material, enhance the mechanical strength and to improve the compatibility of the membrane material with the working fluid mixtures. Membrane contactors do not suffer corrosion problems as it occurs in conventional absorption refrigeration components. However, fouling of membrane contactors means that more need for research is necessary with regard to absorption refrigeration components employing membrane contactors, so that durability and life span cost of the absorption refrigeration system can be evaluated more precisely. Membrane module desorbers should be tested and analysed at higher operating temperatures to investigate the effect of high temperatures on membrane materials and performance.

Acknowledgements

This study is part of an R&D project funded by the Spanish Ministry of Economy and Competitiveness (DPI2012-38841-C02-02). Faisal Asfand gratefully acknowledges the Rovira i Virgili University for granting the Martí-Franquès research fellowship 2012 (2012BPURV-50) to pursue a doctorate degree.

References

[1] Drost K, Liburdy J, Paul B, Peterson R. Enhancement of heat and mass transfer in mechanically constrained ultra thin films. DOE final Report no.: FC36-01GO11049; 2005.
[2] Yu JS, Chang WS, Haskin WL. Use of membrane transport in an absorption thermal transfer cycle. J Thermophys Heat Transfer 1992;6:371–6.
[3] Riffat SB, Wu S, Bol B. Pervaporation membrane process for vapour absorption system. Int. J. Refrig 2004;27:604–11.
[4] Schaal F, Weimer T, Hasse H. Membrane contactors for absorption refrigeration. In: International sorption heat pump conference 2008, Seoul, Korea; September 2008.
[5] Thorud JD, Liburdy JA, Pence DV. Microchannel membrane separation applied to confined thin film desorption. J Exp Ther Fluid Sci 2006;30:713–23.
[6] Wang Z, Gu Z, Feng S, Li Y. Application of vacuum membrane distillation to lithium bromide absorption refrigeration system. Int J Refrig 2009;32:1587–96.
[7] Ali AHH, Schwerdt P. Characteristics of the membrane utilized in a compact absorber for lithium bromide–water absorption chillers. Int J Refrig 2009;32:1886–96.
[8] Isfahani RN, Sampath K, Moghaddam S. Nanofibrous membrane-based absorption refrigeration system. Int J Refrig 2013;36:2297–307.
[9] Isfahani RN, Fazeli A, Bigham S, Moghaddam S. Physics of lithium bromide (LiBr) solution dewatering through vapor venting membranes. Int J Multiphase Flow 2014;58:27–38.
[10] Isfahani RN, Moghaddam S. Absorption characteristics of lithium bromide (LiBr) solution constrained by superhydrophobic nanofibrous structures. Int J Heat Mass Transfer 2013;63:82–90.
[11] Bigham S, Yu D, Chugh D, Moghaddam S. Moving beyond the limits of mass transport in liquid absorbent microfilms through the implementation of surface-induced vortices. Energy 2014;65:621–30.
[12] Bigham S, Isfahani RN, Moghaddam S. Direct molecular diffusion and micromixing for rapid dewatering of LiBr solution. Appl Therm Eng 2014;64:371–5.

[13] Deerberg G, Gehrke I. Personal communication. Fraunhofer Institut Umwelt-, Sicherheits-und Energietechnik UMSICHT. Oberhausen. Germany; August 2007.
[14] Iversen SB, Bhatia VK, Dam-Johansen K, Jonsson G. Characterization of microporous membranes for use in membrane contactors. J Membr Sci 1997;130:205–17.
[15] Ali AHH, Schwerdt P. For designing a compact absorber with membrane contactor at liquid–vapor interface–Influence of membrane properties on water vapor transfer. ASHRAE Trans 2010;116:398–407.
[16] Yu D, Chung J, Moghaddam S. Parametric study of water vapor absorption into a constrained thin film of lithium bromide solution. Int J Heat Mass Transfer 2012;55:5687–95.
[17] Smolders A, ACM. Franken. Terminology for membrane distillation. Desalination 1989;72:249–62.
[18] Martınez L, Rodrıguez-Maroto JM. Characterization of membrane distillation modules and analysis of mass flux enhancement by channel spacers. J Membr Sci 2006;274:123–37.
[19] Mackie JS, Meares P. The diffusion of electrolytes in a cation-exchange resin membrane. I. Theoretical. Proc R Soc A 1955;232:498–509.
[20] Alkhudhiri A, Darwish N, Hilal N. Membrane distillation: a comprehensive review. Desalination 2012;287:2–18.
[21] Gabino F, Belleville MP, Preziosi-Belloy L, Dornier M, Sanche J. Evaluation of the cleaning of a new hydrophobic membrane for osmotic evaporation. Sep Purif Technol 2007;55:91–197.
[22] Zidu MA. Membrane contactors for absorption refrigeration. International Publication No WO 2009/052582 A1, 2009.
[23] Sperati CA. DuPont de Nemours EI. In: Brandrup J, Immergut EH, editors. Polymer handbook. 2nd ed.. New York: John Wiley; 1975.
[24] Jönsson AS, Wimmerstedt R, Harrysson AC. Membrane distillation—a theoretical study of evaporation through microporous membranes. Desalination 1985;56:237–49.
[25] Martínez L, Florido-Díaz F, Hernández A, Prádanos P. Characterisation of three hydrophobic porous membranes used in membrane distillation modelling and evaluation of their water vapour permeabilities. J Membr Sci 2002;203:15–27.
[26] Albrecht W, Hilke R, Kneifel K, Th Weigel, Peinemann KV. Selection of microporous hydrophobic membranes for use in gas/liquid contactors: an experimental approach. J Membr Sci 2005;263:66–76.
[27] Rautenbach R, Albrecht R. On the behaviour of asymmetric membranes in pervaporation. J Membr Sci 1984;19:1–22.
[28] Lawson KW, Lloyd DL. Membrane distillation. J Membr Sci 1996;124:1–25.
[29] Alklaibi AM, Lior N. Membrane-distillation desalination: status and potential. Desalination 2005;171:111–31.
[30] Shirazi S, Lin CJ, Chen D. Inorganic fouling of pressure-driven membrane processes—a critical review. Desalination 2010;250:236–48.
[31] Gryta M. Long-term performance of membrane distillation process. J Membr Sci 2005;265:153–9.
[32] Gryta M. Fouling in direct contact membrane distillation process. J Membr Sci 2008;325:383–94.
[33] Griesheim MS, Rodenbach BG. Absorption refrigeration machine. US Patent no. 2010/0326126 A1; 2010.
[34] Oronel C, Amaris C, Bourouis M, Vallès M. Heat and mass transfer in a bubble plate absorber with $NH_3/LiNO_3$ and $NH_3/(LiNO_3+H_2O)$ mixtures. Int J Therm Sci 2013;63:105–14.
[35] Bourouis M, Vallès M, Medrano M, Coronas A. Performance of air-cooled absorption air conditioning systems working with water-(LiBr+LiI+$LiNO_3$+LiCl). J Process Mech Eng 2005;219:205–12.
[36] Bourouis M, Vallès M, Medrano M, Coronas A. Absorption of water vapour in the falling film of water-(LiBr+LiI+$LiNO_3$+LiCl) in a vertical tube at air-cooling thermal conditions. Int J Therm Sci 2005;44:491–8.
[37] Mesones J. Experimental and theoretical study of solubility of new absorbents in natural refrigerants. (Doctoral thesis). Spain: Universitat Rovira I Virgili; 2014.
[38] Marsh KN, Boxall JA, Lichtenthaler R. Room temperature ionic liquids and their mixtures—a review. Fluid Phase Equilib 2004;219:93–8.
[39] Valkenburg MEV, Vaughn RL, Williams M, Wilkes JS. Thermochemistry of ionic liquid heat-transfer fluids. Thermochim Acta 2005;425:181–8.
[40] Khamooshi M, Parham K, Atikol U. Overview of ionic liquids used as working fluids in absorption cycles. Adv Mech Eng 2013. http://dx.doi.org/10.1155/2013/620592.
[41] Yokozeki A, Shiflett MB. Water solubility in ionic liquids and application to absorption cycles. Ind Eng Chem Res 2010;49(19):9496–503.
[42] Yokozeki A, Shiflett MB. Vapor–liquid equilibria of ammonia+ionic liquid mixtures. Appl Energy 2007;84(12):1258–73.
[43] Yokozeki A, Shiflett MB. Ammonia solubilities in room-temperature ionic liquids. Ind Eng Chem Res 2007;46(5):1605–10.
[44] Martin A, Bermejo MD. Thermodynamic analysis of absorption refrigeration cycles using ionic liquid+supercritical CO_2 pairs. J Supercrit Fluids 2010;55(2):852–9.
[45] Kim YJ, Kim S, Joshi YK, Fedorov AG, Kohl PA. Thermodynamic analysis of an absorption refrigeration system with ionic–liquid/refrigerant mixture as a working fluid. Energy 2012;44:1005–16.
[46] Mesones J, Altamash T, Pérez E, Salavera D, Coronas A. New device for measuring the solubility of inorganic salts in liquid ammonia. Fluid Phase Equilib 2013;355:46–51.
[47] Salavera D, Esteve X, Patil KR, Mainar AM, Coronas A. Solubility, heat capacity, and density of lithium bromide+lithium iodide+lithium nitrate+lithium chloride aqueous solutions at several compositions and temperatures. J Chem Eng Data 2004;49:613–9.
[48] Koo KK, Lee HR, Jeong S, Oh YS, Park DR, Solubilities Back YS. Vapor pressures, and heat capacities of the water+lithium bromide+lithium nitrate+lithium iodide+lithium chloride system. Int J Thermodyn 1999;20:589–600.
[49] Ali AHH. Design of a compact absorber with a hydrophobic membrane contactor at the liquid–vapor interface for lithium bromide–water absorption chillers. Appl Energy 2010;87:1112–21.
[50] AHH. Ali. Performance of an absorber with hydrophobic membrane contactor at aqueous solution–water vapor interface. J Therm Sci Eng Appl 2010;2:031007.
[51] Baker RW. Membrane technology and applications. 2nd ed.. New York: Wiley; 2004.
[52] Zarkadas DM, Sirkar KK. Polymeric hollow fiber heat exchangers: an alternative for lower temperature applications. Ind Eng Chem Res 2004;43:8093–106.
[53] Chen J, Chang H, Chen S. Simulation study of a hybrid absorber–heat exchanger using hollow fiber membrane module for the ammonia–water absorption cycle. Int J Refrig 2006;29:1043–52.
[54] Wang Z, Feng S, Shi X, Gu Z Experimental study on concentration of aqueous lithium bromide solution by vacuum membrane distillation process. In: International refrigeration and air conditioning conference; 2008. ⟨http://docs.lib.purdue.edu/iracc/915⟩.
[55] Wang Z, Feng S, Li Y, Gu Z. Simulation of heat and mass transfer in solution heat exchanger with hollow fiber membrane. J Xi'an Jiaotong Univ 2009;43:36–41.
[56] Wang Z, Feng S, Li Y, Gu Z. Experimental and theoretical study on heat and mass transfer of hollow fiber membrane heat exchanger. J Xi'an Jiaotong Univ 2009;43:40–5.
[57] Wang ZS, Gu ZL, Wang GZ, Cui F, Feng SY. Analysis on membrane heat exchanger applied to absorption chiller. Int J Air-Cond Refrig 2011;19:167–75.
[58] Mengual JI, Khayet M, Godino MP. Heat and mass transfer in vacuum membrane distillation. Int J Heat Mass Transfer 2004;47:865–75.
[59] Qtaishat M, Matsuura T, Kruczek B, Khayet M. Heat and mass transfer analysis in direct contact membrane distillation. Desalination 2008;219:272–92.
[60] Riffat SB, Su YH. Analysis of a novel absorption refrigeration cycle using centrifugal separation. Energy 2001;26:177–85.
[61] Su YH, Riffat SB. A thermodynamic approach to calculating the operating osmotic pressure of pressure driven membrane separation absorption cycles. Int J Therm Sci 2004;43:1197–201.
[62] Kim YJ, Joshi YK, Fedorov AG. An absorption based miniature heat pump system for electronics cooling. Int J Refrig 2008;31:23–33.
[63] Zerweck G. Ein-oder mehrstufige Absorptionswarmepumpe, German Patent no. DE 30 09 820A1, 1980.

A.2 Estimation of differential heat of dilution for aqueous lithium (bromide, iodide, nitrate, chloride) solution and aqueous (lithium, potassium, sodium) nitrate solution used in absorption cooling systems.

INTERNATIONAL JOURNAL OF REFRIGERATION 71 (2016) 18–25

Available online at www.sciencedirect.com

ScienceDirect

journal homepage: www.elsevier.com/locate/ijrefrig

Estimation of differential heat of dilution for aqueous lithium (bromide, iodide, nitrate, chloride) solution and aqueous (lithium, potassium, sodium) nitrate solution used in absorption cooling systems

Faisal Asfand, Mahmoud Bourouis *

Department of Mechanical Engineering, Universitat Rovira i Virgili, Av. Països Catalans No. 26, 43007 Tarragona, Spain

ARTICLE INFO

Article history:
Received 18 March 2016
Received in revised form 4 August 2016
Accepted 20 August 2016
Available online 24 August 2016

Keywords:
Differential heat of dilution
Duhring's diagram
Water/LiBr
Water/(LiBr + LiI + $LiNO_3$ + LiCL)
Water/($LiNO_3$ + KNO_3 + $NaNO_3$)
Absorption cooling

ABSTRACT

The differential heat of dilution data are estimated theoretically using Duhring's diagrams for water/LiBr, water/(LiBr + LiI + $LiNO_3$ + LiCl) with mass compositions in salts of 60.16%, 9.55%, 18.54% and 11.75%, respectively, and water/($LiNO_3$ + KNO_3 + $NaNO_3$) with mass compositions in salts of 53%, 28% and 19%, respectively, as these can be potentially utilized as working fluids in absorption cooling systems. The differential heat of dilution data obtained were correlated with simple polynomial equations for the three working fluids as a function of the solution concentration and temperature. The results showed that the differential heat of dilution of the non-conventional working fluid mixtures is lower than that of water/LiBr at typical operating temperature and concentration of interest in absorption cooling cycles employing these working fluid mixtures. The correlations developed could be useful in predicting the differential heat of dilution value while performing heat and mass transfer analyses of these potential non-conventional working fluid mixtures in absorption cooling systems.

Estimation de la chaleur différentielle de dilution pour une solution aqueuse de (bromure, iodure, nitrate, chlorure) de lithium et une solution aqueuse de nitrate de (lithium, potassium, sodium) utilisées dans les systèmes de refroidissement à absorption

Mots-clés : Chaleur différentielle de dilution ; Diagramme de Duhring ; Eau/LiBr ; Eau/(LiBr + LiI + LiNO3 + LiCl) ; Eau/(LiNO3 + KNO3 + NaNO3) ; Refroidissement par absorption

* *Corresponding author.* Department of Mechanical Engineering, Universitat Rovira i Virgili, Av. Països Catalans No. 26, 43007 Tarragona, Spain. Fax: +34 977 55 96 91.
E-mail address: mahmoud.bourouis@urv.cat (M. Bourouis).
http://dx.doi.org/10.1016/j.ijrefrig.2016.08.008

Nomenclature

a, b, c	constants
H	enthalpy [kJ kg^{-1}]
i	i^{th} term
m	slope
P	pressure [Pa]
T	temperature [K]
V	volume [m^3 kg^{-1}]
w	mass fraction
y	y-coordinate intercept

Superscripts

s	solution
sup	superheated
sat	saturated
w	water

Subscripts

d	dilution
f	liquid state
v	vapour state

Chemical formula

H_2O	water
KNO_3	potassium nitrate
LiBr	lithium bromide
LiCl	lithium chloride
LiI	lithium iodide
$LiNO_3$	lithium nitrate
$NaNO_3$	sodium nitrate

1. Introduction

Absorption air-conditioning systems driven by solar thermal energy are gaining global acceptance for space cooling in summer due to their potential to utilize the free solar thermal energy efficiently. Working fluid mixtures employed in the absorption air-conditioning systems are environmental friendly and do not contribute to greenhouse gas emissions unlike vapour compression systems which also use costly mechanical energy input. Intensive research has been carried out to improve the performance and thermal efficiency of absorption air-conditioning systems by adopting suitable operating conditions and improved design and configuration of the components. In commercial absorption air-conditioning systems, water/LiBr is mainly employed as a working fluid mixture and offers outstanding features such as the non-volatility of LiBr absorbent and high heat of vaporization of water. However, water/LiBr based absorption air-conditioning systems suffer from corrosion problems and exhibit a high risk of crystallization when operated at air-cooled thermal conditions. At high cooling-water temperatures and high concentrations, the solution is prone to crystallization. In addition, because of the risk of crystallization, corrosion problems and thermal instability at higher temperatures, water/LiBr working fluid mixture limits the use of high temperature heat sources in triple-effect cycles which are intended to improve the thermal utilization and increase the coefficient of performance of absorption air-conditioning systems. In view of the above mentioned problems associated with water/LiBr working fluid mixture, new working fluid mixtures have been investigated to overcome problems associated with the conventional working fluid mixture.

The addition of other salts to water/LiBr can improve the solubility of the solution. Bourouis et al (2005a, 2005b) and Medrano et al (2002) investigated and recommended the use of an aqueous multi-component salt solution (LiBr + LiI + $LiNO_3$ + LiCl) with mass compositions in salts of 60.16%, 9.55%, 18.54% and 11.75%, respectively, as a potential absorbent with water as a refrigerant. The multi component salt solution exhibits higher solubility and also reduces the risk of crystallization. Bourouis et al (2005a) reported that the presence of lithium chloride decreases the vapour pressure, both lithium iodide and lithium nitrate improve the solubility, and lithium nitrate reduces corrosion in the system. The safety margin for crystallization is much higher as its crystallization temperature is about 30 K lower than that of water/LiBr. Thus, the use of the multi-salt working fluid mixture cannot only mitigate the problems associated with the conventional water/LiBr working fluid mixture but can also enhance the performance of an absorber operating at air-cooled thermal conditions.

Similarly, as water/LiBr cannot be used in triple-effect cycles driven by high temperature heat sources (above 180 °C) due to corrosion problems and thermal instability, investigations are being performed on the development of potential absorbents that are non-corrosive and thermally stable at higher temperatures so as to efficiently utilize the thermal potential of high temperature heat sources. Aqueous (lithium, potassium, sodium) nitrate solution (Alkitrate) has been suggested as a working fluid in the high temperature stage of a triple-effect cycle (Álvarez et al., 2015; Davidson and Erickson, 1986; Erickson et al., 1996; Howe and Erickson, 1990). The working fluid mixture is composed of water as a refrigerant, and a ternary salt mixture of lithium nitrate, potassium nitrate and sodium nitrate as an absorbent with a mass composition in salts of 53%, 28% and 19%, respectively. The use of an Alkitrate solution can be potentially useful in applications in which the available heat source temperature is very high because it is non-corrosive and has high thermal stability up to a temperature of about 260°C.

The aqueous multi-component salt solution (LiBr + LiI + $LiNO_3$ + LiCl) and aqueous (lithium, potassium, sodium) nitrate solution can be considered as promising alternatives to the conventional water/LiBr working fluid mixture to enhance the performance of absorption air-conditioning systems operating at air-cooled thermal conditions and high temperature heat source conditions, respectively.

Many researchers have investigated the thermophysical properties of these non-conventional working fluids such as vapour pressure, density, viscosity, specific heat, thermal conductivity, etc. Although thermodynamic simulations have been performed with these non-conventional working fluid mixtures to investigate the cycle performance, there is very scarce information in the literature about the absorption and desorption processes. Heat and mass transfer phenomena which simultaneously occur in the absorber and desorber of an

absorption air-conditioning system have to be investigated in order to evaluate the performance of the component. In many numerical approaches for analysis of heat and mass transfer phenomena in an absorber the differential heat of dilution is an important property to be known. Differential heat of dilution is the heat which evolves when a unit weight of solvent is added to an infinite weight of solution at a constant temperature and concentration. In the absorber of an absorption air-conditioning system, when the refrigerant is absorbed in the solution, heat evolves as a result of mixing and condensation and is known as heat of absorption. The heat of absorption is calculated from the enthalpies of the liquid state and vapour state and the differential heat of dilution. Therefore, differential heat of dilution is needed in the numerical modelling of heat transfer in the absorber. However, the differential heat of dilution data of the above non-conventional working fluid mixtures are not known.

Although differential heat of dilution can be determined experimentally using a calorimeter, another way is to estimate the differential heat of dilution from the enthalpy-concentration charts or vapour pressure data. Analytical method of calculating differential heat of dilution is simple and easy as the vapour pressure data of the examined working fluid mixtures are available. Brown (1935) described that the Clapeyron equation for a liquid substance and a solution containing that liquid as a solvent can be combined to derive a relation in which the differential term represents the slope of the Duhring line. Haltenberger (1939) reported that the slopes of the Duhring lines are constant at low concentrations and vary slightly at higher concentrations. He explained that an exact relation is obtained using the Clapeyron equation, which is applicable to all systems containing a single volatile constituent. The author used the vapour pressure of sodium hydroxide solutions to construct a Duhring chart from which he calculated the enthalpy of solution. The calculated values of differential heat of dilution using experimental data of heat capacity were used to construct an enthalpy-concentration chart. A similar approach was followed by McNeely (1979) who derived the differential heat of dilution data of water/LiBr theoretically from the Duhring's diagram using the Clapeyron equation. In this work, a similar theoretical procedure has been adopted to calculate the differential heat of dilution from the Duhring's diagram; however a new database for the vapour pressure calculation of water/LiBr is used. Further, a polynomial correlation has been derived for the calculation of the differential heat of dilution value for a range of concentration at different temperatures. The analytically calculated data obtained for water/LiBr were validated against the experimental data available in the literature and are found well in agreement with the experimental values. Further, the same procedure is used to estimate the differential heat of dilution of the multi-component salt aqueous solution (LiBr + LiI + $LiNO_3$ + LiCl) and aqueous (lithium, potassium, sodium) nitrate solution, and the data were correlated using a polynomial equation as a function of temperature and concentration. The obtained correlations to calculate the differential heat of dilution could be useful in performing a heat and mass transfer analysis of these non-conventional working fluid mixtures in the components of absorption cooling systems.

2. Calculation methodology

The Clausius–Clapeyron equation which is used for characterizing a discontinuous phase transition between two phases of matter of a single constituent can be written in a differential form as:

$$\frac{dP}{dT} = \frac{\Delta H}{\Delta V T} \tag{1}$$

Applying the Clausius–Clapeyron equation for the refrigerant which is water and the absorbent which is an aqueous solution of salt or mixture of salts, we obtain:

$$\frac{dP^w}{dT^w} = \frac{\Delta H^w}{\Delta V^w T^w} \tag{2}$$

and

$$\frac{dP^s}{dT^s} = \frac{\Delta H^s}{\Delta V^s T^s} \tag{3}$$

where, the superscript w denotes water and s denotes solution. T is the absolute saturation temperature in K, P is the saturation pressure in Pa, ΔH is the latent heat at temperature T and pressure P in kJ kg^{-1} and ΔV is the difference between vapour and liquid volumes in m^3 kg^{-1}.

For the same water vapour pressure, when $P^w = P^s$, dividing Eq. (2) by Eq. (3), we obtain:

$$\frac{dT^s}{dT^w} = \frac{\Delta H^w \Delta V^s T^s}{\Delta H^s \Delta V^w T^w} \tag{4}$$

As the liquid volume is negligible in comparison with its volume in the vapour phase, therefore, ΔV can be replaced by the vapour volume.

$$\frac{dT^s}{dT^w} = \frac{\Delta H^w V^{sup} T^s}{\Delta H^s V^{sat} T^w} \tag{5}$$

where V^{sat} is the volume of saturated water vapour and V^{sup} is the volume of superheated water vapour at saturation temperature of the solution. The degree of superheat is equal to T^s-T^w. Equation 5 represents the Duhring equation derived from the Clausius–Clapeyron equation.

According to Duhring's rule, if the boiling point of the solution is plotted against the boiling point of its solvent at the same pressure, the resultant plot will be a straight line. The equation of a straight line can be represented as:

$$T^s = mT^w + y \tag{6}$$

where m is the slope of the line and y is the y-coordinate intercept.

By differentiating Eq. (6), we obtain:

$$\frac{dT^s}{dT^w} = m \tag{7}$$

Similarly the Duhring equation can be represented by an equation of a straight line where m and y are constants for any given concentration.

$$\frac{dT^s}{dT^w} = \frac{\Delta H^w V^{sup} T^s}{\Delta H^s V^{sat} T^w} = m \tag{8}$$

The slope m of each line for each concentration is calculated from the Duhring's diagram. Saturation temperature of water vapour, specific volume of saturated water vapour and super heated water vapour are calculated from the steam table. Latent heat of water ΔH^w is given as:

$$\Delta H^w = H_v^w - H_f^w \tag{9}$$

where H_v^w is the saturated water vapour enthalpy and H_f^w is the saturated water enthalpy at temperature T^w. All values in Eq. (8) are known except ΔH^s. By rearranging Eq. (8) we get:

$$\Delta H^s = \frac{\Delta H^w V^{sup} T^s}{m V^{sat} T^w} \tag{10}$$

The differential heat of dilution is given as:

$$H_d = \bar{H} - H_f \tag{11}$$

where H_f is the enthalpy of water at temperature T^s and $\bar{H}$ is the partial enthalpy of water and is given as:

$$\bar{H} = H_v - \Delta H^s \tag{12}$$

where H_v is the superheated water vapour enthalpy at temperature T^s. By substituting the variables, the differential heat of dilution can be expressed as:

$$H_d = H_v - \frac{\Delta H^w V^{sup} T^s}{m V^{sat} T^w} - H_f \tag{13}$$

By substituting all the values in Eq. (13), the differential heat of dilution is calculated for different solution concentration at different temperature.

3. Vapour pressure data

Vapour liquid equilibria of all the working fluid mixtures were taken from the recent available experimental data. The correlation developed by Patek and Klomfar (2006) to calculate the thermodynamic properties of water/LiBr was used to calculate the saturation temperature of the water/LiBr solution. The vapour pressure data of Koo et al (1999) and the correlation developed by the research group CREVER from Rovira i Virgili University (Confidential Report, 2012) were used to calculate the saturation temperature of the quaternary salt working fluid mixture. To calculate the saturation temperature of the solution of Alkitrate, the correlation developed by Álvarez et al (2011) was used. The thermodynamic properties of water were calculated using the IAPWS formulation 1995 reported by Wagner and Pruß (2002).

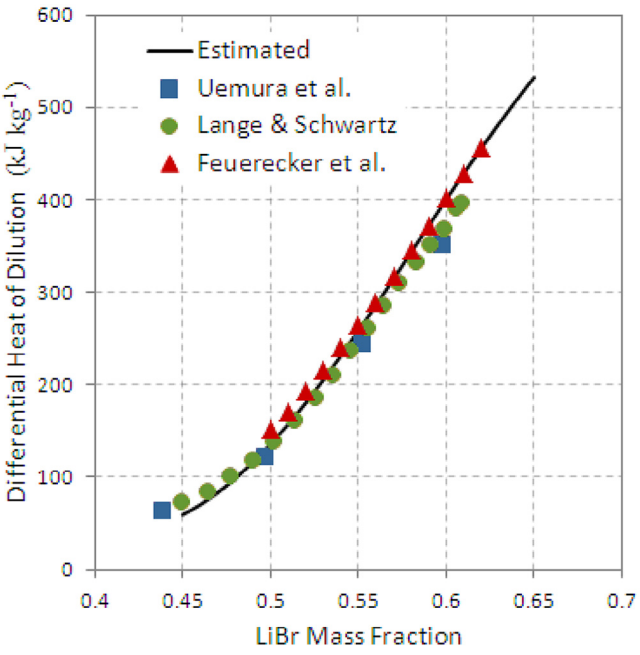

Fig. 1 – Validation of differential heat of dilution for water/LiBr at 25 °C.

4. Validation

Differential heat of dilution was theoretically calculated for water/LiBr solution using the above procedure and thermophysical properties, and the data obtained were validated against the experimental data of Uemura et al (1964), Lange and Schwartz (1928) and Feuerecker et al. (1993). As the differential heat of dilution data reported in the literature is measured at 25 °C therefore, in the derived polynomial correlation the temperature is kept constant at 25 °C. Fig. 1 shows the comparison of the analytically estimated and experimentally reported data. The estimated result is well in agreement with the experimental data with an absolute mean percentage error of 5.46%.

5. Results and discussion

The differential heat of dilution is theoretically calculated for all the three working fluid mixtures considered in the present work for a range of concentrations at different temperatures and covering the typical operating conditions of each working fluid mixture in absorption cooling systems. The saturation temperature of the solution was plotted against the saturation temperature of the water at the same pressure. The procedure was repeated for different solution concentrations of interest for absorption cooling cycles operating with the three working fluid mixtures. For each solution concentration, a straight line was obtained and the slope of the line was calculated. The slope m of the straight line at a given concentration, solution temperatures and corresponding dew point temperatures for water/LiBr, water/(LiBr + LiI + $LiNO_3$ + LiCl) and water/

Table 1 – Dew point and solution temperatures of the water/LiBr solution at different concentrations with the corresponding slope of the line on the Duhring's diagram.

Absorbent mass fraction	Slope m	Solution temperature (°C)							
		20	40	60	80	100	120	140	160
		Corresponding dew point temperature (°C)							
0.45	1.1013	5.90	24.06	42.22	60.39	78.55	96.71	114.90	133.00
0.46	1.1056	4.84	22.93	41.01	59.10	77.18	95.27	113.40	131.40
0.47	1.1104	3.71	21.72	39.73	57.75	75.76	93.77	111.80	129.80
0.48	1.1153	2.52	20.45	38.39	56.33	74.27	92.20	110.10	128.10
0.49	1.1194	1.25	19.11	36.98	54.85	72.71	90.58	108.40	126.30
0.50	1.1238	–0.09	17.71	35.51	53.31	71.10	88.90	106.70	124.50
0.51	1.1279	–1.49	16.24	33.98	51.71	69.44	87.17	104.90	122.60
0.52	1.1321	–2.95	14.72	32.39	50.05	67.72	85.39	103.10	120.70
0.53	1.1360	–4.47	13.14	30.74	48.35	65.96	83.57	101.20	118.80
0.54	1.1399	–6.04	11.51	29.06	46.60	64.15	81.70	99.25	116.80
0.55	1.1433	–7.65	9.84	27.33	44.82	62.31	79.80	97.29	114.80
0.56	1.1473	–9.29	8.14	25.57	43.00	60.43	77.86	95.29	112.70
0.57	1.1511	–10.97	6.41	23.78	41.15	58.53	75.90	93.27	110.60
0.58	1.1551	–12.65	4.66	21.98	39.29	56.60	73.92	91.23	108.50
0.59	1.1595	–14.34	2.91	20.16	37.41	54.66	71.91	89.17	106.40
0.60	1.1637	–16.03	1.15	18.34	35.53	52.71	69.90	87.09	104.30
0.61	1.1684	–17.71	–0.59	16.52	33.64	50.76	67.87	84.99	102.10
0.62	1.1737	–19.36	–2.32	14.72	31.76	48.80	65.84	82.88	99.91
0.63	1.1795	–20.97	–4.02	12.93	29.89	46.84	63.80	80.75	97.71
0.64	1.1859	–22.55	–5.69	11.17	28.03	44.89	61.75	78.61	95.47
0.65	1.1934	–24.08	–7.33	9.43	26.19	42.95	59.70	76.46	93.22

($LiNO_3 + KNO_3 + NaNO_3$) are tabulated in Tables 1, 2 and 3, respectively. The slope of each line was used to calculate the differential heat of dilution for the given concentration of solution at different temperatures. Figs. 2, 3 and 4 show the variation of the differential heat of dilution as a function of temperature and concentration. Figs. 2 and 3 show that the differential heat of dilution increases significantly with an increase in solution concentration; however, a slight increase is observed with an increase in temperature at a given concentration of the solution. It can be seen from Fig. 3 that the differential heat of dilution varies linearly with temperature in the case of lower absorbent concentration. Whereas, in the case of higher absorbent concentration, no significant increase in the differential heat of dilution is observed with the increase in temperature initially in the range of 298–320 K, however, a significant increase in the differential heat of dilution is observed above 320 K. It shows that the increase in the differential heat of dilution is less prominent at higher solution concentration and lower temperatures. In addition, it is worth noting that the differential heat of dilution of the non-conventional working fluid mixtures, water/(LiBr + LiI + $LiNO_3$ + LiCl) and water/($LiNO_3 + KNO_3 + NaNO_3$), at a given concentration and temperature of interest for absorption cooling cycles is lower than that of the water/LiBr solution, which results in a lower contribution to the heat of absorption. This makes these working fluid mixtures more appropriate for the absorption process taking place in the absorber which is the main component in absorption cooling systems. The estimated differential heat of dilution data for each working fluid mixture was correlated with the simple polynomial equation given below:

$$H_d = \sum_{i=0}^{3} \left[\left(a_i + b_i T + c_i T^2 \right) w^i \right] \quad (14)$$

Equation 14 represents the correlation to estimate the differential heat of dilution of each working fluid mixture as a function of concentration and temperature. In the above correlation, T represents temperature in K and w represents concentration of the absorbent in mass fraction. The values of the regressed parameters in the equation are tabulated in Table 4 for each working fluid mixture. The correlation is able to predict the differential heat of dilution with a mean absolute percentage error of 0.54%, 0.70% and 1.66% for water/LiBr, water/(LiBr + LiI + $LiNO_3$ + LiCl) and water/($LiNO_3 + KNO_3 + NaNO_3$), respectively. The correlation is valid for a concentration range of 45–65%, 55–67% and 60–85% and a temperature range of 20–50 °C, 25–60 °C and 80–150 °C for water/LiBr, water/(LiBr + LiI + $LiNO_3$ + LiCl) and water/($LiNO_3 + KNO_3 + NaNO_3$), respectively. The concentration ranges for the validity of the correlations depend on the use of the examined fluid mixtures. In this paper, the concentration and temperature ranges are taken in context of absorption cooling applications. The examined fluid mixtures are considered potential working pairs in absorption cooling systems. As this work is intended to estimate the differential heat of dilution which is used in the heat transfer calculation in the absorber of absorption cooling systems, the selection of composition and temperature ranges in the calculation are based on the typical operating conditions of these systems employing the examined working fluid mixtures.

6. Conclusion

The differential heat of dilution, which contributes in the heat evolved during the absorption process, is required in many numerical approaches to analyse the heat and mass transfer

Table 2 – Dew point and solution temperatures of the water/(LiBr + LiI + $LiNO_3$ + LiCl) solution at different concentrations with the corresponding slope of the line on the Duhring's diagram.

Absorbent mass fraction	Slope m	Solution temperature (°C)							
		30	40	60	80	100	120	140	160
		Corresponding dew point temperature (°C)							
0.55	1.1879	4.30	12.82	29.83	46.63	63.03	82.65	101.30	120.10
0.56	1.1889	2.69	11.25	28.30	45.10	61.46	80.71	99.09	117.60
0.57	1.1899	1.02	9.61	26.71	43.53	59.86	78.64	96.77	115.00
0.58	1.1910	–0.62	7.92	25.07	41.92	58.23	76.50	94.42	112.40
0.59	1.1921	–2.21	6.16	23.38	40.26	56.57	74.30	92.07	109.90
0.60	1.1934	–3.84	4.36	21.63	38.56	54.88	72.07	89.77	107.50
0.61	1.1945	–5.53	2.50	19.84	36.82	53.17	69.85	87.55	105.30
0.62	1.1958	–7.26	0.59	18.00	35.04	51.43	67.66	85.41	103.30
0.63	1.1969	–9.05	–1.21	16.12	33.23	49.66	65.52	83.36	101.30
0.64	1.1981	–10.87	–2.97	14.20	31.38	47.87	63.44	81.39	99.49
0.65	1.1991	–12.74	–4.79	12.24	29.50	46.07	61.45	79.50	97.72
0.66	1.2003	–14.65	–6.63	10.25	27.59	44.24	59.56	77.65	95.94
0.67	1.2013	–16.59	–8.52	8.22	25.66	42.39	57.78	75.82	94.07

phenomena. The differential heat of dilution of water/lithium bromide, water/(lithium bromide + lithium iodide +lithium nitrate + lithium chloride) with mass compositions in salts of 60.16%, 9.55%, 18.54% and 11.75%, respectively, and water/(lithium nitrate + potassium nitrate + sodium nitrate) with mass compositions in salts of 53%, 28% and 19%, respectively was analytically calculated in this paper. The analytical procedure to estimate the differential heat of dilution from Duhring's diagram using the vapour pressure data is an interesting alternative to experimental techniques, as the analytically calculated values are well in agreement with the experimental values. In this study, the Clausius–Clapeyron equation was used to derive the Duhring equation, and using the vapour pressure data of the examined mixtures, the differential heat of dilution data were estimated from the Duhring's diagrams. The differential heat of dilution data obtained were correlated with simple polynomial equations for the three working fluids as a function of the solution concentration and temperature. The correlation is able to predict the differential heat of dilution with a mean absolute percentage error of 0.54%, 0.70% and 1.66% for water/LiBr, water/(LiBr + LiI + $LiNO_3$ + LiCl) and water/($LiNO_3$ + KNO_3 + $NaNO_3$), respectively. The results showed that the differential heat of dilution of the non-conventional working fluid mixtures is lower than that of water/LiBr at typical operating temperature and concentration of interest in absorption cooling cycles employing these working fluid mixtures. For instance, the differential heat of dilution of water/LiBr at typical operating conditions lies in the range

Table 3 – Dew point and solution temperatures of the water/($LiNO_3$ + KNO_3 + $NaNO_3$) solution at different concentrations with the corresponding slope of the line on the Duhring's diagram.

Absorbent mass fraction	Slope m	Solution temperature (°C)							
		70	80	90	100	110	120	130	140
		Corresponding Dew Point Temperature (°C)							
0.6	1.1118	54.69	63.51	72.37	81.26	90.18	99.14	108.10	117.20
0.65	1.1240	51.07	59.78	68.53	77.31	86.12	94.96	103.80	112.80
0.7	1.1505	46.85	55.38	63.92	72.49	81.09	89.72	98.38	107.10
0.75	1.1931	41.86	50.10	58.37	66.64	74.94	83.26	91.60	99.96
0.76	1.2036	40.79	48.97	57.17	65.38	73.60	81.85	90.11	98.40
0.77	1.2150	39.69	47.81	55.94	64.08	72.23	80.40	88.59	96.80
0.78	1.2272	38.58	46.63	54.69	62.75	70.83	78.92	87.03	95.15
0.79	1.2403	37.44	45.42	53.40	61.40	69.40	77.41	85.43	93.47
0.8	1.2544	36.28	44.19	52.10	60.01	67.93	75.86	83.80	91.75
0.81	1.2692	35.10	42.94	50.77	58.60	66.44	74.28	82.13	89.99
0.82	1.2851	33.91	41.66	49.42	57.17	64.92	72.67	80.43	88.19
0.83	1.3019	32.69	40.37	48.04	55.71	63.37	71.03	78.70	86.37
0.84	1.3200	31.46	39.05	46.64	54.22	61.80	69.37	76.94	84.51
0.85	1.3392	30.21	37.72	45.22	52.71	60.20	67.67	75.15	82.62
0.86	1.3595	28.94	36.37	43.78	51.18	58.57	65.96	73.33	80.70
0.87	1.3812	27.65	35.00	42.32	49.63	56.93	64.21	71.49	78.75
0.88	1.4042	26.35	33.61	40.85	48.06	55.26	62.45	69.62	76.78
0.89	1.4287	25.04	32.21	39.35	46.47	53.57	60.66	67.73	74.78
0.9	1.4548	23.71	30.79	37.84	44.86	51.87	58.85	65.81	72.76
0.95	1.6129	16.77	23.38	29.95	36.48	42.98	49.44	55.86	62.25

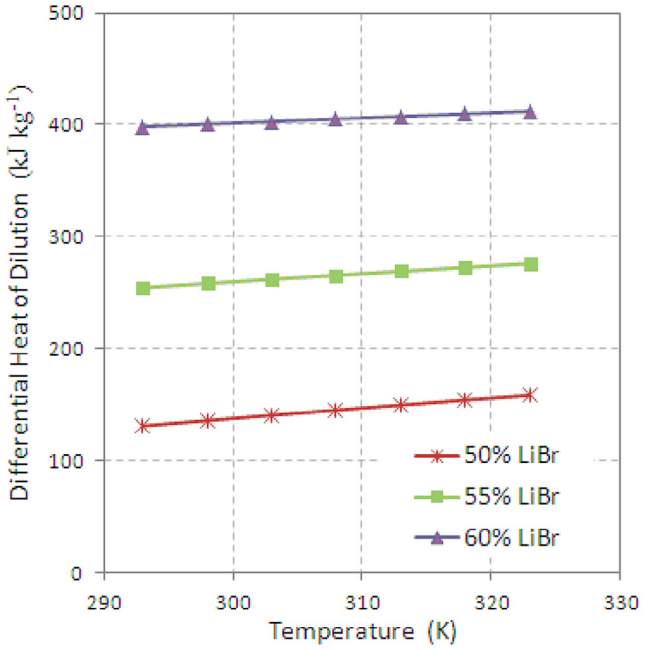

Fig. 2 – Differential heat of dilution for water/LiBr working fluid.

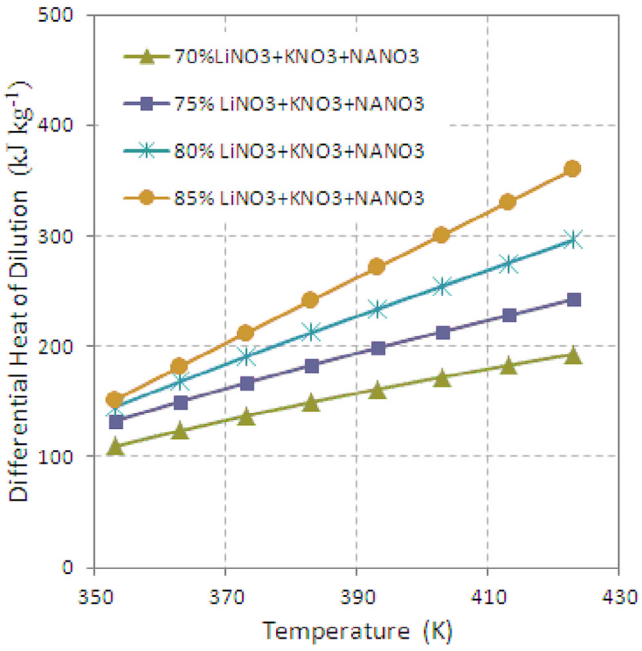

Fig. 4 – Differential heat of dilution for water/(LiNO3 + KNO3 + NaNO3) working fluid.

of 300–400 kJ kg^{-1}, whereas the differential heat of dilution of the quaternary working fluid and Alkitrate solution lies in the range of 250–350 kJ kg^{-1} and 200–300 kJ kg^{-1}, respectively, at typical operating conditions of these working fluid mixtures. Therefore, it is concluded that the performance of the absorber could be improved with these non-conventional working fluid mixtures because of the lower heat of absorption. Reduction in the heat of absorption released at the solution

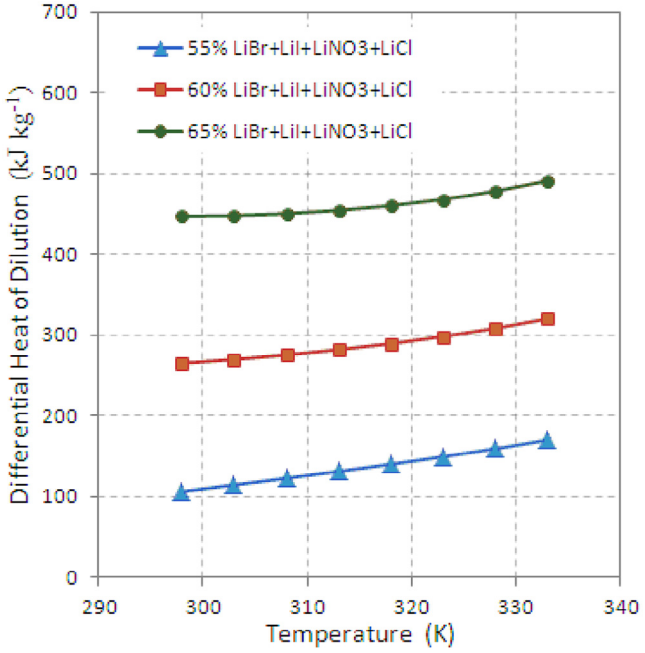

Fig. 3 – Differential heat of dilution for water/(LiBr + LiI + $LiNO_3$ + LICl) working fluid.

Table 4 – Regressed values of the coefficients in Eq. (14).

	a_i	b_i	c_i
Water/LiBr working fluid			
i = 0	0.992786	–3.80487	0.06707
i = 1	1.017947	–0.3167	–0.31698
i = 2	1.06683	12.75037	0.548797
i = 3	1.044128	6.897941	–0.35639
Water/(LiBr + LiI + $LiNO_3$ + LiCl) working fluid			
i = 0	0.932142	–8.91989	0.053392
i = 1	1.032266	6.815861	–0.17187
i = 2	1.062847	9.656643	0.229848
i = 3	1.063738	7.55447	–0.14364
Water/($LiNO_3$ + KNO_3 + $NaNO_3$) working fluid			
i = 0	1.005307	–8.70613	0.016192
i = 1	0.841477	19.01825	–0.02999
i = 2	0.692006	0.003384	–0.0169
i = 3	0.5949	–14.7523	0.044434

vapour interface allows for a reduction in the partial pressure of water vapour in the solution at the interface, consequently increasing the absorption capability of the solution. The correlations developed could be useful in predicting the differential heat of dilution value while performing heat and mass transfer analyses of these potential non-conventional working fluid mixtures in the absorption process of absorption cooling systems.

Acknowledgements

Faisal Asfand gratefully acknowledges the Rovira i Virgili University for granting the Martí-Franquès research fellowship 2012 (2012BPURV-50) to pursue a doctorate degree.

REFERENCES

Álvarez, M.E., Bourouis, M., Esteve, X., 2011. Vapor–liquid equilibrium of aqueous alkaline nitrate and nitrite solutions for absorption refrigeration cycles with high temperature driving heat. J. Chem. Eng. Data 56, 491–496.

Álvarez, M.E., Esteve, X., Bourouis, M., 2015. Performance analysis of a triple-effect absorption cooling cycle using aqueous (lithium, potassium, sodium) nitrate solution as a working pair. Appl. Therm. Eng. 79, 27–36.

Bourouis, M., Vallès, M., Medrano, M., Coronas, A., 2005a. Absorption of water vapour in the falling film of water-(LiBr + LiI + $LiNO_3$ + LiCl) in a vertical tube at air-cooling thermal conditions. Int. J. Therm. Sci. 44, 491–498.

Bourouis, M., Vallès, M., Medrano, M., Coronas, A., 2005b. Performance of air-cooled absorption air conditioning systems working with water-(LiBr + LiI + $LiNO_3$ + LiCl). J. Process Mech. Eng. 219, 205–212.

Brown, G.G., 1935. Solution cycles as applied to set-up transformers for temperatures. J. Franklin Inst. 219, 405–432.

CREVER-URV, 2012. Thermophysical properties of the fluid mixture water/(LiBr + LiI+$LINO_3$+LICl). Confidential Report. Universitat Rovira i Virgili.

Davidson, W., Erickson, D., 1986. 260 °C aqueous absorption working pair under development. Newsl. IEA Heat Pump Cent. 4, 29–31.

Erickson, D., Potnis, S.V., Tang, J. Triple effect absorption cycles. Energy Conversion Engineering Conference IECEC 96. Proceedings of The 31st Intersociety. 1996; 1072–7.

Feuerecker, G., Scharfe, J., Greiter, I., Frank, C., Alefeld, G., 1993. Measurement of thermophysical properties of aqueous LiBr-solutions at high temperatures and concentrations. Proc. Int. Absorption Heat Pump Conf. ASME 31, 493–499.

Haltenberger, W., 1939. Enthalpy-concentration charts from vapor pressure data. Ind. Eng. Chem. 31, 783–786.

Howe, L., Erickson, D. Proof-of-concept testing of alkitrate. Phase III. Final Report- Energy Concepts Co. 1990. USA.

Koo, K.K., Lee, H.R., Jeong, S., Oh, Y.S., Park, D.R., Baek, Y.S., 1999. Solubilities, vapor pressures, and heat capacities of the water + lithium bromide + lithium nitrate + lithium iodide + lithium chloride system. Int. J. Thermophys. 20, 589–600.

Lange, E., Schwartz, E., 1928. Lösungs and verdünnungswärmen von salzen von äussersten verdünnung bis zur sättigung-IV Lithiumbromid. Z. Physikal. Chem. 133, 129–150.

McNeely, N.A., 1979. Thermodynamics properties of aqueous solutions of lithium bromide. ASHRAE Trans. 85, 413–434.

Medrano, M., Bourouis, M., Coronas, A., 2002. Absorption of water vapour in the falling film of water-lithium bromide inside a vertical tube at air-cooling thermal conditions. Int. J. Therm. Sci. 41, 891–898.

Patek, J., Klomfar, J., 2006. A computationally effective formulation of the thermodynamic properties of LiBr-H2O from 273 to 500 K over full composition range. Int. J. Refrigeration 29, 566–578.

Uemura, T., Hasaba, S., 1964. Studies on the lithium bromide-water absorption refrigeration machine. Tech. Rep. Kansai Univ. 6, 31–55.

Wagner, W., Pruß, A., 2002. The IAPWS formulation 1995 for the thermodynamic properties of ordinary water substance for general and scientific use. J. Phys. Chem. Ref. Data 31, 387–535.

A.3 CFD simulation to investigate heat and mass transfer processes in a membrane-based absorber for water-LiBr absorption cooling systems.

Energy 91 (2015) 517–530

Contents lists available at ScienceDirect

Energy

journal homepage: www.elsevier.com/locate/energy

CFD simulation to investigate heat and mass transfer processes in a membrane-based absorber for water-LiBr absorption cooling systems

Faisal Asfand, Youssef Stiriba, Mahmoud Bourouis*

Department of Mechanical Engineering, Universitat Rovira i Virgili, Av. Països Catalans No. 26, 43007 Tarragona, Spain

ARTICLE INFO

Article history:
Received 25 January 2015
Received in revised form
28 June 2015
Accepted 8 August 2015
Available online 12 September 2015

Keywords:
Heat and mass transfer
Membrane contactors
Plate-and-frame membrane absorber
Water-lithium bromide
Absorption cooling systems
CFD simulation

ABSTRACT

Absorption cooling systems employing membrane based components provide an interesting opportunity to use the technology for small scale applications. Steady-state heat and mass transfer analyses of a water-lithium bromide membrane based absorber are performed. CFD (computational fluid dynamics) tool ANSYS/FLUENT 14.0 is used to perform the simulation and investigate the behaviour of the heat and mass transfer mechanisms at local levels in the channels. Results show that the solution film thickness is an important parameter which significantly affects the mass transfer mechanism. It was observed that the absorption rate increased by a factor of 3 when the solution channel thickness was reduced from 2 mm to 0.5 mm. In addition, the absorption rate was increased by a factor of 2.5 when the solution inlet flow velocity was increased from 0.00118 m/s to 0.00472 m/s. The solution film thickness and velocity can be independently controlled in plate-and-frame membrane based absorbers. Therefore to design a compact and efficient plate-and-frame membrane absorber with water as a refrigerant, an optimum value of 0.5 mm for the solution channel thickness is suggested and a solution inlet velocity of about 0.005 m/s is recommended to achieve high absorption rates with acceptable pressure drop along the solution channel.

1. Introduction

Absorption refrigeration technology is gaining global acceptance due to its potential to use thermal energy, available from solar thermal energy or waste heat energy sources, instead of mechanical energy. The absorber is an important component of the absorption refrigeration system and plays a critical role in the overall performance, size, and capital cost of the system. Both heat and mass transfer take place simultaneously in the absorber. The design and configuration of the absorber significantly influence its performance. Continued improvements in the design and configuration of the absorber have been suggested by many researchers to improve its performance and thermal efficiency. Both active and passive techniques have been investigated for enhancing the absorption rate in the absorbers of absorption refrigeration systems. These techniques are generally categorized into chemical and mechanical treatments [1,2]. In mechanical treatments, corrugated surfaces are produced to enhance the heat and mass transfer coefficients. In chemical treatments, the addition of small quantities of additives (surfactants, nanoparticles, etc.) has been extensively investigated. The heat and mass transfer coefficients are enhanced by causing interfacial turbulence. Numerical and experimental research has been performed, using water-LiBr as a working fluid on horizontal and vertical tubes, to investigate the absorption process. Medrano et al. [3] performed an experimental study and achieved an absorption rate of 0.0020 kg/m^2 s for a vertical tube falling film absorber. Jeong and Garimella [4] numerically investigated a horizontal tube falling film absorber and obtained an absorption rate of 0.0023 kg/m^2 s. Islam et al. [5] experimentally analysed a horizontal tube falling film absorber with film inversion and achieved an absorption rate of 0.0041 kg/m^2 s. Yoon et al. [6] experimentally investigated a helical tube absorber and obtained an absorption rate of 0.0021 kg/m^2 s.

The use of membrane contactor technology is well-known in the process industry and is growing due to the relative simplicity, reliability, high parameters of separation, large interfacial area and lower energy consumption with improved heat and mass transfer. In recent years, research has been carried out regarding the use of membrane contactors in the form of plate-and-frame membrane modules and hollow fibre membrane modules in absorption

* Corresponding author. Tel.: +34 977 55 86 13; fax: +34 977 55 96 91.
E-mail address: mahmoud.bourouis@urv.cat (M. Bourouis).

http://dx.doi.org/10.1016/j.energy.2015.08.018
0360-5442/

Nomenclature

D	mass diffusion coefficient (m^2/s)
d	membrane pore mean diameter (μm)
E	energy (J)
$\vec{F}$	external body force (N)
$\vec{g}$	gravitational force (m/s^2)
h	enthalpy (J/kg)
I	unit tensor
J	mass transfer flux (kg/m^2 s)
k	mass transfer coefficient (kg/m^2 s Pa)
M	molecular weight (g/mol)
P	pressure (Pa)
p	static pressure (Pa)
p_{ms}	vapour pressure of solution (Pa)
R	universal gas constant (J/mol K)
S_h	heat source term (J/m^3 s)
S_m	mass source term (kg/m^3 s)
T	temperature (°C, K)
Y	mass fraction

Greek letters

ρ	density (kg/m^3)
$\vec{v}$	velocity vector (m/s)
ε	porosity
δ	thickness (μm)
τ	tortuosity
λ	thermal conductivity (W/m K)
$\bar{\tau}$	stress tensor
μ	dynamic viscosity (kg/m s)

Subscripts

dil	dilution
eff	effective
i	*ith* specie
m	membrane
p	pore
s	solution
v	vapour

Chemical formula

H_2O	water
LiBr	lithium bromide

refrigeration systems. In the open literature, the plate-and-frame membrane absorber is selected for the absorption refrigeration systems employing water-LiBr as a working fluid mixture, whereas the hollow fibre membrane absorber is selected for the ammonia-water based absorption refrigeration system. The pressure drop in the plate-and-frame membrane module is small; therefore, it is considered a better choice for the water-LiBr working fluid pair. The driving force for the vapour transfer in the case of ammonia-water and water-LiBr solution is considered to be the concentration difference and the water vapour partial pressure difference across the membrane, respectively.

Membrane contactors have been extensively investigated for the desorption process in absorption refrigeration systems, as the process in the desorber resembles that of a membrane distillation process. In recent years, research is being performed to analyse the use of membrane contactors in the absorber and solution heat exchanger. The principle of operation and the use of membrane contactors in the desorber of absorption refrigeration systems can alter the configuration of the cycle. However, the use of membrane contactors in the absorber and solution heat exchanger has no effect on the configuration of the cycle.

Asfand and Bourouis [7] have performed an extensive review on the application of membrane contactors in absorption refrigeration systems. They have concluded from their review that the use of membrane contactors in the absorber and desorber of an absorption refrigeration system can not only enhance the heat and mass transfer performance of the component, but can also allow for a reduction in the size of the component. Thus, introducing polymeric hydrophobic microporous membranes into the absorber design could provide one of the alternatives for achieving highly compact absorbers, as microporous membrane contactors can provide a high specific surface area. Chen et al. [8] performed numerical simulations to study and evaluate the performance of an innovative hybrid hollow fibre membrane absorber. They reported that, for the same absorption rates, the volume of a hollow fibre membrane absorber was only 31% of that of a plate heat exchanger falling film absorber, while the mass transfer interfacial area was 4.3 times of that of a plate heat exchanger falling film absorber. Schaal et al. [9] analytically and experimentally analysed a hollow fibre membrane absorber and reported that the membrane based absorber had a higher mass transfer rate when compared to the plate absorber. They concluded that the size of the absorber could be reduced up to 10 times more than plate absorbers, by utilizing the micro-porous hollow fibre membrane module. However, in their design cooling was not integrated into the hollow fibre absorber module. Ali [10] performed an analytical analysis to design a compact plate-and-frame absorber possessing a hydrophobic microporous membrane contactor at the aqueous solution–water vapour interface. His results demonstrated that the aqueous solution channel thickness greatly influences the absorber size compactness. Ali and Schwerdt [11] investigated experimentally and analytically the characteristics of membrane used in plate-and-frame membrane absorbers. In their experimental study, a solution film thickness of 4 mm was used and a differential pressure of nearly three times the pressure available in a typical absorber was applied. However, the absorption rate was approximately half that of the conventional absorbers. In a conventional absorber, the solution thickness flowing over a tube bundle varies from 0.1 to 1.0 mm. Ali [10] observed that reducing the solution film thickness from 2.5 to 1.0 mm can result in about a 20% increase in the absorption rate. In addition, results reported by Yu et al. [12] showed that a 3-fold increase in the absorption rate can be achieved when the solution film thickness is reduced from 0.15 mm to 0.05 mm. Thus, the low absorption rates obtained in the Ali and Schwerdt [11] analysis could be due to the higher values of the solution film thickness. Also they did not observe a change in the absorption rate when the vapour pressure potential was increased. They ascribed this behaviour to the dominant mass transfer resistance of their membrane. However, recent studies [13,14] suggest that vapour pressure potential has a direct effect on the vapour mass transfer flux across the membrane and that the mass transfer through the solution is the dominant resistance rather than the membrane mass transfer resistance. Isfahani et al. [13] experimentally investigated a membrane based absorber for the absorption of water vapour in the aqueous solution of LiBr and reported that the absorption rate was 2.5 times higher than that in

falling film absorbers. Isfahani and Moghaddam [14] experimentally analysed absorption characteristics of water vapour into a thin LiBr solution constrained by superhydrophobic nanofibrous membrane structures. They studied the effect of water vapour pressure, cooling temperature, solution film thickness and solution mass flow rate on the absorption rate in a membrane based absorber. They achieved an absorption rate of 0.006 kg/m^{2}s with a solution film thickness of 0.1 mm and a velocity of 0.005 m/s. Bigham et al. [15] experimentally and numerically investigated the implementation of micro-scale features on the flow channel surface to induce vortices within the solution film. They reported that the mass transport mode in such a configuration could be changed from a diffusive to an advective mode. They obtained an increase in the absorption rate by a factor of 2.5 i.e. from 0.0016 kg/m^{2}s to 0.004 kg/m^{2}s for the flow channel surface with micro-scale features.

Experimental and analytical analyses have been carried out to investigate the performance of the membrane based absorbers, however, detailed behaviour of the heat and mass transfer mechanisms at local levels in the channels and the fluid dynamic behaviour need to be investigated to better understand the phenomenon and the effect of flow parameters. The objective of this work is to perform a computational fluid dynamic analysis of heat and mass transfer in a membrane based absorber that will help in designing a compact and efficient absorber. Ali [10] developed a one dimensional model to investigate the performance of a plate-and-frame membrane absorber whereas, Yu et al. [12] used a CFD (computational fluid dynamics) solver based on LBM (lattice Boltzmann method) and finite difference method for the concentration and temperature field. In this work, a commercial CFD solver ANSYS/FLUENT 14.0, which is based on Navier–Stokes equations that are solved using finite volume method, is used to simulate the mass transfer across the membrane and the heat transfer between the solution and coolant in the absorber. Navier–Stokes equations are capable of solving both unsteady (time-dependent) and steady-state equations whereas Lattice Boltzmann equations are inherently unsteady and are more attractive to solve transient simulation. As in this study a steady-state analysis is performed therefore CFD solver based on the Navier–Stokes equation was selected as a favourable option. A plate-and-frame absorber module incorporating membrane contactor at the solution-vapour interface is selected for simulation with water-LiBr as a working fluid pair. A parametric study is performed to investigate the effect on the absorption rate of the solution channel thickness, solution flow rate and coolant wall temperature. The solution pressure drop along the channel length which is an important parameter of concern in water-LiBr based absorbers, working under vacuum condition, is investigated in detail. The effect of solution channel thickness and solution mass flow rate on the solution pressure drop along the solution channel length is critically analysed which was not previously reported. Further, the fluid dynamics behaviour of the water-LiBr solution is investigated and the effect of thermophysical properties on the solution flow profile is discussed as well. In addition, a case study is selected to analyse the boundary layers at the solution membrane interface and the local profiles of velocity, temperature and concentration of the working fluid in order to better understand heat and mass transfer phenomena.

2. Membrane absorber configuration

The structural unit of the plate-and-frame absorber with membrane contactor is shown in Fig. 1. The configuration of the plate-and-frame absorber is set as such that the lattice cell consists of a metallic plate for heat transfer and a microporous hydrophobic membrane sheet for both the heat and mass transfer. The membrane contactor is placed at the aqueous solution–water vapour interface in the form of parallel sheet along metallic plates to create individual flow channels. The parallel assembly of the plates and membrane sheets minimizes the pressure drop through the absorber. Three thin channels of refrigerant, coolant and absorbent solution are formed. Each refrigerant channel serves two absorbent solution channels at each side. Similarly the coolant channel also serves two aqueous solution channels. The first and last cells of the module have half width coolant channels.

The absorbent solution and the coolant flow along the metallic plate in a counter flow direction during which only heat transfer takes place. Water vapour and absorbent solution are brought into contact with each other using the microporous membrane contactor. Only refrigerant vapours pass through the pores of the membrane. If the absorbent is a solution containing water, then a hydrophobic microporous membrane can be effectively utilized to stop the solution from passing through the pores of the membrane. As the water vapour pressure is more than the partial pressure of the water vapour inside the solution, the water vapour is absorbed at the solution-vapour interface and then diffused into the solution film.

2.1. Membrane material characteristics

In this study, a flat sheet membrane contactor made of polypropylene material is used. The membrane material characteristics are tabulated in Table 1.

2.2. Thermophysical properties

In the ANSYS/FLUENT 14.0 code material database water-LiBr mixture is not available. Therefore, a mixture of H_2O-LiBr was created in the material panel of ANSYS/FLUENT 14.0 code and the thermophysical properties of the water-LiBr mixture were updated in the ANSYS/FLUENT 14.0 code database using user-defined functions [16,17]. These thermophysical properties of the aqueous solution of lithium bromide are calculated as a function of solution concentration in lithium bromide and temperature. The density and viscosity of the aqueous solution of lithium bromide were calculated using the correlations developed by Lee et al. [18]. The thermal conductivity of the water-LiBr mixture was calculated using the correlation of DiGuilio et al. [19]. Specific heat capacity of the water-LiBr mixture was calculated using the correlation based on McNeely data [20]. The diffusion coefficient of water in the aqueous lithium bromide solution was calculated from the experimental data of Kashiwagi et al. [21] which was determined at constant temperature and different concentrations. However, at other temperature the diffusion coefficient was estimated using the equation given below.

$$\frac{D_1\mu_1}{T_1} = \frac{D_2\mu_2}{T_2} \tag{1}$$

where D is the diffusion coefficient, μ is the dynamic viscosity and T is the temperature. State 1 refers to the values calculated at 25 °C whereas sate 2 refers to the values calculated at any other temperature. A user-defined function was implemented in the ANSYS/FLUENT 14.0 code to estimate the value of diffusion coefficient using the above procedure at different concentration and temperature of the solution.

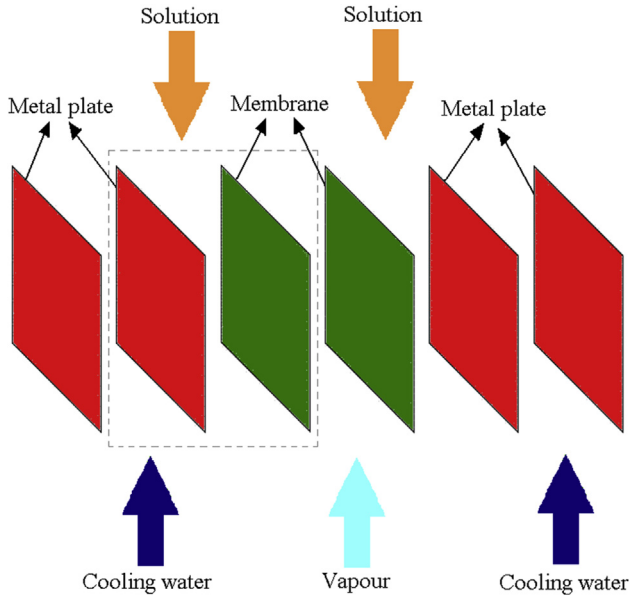

Fig. 1. Plate-and-frame absorber configuration with membrane contactor.

3. Governing equations

In the present simulations of mass transfer across the membrane and heat transfer between the solution and coolant in the absorber, the flow in each channel is a homogeneous single phase flow. As the species in the solution are well mixed, the relative velocity between the species is negligible. In the absence of relative motion the governing mass and momentum conservation equations for homogeneous flow are reduced to the single-phase form. Therefore, instead of a mixture model, single phase equations are used to perform the simulation with less computational effort. The continuity, momentum, energy and species transport equations are solved to perform steady-state heat and mass transfer analyses.

The general steady-state equation of continuity which is based on the conservation of mass is given by:

$$\nabla\cdot(\rho\vec{v}) = S_m \tag{2}$$

where ρ is the density and $\vec{v}$ is the velocity vector. S_m is the mass source term which is added to the continuity equation and it is the vapour mass that is absorbed into the solution at the solution-membrane interface. The mass source term S_m is added using a user-defined function at the solution-membrane interface to model the vapour mass transfer across the membrane. The driving force for the vapour mass transfer flux into the aqueous solution in a H_2O-LiBr absorber is the water vapour partial pressure difference. The mass transfer flux across the membrane is given by Martinez and Rodriguez–Maroto [22] as follows:

$$J = k_m(P_v - p_{ms}) \tag{3}$$

where P_v is the water vapour pressure and p_{ms} is the equilibrium water vapour partial pressure of the solution at the membrane pores entrance and is calculated at the solution-membrane interface as a function of the solution concentration and temperature using the vapour pressure correlation given by Ref. [23]. k_m is the membrane equivalent mass transfer coefficient which is expressed in Ali [10] as follows:

$$k_m = \frac{2}{3}\cdot\frac{\varepsilon}{\tau\cdot\delta_m}\cdot d_p\cdot\sqrt{\frac{2}{\pi}\cdot\frac{M_{H_2O}}{R\cdot T_m}} \tag{4}$$

where, ε is the membrane porosity, τ is the tortuosity of the membrane, δ_m is the membrane thickness and d_p is the membrane pore mean diameter. M_{H_2O} is the molecular weight of water, R is the universal gas constant and T_m is the membrane mean temperature which is calculated as the average of vapour and solution interface temperatures.

The steady-state momentum conservation equation has the following form:

$$\nabla\cdot(\rho\vec{v}\vec{v}) = -\nabla p + \nabla\cdot(\bar{\tau}) + \rho\vec{g} + \vec{F} \tag{5}$$

where p is the static pressure, $\rho\vec{g}$ is the gravitational body force while $\vec{F}$ is the external body force which arises as a result of the interaction of the vapour mass added to the bulk solution. $\bar{\tau}$ is the stress tensor and is given by

$$\bar{\tau} = \mu\left[\left(\nabla\vec{v} + \nabla\vec{v}^T\right) - \frac{2}{3}\nabla\cdot\vec{v}I\right] \tag{6}$$

where μ is the molecular viscosity and I is the unit tensor.

The steady-state energy equation has the following form:

$$\nabla\cdot(\vec{v}(\rho E + p)) = \nabla\cdot\left(k_{eff}\nabla T - \sum_j h_j\vec{J}_j + \left(\bar{\tau}_{eff}\cdot\vec{v}\right)\right) + S_h \tag{7}$$

where T is the temperature in K, k_{eff} is the effective thermal conductivity, $\vec{J}_j$ is the diffusion flux of the specie j, h_j is the enthalpy of specie j and the third term on the right hand side is the energy transfer from viscous dissipation. E is given as:

$$E = h - \frac{p}{\rho} + \frac{v^2}{2} \tag{8}$$

where h is the sensible enthalpy and is defined for the incompressible flow as follows:

$$h = \sum_j Y_j h_j - \frac{p}{\rho} \tag{9}$$

S_h is the heat source term which is included to incorporate the heat of absorption in the solution and is added to the energy equation using a user-defined function. The heat of absorption S_h is calculated as:

$$S_h = h_v - h_s + h_{dil} \tag{10}$$

where h_v is the vapour enthalpy, h_s is the solution enthalpy and h_{dil} is the heat of dilution. h_v was calculated using the correlation reported by Florides et al. [24], h_s was calculated using the correlation reported by Kaita et al. [23], h_{dil} was calculated from the data of McNeely [20].

The steady-state species transport equation for the prediction of the local mass fraction of each specie is given as:

Table 1
Membrane material characteristics.

Thickness, δ_m (μm)	60
Porosity, ε (%)	75
Tortuosity, τ ($\tau = (2-\varepsilon)^2/\varepsilon$)	2.083
Mean pore diameter, d_p (μm)	0.45
Thermal conductivity, λ (W/m K)	0.17

$$\nabla\cdot(\rho\vec{v}Y_i) = -\nabla\cdot\vec{J}_i + S_i \quad (11)$$

where Y_i is the mass fraction of specie i, S_i is the specie source term which is added at the solution-membrane interface using a user-defined function and is equal to the mass of the water vapour transferred to the solution at the interface. $\vec{J}_i$ is the diffusion flux of specie i, which is given as:

$$\vec{J}_i = -\rho D_{H_2O-LiBr}\nabla Y_i \quad (12)$$

where $D_{H_2O-LiBr}$ is the mass diffusion coefficient of water in an aqueous solution of lithium bromide.

4. Numerical simulation

Numerical simulations were performed to analyse the heat and mass transfer processes in a plate-and-frame membrane absorber. CFD commercial code ANSYS/FLUENT 14.0 was utilized for the numerical simulation which employs a finite volume approach to discretize the governing Navier–Stokes equations into a set of linear equations. The computational domain, boundary conditions and numerical schemes adopted in this study are illustrated in the following subsections.

4.1. Computational domain and boundary conditions

A two-dimensional model was developed to simulate the flow, heat and mass transfer phenomena in a single unit of the plate-and-frame membrane module. Fig. 2(a) shows a 2D sectional view of a single unit of the plate-and-frame membrane absorber. To reduce the computational time and get a converged solution without flow instabilities, the vapour pressure of the vapour channel is assumed constant, as the vapour coming from the evaporator is at a constant pressure. Further, heat transfer across the membrane and the consequent temperature rise of the vapour are not significant to considerably affect the mass transfer potential because of the low thermal conductivity of the membrane material. In addition, the mass transfer potential in a plate-and-frame membrane absorber employing water-LiBr as a working fluid is dependent primarily on the vapour pressure difference across the membrane. The rise in the vapour temperature because of heat transfer does not directly affect the mass transfer mechanism. Therefore, the vapour channel is not considered in the computational domain of the simulation. Hence, the mass of water vapour is added as a source term at the solution-membrane interface. Symmetric boundary conditions are considered on the left side of the coolant flow channel to reduce the computational efforts. The computational domain is shown in Fig. 2(b). The heat transfer plate between the solution and coolant is considered as a wall boundary condition. Inlet boundary conditions in the solution and coolant flow channels are considered as velocity inlets, while outlet boundary conditions are specified as pressure outlets. The coolant temperature profile along the channel obtained from the initial converged steady-state simulation was used as a coolant wall temperature profile for the rest of the parametric analysis to minimize the computational time using only the solution channel. A wall temperature function was imposed at the heat transfer plate using a user-defined function to incorporate the linearized change in coolant temperature along the channel.

The spatial domain of the simplified model was discretized into meshes fine enough to produce mesh-independent results. The grids were created in Gambit software and imported into ANSYS/FLUENT 14.0. Different grid sizes were tested for the 0.5 mm solution channel and the 15 × 15,000 cells mesh size, with a minimum edge size of 0.00002 was selected for the simulation analysis. Both the boundary layers on the coolant side and the membrane side comprised of 4 cells each with a growth factor of 1.2. The remaining cells in the middle of the solution channel were of the same size. Grid independence test showed that the maximum error in the absorption rate was less than 1% when the grid size was reduced by a factor of 2.

4.2. Numerical model and discretization scheme

The governing equations of continuity, diffusion and energy are used to perform a numerical analysis of combined heat and mass transfer in a plate-and-frame membrane absorber. As the solution flow Reynolds number is low, a laminar model is selected for the analysis. The calculations were performed by a combination of the SIMPLE (Semi-Implicit Method for Pressure Linked Equations) algorithm for pressure–velocity coupling and the first-order accurate implicit scheme for the linearized discretized equation in the segregated solver. A second-order upwind discretization scheme was used to compute advection terms. For the energy and specie transport equation, a second-order discretization scheme was used. In the present work, the numerical computation is considered to have converged when the scaled residuals of the different variables (continuity, momentum, species and energy equations) are lowered by tenth orders of magnitude and the steady state results are analysed.

5. Results and discussion

CFD simulations are capable of predicting the detailed behaviour of heat and mass transfer at local regions, thus, a clear pattern of the temperature and concentration gradients and velocity profiles are obtained. In the following subsections, the numerical model is validated with data from the open literature and a parametric analysis is performed to investigate the effects of solution channel thickness, solution mass flow rate and coolant wall temperature on the absorption process. Based on the parametric analysis results, a suitable geometry with optimal input operating conditions is selected for a detailed analysis of heat and mass transfer at local levels.

5.1. Validation

The CFD numerical model was validated by reproducing the results of the numerical analysis performed by Yu et al. [12] for a membrane based absorber in which the LBM (lattice Boltzmann method) was used to investigate the heat and mass transfer phenomena in a 20 mm long and 0.05 mm thick solution channel with an inlet solution velocity of 0.0182 m/s, and an inlet solution concentration and temperature of 60% and 55 °C, respectively. The local absorption rate obtained using the CFD simulation is compared with the results reported by Yu et al. [12] for the corresponding case. The CFD results show good agreement with the literature data as shown in Fig. 3. The mean absolute percent error was found to be 4.82% with a standard deviation of 0.0322.

5.2. Parametric study

In this section, the results of the parametric study performed to investigate the effect of operational and geometric parameters on the absorption rate are discussed. Solution channel thickness, solution mass flow rate and coolant wall temperature were varied to investigate their impact on the absorption rate. The input data in the parametric study correspond to the operating conditions of a

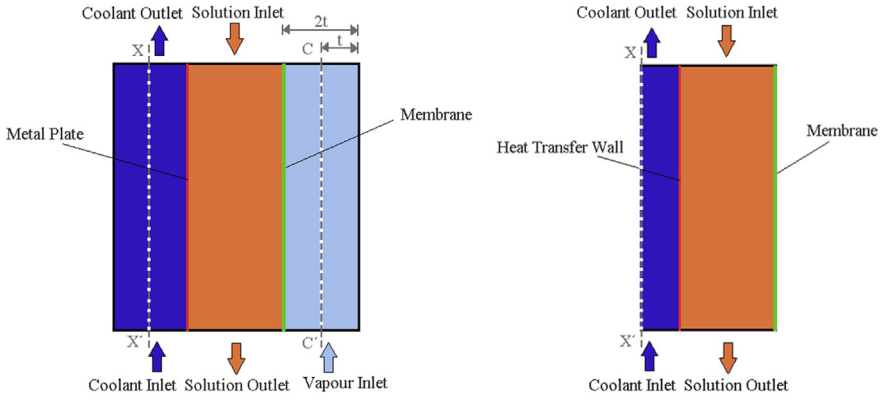

(a) Single unit of the plate-and-frame absorber

(b) Computational domain of the plate-and-frame absorber

Fig. 2. 2D sectional view of a single unit of plate-and-frame absorber.

typical absorption refrigeration system. These operating conditions and geometric dimensions are listed in Table 2.

Fig. 4 shows the results of the analysis carried out to investigate the effect of the solution film thickness on the absorption rate. Solution mass flow rate and other input variables were kept constant in all the cases except the solution channel thickness which was varied from 0.25 mm to 2 mm Fig. 4(a) shows the local mass transfer flux along the channel obtained for different values of the channel thickness. It is observed that the absorption rate increases with a decrease in the solution channel thickness. It can be noted that a higher absorption rate is achieved at the inlet of the absorber due to the low mass fraction of water in the solution at the inlet and a lower solution interface temperature. A decreasing trend in the absorption rate is observed in the first quarter of the absorber while a steady absorption rate is achieved in the later part of the absorber.

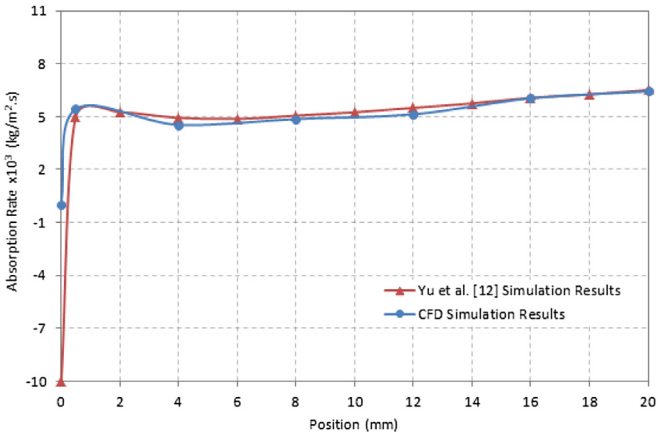

Fig. 3. Comparison of the local absorption rate of the present work with data reported by Yu et al. [12].

Table 2
Input data for the parametric study.

Parameter	Base value	Range
Absorber pressure, Pa	813.5 Pa	NA
Inlet solution temperature, T_s	35.5 °C	NA
Inlet solution concentration, X_s	57.82%	NA
Solution velocity, $\vec{v}$	0.00472 m/s	0.00118–0.00944 m/s
Cooling wall temperature, T_c	25–33 °C	25–43 °C
Solution channel thickness, t	0.5 mm	0.25–2 mm
Solution channel length, L	400 mm	NA

Initially a high mass transfer flux is observed as the solution concentration in LiBr is high, however, the absorption rate decreases sharply as concentration and temperature boundary layers are developed consequently forming a resistance to the absorption of water vapours in the solution. A steady mass transfer occurs in the later part of the channel as the coolant wall linearly dissipates heat of absorption and allows the solution to cool down and maintain the absorption capacity of the solution. Fig. 4(b) shows the overall mass transfer flux obtained for different values of the solution

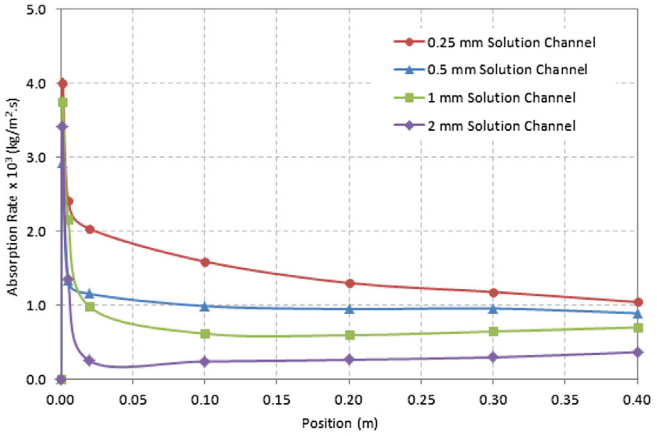

(a) Local mass transfer flux along the channel

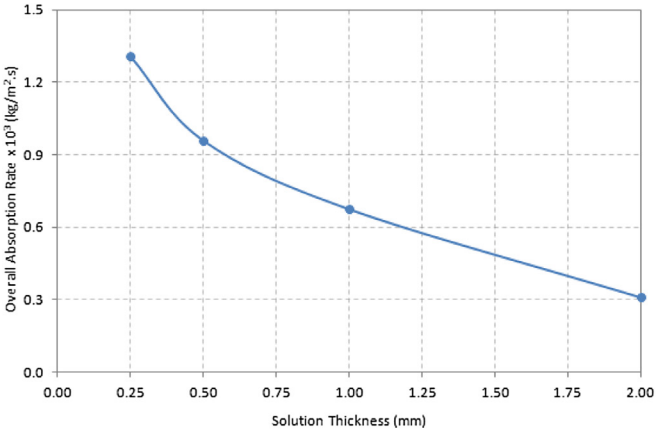

(b) Overall absorption rate

Fig. 4. Effect of the solution channel thickness on the absorption rate along the channel.

channel thickness. It is observed that the overall absorption rate increased by a factor of 3 when the solution channel thickness was reduced from 2 mm to 0.5 mm. Increase in the absorption rate is more significant for lower values of the solution channel thickness as seen in Fig. 4(b). This is because a thinner solution channel leads to a higher solution flow Reynolds number and consequently thinner temperature and concentration boundary layers are formed which enhance the heat and mass transfer coefficients. In addition, the concentration and temperature gradients across the channel are less pronounced in the bulk solution for the thinner channel when compared to the thicker solution channel. Fig. 5(a) shows how the overall percent pressure drop along the channel increases when the solution channel thickness is reduced. In this study, the solution pressure at the absorber exit is set at 813.5 Pa which is the corresponding saturation pressure at a water vapour temperature of 4 °C. The overall percent pressure drop is calculated with reference to absorber inlet pressure. It can be seen that the overall percent pressure drop increases exponentially when the solution film thickness is reduced. A 50% decrease in the solution film thickness causes an increase in the accumulative pressure drop by a factor of approximately 7.5. Fig. 5(b) shows the accumulative pressure drop along the channel length for different values of the solution channel thickness. It is observed that the pressures drop linearly along the channel length for thinner solution channels. However, for thick solution channels the pressure drop in the first quarter is very small when compared to the later part of the channel. The absorption rate is significant in the first quarter of the solution channel up to 100 mm in length. However, the absorption rate decreases and remains constant in the remaining part of the absorber. Thus, reducing the channel length can lead to a higher overall absorption rate and a low pressure drop.

Fig. 6 shows the effect of the solution flow velocity on the absorption rate for a 0.5 mm solution channel thickness. Solution inlet velocity is increased from 0.00118 m/s to 0.00944 m/s while all other input parameters are kept constant in the simulation of each case. Fig. 6(a) shows the local mass transfer flux along the channel obtained for different solution inlet velocities. It can be seen that the absorption rate increases with an increase in the inlet velocity of the solution. Initially a high absorption rate is observed as the solution concentration in LiBr is high, however, the absorption rate decreases sharply as concentration and temperature boundary layers are developed which resist the absorption of water vapours in the solution. A steady mass transfer occurs in the later part of the channel as the coolant wall linearly dissipates heat of absorption and allows the solution to cool down which consequently increases the absorption capacity of the solution. Fig. 6(b) shows the overall absorption rate obtained for different values of the solution inlet velocity. It is observed that the increase in the overall absorption mass flux is more significant initially as the increase in the solution velocity brings fresh layers of solution near the membrane interface which increases the absorption capacity. However, further increasing the solution velocity decreases the solution residence time and minimizes the diffusion of the vapour across the solution causing a negative effect on the absorption mass flux. The absorption rate was increased by a factor of 2.5 when the solution

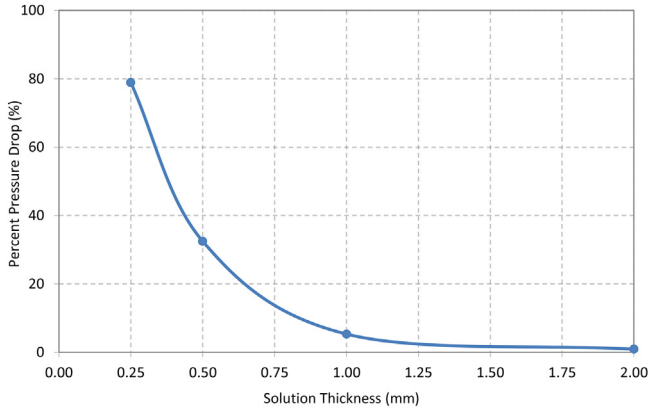

(a) Overall pressure drop vs solution channel thickness

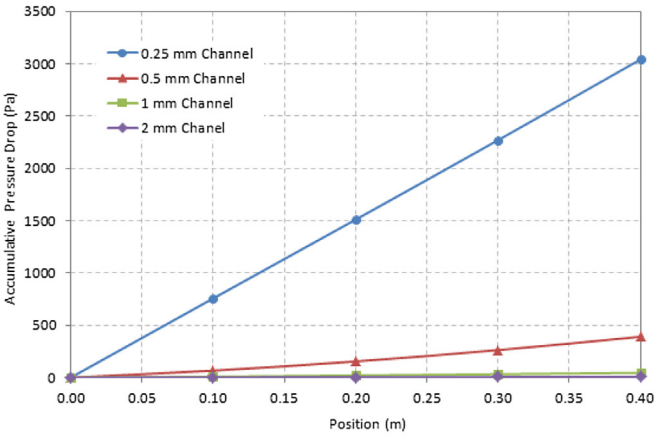

(b) Accumulative pressure drop along the solution channel

Fig. 5. Effect of the solution channel thickness on the pressure drop.

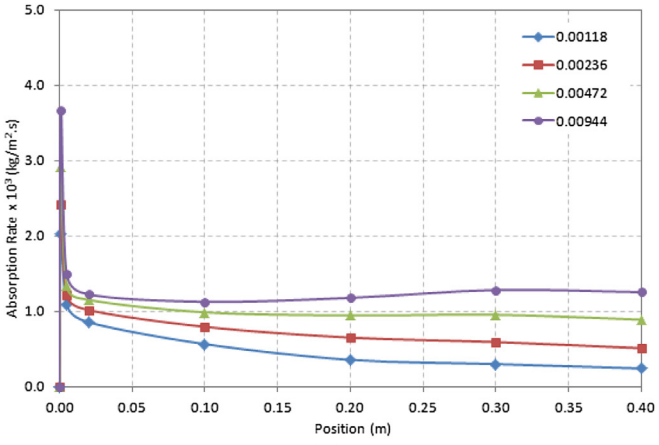

(a) Local mass transfer flux along the channel

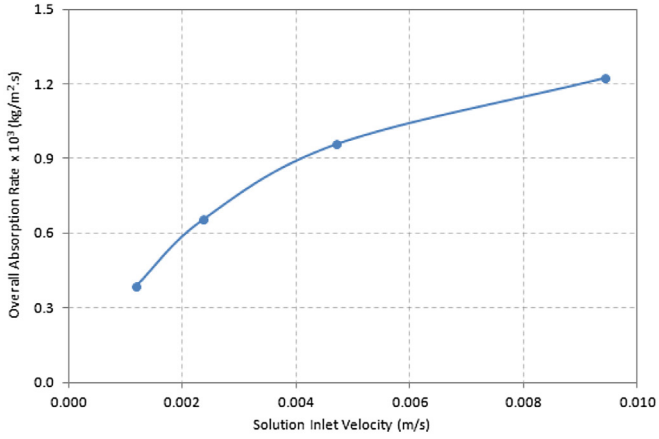

(b) Overall absorption rate

Fig. 6. Effect of the solution flow velocity on the absorption rate along the channel.

inlet velocity was increased from 0.00118 m/s to 0.00472 m/s. The overall percent pressure drop along the channel for different flow velocities is shown in Fig. 7(a). The pressure drop increases by a factor of approximately 2.1 when the solution flow velocity is doubled. For example, increasing the solution flow velocity from 0.00236 m/s to 0.00472 m/s resulted in an increase in the pressure drop from 187 Pa to 391 Pa. However, it is observed that the overall percent pressure drop does not increase more sharply at higher velocities. It was observed that the accumulative pressure drop along the channel increases linearly with an increase in the solution flow velocity. Fig. 7(b) shows the accumulative pressure drop along the 0.5 mm solution channel at different solution inlet velocities. It can be noted that the pressure drop is more significant in the later part of the solution channel for low solution inlet velocities. However, at higher solution inlet velocities, the pressure drops linearly along the channel length. For the solution inlet velocity of 0.00236 m/s, the pressure drop in the first quarter of the channel is only about 2% whereas about 45% of the pressure drop is observed in the last quarter of the solution channel. Thus, it can be concluded that reducing the channel length can significantly minimize the pressure drop along the channel length.

It is important to note that although both solution flow velocity and solution film thickness can be independently varied in a plate-and-frame absorber, an optimum value of solution flow velocity and solution film thickness have to be selected to minimize the pressure drop which can significantly affect the performance of an absorber operating with water as a refrigerant under vacuum conditions.

Fig. 8 shows the effect of the coolant wall temperature on the absorption rate for a 0.5 mm solution channel of 100 mm length. The coolant wall temperature was varied from 25 – 30 °C to 35–40 °C while all other input parameters were kept constant in the simulation of each case. Fig. 8(a) shows the local mass transfer flux along the channel obtained for different coolant wall temperatures. It can be seen that the absorption rate decreases when the coolant wall temperature is increased. This is because with an increase in the coolant wall temperature, the heat of absorption is not well dissipated and thus the solution temperature increases and lowers the absorption capacity of the solution. Fig. 8(b) shows the overall absorption rate for different coolant wall temperatures. It can be seen that the absorption rate decreases linearly with an increase in the coolant wall temperature. The absorption rate decreases by a factor of 5 when the coolant wall temperature is increased from 25 – 30 °C to 35–40 °C.

5.3. Case study

Optimum values of the solution flow velocity and solution channel thickness were selected for detailed analysis and comparison of heat and mass transfer at local levels. A solution channel thickness of 0.5 mm and a solution flow velocity of 0.00472 m/s, yielding a high absorption rate and lower pressure drop along the

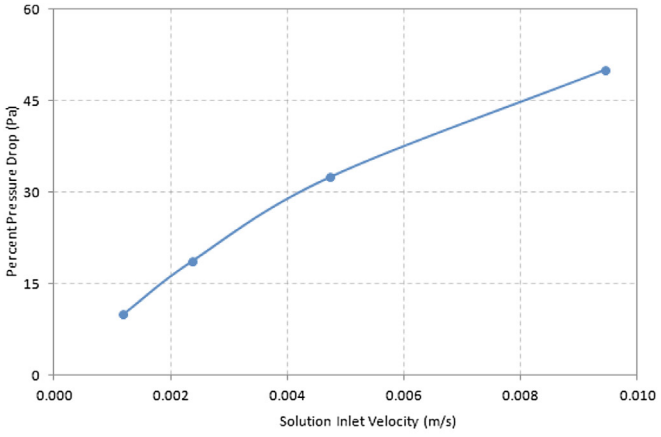

(a) Overall pressure drop vs solution inlet velocity

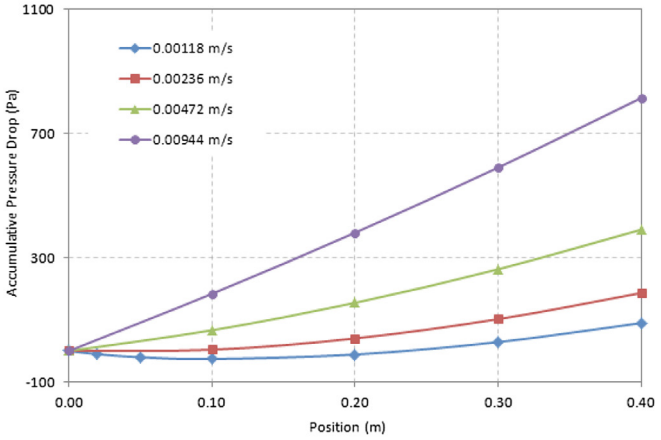

(b) Accumulative pressure drop along the solution channel

Fig. 7. Effect of the solution flow velocity on the pressure drop.

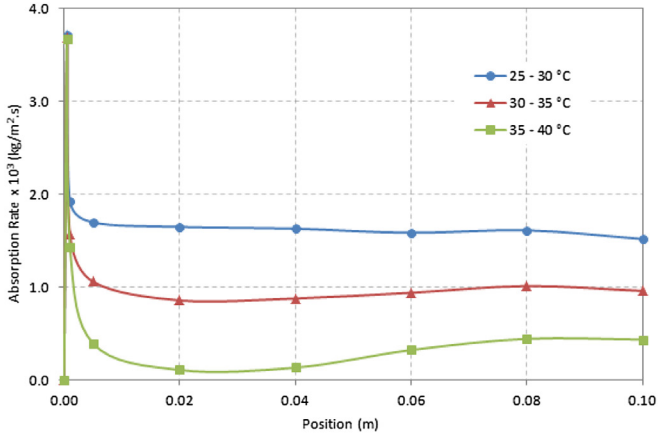

(a) Local absorption rate along the channel

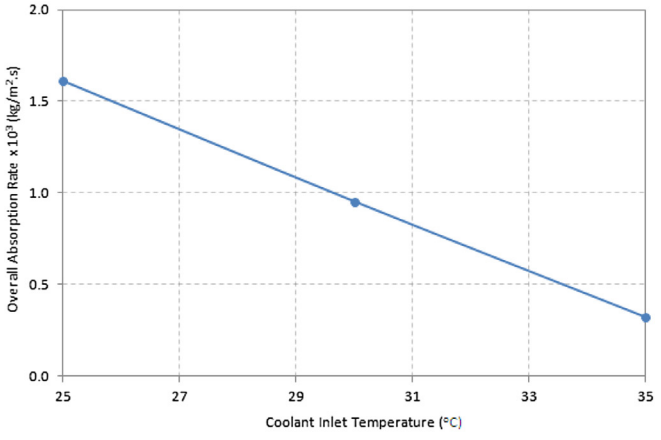

(b) Overall absorption rate

Fig. 8. Effect of the coolant wall temperature on the absorption rate along the channel.

solution channel, were selected for a detailed analysis of the absorption process and comparison with the 2 mm solution channel. Fig. 9 shows the contour of a velocity profile at the exit of the solution channel. It can be seen that a laminar flow profile of the velocity distribution is obtained because of low solution flow rates along the rectangular channel. Fully developed flow profile is obtained at the exit of the 2 mm and 0.5 mm solution channels as shown in Fig. 9(a) and (b), respectively. However, temperature and concentration gradients do slightly affect the flow profile because of the change in the solution density which causes buoyancy forces. It can be observed from Fig. 9(a) that the flow velocity near the solution-membrane interface (right side) along the solution channel is lower compared to the solution velocity near the heat transfer wall (left side). This is because of the effect of buoyancy forces which are observed at the solution-membrane interface due to the change in density. The density of the solution near the solution-membrane interface is lower than in the bulk, as the concentration of water in the solution is higher near the solution-membrane interface due to the absorption of water vapour and also the temperature of the solution is higher at the solution-membrane interface as a result of the heat of absorption. However, in Fig. 9(b) the velocity varies uniformly across the channel at the outlet. This is mainly because of the low temperature gradient across the 0.5 mm channel. Therefore, the variation in buoyancy forces is not significant across the channel. Soret and Dufour effects are negligible in this study as there is a small temperature gradient across the channel and no chemical reaction takes place.

In Fig. 10(a) and (b), contours of temperature profiles at the inlet, exit and at the mid of the channel are shown for the 0.5 mm and 2 mm solution channels, respectively. Fig. 10 depicts temperature values at local regions different to those in the bulk solution and a temperature gradient is observed across the width of the channel. It can be seen that the temperature near the solution-membrane interface (right side) is higher than the bulk solution temperature. This is because of the heat of absorption at the solution-membrane-interface. The temperature difference between the bulk solution and the solution-membrane interface is higher (up to 1.5 °C) near the inlet of the channel and then decreases downward to a steady value of 1 °C along the 0.5 mm solution channel. This is because of the higher absorption rate at the inlet which generates more heat at the solution-membrane interface and thus a higher temperature gradient is observed. However, in case of 2 mm channel the temperature difference between the bulk solution and the solution-membrane interface is higher and is about 5 °C. It is observed that initially the thermal boundary layer formed in the 2 mm channel is about 2–3 times thicker than the thermal boundary layer in the 0.5 mm channel. Due to the formation of the thermal boundary layer a resistance to heat and mass transfer is observed. Therefore, a temperature gradient exists across the solution channel which is about 4 °C higher in the case of the 2 mm channel than the 0.5 mm channel. This shows that in the 0.5 mm channel heat is well dissipated from the solution-membrane interface to the coolant side. Similarly, it can be observed from Fig. 11(a) and (b) that the water concentration in the solution is higher at the solution-membrane interface (right side) due to absorption of water vapour at the interface. The water molecules diffuse across the solution at a low rate due to the low diffusivity which gives rise to a concentration gradient across the solution channel. The concentration boundary layer developed at the solution-membrane interface also plays an important role in limiting the mass transfer rate. The concentration boundary layer in the 2 mm channel is significantly thicker than in the 0.5 mm channel. The effect of the formation of the concentration and thermal boundary layers in the solution channels near the solution-membrane interface is reflected as a low local absorption rate because the formation of these boundary layers limits the absorption capacity of the solution. The LiBr concentration at the solution-membrane interface is approximately 1.8% lower than in the bulk solution in the 0.5 mm channel.

The bulk solution temperature and concentration, coolant wall temperature, and solution-membrane interface temperature and concentration are graphically represented along the channel length in Fig. 12. It can be seen that the bulk solution temperature decreases from 35.5 °C to 26.5 °C as it flows downward along the channel because of the heat transfer to the coolant which temperature is adjusted as a wall temperature and varies linearly from 25 °C to 33 °C in the counter flow direction. Similarly, the interface solution temperature drops from 38.0 to 27.4 °C. The mass fraction of LiBr in the bulk solution decreases along the channel length due to the absorption of water vapour in the solution. It is observed that both the bulk solution concentration and interface solution concentration decrease at the same rate therefore, a transverse concentration gradient along the solution channel exists till the end of the solution channel. As the concentration difference between the bulk solution and solution-membrane interface also acts as a driving force for the mass transfer, water vapour absorption is observed till the channel exit. It is worth to note that the mass fraction of water in the bulk solution and at the solution-membrane interface increase along the channel length, however, both the bulk solution temperature and the solution-membrane interface temperature decrease along the channel length which in turn causes a decrease in the partial pressure of water vapour in the solution and an increase in the absorption capacity.

Fig. 13 shows a comparison of the bulk solution concentration along the 0.5 mm and 2 mm solution channels. It is observed that reducing the solution channel thickness enhances the absorption rate and as a result the exit bulk solution concentration achieved in case of a 2 mm solution channel can be achieved at a length of about 0.115 m in case of 0.5 mm solution channel. Thus, decreasing the channel thickness from 2 mm to 0.5 mm and reducing the absorber length from 400 mm to 100 mm can decrease the solution space requirement by a factor of 16, whereas the absorber size can be reduced by a factor of about 5.5 keeping the same thickness of 1.5 mm and 1 mm for the coolant and vapour channels, respectively. Further, for smaller channel length a lower pressure drop will be observed. Thus, considering a thinner channel with reduced length can both allow a higher absorption rate and a lower pressure drop along the channel. Therefore, reducing the channel thickness and length can allow for the design of highly compact membrane absorbers.

From the contours of the thermophysical properties shown in Fig. 14 for the 0.5 mm solution channel, it can be observed that the solution thermophysical properties vary at local levels based on the local concentration and temperature. It can be seen that the density of the solution near the solution-membrane interface (right side) is lower because of the higher mass fraction of water at the interface and the higher temperature caused by the heat of absorption. Similarly, the viscosity and thermal conductivity of the solution vary at local levels due to the variation of the water mass fraction in the solution and temperature at local levels. The effects of density and viscosity at local levels on the solution flow can be seen in the velocity profile of the solution at the exit of the channel as shown in Fig. 9(a) in which the velocity near the solution-membrane interface is lower due to buoyancy forces caused by the low density of the solution. The low velocity at the interface inversely affects the mass transfer mechanism by developing thermal and concentration boundary layers at the solution-membrane interface thus limiting the absorption process. The higher thermal conductivity near the solution-membrane interface has a positive effect on heat transfer and can enhance heat transfer from the interface to the bulk solution.

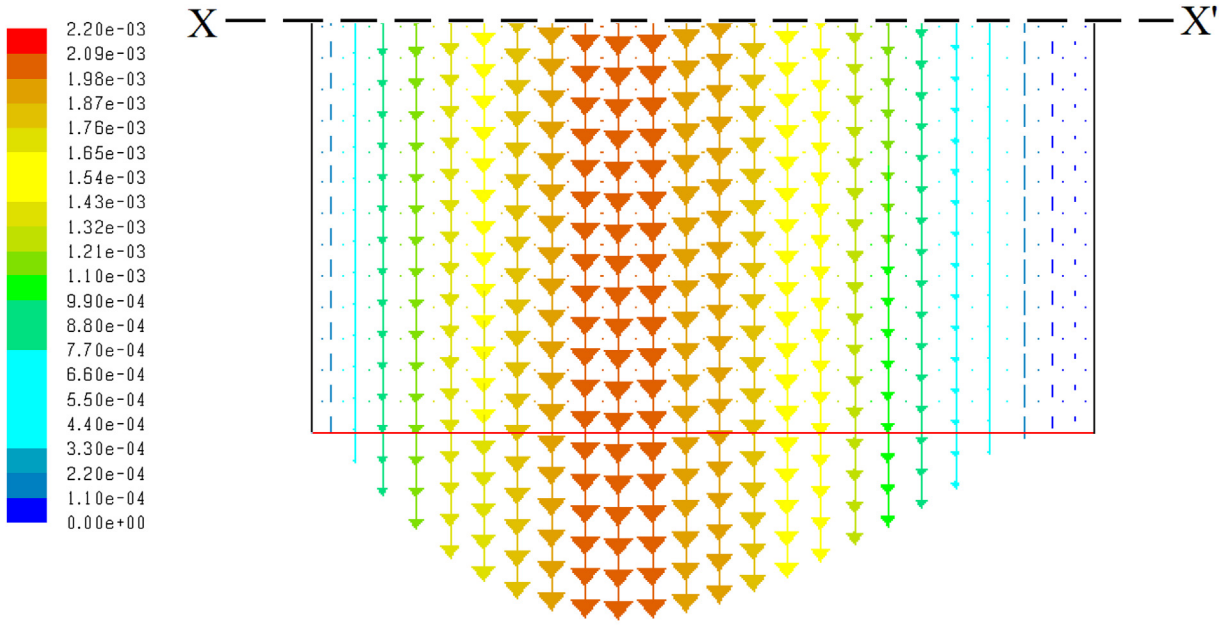

(a) 2 mm Channel

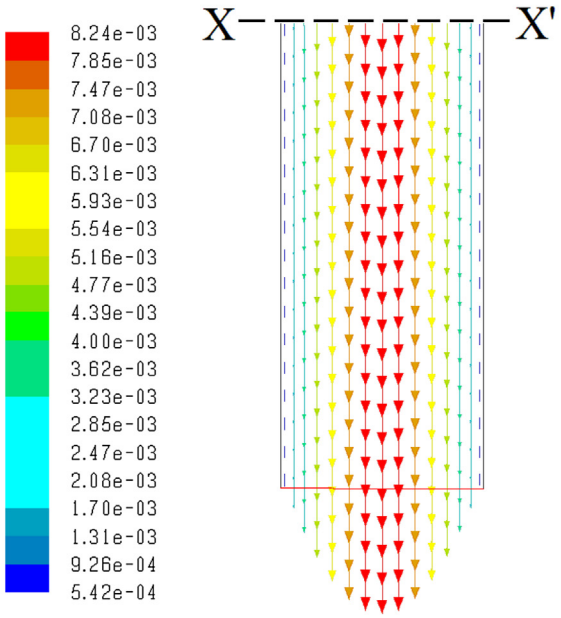

(b) 0.5 mm Channel

Fig. 9. Contours of the velocity vectors (m/s) at the exit of the solution channel.

5.4. Discussion

From the above results, it is clear that a plate-and-frame membrane based absorber employing water-LiBr as a working fluid mixture could be an interesting alternative for the design of compact absorbers with enhanced heat and mass transfer. In this study, for a 0.5 mm solution channel with a solution inlet velocity of 0.00472 m/s, an average absorption rate of the order 0.001 kg/m^2 s was achieved whereas, Isfahani and Moghaddam [14] achieved an average absorption rate of approximately 0.006 kg/m^2 s for a solution channel thickness and flow velocity of 0.1 mm and 0.005 m/s, respectively. Similarly, Yu et al. [12] achieved an overall absorption rate of above 0.009 kg/m^2 s when the solution channel thickness and solution flow velocity were considered of the order 0.05 mm and 0.15 m/s. It is clear that decreasing the solution channel thickness can significantly increase the absorption rate. However, it is worth to mention that the pressure drop increases exponentially with decrease in the solution channel thickness. As the absorber of an absorption refrigeration system employing water-LiBr operates under vacuum pressure therefore the high pressure drop in the solution channel could result in critical problems. Bigham et al. [15] achieved an overall absorption rate of

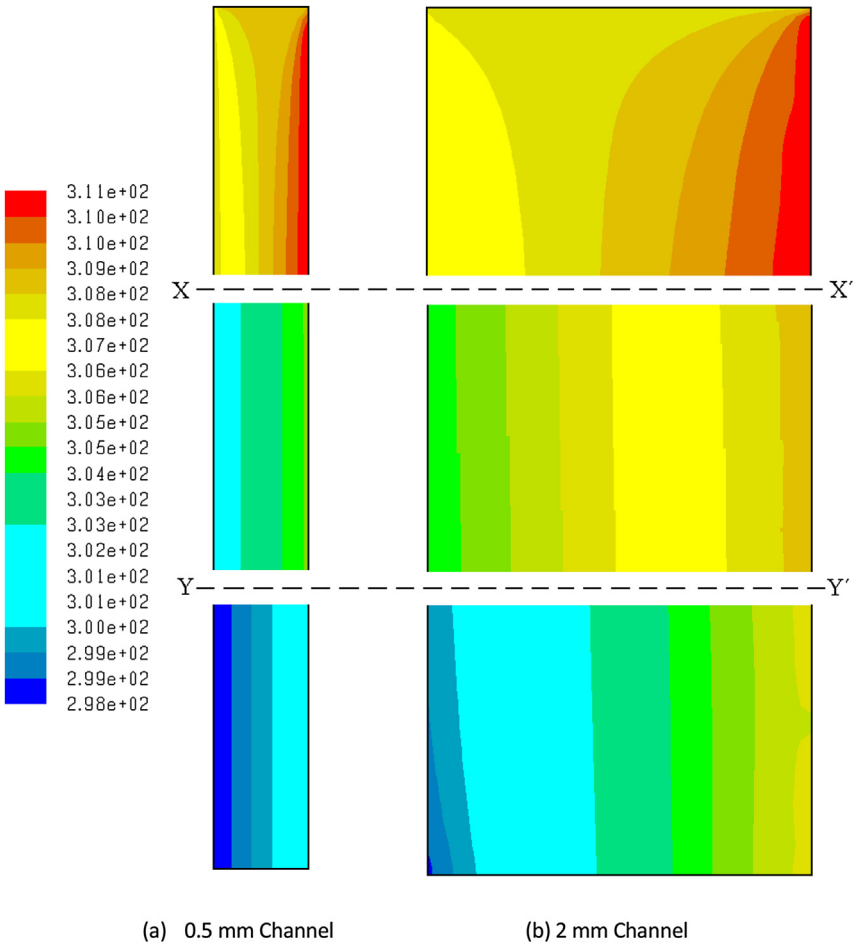

Fig. 10. Contours of the temperature (K) profiles along the solution channel.

0.004 kg/m^2 s at a solution velocity of 0.05 m/s and a channel thickness of 0.5 mm with micro-scale features implemented on the flow channel surface, however, it is expected that the pressure drop could be very high in such a design due to the micro-scale features. Absorption rate in an absorber is also dependent on the operating conditions of the absorber and flow parameters. A higher absorption rate can be achieved in case of a higher inlet concentration of LiBr in the solution and a higher vapour pressure difference. Similarly, low solution and coolant inlet temperature and higher solution inlet velocity can also enhance the absorption rate. Yu et al. [12], Isfahani and Moghaddam [14] and Bigham et al. [15] considered higher vapour pressure and solution inlet concentration which resulted in a higher absorption rate. It can be concluded from the above discussion that although in a plate-and-frame membrane based absorber the solution flow velocity and solution thickness can be varied independently however the increase in the flow velocity and decrease in the solution thickness should be in a manner to achieve higher absorption rate with minimum pressure drop. Similarly, appropriate operating conditions should be adopted to avoid the risk of crystallization. In addition, the membrane contactor characteristics such as pore size, porosity, membrane thickness and tortuosity can also affect the absorption rate. In the above mentioned studies from literature, a pore size in the range of 1 μm–6 μm, membrane thickness of 20 μm, membrane porosity of 60% and a tortuosity of 1 were considered. Membrane with ideal tortuosity equal to 1 means that the membrane pores are assumed straight however, in a microporous membrane, the membrane pores have a meandering path which causes vapour pressure drop and lower the absorption rate due to higher flow resistance. In this study, the membrane tortuosity was calculated using the equation given in Table 1. Similarly decreasing the membrane contactor thickness and increasing the pore size and porosity have a positive effect on the absorption rate however a nominal value must be selected keeping in view the membrane material mechanical strength and liquid entry pressure.

6. Conclusions

The absorber is one of the major components in absorption cooling systems and has a direct effect on the size and performance of the system. Introducing polymeric hydrophobic microporous membranes into the absorber design can be one of the alternatives for achieving highly compact absorbers with enhanced heat and mass transfer. In this study, CFD simulation is used to perform a detailed analysis of heat and mass transfer at local levels in the flow channels. The simulation results provide a deep insight of the heat and mass transfer in the membrane based absorber. The results of CFD simulation are useful and can play an important role in the design of membrane based absorbers that use water as a refrigerant. The effect of important parameters like solution channel thickness, solution flow velocity and coolant temperature on the performance of membrane based absorbers is studied and it can be concluded that

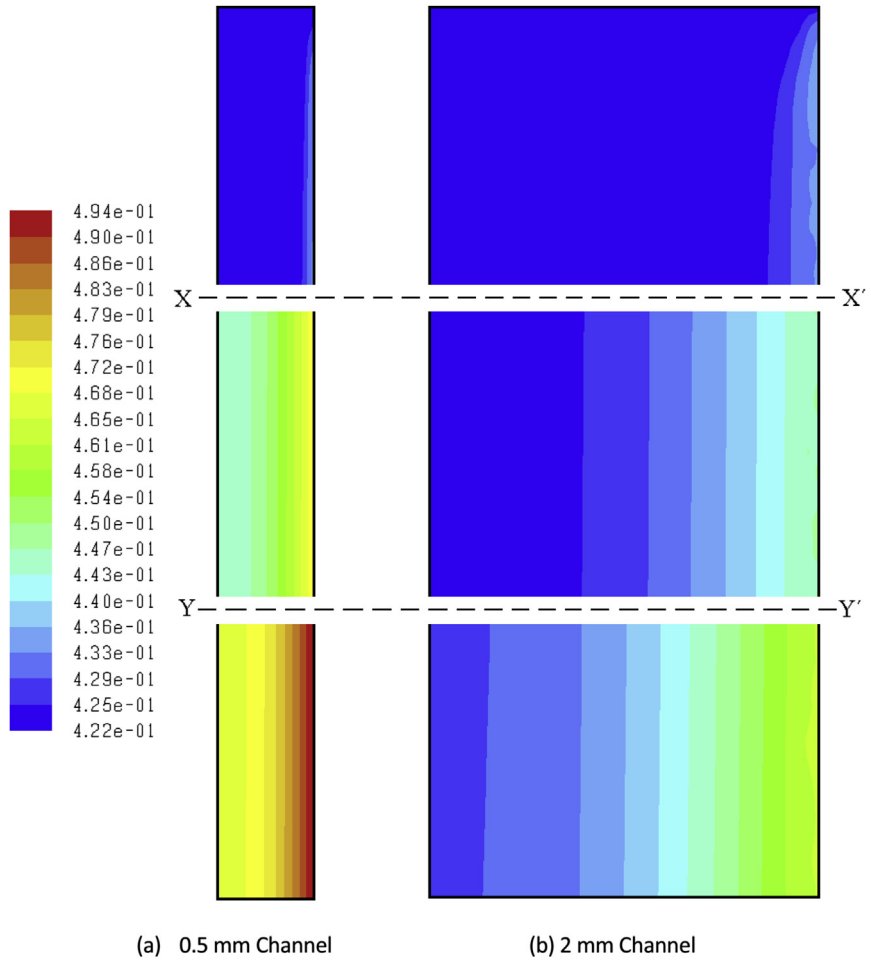

Fig. 11. Contours of the species concentration (H_2O mass fraction) profile along the solution channel.

the solution flow velocity and solution channel thickness are important parameters that can significantly affect the absorption rate across the membrane. The absorption rate was increased by a factor of 2.5 when the solution inlet velocity was increased from 0.00118 m/s to 0.00472 m/s. Moreover, it was observed that the absorption rate increased by a factor of 3 when the solution channel thickness was reduced from 2 mm to 0.5 mm. However, it was observed that the pressure drop increases exponentially with a decrease in the solution channel thickness, while it increases linearly with an increase in the solution velocity. It is recommended that the solution channel thickness and the solution flow rate should be optimized to obtain a higher absorption rate across a membrane with a minimum pressure drop. Therefore to design a compact and

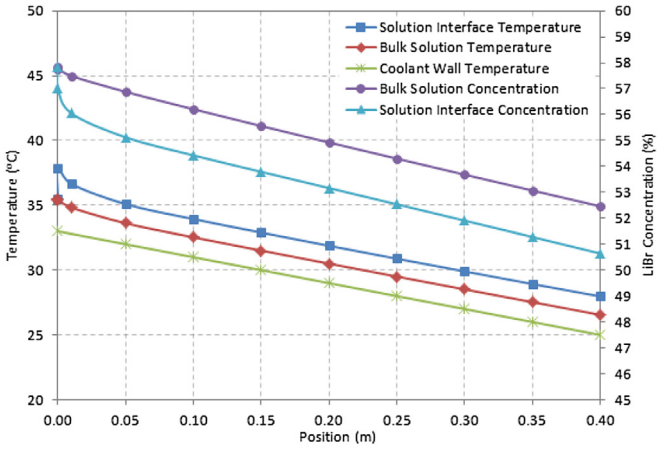

Fig. 12. Temperature and solution concentration profiles along the solution channel.

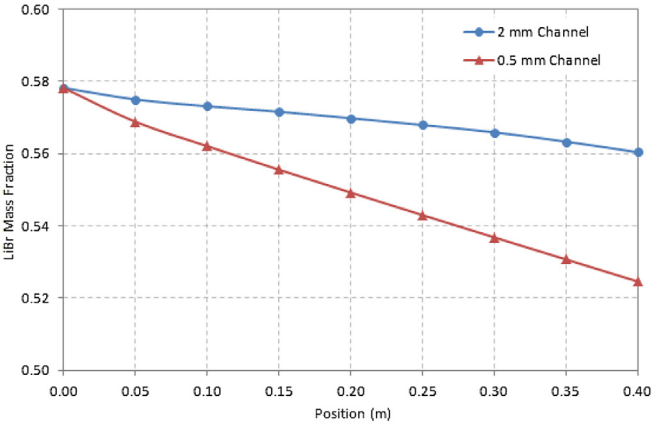

Fig. 13. Concentration profiles in the bulk solution along the 0.5 mm and 2 mm solution channels.

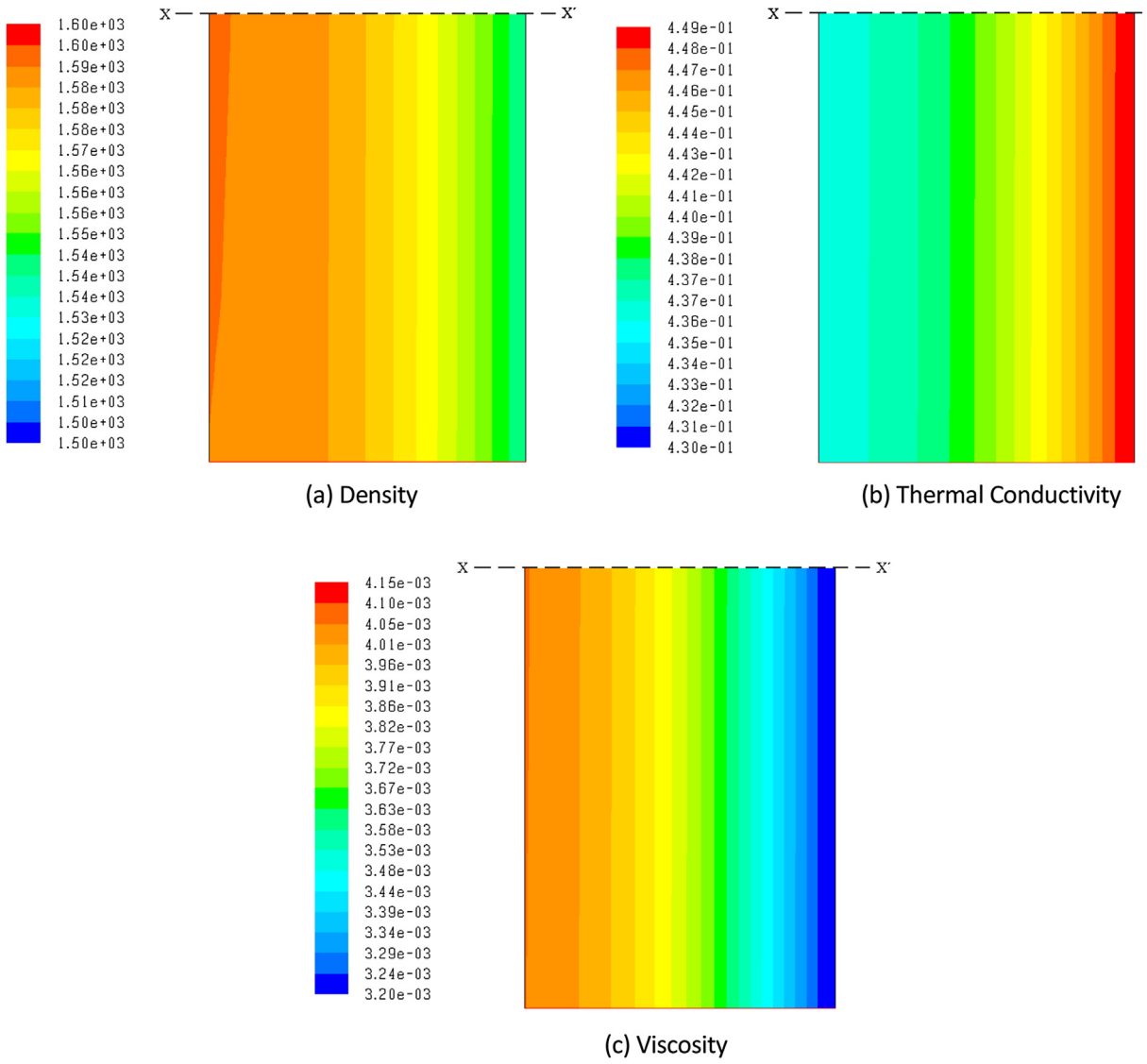

Fig. 14. Thermophysical properties of the aqueous solution of LiBr corresponding to the solution concentration and temperature at the solution channel exit.

efficient plate-and-frame membrane absorber, an optimum value of 0.5 mm for the solution channel thickness is suggested and a solution inlet velocity of about 0.005 m/s is recommended. It was observed that the local absorption rate decreases slightly along the length of the channel which affects the performance of the absorber. In addition, the pressure drop down the channel length is more significant thus an absorber length in the range of 100–200 mm is suggested for a plate and frame membrane absorber.

Acknowledgements

This study is part of an R&D project funded by the Spanish Ministry of Economy and Competitiveness (DPI2012-38841-C02-02). The authors gratefully acknowledge the Spanish Ministry of Economy and Competitiveness (CTQ2013-46799-C2-1-P) for funding the ANSYS/FLUENT licence. Faisal Asfand gratefully acknowledges the Rovira i Virgili University for granting the Martí-Franquès research fellowship 2012 (2012BPURV-50) to pursue a doctorate degree.

References

[1] Amaris C, Bourouis M, Vallès M. Effect of advanced surfaces on the ammonia absorption process with $NH_3/LiNO_3$ in a tubular bubble absorber. Int J Heat Mass Transf 2014;72:544–52.
[2] Amaris C, Bourouis M, Vallès M. Passive intensification of the ammonia absorption process with $NH_3/LiNO_3$ using carbon nanotubes and advanced surfaces in a tubular bubble absorber. Energy 2014;68:519–28.
[3] Medrano M, Bourouis M, Coronas A. Absorption of water vapour in the falling film of water-lithium bromide inside a vertical tube at air-cooling thermal conditions. Int J Therm Sci 2002;41:891–8.
[4] Jeong S, Garimella S. Falling-film and droplet mode heat and mass transfer in a horizontal tube LiBr/water absorber. Int J Heat Mass Transf 2002;45:1445–58.
[5] Islam MR, Wijeysundera NE, Ho JC. Performance study of a falling-film absorber with a film-inverting configuration. Int J Refrig 2003;26:909–17.
[6] Yoon JI, Kwon OK, Bansal PK, Moon CG, Lee HS. Heat and mass transfer characteristics of a small helical absorber. Appl Therm Energy 2006;26:186–92.
[7] Asfand F, Bourouis M. A review of membrane contactors applied in absorption refrigeration systems. Renew Sustain Energy Rev 2015;45:173–91.
[8] Chen J, Chang H, Chen S. Simulation study of a hybrid absorber–heat exchanger using hollow fiber membrane module for the ammonia–water absorption cycle. Int J Refrig 2006;29:1043–52.

[9] Schaal F, Weimer T, Hasse H. Membrane contactors for absorption refrigeration. In: International Sorption Heat Pump Conference 2008. Seoul: KOREA; September 2008.
[10] Ali AHH. Design of a compact absorber with a hydrophobic membrane contactor at the liquid–vapor interface for lithium bromide–water absorption chillers. Appl Energy 2010;87:1112–21.
[11] Ali AHH, Schwerdt P. Characteristics of the membrane utilized in a compact absorber for lithium bromide–water absorption chillers. Int J Refrig 2009;32:1886–96.
[12] Yu D, Chung J, Moghaddam S. Parametric study of water vapor absorption into a constrained thin film of lithium bromide solution. Int J Heat Mass Transf 2012;55:5687–95.
[13] Isfahani RN, Sampath K, Moghaddam S. Nanofibrous membrane-based absorption refrigeration system. Int J Refrig 2013;36:2297–307.
[14] Isfahani RN, Moghaddam S. Absorption characteristics of lithium bromide (LiBr) solution constrained by superhydrophobic nanofibrous structures. Int J Heat Mass Transf 2013;63:82–90.
[15] Bigham S, Yu D, Chugh D, Moghaddam S. Moving beyond the limits of mass transport in liquid absorbent microfilms through the implementation of surface-induced vortices. Energy 2014;65:621–30.
[16] ANSYS FLUENT UDF Manual. ANSYS Inc. Release 14.0. November 2011.
[17] ANSYS FLUENT Theory Guide. ANSYS Inc. Release 14.0. November 2011.
[18] Lee RJ, DiGuilio RM, Jeter SM, Teja AS. Properties of lithium bromide-water solutions at high temperatures and concentrations – II density and viscosity. ASHRAE Trans 1990:709–14. Paper 3381. RP-527.
[19] DiGuilio RM, Lee RJ, Jeter SM, Teja AS. Properties of lithium bromide-water solutions at high temperatures and concentrations - I thermal conductivity. ASHRAE Trans 1990:702–8. Paper 3380. RP-527.
[20] McNeely NA. Thermodynamics properties of aqueous solutions of lithium bromide. ASHRAE Trans 1979;85:413–34.
[21] Kashiwagi T, Kurosaki Y, Nikai I. Heat and mass diffusions in the absorption of water vapor by aqueous solution of lithium bromide. Trans Jpn Soc Refrig Air Cond Eng 2012;1:89–98.
[22] Martınez L, Rodrıguez-Maroto JM. On transport resistances in direct contact membrane distillation. J Membr Sci 2007;295:28–39.
[23] Kaita Y. Thermodynamic properties of lithium bromide–water solutions at high temperatures. Int J Refrig 2001;24:374–90.
[24] Florides GA, Kalogirou SA, Tassou SA, Wrobel LC. Design and construction of a LiBr–water absorption machine. Energy Convers Manage 2003;44:2483–508.

A.4 Performance evaluation of membrane-based absorbers employing $H_2O/(LiBr+LiI+LiNO_3+LiCl)$ and $H_2O/(LiNO_3+KNO_3+NaNO_3)$ as working pairs in absorption cooling systems.

Energy 115 (2016) 781–790

Contents lists available at ScienceDirect

Energy

journal homepage: www.elsevier.com/locate/energy

Performance evaluation of membrane-based absorbers employing H_2O/(LiBr + LiI + $LiNO_3$ + LiCl) and H_2O/($LiNO_3$ + KNO_3 + $NaNO_3$) as working pairs in absorption cooling systems

Faisal Asfand, Youssef Stiriba, Mahmoud Bourouis*

Department of Mechanical Engineering – Universitat Rovira i Virgili, Av. Països Catalans No. 26, 43007 Tarragona, Spain

ARTICLE INFO

Article history:
Received 20 February 2016
Received in revised form
21 August 2016
Accepted 30 August 2016

Keywords:
Absorption cooling systems
Membrane contactors
CFD simulation
Plate-and-frame membrane absorber
H_2O/(LiBr + LiI + $LiNO_3$ + LiCl)
H_2O/($LiNO_3$ + KNO_3 + $NaNO_3$)

ABSTRACT

In recent years, rigorous research has been carried out on the use of membrane contactors to design compact absorbers for absorption cooling systems and to extend their use in small scale applications. Moreover, the use of new working fluid mixtures has been suggested for the absorption cooling systems to cope with the limitations and problems associated with the conventional working fluid mixtures. In this study, water/(LiBr + LiI + $LiNO_3$ + LiCl) with mass compositions in salts of 60.16%, 9.55%, 18.54% and 11.75%, respectively, and water/($LiNO_3$ + KNO_3 + $NaNO_3$) with mass compositions in salts of 53%, 28% and 19%, respectively, were investigated for air-cooled and multi-stage high temperature absorption cooling systems, respectively. Results show that a 25% increase in the absorption rate can be achieved by using water/(LiBr + Li + $LiNO_3$ + LiCl) when compared to water/LiBr at air-cooling thermal conditions. Furthermore, an absorption rate as high as 0.00523 kg/m^2 s is achieved when the water/($LiNO_3$ + KNO_3 + $NaNO_3$) working fluid mixture is used in the membrane-based absorber of the third stage of a triple effect absorption cooling cycle. In addition, the pressure drop percentage in the case of water/($LiNO_3$ + KNO_3 + $NaNO_3$) working fluid mixture is significantly lower than the water/LiBr and water/(LiBr + LiI + $LiNO_3$ + LiCl) working fluid mixtures because of the higher operating pressure.

1. Introduction

Absorption air-conditioning systems, which can use solar thermal energy, are an interesting alternative for space cooling in summer when compared to vapour compression systems, which use costly mechanical energy input. In summer, the intensity of solar thermal radiation is high and thus an absorption air-conditioning system using solar thermal radiations can better satisfy the cooling demand during the day. Moreover, the refrigerants used in conventional vapour compression air-conditioning systems are not environmental friendly and can contribute to ozone depletion and greenhouse effects, whereas in the absorption air-conditioning systems the working fluid mixtures are environmental friendly. Absorption air-conditioning has been an attractive alternative since the early stages of air-conditioning technologies and continued improvements in the design and configuration of the components of absorption air-conditioning systems have been suggested and implemented on a commercial scale to improve their performance. The absorber is an important component of an absorption air-conditioning system and as such plays a critical role in the overall performance, size, and capital cost of the system. Both the design and configuration of the absorber significantly influence its performance as heat and mass transfer take place simultaneously in this component. Absorbers used in absorption cooling technology employing water as a refrigerant, operate under static vacuum pressure conditions and are accompanied by a high specific volume of water vapour. This means that the absorber has a direct effect on the size, weight and space requirements of absorption air-conditioning systems. Research is currently being carried out to design more compact absorbers for absorption air-conditioning systems. Recently, research has shown that membrane contactor technology can be used in these systems, especially in the case of the absorber and desorber. The aim is to reduce the size, weight and cost of the system while significantly enhancing the heat and mass transport processes taking place in these components. The use of polymeric hydrophobic microporous membrane contactors in the absorber could also mean a reduction in manufacturing cost. Both numerical and experimental studies

* Corresponding author.
E-mail address: mahmoud.bourouis@urv.cat (M. Bourouis).

http://dx.doi.org/10.1016/j.energy.2016.08.103
0360-5442/

Nomenclature

c_B	Boltzmann constant (J/K)
D	diffusion coefficient (m^2/s)
d_p	membrane pore mean diameter (μm)
d_h	hydraulic diameter (m)
J	mass transfer flux (kg/m^2 s)
K	mass transfer coefficient (kg/m^2 s Pa)
Kn	Knudsen number, $Kn = \lambda/d_p$
k	thermal conductivity (W/m K)
L	channel length (m)
M	molecular weight (g/mol)
P	pressure (Pa)
p	vapour pressure of solution (Pa)
R	universal gas constant (J/mol K)
Re	Reynolds number, $Re = \rho.u.d_h/\mu$
T	temperature (°C, K)
t	channel thickness (m)
X	LiBr mass fraction

Greek letters

ρ	density (kg/m^3)
ε	porosity
δ_m	membrane thickness (μm)
σ	molecular collision diameter (m)
τ	tortuosity
λ	mean free path (m)
μ	dynamic viscosity (kg/m s)

Subscripts

c	coolant
$H2O$	water
int	solution-membrane interface
m	membrane
s	solution
v	vapour
w	wall

Abbreviations

AMD	Advanced Micro Devices
CFD	Computational Fluid Dynamics

are being carried out to investigate the heat and mass transfer processes in microporous hydrophobic membrane based components. Asfand and Bourouis [1] have extensively reviewed the application of membrane contactors in absorption refrigeration systems. They have reported that the use of microporous membrane contactors in the absorber and desorber of an absorption refrigeration system can, not only enhance the heat and mass transfer performance of the component, but can also allow for a reduction in the size and weight of the component. Thus, introducing polymeric hydrophobic microporous membranes into the design of the absorber and desorber could provide an alternative to achieve highly compact components, which would permit the use of absorption air-conditioning systems in small scale cooling applications, heat-driven automotive air conditioning, and portable cooling. The heat and mass transfer processes can be significantly improved because the microporous membrane contactors provide a wider interfacial area. Microporous membrane contactors in the form of plate-and-frame membrane modules and hollow fiber membrane modules have been investigated to replace the conventional components in absorption refrigeration and air-conditioning systems. The plate-and-frame module is generally selected when water is used as a refrigerant, whereas the hollow fibre module is usually selected for ammonia based absorption systems. The driving force for the refrigerant mass transfer in the case of ammonia/water solution is considered to be the difference in ammonia concentration in the solution and vapour phase whereas in the case of water/LiBr, water vapour partial pressure difference across the membrane is responsible for the refrigerant mass transfer.

Table 1 compares the vapour absorption rates achieved in experimental and numerical studies of plate-and-frame membrane based absorbers employing water/LiBr as a working fluid mixture. In addition to the solution channel thickness, the solution inlet temperature and concentration, the solution mass flow rate at the inlet, the cooling water inlet temperature, and the water vapour pressure are also listed in the table. It is evaluated from the reported data in Table 1 that both the solution channel thickness and the operating conditions significantly affect the absorption performance of the absorber. This is evident from the large discrepancy in the absorption rate at different conditions. Ali & Schwerdt [2] experimentally analysed a plate-and-frame membrane based absorber and achieved an absorption rate of 0.00125 kg/m^2 s at a water vapour pressure of 2.339 kPa, which is more than twice the available pressure in a typical absorber. Ali and Schwerdt [2] reported that their membrane mass transport resistance could have dominated the overall mass transfer process which resulted in poor absorption rates. Numerical simulations performed by Yu et al. [3] show that reducing the solution channel thickness can significantly enhance the absorption rate. They reported that an absorption rate of approximately 0.0092 kg/m^2 s is achievable if the solution channel is constrained to a thickness of 0.05 mm. Similarly, Isfahani et al. [4] and Isfahani and Moghaddam [5] experimentally investigated plate-and-frame membrane based absorbers and obtained absorption rates of 0.00355 kg/m^2 s and 0.0060 kg/m^2 s respectively. In their study, they used solution channel thicknesses of 0.16 mm and 0.10 mm, respectively. It can be concluded from the investigations reported above that the lower absorption rate achieved by Ali and Schwerdt [2] is due to the fact that, in their study, they used solution channel thicknesses of 4.0 mm and 2.0 mm respectively. Furthermore, the experimental studies carried out by Isfahani et al. [4] and Isfahani and Moghaddam [5] suggest that the mass transfer through the solution is the dominant resistance as opposed to the membrane mass transfer resistance. In addition, numerical results reported by Asfand et al. [6] critically evaluated the impact of solution channel thicknesses while investigating the effect of membrane characteristics. They reported that the membrane mass transfer resistance is considerable only when the solution channel thickness is of the order 0.1 mm or lower. It was observed from their results that the membrane characteristics have a less prominent effect on the absorption rate in the case of solution channels with a thickness of the order 0.5 mm or more. They concluded that the solution resistance is the dominant resistance to the refrigerant mass transfer. As opposed to conventional absorbers, the solution film thickness and the velocity can be independently controlled in plate-and-frame membrane absorbers. However, decreasing the solution channel thickness and increasing the solution mass flow rate in order to achieve a higher absorption rate can cause an unacceptable pressure drop along the solution

Table 1
Absorption rate achieved during experimental and numerical analyses of plate-and-frame membrane based absorbers employing water/LiBr working fluid mixture.

Reference	Study	Solution channel thickness (mm)	Operating conditions					Absorption rate $\times 10^3$ (kg/m^2 s)
			Solution mass flow rate/Inlet velocity	Solution inlet temperature (°C)	Solution inlet concentration (%)	Vapour pressure (kPa)	Coolant inlet temperature (°C)	
Ali & Schwerdt [2]	Experimental	4.00	8.0 kg/h	27.0	53.55	2.339	NA	1.25
Yu et al. [3]	Numerical	0.05	0.15 m/s	45.0	60.00	0.873	27.0	9.20
Isfahani et al. [4]	Experimental	0.16	0.6 kg/h	25.0	60.00	1.100	25.0	3.55
Isfahani & Moghaddam [5]	Experimental	0.10	0.6 kg/h	25.0	60.00	1.350	25.0	6.00
Asfand et al. [7]	Numerical	0.50	0.005 m/s	35.5	57.82	0.813	25.0	1.00
Bigham et al. [8]	Experimental	0.50	0.05 m/s	32.5	60.00	0.873	27.5	4.00

channel. The higher pressure drop along the solution channel can hinder the performance of the plate-and-frame membrane absorber operating with water as a refrigerant under vacuum conditions. Asfand et al. [7] observed that the pressure drop increases exponentially when the solution channel thickness is reduced. They reported that a 50% decrease in the solution film thickness causes an increase in the accumulative pressure drop by a factor of approximately 7.5, keeping the same solution mass flow rate. They recommended that a solution channel thickness of the order 0.5 mm should be used to avoid higher pressure drops in the solution channel. They numerically investigated the plate-and-frame membrane absorber and achieved an absorption rate of 0.001 kg/m^2 s with a solution channel thickness of 0.5 mm. However, the absorption rate can be enhanced if favourable operating conditions are adopted. It can be seen from Table 1 that a higher absorption rate is achievable if the solution mass flow rate, solution inlet concentration and water vapour pressure difference across the membrane are higher and the solution and coolant inlet temperatures are lower. Bigham et al. [8] experimentally and numerically investigated a plate-and-frame membrane absorber with a solution channel thickness of 0.5 mm and achieved an increase in the absorption rate by a factor of 2.5 from 0.0016 kg/m^{2}s to 0.004 kg/m^{2}s by the implementation of micro-scale features on the flow channel surface. They reported that the laminar streamlines within the solution film are stretched and folded as a result of the vortices and that the mass transport mode in such a configuration could be changed from a diffusive to an advective mode.

Most of the research in the absorption technology is done using the conventional working fluid mixtures, water/LiBr and ammonia/water with water as a cooling medium. However, many new working fluid mixtures have been proposed and investigated for absorption air-conditioning systems for them to cope with the problems and deficiencies associated with the conventional working fluid mixtures, NH_3/H_2O and H_2O/LiBr and to enhance the performance of the absorber. Moreover, there is a growing interest in air-cooled absorption chillers, for which water/multi-salts mixture is proposed as a working fluid due to its wider range of solubility. However, there is very scarce information in the literature about the absorption process with this non-conventional working fluid. Conventional water/LiBr absorption systems are widely used to supply chilled water for industrial and space cooling applications that require huge cooling capacities. In these systems, cooling towers are used for cooling water to dissipate the heat released in the absorber and condenser. Whereas, the transport sector and the residential sector in which the cooling demand is lower, are currently dominated by vapour compression systems that are run by costly mechanical energy systems. If the heat rejected in the absorber and condenser of an absorption system is directly dissipated to ambient air instead of employing cooling towers, then it can favour the use of absorption systems in small scale applications. Furthermore, it will not only reduce the investment cost of the installation but also eliminate the maintenance cost of cooling towers. However, the absorber and condenser must operate at higher temperatures to effectively dissipate the heat released into the ambient air and this in turn can increase the risk of crystallization of the solution. Water/LiBr solution has a limited range of solubility which restricts the range of temperatures feasible for air-cooled absorbers and hinders the development of air-cooled absorption systems for cooling applications. Recent research has shown that the addition of other salts to LiBr aqueous solutions can significantly improve their solubility. However, the criteria for selecting an appropriate salt mixture should not only include an increase in the range of solubility but also other aspects of the operation of the machine, such as vapour pressure, viscosity, corrosivity, and thermal and chemical stability. Bourouis et al. [9,10] and Medrano et al. [11] experimentally and numerically investigated an aqueous solution of the quaternary salt system (LiBr + LiI + $LiNO_3$ + LiCl) with mass compositions in salts of 60.16%, 9.55%, 18.54% and 11.75%, respectively, for air-cooled absorption systems and reported that it is less corrosive and its crystallization temperature is about 35 K lower than that of water/LiBr. The presence of lithium chloride decreases the vapour pressure of the solution. Lithium iodide and lithium nitrate improve the solubility and lithium nitrate reduces corrosion in the system. Thus, the use of a multi-salt mixture can overcome the crystallization problem and allow for the development of air-cooled absorption systems with membrane contactor based components for small scale applications.

Currently, numerical and experimental analyses are being carried out in order to improve the thermal efficiency and increase the COP (coefficient of performance) of absorption cooling systems. Double-effect water/LiBr absorption systems have already been developed for commercial cooling applications. However, the COP achieved in these applications does not reach levels high enough to use the thermal potential of high temperature heat sources efficiently, between 1 and 1.3. In order to make better use of the thermal energy produced by high temperature heat sources and improve the efficiency of absorption cooling systems, the installation of different triple-effect absorption systems has been proposed. The triple-effect absorption cooling cycles are intended, not only to improve the COP, but also to miniaturize the size of the equipment for use in small scale applications. However, the thermal instability, corrosion and crystallization problems of water/LiBr at high temperatures restrict the development of water/LiBr triple-effect cycles for efficient use of thermal energy produced by high temperature heat sources. The conventional water/LiBr working fluid mixture suffers serious problems of corrosion and thermal decomposition at temperatures of over 180 °C.

Davidson and Erickson [12] proposed the use of an aqueous solution of three alkali-metal nitrate salts ($LiNO_3 + KNO_3 + NaNO_3$), called Alkitrate, with mass compositions in salts of 53%, 28% and 19%, respectively, to increase the maximum temperature limit to 260 °C or above for absorption systems. Although the working fluid mixture is compatible with austenitic stainless steel materials at high temperatures, Howe and Erickson [13] reported that this working fluid mixture does not exhibit a wide range of solubility, and consequently its use at low temperatures is limited due to crystallization problems. Therefore, Erickson et al. [14] suggested that Alkitrate can be used in the high temperature components of triple-effect absorption cooling cycles, while the conventional working fluid water/LiBr could be used in the low temperature components. The working fluid Alkitrate is potentially useful when operating at high temperatures in the last stage of a triple-effect cycle because of its non-corrosive nature and high thermal stability up to temperatures of about 260 °C [15]. Moreover, it contains water as a refrigerant, so a membrane based absorber employing microporous hydrophobic membrane contactors can be effective in improving the heat and mass transfer processes and reducing the size of the system.

Experimental and numerical analyses have been carried out to investigate the performance of membrane based absorbers with conventional working fluid mixtures, i.e. water/LiBr and ammonia/water. However, at local levels in the channels, detailed fluid dynamics behaviour and the heat and mass transfer processes of the two non-conventional working fluid mixtures mentioned above needs further investigation. This way the phenomena and the effect of different working fluid mixtures on the heat and mass transfer and flow parameters would be better understood. The purpose of this study is to numerically investigate the use of non-conventional working fluid mixtures in air-cooled and triple-effect absorption cooling systems employing membrane based absorbers. In this work, the CFD code ANSYS/FLUENT 14.0 has been used to perform the simulation of heat and mass transfers in a plate-and-frame membrane absorber. The water/($LiBr + LiI + LiNO_3 + LiCl$) working fluid mixture which is considered as an attractive alternative to water/LiBr in air-cooled absorption cooling systems and the water/($LiNO_3 + KNO_3 + NaNO_3$) working fluid mixture, which can be utilized in the last stage of triple-effect absorption cooling systems, are both numerically investigated. Absorption rate, local temperature and concentration profiles as well as pressure drop along the solution channel are analysed in detail.

2. Absorber module

A plate-and-frame membrane absorber has been selected for the analysis in this study. As in the case of absorption cooling system employing water as a refrigerant, the absorber operates under vacuum conditions, so the plate-and-frame membrane module which presents a minimum pressure drop, could be an interesting choice. The structural unit of the absorber configuration with membrane contactors and the sectional view of the absorber are shown in Fig. 1. The configuration of the plate-and-frame absorber is set as such that the solution, coolant and vapour flow in individual flow channels. Each coolant channel serves two solution channels and is fed in a counter flow direction in order to dissipate the heat of absorption from the solution. The first and last cells of the module have half width coolant channels. Similarly, each vapour channel serves two solution channels and can move in a counter flow or co-current flow. The coolant and solution are separated using a metallic plate across which only heat transfer takes place. A microporous hydrophobic membrane sheet is placed at the aqueous solution–water vapour interface in the form of a parallel sheet along the metallic plate. Both heat and mass transfer processes take place across the membrane sheet. The parallel assembly of the plates and membrane sheets minimizes the pressure drop through the absorber. In this study, a flat sheet membrane contactor made of polypropylene material is considered. Because of the corrosive nature of LiBr solution, Hastelloy C-22 alloy has been used to separate the coolant and solution channels. Hastelloy C-22 has exceptional resistance to a wide variety of chemical process environments. The membrane material characteristics and absorber dimensions are summarized in Table 2.

3. Working fluid mixture

The quaternary salt system ($LiBr + LiI + LiNO_3 + LiCl$) and the ternary mixture of alkali nitrates ($LiNO_3 + KNO_3 + NaNO_3$) were used as absorbents with water as a refrigerant. Numerical simulations were carried out and the results were compared to those of the conventional working fluid mixture water/LiBr.

3.1. Thermophysical properties

In the ANSYS/FLUENT 14.0 code material database water/($LiBr + LiI + LiNO_3 + LiCl$), water/($LiNO_3$°+°$KNO_3$°+°$NaNO_3$) as well as water/LiBr mixture are not available. Therefore, these working fluid mixtures were created in the material panel of the ANSYS/FLUENT 14.0 code and the thermophysical properties of the mixtures were updated in the ANSYS/FLUENT 14.0 code database with user defined functions. Density, viscosity, thermal conductivity, specific heat capacity and diffusion coefficient of the aqueous solutions of the examined working fluid mixtures were estimated as a function of solution concentration and temperature.

3.1.1. Vapour liquid equilibria

The correlation developed by Uemura and Hasaba [16] was used to calculate the vapour pressure of the water/LiBr solution. The vapour pressure data of Koo et al. [17] and the correlation developed by the research group CREVER from Rovira i Virgili University [18] were used to calculate the vapour pressure of the quaternary salt working fluid mixture. To calculate the vapour pressure of the Alkitrate solution, the correlation developed by Álvarez et al. [19] was used.

3.1.2. Density and viscosity

The density and viscosity of the aqueous solution of lithium bromide was calculated using the correlation developed by Lee et al. [20]. The correlation developed by the research group CREVER from Rovira i Virgili University [18] was used to calculate the density and viscosity of the quaternary salt working fluid mixture. To calculate the density and viscosity of the Alkitrate solution, the correlation developed by Álvarez [21] was used.

3.1.3. Specific heat capacity

The correlation reported in Kaita [22] was used to calculate the specific heat capacity of the water/LiBr fluid mixture. The correlations reported in Salavera et al. [23] and Koo et al. [17] were used to calculate the specific heat capacity of the quaternary salt working fluid mixture. The procedure reported by Laliberté [24] was used to calculate the specific heat capacity of the Alkitrate solution.

3.1.4. Thermal conductivity

The thermal conductivity of the water/LiBr fluid mixture was calculated using the correlation of DiGuilio et al. [25]. The correlation developed by the research group CREVER from Rovira i Virgili University [18] was used to calculate the thermal conductivity of the quaternary salt working fluid mixture. To calculate the thermal conductivity of the Alkitrate solution, the method of Aseyev [26]

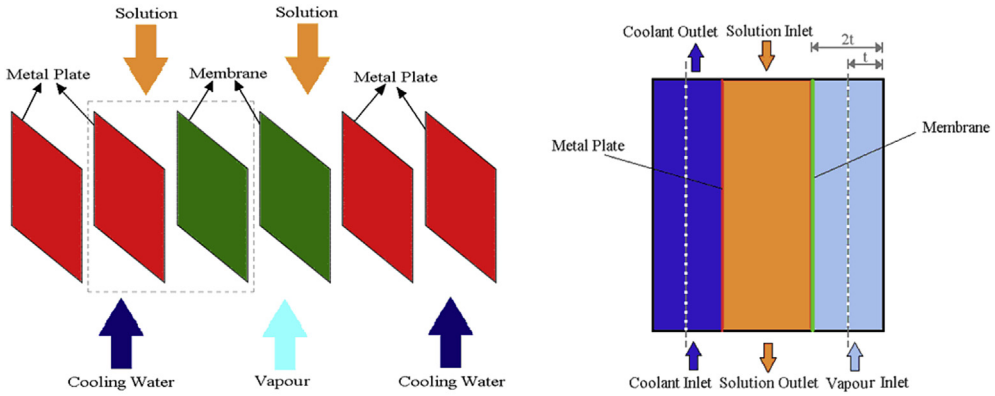

(a) Flow channel configuration (b) 2D sectional view of a single unit

Fig. 1. Plate-and-frame absorber configuration with membrane contactor.

Table 2
Membrane material characteristics and absorber dimensions.

Thickness, δ_m (μm)	40
Porosity, ε (%)	85
Tortuosity, τ ($\tau = (2-\varepsilon)^2/\varepsilon$)	1.56
Mean pore diameter, d_p (μm)	1.0
Thermal conductivity, k_m (W/m K)	0.17
Thermal conductivity, k_w (W/m°K)	10
Solution channel thickness, t (mm)	0.5
Solution channel length, L (mm)	200

was used.

3.1.5. Enthalpy

The enthalpy of water vapour was calculated using the correlation reported in Florides et al. [27]. The differential enthalpy of dilution was estimated using the procedure reported in Asfand and Bourouis [28]. The specific enthalpy of the aqueous solutions of LiBr, quaternary salt system and Alkitrate were calculated using the correlations reported in Refs. [22]·[18], and [29], respectively.

3.1.6. Coefficient of diffusion

The diffusion coefficient of water in the aqueous lithium bromide solution was calculated from the experimental data of Gierow and Jernqvist [30] which was determined at constant temperature and different concentrations. However, at other temperatures the diffusion coefficient was estimated using the equation given below.

$$\frac{D_1\mu_1}{T_1} = \frac{D_2\mu_2}{T_2} \quad (1)$$

where D is the diffusion coefficient, μ is the dynamic viscosity and T is the temperature. State 1 refers to the values calculated at 25 °C whereas state 2 refers to the values calculated at any other temperature.

Mass diffusivity coefficient of the Alkitrate and quaternary salt working fluid mixtures were estimated using the Stokes-Einstein equation reported in Bird [31]. The method was validated against the known diffusion coefficient of water/LiBr working fluid mixture.

4. Numerical model

In this study, CFD numerical simulations were preformed in a workstation cluster of 24 AMD Opteron 248 dual core processors (64 bits) and 7 Intel 3 Ghz processors, with 3 terabytes of disk, linked with a Giga Ethernet in a Linux environment. Simulations were performed in parallel using four processors and each case simulated took approximately 6 days to achieve a steady-state condition. The CFD commercial code ANSYS Fluent 14.0 was used for the numerical simulation which employs a finite volume approach to discretize the governing Navier-Stokes equations into a set of linear equations. The computational domain, boundary conditions and numerical schemes adopted in this study are illustrated in the following subsections.

4.1. Model assumptions

The following assumptions are considered in the analytical model for the simulation:

- Steady state conditions.
- Linear coolant temperature rise.
- Vapour channel pressure and temperature are assumed constant.
- Coolant thermophysical properties are assumed constant.
- No heat losses to/or gained from the surroundings of the absorber cells.

4.2. Computational domain

A two-dimensional model was developed to simulate the flow, heat and mass transfer processes in a single unit of the plate-and-frame membrane module. To reduce the computational time and reach a converged solution without flow instabilities, the vapour pressure and temperature of the vapour channel were assumed constant. Similarly, a coolant wall temperature function was imposed at the heat transfer plate with a user defined function to incorporate the linearized change in coolant temperature along the channel. The Inlet boundary in the solution flow channel was considered the velocity inlet whereas the outlet boundary condition was specified as the pressure outlet.

The spatial domain of the simplified model was discretized into meshes fine enough to get mesh-independent results based on the independency test. The grids were created in Gambit software and imported into ANSYS Fluent 14.0. Different grid sizes were tested for the 0.5 mm solution channel. The mesh size of 15 × 15000 cells, with a minimum edge size of 0.00002 and a growth factor of 1.2 in the boundary layer, was selected for the simulation analysis. A grid

independence test showed that the maximum error in the absorption rate was less than 1% when the grid size was reduced by a factor of 2.

4.3. Governing equation

In the present numerical simulation of heat and mass transfer, the flow in the solution channel is a homogeneous single phase flow. As the species in the solution are well mixed, the relative velocity between the species is negligible. In the absence of relative motion, the governing mass and momentum conservation equations for homogeneous flow are reduced to the single-phase form, therefore, instead of the mixture model, single phase equations are used to perform the simulation with less computational effort. The flow is governed by the Navier-Stokes equations. The continuity, momentum, energy and specie transport equations are solved to perform steady-state heat and mass transfer analyses. These equations are given in the ANSYS/FLUENT 14.0 theory guide.

The driving force for the refrigerant vapour mass transfer across the membrane in a water-LiBr absorber is the difference in vapour pressure and partial pressure of water vapour in the aqueous solution. The mass transfer flux across the membrane is given by Martinez and Rodriguez-Maroto [32] as follows:

$$J = K_m(P_v - p_{\text{int}}) \tag{2}$$

where J is the mass transfer flux of water vapour absorbed in the solution, P_v is the water vapour pressure and p_{int} is the equilibrium water vapour partial pressure of the solution at the solution-membrane interface. K_m is the membrane equivalent mass transfer coefficient.

Mass transport through a microporous membrane can take place by different mechanisms depending on the flow regime. Thus, it is important to determine the flow regime in order to accurately calculate the mass flux through the membrane. Flow through a porous membrane can be classified into viscous, transitional, or free molecular flow regimes, depending on the magnitude of the Knudsen (Kn) number. The Kn number is defined as the ratio of the mean free path (λ) to the pore diameter (d_p):

$$Kn = \lambda / d_p \tag{3}$$

where λ is the mean free path and is calculated as:

$$\lambda = \frac{c_B \cdot T}{\sqrt{2} \cdot \pi \cdot \sigma^2 P} \tag{4}$$

where c_B is the Boltzmann constant (1.38×10^{-23} J/K), σ is the molecular collision diameter (2.7×10^{-10} m for water vapour), T is the absolute temperature in K and P is mean total pressure within the membrane pore in Pa.

For Kn > 10, collision between molecules and pore walls is dominant, the gas transport takes place in the free molecular regime and the flow is known as Knudesn flow. When Kn < 0.01, collisions between gas molecules dominate and viscous flow occurs which results in rapid convective transport. A transitional flow regime exists if 0.01 < Kn < 10 and according to the Dusty-Gas model, the mass transfer through a membrane consists of both diffusion and viscous fluxes.

In this study, the mean membrane pore diameter is 1 μm and at vapour pressure of 1.3 kPa and 30 kPa, the mean free path of water molecules is 9.8 μm and 0.5 μm, respectively, therefore the Knudsen number value lays in the transitional flow regime for both cases and the vapour transport through the microporous membrane pores takes place via both the diffusion and convective transport mechanisms. The membrane mass transfer coefficient in the transitional flow regime can be calculated as:

$$K_m = \frac{M_{H_2O}}{\delta_m}\left(\frac{D_k}{RT_m} + \frac{P_m B_0}{RT_m \mu_v}\right) \tag{5}$$

where M_{H2O} is the molecular weight of water, δ_m is the membrane thickness, R is the universal gas constant and T_m is the mean membrane temperature which is calculated as the average of vapour and solution interface temperatures. D_k is the Knudsen diffusion coefficient and for porous solid it can be calculated as:

$$D_k = \frac{\varepsilon d_p}{3\tau}\left(\frac{8RT_m}{\pi M_{H_2O}}\right)^{\frac{1}{2}} \tag{6}$$

where, ε is the membrane porosity, τ is the tortuosity of the membrane and d_p is the mean membrane pore diameter.

$$B_0 = \frac{\varepsilon d_p^2}{32\tau} \tag{7}$$

where, μ is the viscosity and P is the pressure.

The mass transfer flux, which is the vapour mass that is absorbed in the solution, is added as a mass source term in the continuity equation and a specie source term in the species transport equation. A user defined function is implemented at the solution-membrane interface to model the vapour mass transfer across the membrane. Similarly, with a user defined function at the solution-membrane interface, the heat of absorption in the solution is added to the energy equation as a source term. The heat of absorption is expressed as the change in the enthalpy of water as it undergoes a phase change from vapour to liquid phase plus the differential heat of dilution of the absorbent.

4.4. Numerical scheme

The governing equations of continuity, diffusion and energy are used to perform a numerical analysis of coupled heat and mass transfer processes in a plate-and-frame membrane absorber. As the solution flow Reynolds number is low, a laminar model is selected for the analysis. The calculations were performed by a combination of the PISO (Pressure-Implicit with Splitting of Operators) pressure-velocity coupling scheme, part of the SIMPLE family of algorithms, and the first-order accurate implicit scheme for the linearized discretized equations in the segregated solver [33,34]. The Second-order upwind discretization scheme is used to compute advection terms. For the energy and species equations, the second-order discretization scheme was used. In the present work, the numerical computation is considered to have converged when the scaled residuals of the different variables are lowered by tenth orders of magnitude and the steady state results are analysed.

5. Results and discussion

CFD simulations are capable of predicting the detailed behaviour of heat and mass transfer phenomena at local regions, thus, a clear pattern of the temperature and concentration gradients and the velocity profiles are obtained.

The current CFD numerical model was validated in a previous study [7] by comparing the local absorption rates predicted along the length of the channel with the numerical results reported by Yu et al. [3]. These authors considered water/LiBr as a working pair and a solution channel of 0.05 mm thickness and 20 mm long. A solution inlet velocity of 0.0182 m/s, and an inlet solution concentration and temperature of 60% and 55 °C, respectively, were considered in

their study. A linear temperature profile was considered along the coolant wall. The local absorption rates predicted by the CFD model were compared with the local absorption rates obtained by Yu et al. [3] at the same operating conditions. The CFD results showed close agreement with the literature data producing a mean absolute percentage error of 4.82%.

In this section, an analysis is carried out to study in detail the absorption performance of a water/(LiBr + LiI + $LiNO_3$°+°LiCl) working fluid mixture with mass compositions in salts of 60.16%, 9.55%, 18.54% and 11.75%, respectively, at thermal operating conditions of an air-cooled absorption cooling system and compare the results with those of a water/LiBr solution. In addition, a parametric study is performed to investigate in detail the performance of a water/($LiNO_3$°+°KNO_3°+°$NaNO_3$) working fluid mixture with mass compositions in salts of 53%, 28% and 19%, respectively, at the operating conditions of the last stage of a triple-effect absorption cooling system. It is worth noting that the selected operating conditions at which the simulations are carried out in this study lie in the regime where the solutions are not prone to crystallization problem.

Fig. 2 shows the results of the analysis carried out to investigate the performance of a membrane-based absorber at air-cooling thermal conditions employing water/(LiBr + LiI + $LiNO_3$+LiCl) and water/LiBr working fluid mixtures. Solution Reynolds number and other input variables were kept constant. The input variables for the analysis correspond to the operating conditions considered in the experimental analysis performed by Bourouis et al. [9,10] given in Table 3. It can be seen that a higher absorption rate is achieved in the case of water/(LiBr + LiI + $LiNO_3$+LiCl) with a 64.2% inlet solution concentration when compared to water/LiBr with a 60% inlet solution concentration. However, the water/(LiBr + LiI + $LiNO_3$+LiCl) working fluid mixture with a 61% inlet solution concentration yields a lower absorption rate. It is evaluated that a water/(LiBr + LiI + $LiNO_3$+LiCl) working fluid mixture is more advantageous at higher solution concentrations and this makes it a better choice for air-cooled absorption cooling systems. In contrast, water/LiBr cannot operate at higher concentrations due to the crystallization problem. It is noted that a higher absorption rate is achieved at the inlet of the absorber due to the low mass fraction of water in the solution at the inlet and a lower solution interface temperature. A tendency for the absorption rate to decrease is observed in the first quarter of the absorber whereas almost a steady absorption rate is achieved in the latter part of the absorber. Initially, a high mass transfer flux is observed as the solution concentration in the absorbent is high, however, the absorption rate decreases sharply as concentration and temperature boundary layers are developed consequently forming a resistance to the absorption of refrigerant molecules into the solution. A steady mass transfer occurs in the latter part of the channel as in addition to the refrigerant molecules diffusion into the bulk solution, the coolant wall linearly dissipates the heat of absorption and allows the solution to cool down and maintain the absorption capacity of the solution. It is observed that a 25% increase in the overall absorption rate can be achieved by using a water/(LiBr + LiI + $LiNO_3$+LiCl) working fluid mixture with a 64.2% inlet solution concentration. In addition, the absorption rate is higher by a factor of 1.67 when the solution inlet concentration of 64.2% is used instead of the 61% concentration in the case of the water/(LiBr + LiI + $LiNO_3$°+°LiCl) working fluid mixture.

Table 3
Input conditions for the CFD analysis of water/LiBr and water/(LiBr + LiI + $LiNO_3$°+°LiCl) working fluid mixtures.

Parameter	Base value
Absorber pressure, Pa	1.3 kPa
Inlet solution temperature, T_s	45 °C
Inlet solution concentration, X_s	60, 61, 64.2%
Solution Reynolds Number, Re	2
Cooling wall temperature, T_c	35–43 °C

The bulk solution temperature, coolant temperature and the solution-membrane interface temperature are graphically represented along the channel length in Fig. 3. The bulk solution temperature decreases from 318.15 K to 310.30 K, 309.94 K and 310.80 K in the case of water/LiBr, water/(LiBr + LiI + $LiNO_3$°+°LiCl) with a solution inlet concentration of 61% and water-(LiBr + LiI + $LiNO_3$ + LiCl) with a solution inlet concentration of

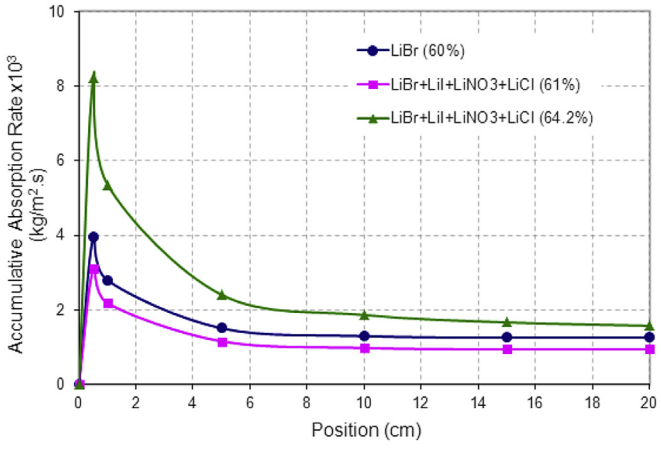

Fig. 2. Comparison of accumulative absorption rate of the working fluid mixtures along the channel length.

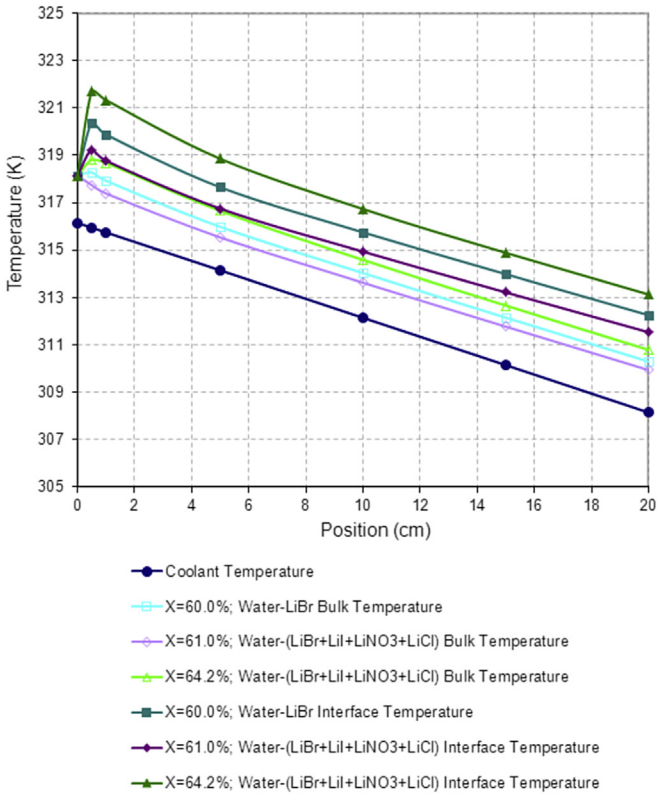

Fig. 3. Temperature profiles of the working fluid mixtures along the channel length.

64.2%, respectively. It can be seen that the solution-membrane interface temperature is higher than the bulk solution temperature for all the working fluid mixtures. This is because of the heat of absorption which is generated at the solution-membrane interface. A sharp increase in the interface temperature is observed initially because of the higher absorption rate achieved at first as a result of the higher concentration of the absorbent. The solution-membrane interface temperature decreases from 320.39 K, 319.25 K and 321.69 K–312.26 K, 311.54 K and 313.13 K in the case of water/LiBr, water/(LiBr + LiI + $LiNO_3$°+°LiCl) with a solution inlet concentration of 61% and water/(LiBr + LiI + $LiNO_3$°+°LiCl) with a solution inlet concentration of 64.2%, respectively. It was observed that both the bulk solution and the solution membrane interface temperature of the water/(LiBr + LiI + $LiNO_3$°+°LiCl) working fluid mixture with a solution inlet concentration of 64.2% was higher than that of the water/LiBr solution because the higher absorption rate leads to generation of higher heat of absorption.

Fig. 4 shows the bulk solution concentration and the solution-membrane interface concentration along the channel length. The mass fraction of the absorbent in the bulk solution decreases along the channel length due to the absorption of refrigerant molecules into the solution. It is observed that both the bulk solution concentration and the interfacial solution concentration decrease at the same rate thus producing a transverse concentration gradient along the solution channel to the end. As the concentration difference between the bulk solution and the solution-membrane interface also acts as a driving force for the mass transfer, water vapour absorption is observed up to the channel exit. It is worth noting that the mass fraction of water in the bulk solution and at the solution-membrane interface increases along the channel length, however, both the bulk solution temperature and the solution-membrane interface temperature decrease along the channel length. This causes a decrease in the partial pressure of the water vapour in the solution and an increase in the absorption capacity.

Fig. 5 shows the accumulative absorption rate achieved considering the water/($LiNO_3$°+°KNO_3°+°$NaNO_3$) working fluid mixture at different solution flow Reynolds numbers. The solution flow Reynolds number was increased from 1 to 8 while all other input parameters were kept constant in the simulation. The input variables for the analysis correspond to the operating conditions considered in the experimental analysis performed by Álvarez [21] given in Table 4. It can be seen that the absorption rate increases with an increase in the inlet velocity of the solution. Initially a high mass transfer flux is observed as the solution concentration is high, however, the absorption rate decreases sharply as concentration and temperature boundary layers are developed and resist the absorption of refrigerant molecules into the solution. A steady mass transfer occurs in the latter part of the channel as the coolant wall linearly dissipates the heat of absorption and allows the solution to cool down which increase the absorption capacity of the solution. Initially, the increase in the overall absorption rate is more significant below the solution flow Reynolds number of 2, whereas a linear increase in the absorption rate is achieved when the solution flow Reynolds number is increased from 2 to 8.The increase in the solution velocity brings fresh layers of solution near the membrane interface and increases the absorption capacity, however further-increasing the solution velocity decreases the solution residence time and minimizes the diffusion of water vapours across the solution causing a negative effect on the absorption mass flux. Consequently, the increase in the absorption rate is not very significant when the solution mass flow rate is increased at very high solution flow Reynolds numbers. The absorption rate was increased by a factor of 2 when the solution flow Reynolds number was increased from 1 to 8.

Figs. 6 and 7 show the contours of temperature and the concentration profiles at local levels in the case of water/($LiNO_3$°+°KNO_3°+°$NaNO_3$) working fluid mixture. Due to the higher aspect ratio of the channel, only the inlet, exit and the middle part of the channel are shown for the 0.5 mm solution channel. Fig. 6 depicts temperature values at local regions from which it can be observed that a temperature gradient exists across the width of the channel. It can be seen that the temperature near the solution-membrane interface (right side) is higher than the bulk solution temperature. This is because of the heat of absorption which is generated at the solution-membrane-interface. The temperature gradient in the transverse direction is higher in the case of higher Reynolds

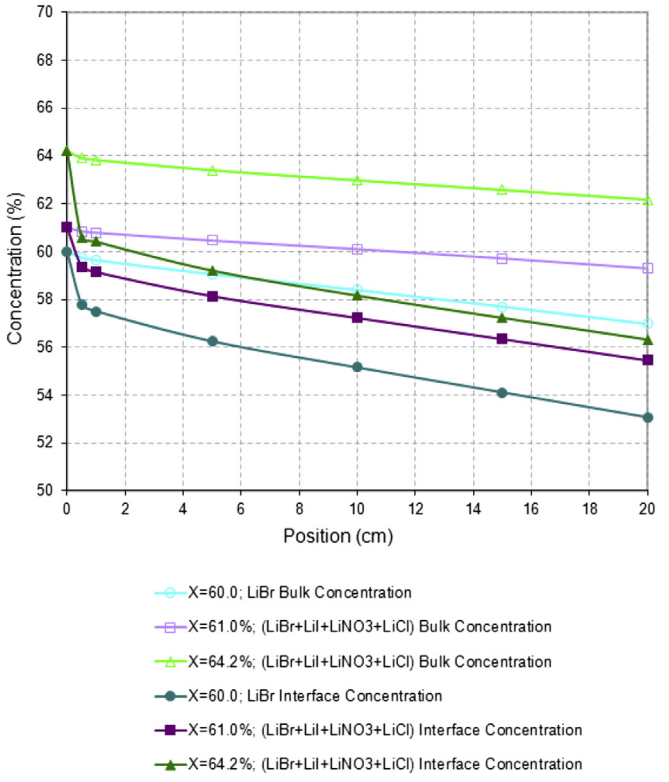

Fig. 4. Concentration profiles of the working fluid mixtures along the channel length.

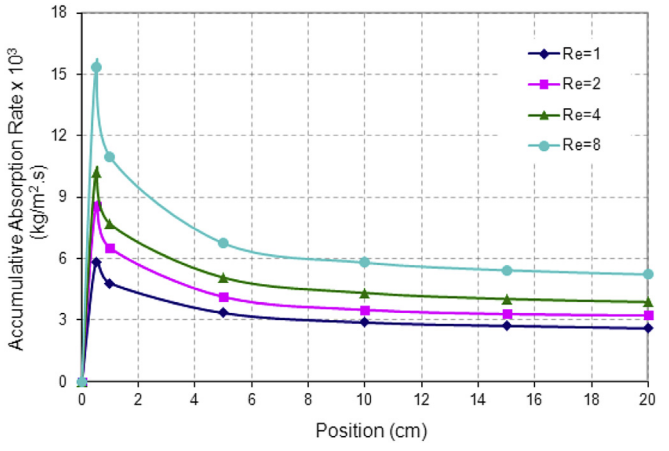

Fig. 5. Accumulative absorption rate along the channel length at different solution Reynolds number.

Table 4
Input conditions for the CFD analysis of water/($LiNO_3$ + KNO_3 + $NaNO_3$) working fluid mixture.

Parameter	Base value
Absorber pressure, Pa	30 kPa
Inlet solution temperature, T_s	93 °C
Inlet solution concentration, X_s	82%
Solution Reynolds Number, Re	1–8
Cooling wall temperature, T_c	80–88 °C

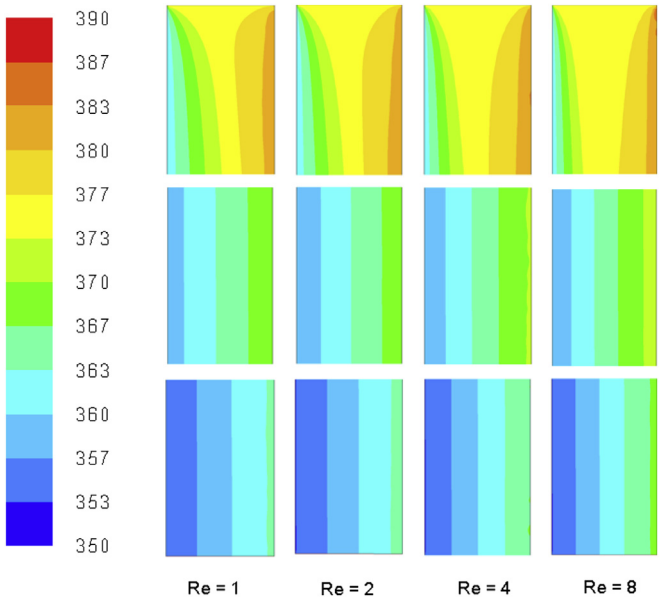

Fig. 6. Contours of temperature profile at different solution Reynolds numbers in the case of water/($LiNO_3$ + KNO_3 + $NaNO_3$) working fluid mixture.

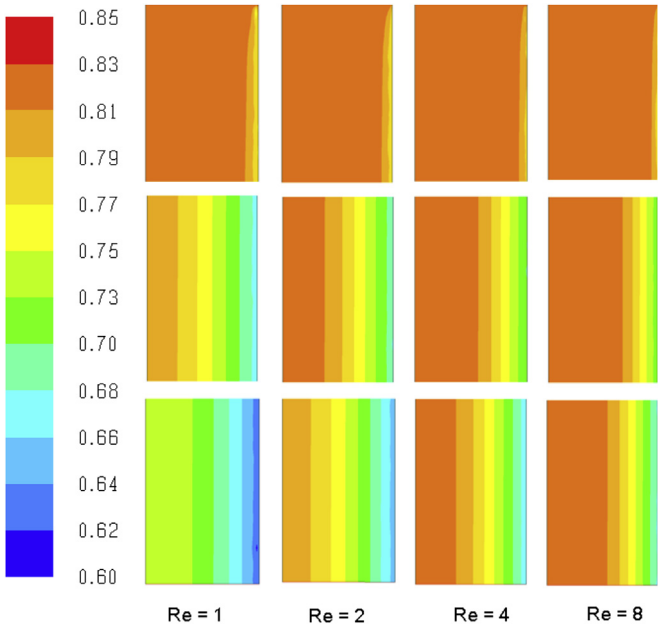

Fig. 7. Contours of concentration profile at different solution Reynolds numbers in the case of water/($LiNO_3$ + KNO_3 + $NaNO_3$) working fluid mixture.

number because of the higher absorption rate which leads to the generation of higher heat of absorption. In addition, the temperature difference between the bulk solution and the solution-membrane interface is higher near the inlet of the channel and then decreases downwards by about 6 K. This is because of the higher absorption rate at the inlet which generates more heat at the solution-membrane interface and thus a higher temperature gradient is observed. Fig. 7 shows the solution concentration at a local level. It can be seen that the absorbent concentration in the solution is lower at the solution-membrane interface (right side) due to the absorption of refrigerant molecules at the interface. The refrigerant molecules diffuse across the solution at a low rate due to the low diffusivity which gives rise to a concentration gradient across the solution channel. The concentration boundary layer developed at the solution-membrane interface also plays an important role in limiting the mass transfer rate across the membrane. The concentration boundary layer decreases when the solution flow Reynolds number is increased. This occurs as the increase in the solution velocity brings fresh layers of solution with higher absorbent concentration near the membrane interface which increases the absorption capacity.

Fig. 8 shows the overall pressure drop percentage along the solution channel for the three working pairs, namely water/($LiNO_3$°+°KNO_3°+°$NaNO_3$), water/LiBr and water/(LiBr + LiI + $LiNO_3$°+°LiCl). The solution pressure at the absorber exit is set as the absorber operating pressure which is 1.3 kPa in the case of water/LiBr and water/(LiBr + LiI + $LiNO_3$°+°LiCl) and 30 kPa in the case of water/($LiNO_3$°+°KNO_3°+°$NaNO_3$). The overall pressure drop percentage is calculated with reference to absorber inlet pressure. It can be seen that the overall pressure drop percentage is higher in the case of the water/(LiBr + LiI + $LiNO_3$°+°LiCl) working fluid mixture as opposed to the water/LiBr solution. This is because of the higher viscosity of water/(LiBr + LiI + $LiNO_3$°+°LiCl). Despite the higher viscosity of the Alkitrate solution, the pressure drop percentage is lower compared to water/LiBr and water/(LiBr + LiI + $LiNO_3$°+°LiCl) working fluid mixtures because of the higher operating pressure of the absorber. It means that in case of water/($LiNO_3$°+°KNO_3°+°$NaNO_3$), higher solution mass flow rate can be used to achieve a higher absorption rate without affecting the performance of the absorber. The pressure drop percentage of water/(LiBr + LiI + $LiNO_3$°+°LiCl) with a 64.2% solution inlet concentration is about 9 times higher compared to that of a water/($LiNO_3$°+°KNO_3°+°$NaNO_3$) working fluid mixture.

6. Conclusion

In this study, a detailed analysis of a membrane based absorber has been performed to investigate the heat and mass transfer

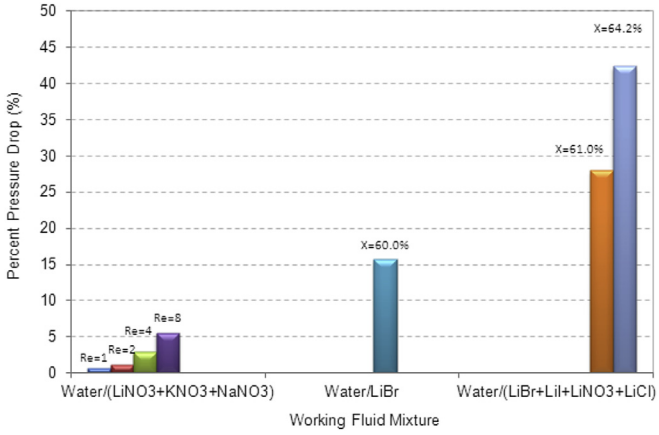

Fig. 8. Comparison of percent pressure drop along the solution channel length.

processes at local levels in the flow channels using CFD approach. Introducing polymeric hydrophobic microporous membranes into the absorber design can be one of the alternatives for achieving highly compact absorbers with enhanced heat and mass transfer processes. Working fluid mixtures, water/(LiBr + LiI + $LiNO_3$°+°LiCl) with mass compositions in salts of 60.16%, 9.55%, 18.54% and 11.75%, respectively, and water/($LiNO_3$°+°KNO_3°+°$NaNO_3$) with mass compositions in salts of 53%, 28% and 19%, respectively, were investigated for air cooled and multi-stage high temperature heat source absorption cooling systems, respectively. These non-conventional working fluid mixtures are able to cope with the limitations of the conventional water/LiBr working pair. Water/LiBr fluid mixture is prone to crystallization at air-cooling thermal conditions. In addition, it cannot operate in the last stage of a triple-effect absorption cooling system driven by high temperature heat sources (>200 °C) because of thermal instability, crystallization and corrosion problems.

The simulation results provide a deep insight into the heat and mass transfer processes in membrane based absorbers. The results of the CFD simulations are useful and play an important role in the design of membrane based absorbers using non-conventional working fluid mixtures. Results show that a 25% increase in the absorption rate can be achieved by using water/(LiBr + LiI + $LiNO_3$°+°LiCl) rather than water/LiBr at air cooling thermal conditions. Furthermore, an absorption rate as high as 0.00523 kg/m^2 s is achieved when a water/($LiNO_3$°+°KNO_3°+°$NaNO_3$) working fluid mixture is used in the membrane-based absorber of the third stage of a triple-effect absorption cooling cycle. In addition, the pressure drop percentage in the case of the water/($LiNO_3$°+°KNO_3°+°$NaNO_3$) working fluid mixture is significantly lower than that of the water/LiBr and water/(LiBr + LiI + $LiNO_3$°+°LiCl) working fluid mixtures because of the higher operating pressure.

Acknowledgements

This study is part of an R&D project funded by the Spanish Ministry of Economy and Competitiveness (DPI2012-38841-C02-02). The authors gratefully acknowledge the Spanish Ministry of Economy and Competitiveness (CTQ2013-46799-C2-1-P) for funding the ANSYS/FLUENT licence. Faisal Asfand gratefully acknowledges the Rovira i Virgili University for granting the Martí-Franquès research fellowship 2012 (2012BPURV-50) to pursue a doctorate degree.

References

[1] Asfand F, Bourouis M. A review of membrane contactors applied in absorption refrigeration systems. Renew Sustain Energy Rev 2015;45:173–91.
[2] Ali AHH, Schwerdt P. Characteristics of the membrane utilized in a compact absorber for lithium bromide–water absorption chillers. Int J Refrig 2009;32:1886–96.
[3] Yu D, Chung J, Moghaddam S. Parametric study of water vapor absorption into a constrained thin film of lithium bromide solution. Int J Heat Mass Transf 2012;55:5687–95.
[4] Isfahani RN, Sampath K, Moghaddam S. Nanofibrous membrane-based absorption refrigeration system. Int J Refrig 2013;36:2297–307.
[5] Isfahani RN, Moghaddam S. Absorption characteristics of lithium bromide (LiBr) solution constrained by superhydrophobic nanofibrous structures. Int J Heat Mass Transf 2013;63:82–90.
[6] Asfand F, Stiriba Y, Bourouis M. Impact of the solution channel thickness while investigating the effect of membrane characteristics and operating conditions on the performance of water-LiBr membrane-based absorbers. Appl Therm Eng 2016;108:866–77.
[7] Asfand F, Stiriba Y, Bourouis M. CFD simulation to investigate heat and mass transfer processes in a membrane-based absorber for water-LiBr absorption cooling systems. Energy 2015;91:517–30.
[8] Bigham S, Yu D, Chugh D, Moghaddam S. Moving beyond the limits of mass transport in liquid absorbent microfilms through the implementation of surface-induced vortices. Energy 2014;65:621–30.
[9] Bourouis M, Vallès M, Medrano M, Coronas A. Absorption of water vapour in the falling film of water-(LiBr + LiI + $LiNO_3$ + LiCl) in a vertical tube at air-cooling thermal conditions. Int J Therm Sci 2005;44:491–8.
[10] Bourouis M, Vallès M, Medrano M, Coronas A. Performance of air-cooled absorption air conditioning systems working with water-(LiBr + LiI + $LiNO_3$ + LiCl). J Process Mech Eng 2005;219:205–12.
[11] Medrano M, Bourouis M, Coronas A. Absorption of water vapour in the falling film of water-lithium bromide inside a vertical tube at air-cooling thermal conditions. Int J Therm Sci 2002;41:891–8.
[12] Davidson W, Erickson D. 260 °C Aqueous absorption working pair under development. Newsl IEA Heat Pump Cent 1986;4:29–31.
[13] Howe L, Erickson D. Proof-of-Concept testing of alkitrate. Phase III. Final Report. USA: Energy Concepts Co.; 1990.
[14] Erickson D, Potnis SV, Tang J. Triple effect absorption cycles. In: Energy conversion engineering conference IECEC 96. Proceedings of the 31st Intersociety; 1996. p. 1072–7.
[15] Álvarez M, Esteve X, Bourouis M. Performance analysis of a triple-effect absorption cooling cycle using aqueous (lithium, potassium, sodium) nitrate solution as a working pair. Appl Therm Eng 2015;79:27–36.
[16] Uemura T, Hasaba S. Studies on the lithium bromide-water absorption refrigeration machine, vol. 6. Technology Reports of Kansai University; 1964. p. 31–55.
[17] Koo KK, Lee HR, Jeong S, Oh YS, Park DR, Baek YS. Solubilities, vapor pressures, and heat capacities of the water + lithium bromide + lithium nitrate + lithium iodide + lithium chloride system. Int J Thermophys 1999;20:589–600.
[18] CREVER-URV. Thermophysical properties of the fluid mixture water/(LiBr + LiI + $LINO_3$ + LICl). Confidential Report. Spain: Universitat Rovira i Virgili; 2012.
[19] Álvarez M, Bourouis M, Esteve X. Vapor-liquid equilibrium of aqueous alkaline nitrate and nitrite solutions for absorption refrigeration cycles with high temperature driving heat. J Chem Eng Data 2011;56:491–6.
[20] Lee RJ, DiGuilio RM, Jeter SM, Teja AS. Properties of lithium bromide-water solutions at high temperatures and concentrations - II Density and viscosity. ASHRAE Trans 1990:709–14. Paper 3381. RP-527.
[21] Álvarez ME. Theoretical and experimental study of the aqueous solution of lithium, sodium and potassium nitrates as a working fluid in absorption chillers driven by high temperature heat sources. PhD Thesis. Spain: Universitat Rovira i Virgili; 2013.
[22] Kaita Y. Thermodynamic properties of lithium bromide–water solutions at high temperatures. Int J Refrig 2001;24:374–90.
[23] Salavera D, Esteve X, Patil KR, Mainar AM, Coronas A. Solubility, heat capacity, and density of lithium bromide+lithium iodide+lithium nitrate+lithium chloride aqueous solutions al several compositionss and temperature. J Chem Eng Data 2004;49:613–9.
[24] Laliberté M. A model for calculating the heat capacity of aqueous solutions, with updated density and viscosity data. J Chem Eng Data 2009;54:1725–60.
[25] DiGuilio RM, Lee RJ, Jeter SM, Teja AS. Properties of lithium bromide-water solutions at high temperatures and concentrations - I Thermal conductivity. ASHRAE Trans 1990:702–8. Paper 3380. RP-527.
[26] Aseyev G. Electrolytes - properties of solutions methods for calculation of multicomponent systems, and experimental data on thermal conductivity and surface tension. New York: Begell House Publishers; 1998.
[27] Florides GA, Kalogirou SA, Tassou SA, Wrobel LC. Design and construction of a LiBr–water absorption machine. Energy Convers Manag 2003;44:2483–508.
[28] Asfand F, Bourouis M. Estimation of differential heat of dilution for aqueous lithium (bromide, iodide, nitrate, chloride) solution and aqueous (lithium, potassium, sodium) nitrate solution used in absorption cooling systems. Int J Refrig 2016. http://dx.doi.org/10.1016/j.ijrefrig.2016.08.008.
[29] Ally M. Thermodynamic properties of aqueous ternary solutions relevant to chemical heat pumps. Final Report. ORNL/TM-10258. Oak Ridge National Laboratory; 1987.
[30] Gierow M, Jernqvist A. Measurement of mass diffusivity with holographic interferometry for H2O/NaOH and H2O/LiBr working pairs. Int Abs Heat Pump Conf 1993;31:525–32.
[31] Bird R, Stewart W, Lightfoot E. Transport phenomena. second ed. OUP; 2001.
[32] Martınez L, Rodrıguez-Maroto JM. On transport resistances in direct contact membrane distillation. J Membr Sci 2007;295:28–39.
[33] ANSYS FLUENT UDF manual. ANSYS Inc.; November 2011. Release 14.0.
[34] ANSYS FLUENT theory guide. ANSYS Inc.; November 2011. Release 14.0.

A.5 Impact of the solution channel thickness while investigating the effect of membrane characteristics and operating conditions on the absorption performance of a membrane-based absorber.

Applied Thermal Engineering 108 (2016) 866–877

Contents lists available at ScienceDirect

Applied Thermal Engineering

journal homepage: www.elsevier.com/locate/apthermeng

Research Paper

Impact of the solution channel thickness while investigating the effect of membrane characteristics and operating conditions on the performance of water-LiBr membrane-based absorbers

Faisal Asfand, Youssef Stiriba, Mahmoud Bourouis *

Department of Mechanical Engineering – Universitat Rovira i Virgili, Av. Països Catalans No. 26, 43007 Tarragona, Spain

HIGHLIGHTS

- A steady-state global heat and mass transfer model is developed for water-LiBr membrane-based absorbers.
- Solution mass transfer resistance is dominant in thicker solution channels.
- Membrane mass transfer resistance is considerable in thinner solution channels.
- High absorption rate is achievable in the case of thinner solution channels.

ARTICLE INFO

Article history:
Received 4 February 2016
Revised 17 July 2016
Accepted 19 July 2016
Available online 20 July 2016

Keywords:
Membrane contactor characteristics
Plate-and-frame membrane absorber
Water-LiBr
Absorption cooling systems

ABSTRACT

In this study, a numerical analysis is performed to investigate the effect of membrane contactor characteristics and operating conditions on the absorption performance in plate-and-frame membrane-based absorbers used in water-LiBr absorption cooling systems. This paper critically evaluates the impact of the solution channel thickness while investigating the effect of membrane characteristics. Results show that the effect of membrane characteristics is different in the case of different solution channel thicknesses. For instance, increasing the membrane mean pore size from 0.25 μm to 1 μm enhances the absorption rate by 75% in the case of a 0.1 mm solution channel, whereas in a 0.5 mm solution channel the absorption rate increases by 40%. In addition, a parametric study is performed to study the effect of solution mass flow rate, vapour pressure, solution inlet concentration and cooling water temperature on the absorption performance, taking into consideration different solution channel thicknesses. Results show that a high absorption rate can be achieved in the case of thinner solution channels. Moreover, the percentage change in the absorption rate remains almost the same when the vapour pressure, solution inlet concentration and coolant inlet temperature are varied in the case of different solution channel thicknesses.

1. Introduction

Absorption technology, which has the ability to utilize heat directly for cooling purposes, has been one of the most widely used technologies for refrigeration and cooling applications since the early stages of refrigeration technology. Working fluid mixtures employed in absorption cooling systems are environmentally friendly and do not contribute to greenhouse gas emissions, whereas vapour compression systems, which also use costly mechanical energy input, do. The absorber is an important component of the absorption cooling system and plays a critical role in the overall performance, size, and capital cost of the system. Both heat and mass transfer take place simultaneously in the absorber. Both the design and configuration of the absorber significantly influence its performance. Many researchers have suggested continued improvements in the design and configuration of the absorber to improve its performance and thermal efficiency. In recent years, research has been carried out regarding the use in absorption cooling systems of membrane contactors in the form of plate-and-frame membrane modules and hollow fiber membrane modules. A comprehensive review on the application of membrane contactors in absorption refrigeration systems has been carried out by Asfand and Bourouis [1]. The authors reviewed in detail, the types of membrane modules used in absorption cooling systems

* Corresponding author.
E-mail address: mahmoud.bourouis@urv.cat (M. Bourouis).

http://dx.doi.org/10.1016/j.applthermaleng.2016.07.139
1359-4311/

Nomenclature

A	area (m^2)
C_p	specific heat (J/kg K)
c_B	Boltzmann constant (J/K)
D	diffusion coefficient (m^2/s)
d_p	membrane pore mean diameter (μm)
d_h	hydraulic diameter (m)
dz	discretization length (m)
H	enthalpy (J/kg)
h	convection heat transfer coefficient (W/m^2 K)
J	mass transfer flux (kg/m^2 s)
K	mass transfer coefficient (kg/m^2 s Pa)
Kn	Knudsen number, $Kn = \lambda/d_p$
k	thermal conductivity (W/m K)
L	channel length (m)
L^*	flow length (m)
M	molecular weight (g/mol)
$\dot{m}$	mass flow rate (kg/s)
Nu	Nusselt number, $Nu = h \cdot d_h/k$
P	pressure (Pa)
p	vapour pressure of solution (Pa)
R	universal gas constant (J/mol K)
Sc	Schmidt number, $Sc = \mu/(\rho \cdot D)$
Sh	Sherwood number, $Sh = K \cdot d_h/D$
Re	Reynolds number, $Re = \rho \cdot u \cdot d_h/\mu$
T	temperature (°C, K)
t	channel thickness (m)
U	global heat transfer coefficient (W/m^2 K)
u	velocity (m/s)
w	channel width (m)
X	LiBr mass fraction

Greek letters

α	channel aspect ratio, $\alpha = t/w$
ρ	density (kg/m^3)
ε	porosity
δ_m	membrane thickness (μm)
σ	molecular collision diameter (m)
τ	tortuosity
λ	mean free path (m)
μ	dynamic viscosity (kg/m s)

Subscripts

c	coolant
H_2O	water
int	solution-membrane interface
m	membrane
s	solution
v	vapour
w	wall

Abbreviations

AMD	Advanced Micro Devices
CFD	Computational Fluid Dynamics
MATLAB	MATrix LABoratory

and the effect of membrane-based components on the cycle configuration. In addition, membrane material characteristics were also discussed. They concluded, from their review, that the use of membrane contactors in the absorber and desorber of an absorption refrigeration system can not only enhance the heat and mass transfer performance of the component, but can also allow for a reduction in the size of the component. Thus, introducing polymeric hydrophobic microporous membranes into the absorber design could provide one of the alternatives for achieving highly compact absorbers, as microporous membrane contactors can provide a high specific surface area. Ali and Schwerdt [2] analytically and experimentally analysed a plate-and-frame membrane based absorber and achieved an absorption rate of 0.00125 kg/m^2 s at a water vapour pressure of 2.339 kPa which is more than twice the available pressure in a typical absorber. Their experimental results show no change in absorption rate when the vapour pressure difference across the membrane was increased. Ali and Schwerdt [2] reported that their membrane mass transport resistance could have dominated the overall mass transfer process which resulted in poor absorption rates. However, the experimental studies carried out by Isfahani and Moghaddam [3] suggest that the mass transfer through the solution is the dominant resistance as compared to the membrane mass transfer resistance. Yu et al. [4] performed numerical simulations to investigate a plate-and-frame membrane absorber and observed that a 3-fold increase in the absorption rate can be achieved when the solution film thickness is reduced from 0.15 mm to 0.05 mm. Isfahani et al. [5] experimentally investigated a membrane based absorber for the absorption of water vapour in the aqueous solution of LiBr and reported that the absorption rate was 2.5 times higher than that in falling film absorbers. Isfahani and Moghaddam [3] experimentally analysed the absorption characteristics of water vapour in a thin LiBr solution constrained by superhydrophobic nanofibrous membrane structures. They studied the effect of water vapour pressure, cooling temperature, solution film thickness and solution mass flow rate on the absorption rate in a membrane based absorber. They achieved an absorption rate of 0.006 kg/m^2 s with a solution film thickness of 0.1 mm and a velocity of 0.005 m/s. Bigham et al. [6] experimentally and numerically investigated the implementation of micro-scale features on the flow channel surface to induce vortices within the solution film. They reported that the mass transport mode in such a configuration could be changed from a diffusive to an advective mode. They obtained an increase in the absorption rate by a factor of 2.5 i.e. from 0.0016 kg/m^2 s to 0.004 kg/m^2 s for the flow channel with micro-scale features on the surface. Asfand et al. [7] performed numerical simulations to investigate heat and mass transfer behaviour in a plate-and frame absorber and observed that the absorption rate can be significantly enhanced if the solution channel thickness is reduced. However, they reported that the solution pressure drop along the channel increases exponentially with the decrease in solution channel thickness and this can significantly affect the performance of an absorber operating with water as a refrigerant under vacuum conditions. They recommended an optimal solution channel thickness of 0.5 mm and a solution velocity of about 0.005 m/s to achieve a higher absorption rate with an acceptable solution pressure drop along the channel. Venegas et al. [8] developed a numerical model to predict the performance of a membrane-based absorber. They reported that by using a plate-and-frame membrane absorber the size was reduced by 50% as opposed to using a falling film absorber for the same cooling capacity. Later, Venegas et al. [9] used this model to perform a parametric study of design and operating conditions. They evaluated the effect of these parameters on the cooling capacity and absorber size.

The selection of appropriate membrane contactor material with suitable characteristics, i.e. porosity, pore size, thickness, tortuosity, etc. is crucial when designing a membrane-based component. In addition, the mechanical strength of the membrane contactor

is dependent on the above mentioned characteristics. The objective of the present work is to analyse in detail, the effect of membrane contactor characteristics and operating conditions on the performance of a plate-and-frame membrane absorber. Although membrane material characteristics were investigated analytically in previous studies, in each case the analysis was performed for a specific solution channel thickness. As the concentration and thickness of the thermal boundary layers decrease when the solution channel thickness is decreased, the absorption potential varies for different solution channel thicknesses. Further, the resistance to the refrigerant mass transfer also differs, which means that the impact of membrane mass transfer resistance and solution mass transfer resistance varies and the relative contribution of each resistance can change. In this regard, this study critically evaluates the impact of different solution channel thicknesses while investigating the effect of membrane characteristics. A range of different membrane properties i.e. porosity, membrane thickness and mean membrane pore size is applied, so as to investigate their effect on the absorption performance. In addition, to select the most suitable operating conditions for efficient performance, a parametric study is performed to assess the effect of the operating conditions on the absorption rate in a plate-and-frame absorber. In previous studies, heat and mass transfer processes in a plate-and-frame membrane absorber were investigated by the authors at a local level using computational fluid dynamics codes [7]. However, because of the higher computational time needed for a CFD based simulation to reach converged results, it is time consuming to perform a parametric study to evaluate in detail the effect of membrane contactor characteristics and operating conditions. Therefore, the aim of this work is to develop an efficient global model using simplified one dimensional heat and mass transfer equations which can perform steady-state analysis with less computation efforts and CPU time. The numerical model can be useful to integrate into a system analysis model to evaluate the absorption cycle performance employing a membrane-based absorber and to evaluate the effect of different parameters on the size and performance of the absorber. The model can be of use to design a compact membrane-based absorber for absorption cooling systems to enhance their performance and reduce their size. This would also enable the use of absorption cooling in small scale applications.

2. Absorber configuration

A plate-and-frame membrane absorber was selected for the analysis in this study. As in a water-LiBr based absorption cooling system, the absorber operates under vacuum conditions and therefore the plate-and-frame membrane module, which offers minimum pressure drop, could be an interesting choice. The structural unit of the absorber configuration with a membrane contactor and the sectional view of the absorber are shown in Fig. 1. The configuration of the plate-and-frame absorber is set as such that the solution, coolant and vapour all flow in individual flow channels. Each coolant channel serves two solution channels and is fed in a counter flow direction. The first and last cells of the module have half the width of the coolant channels. Similarly, each vapour channel serves two solution channels and can be counter flow or co-current flow. The coolant and solution are separated using a metallic plate across which heat transfer takes place. A microporous hydrophobic membrane sheet is placed at the aqueous solution–water vapour interface in the form of a parallel sheet along the metallic plate. Both heat and mass transfer processes take place across the membrane sheet. The parallel assembly of the plates and membrane sheets minimizes the pressure drop through the absorber.

3. Methodology

Fig. 2 shows the detailed modelling of the heat and mass transfer processes in a single element of the absorber cell. The vapour pressure difference across the membrane causes the refrigerant vapour to pass through the membrane pores from the refrigerant side to the solution side, where the vapour condenses and dilutes the solution at the solution-membrane interface. During the process, the heat of condensation and mixing, known as heat of absorption, releases at the solution membrane interface. As a result, the temperature of the solution increases, whereas the solution concentration decreases at the solution-membrane interface and differs from that of the bulk solution. Consequently, the water vapour partial pressure near the solution-membrane interface increases and limits further absorption of the refrigerant vapours. The formation of the concentration and thermal boundary layers

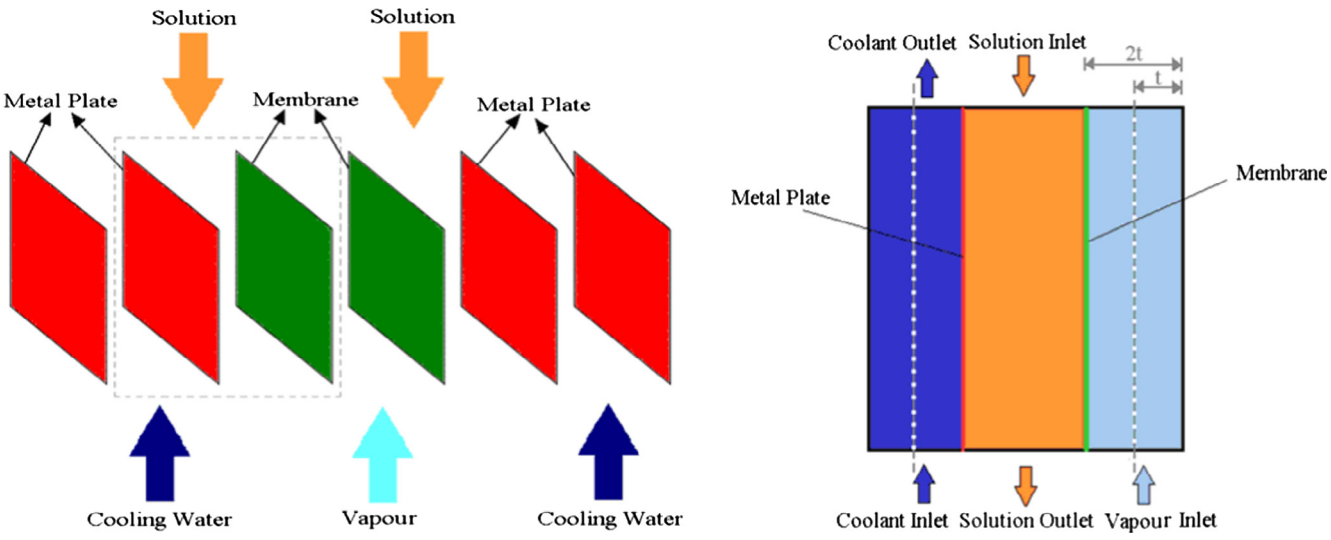

(a) Flow channel configuration (b) 2D sectional view of a single unit

Fig. 1. Configuration of a plate-and-frame absorber with membrane contactor.

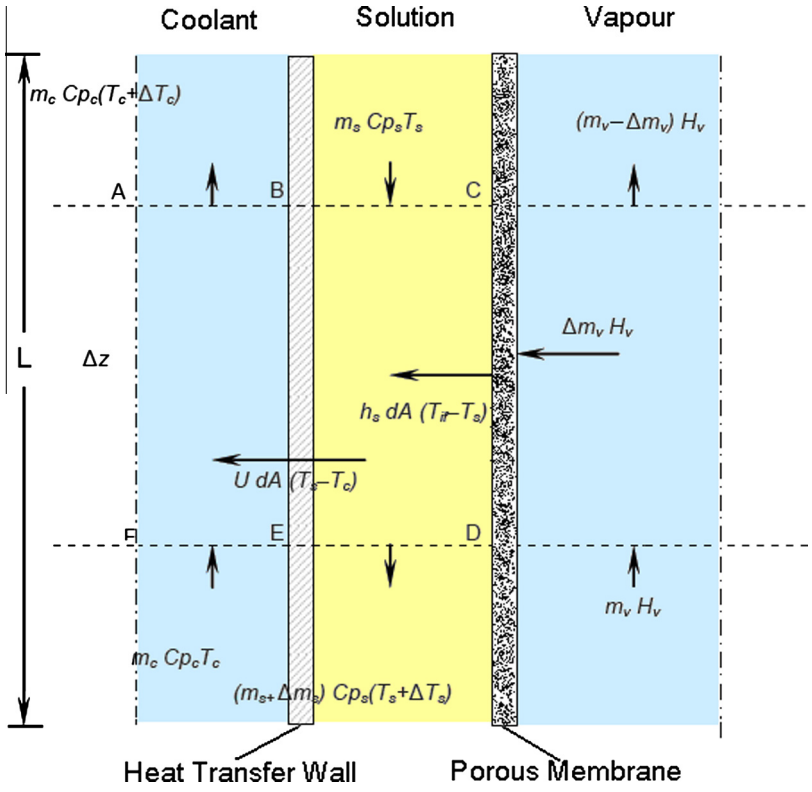

Fig. 2. Schematic of heat and mass transfer processes in an absorber cell segment.

represents an additional thermal and mass transfer resistance to the refrigerant mass transfer and heat transfer fluxes. Refrigerant molecules diffuse from the solution-membrane interface into the bulk solution as a result of the difference in concentration. Similarly, heat flows from the solution-membrane interface towards the coolant wall, due to the difference in temperatures of the bulk solution and the solution near the interface. This heat is dissipated by the coolant which flows in a counter current direction. The interface temperature and interface concentration are lowered, as a result of the heat dissipated by the coolant and the diffusion of the refrigerant molecules into the bulk solution, respectively. Consequently, the partial pressure of water vapour at the solution-membrane interface decreases and promotes further absorption of refrigerant vapours.

In the present simulation of heat and mass transfer, the mathematical model is based on the energy and mass balance equations in an infinitesimal area along the channel. This yields a coupled heat and mass transfer model. A one dimension analysis was carried out along the channel length using a MATLAB code. Each channel was discretized into 200 cells along the length and the governing non-linear and differential equations were solved simultaneously in each cell using the Newton-Raphson and the Runge–Kutta methods, respectively. A convergence criterion of 2×10^{-07} was used to obtain a steady-state converged solution.

The current model is simple and can predict the absorption rate and other parameters with fine accuracy. The model is able to calculate the interface temperature and interface concentration of the solution. These values are used to calculate the partial pressure of water vapour in the solution at the solution-membrane interface. In the previous numerical models [2,8], the bulk solution temperature and the concentration were used to calculate the partial pressure of vapour in the bulk solution from which the mass transfer flux was calculated. In a previous study [7], calculations were performed by the authors to investigate heat and mass transfer processes in a water-LiBr membrane-based absorber using CFD approach. Numerical simulations were preformed in a workstation cluster of 24 AMD Opteron 248 dual core processors (64 bits) and 7 Intel 3 GHz processors, with 3 terabytes of disk, linked with a Giga Ethernet in a Linux environment. Simulations were performed in parallel using four processors and each case simulated took approximately 6 days to achieve a steady-state condition. The same case was simulated using the global model developed in MATLAB and a desktop computer with a 3.0 MHz processor was used to perform the simulation. In this case, steady-state results were obtained within approximately 3 min in the case of the coolant flowing in the counter flow direction whereas when the coolant flow was considered in the co-current direction, steady-state results were obtained in less than 20 s.

3.1. Model assumptions

The following assumptions are considered in the analytical model for the simulation

- Steady state conditions.
- One dimensional transfer in the flow direction along the length.
- Vapour channel pressure and temperature are assumed constant.
- Coolant thermophysical properties are assumed constant.
- No heat lost or gained from the surroundings to the absorber cells.

3.2. Governing equations

The driving force for the refrigerant vapour mass transfer across the membrane in a water-LiBr absorber is the difference in vapour pressure and partial pressure of water vapour in the aqueous solu-

tion. The mass transfer flux across the membrane is given by Martinez and Rodriguez-Maroto [10] as follows:

$$J^i = m^i/(w \cdot dz) = K_m^i\left(P_v^i - p_{\text{int}}^i\right) \tag{1}$$

where J is the mass transfer flux of water vapour absorbed in the solution, P_v is the water vapour pressure and p_{int} is the equilibrium water vapour partial pressure of the solution at the solution-membrane interface. It is calculated at the solution-membrane interface as a function of the solution concentration and temperature using the vapour pressure correlation given by Uemura and Hasaba [11]. m is the mass of water vapour absorbed, dz is the differential length of the segment. w is the width of the channel. K_m is the membrane equivalent mass transfer coefficient.

The bulk solution concentration is calculated from the mass balance equation given below

$$m_{s,out}^i = m_{s,in}^i + m^i \tag{2}$$

$$X_{s,out} = \frac{m_{s,in}}{m_{s,out}} X_{s,in} \tag{3}$$

The solution-membrane interface concentration is calculated using the equation given by Martinez and Rodriguez-Maroto [10]:

$$X_{\text{int}}^i = X_s^i \exp\left(-\frac{J^i}{K_{\text{int}}^i \rho_{\text{H}_2\text{O}}^i}\right) \tag{4}$$

where X_{int} is the interface concentration and K_{int} is the interface mass transfer coefficient. The solution-membrane interface temperature is calculated using the equation given below

$$T_{\text{int}}^i = T_s^i + \frac{H_v}{wh_s^i}\frac{m^i}{dz} \tag{5}$$

where T_{int} is the interface temperature, h_s is the solution heat transfer coefficient and H_v is the vapour enthalpy. The heat transfer equation in the solution channel is derived by considering a control volume and applying an energy balance. The differential equation derived to calculate the solution temperature in each segment can be written as:

$$\frac{dT_s^i}{dz} = \frac{H_v - Cp_s^i T_s^i}{m_s^i Cp_s^i}\frac{m^i}{dz} - \frac{U^i w\left(T_s^i - T_c^i\right)}{m_s^i Cp_s^i} \tag{6}$$

where T_s is the solution temperature and T_c is the coolant temperature. U is the overall heat transfer coefficient Cp_s and Cp_c are the solution and coolant specific heat capacities, respectively. Similarly, the heat transfer equation in the coolant channel is derived by considering a control volume along the coolant channel and applying an energy balance. The differential equation derived to calculate the coolant temperature in each segment can be written as:

$$\frac{dT_c^i}{dz^i} = \frac{U^i w\left(T_s^i - T_c^i\right)}{m_c^i Cp_c^i} \tag{7}$$

3.3. Heat and mass transfer coefficients

Mass transport through a microporous membrane can take place by different mechanisms depending on the flow regime. Thus, it is important to determine the flow regime in order to accurately calculate the mass flux through the membrane. Flow through a porous membrane can be classified into viscous, transitional, or free molecular flow regimes, depending on the magnitude of the Knudsen (Kn) number. The Kn number is defined as the ratio of the mean free path (λ) to the pore diameter (d_p):

$$Kn = \lambda/d_p \tag{8}$$

where λ is the mean free path and is calculated as:

$$\lambda = \frac{c_B \cdot T}{\sqrt{2} \cdot \pi \cdot \sigma^2 P} \tag{9}$$

where c_B is the Boltzmann constant (1.38×10^{-23} J/K), σ is the molecular collision diameter (2.7×10^{-10} m for water vapour), T is the absolute temperature in K and P is mean total pressure within the membrane pore in Pa.

For $Kn > 10$, collision between molecules and pore walls is dominant, the gas transport takes place in the free molecular regime and the flow is known as Knudesn flow, for which the membrane mass transfer coefficient can be calculated as:

$$K_m^i = \frac{M_{\text{H}_2\text{O}}}{\delta_m}\left(\frac{D_k}{RT_m^i}\right) \tag{10}$$

where M_{H2O} is the molecular weight of water, δ_{m} is the membrane thickness, R is the universal gas constant and T_m is the mean membrane temperature which is calculated as the average of vapour and solution interface temperatures. D_k is the Knudsen diffusion coefficient and for porous solid it can be calculated as:

$$D_k = \frac{\varepsilon d_p}{3\tau}\left(\frac{8RT_m^i}{\pi M_{\text{H}_2\text{O}}}\right)^{\frac{1}{2}} \tag{11}$$

where ε is the membrane porosity, τ is the tortuosity of the membrane and d_p is the mean membrane pore diameter.

When $Kn < 0.01$, collisions between gas molecules dominate and viscous flow occurs which results in rapid convective transport. The membrane mass transfer coefficient in the viscous flow regime can be calculated as:

$$K_m^i = \frac{M_{\text{H}_2\text{O}}}{\delta_m}\left(\frac{P_m B_0}{RT_m^i \mu_v}\right) \tag{12}$$

$$B_0 = \frac{\varepsilon d_p^2}{32\tau} \tag{13}$$

where μ is the viscosity and P is the pressure.

A transitional flow regime exists if $0.01 < Kn < 10$ and according to the Dusty-Gas model, the mass transfer through a membrane consists of both diffusion and viscous fluxes.

$$K_m^i = \frac{M_{\text{H}_2\text{O}}}{\delta_m}\left(\frac{D_k}{RT_m^i} + \frac{P_m B_0}{RT_m^i \mu_v}\right) \tag{14}$$

In this study, the base value of the mean membrane pore size is 1 μm and at a vapour pressure of 1 kPa and a temperature of 7 °C, the mean free path of water molecules is 13.2 μm, therefore the Knudsen number value lays in the free molecular regime for the base case and the vapour transport through the microporous membrane pores takes place via Knudsen diffusion mechanism. However, in some cases, particularly in the parametric study of membrane mean pore size and vapour pressure, the Knudsen number value lays in the transitional flow regime. In the code developed in MATLAB, the Knudsen number was calculated for each case study simulated and depending on the value of the Knudsen number an appropriate equation was used for the calculation.

The interface mass transfer coefficient K_{int} between the solution-membrane interface and the bulk solution, which is needed in Eq. (4) to calculate the interface solution concentration, is calculated using the Lévêque's equation. For laminar flow in thin rectangular channels, the mass transfer coefficient is related to the Sherwood number through the following relationship:

$$K_{\text{int}} = Sh \cdot \frac{D}{d_h} = 1.85 \cdot \left(Re \cdot Sc \cdot \frac{d_h}{L^*}\right)^{\frac{1}{3}} \cdot \frac{D}{d_h} \tag{15}$$

where *Re* is the Reynolds number, *Sc* is the Schmidt number and d_h is the hydraulic diameter, and L^* represents the flow length which is the distance from the mass transfer leading edge. Simplifying the above equation, we get:

$$K_{\text{int}} = 1.85 \cdot \left(u \cdot \frac{D^2}{d_h \cdot L^*} \right)^{\frac{1}{3}} \tag{16}$$

where u is the average solution velocity and D is the mass diffusivity of water molecules in the bulk LiBr solution.

The global heat transfer coefficient U, is calculated as:

$$\frac{1}{U^i} = \frac{1}{h_c^i} + \frac{t_w}{k_w^i} + \frac{1}{h_s^i} \tag{17}$$

where h_c and h_s are the local heat transfer coefficient of the coolant and solution and k_w is the thermal conductivity of the wall. As the ratio of the channel length to the thickness of the channel in both the coolant and solution channels is very high, the entrance region is not taken into account in the calculation and a fully developed laminar flow is considered in both the channels. The entrance region is very small in case of the flow channel with an increased length to thickness ratio and for simplification it can be neglected in the calculation as it does not significantly affect the results.

The convection heat transfer coefficient is linked to the Nusselt number through the following relationship:

$$h = Nu \cdot k/d_h \tag{18}$$

For fully developed flow in thin rectangular channels, the correlation developed by Shah and London [12] was used to calculate the Nusselt number.

$$Nu = 8.235 \cdot (1 - 2.0421 \cdot \alpha + 3.0853 \cdot \alpha^2 - 2.4765 \cdot \alpha^3 + 1.0578 \cdot \alpha^4 - 0.1861 \cdot \alpha^5) \tag{19}$$

where α is the channel aspect ratio.

3.4. Calculation sequence

Fig. 3 depicts the calculation sequence used in the global model developed in the present work. After the input values have been set, the inlet conditions are calculated. At the given operating conditions and initial guess values, the thermophysical properties of the solution are calculated, followed by the calculation of the first cell in which the Newton-Raphson method is used to calculate the refrigerant mass transfer across the membrane, absorption rate, interface temperature and concentration of the solution. A loop over the flow length starts with the calculation of the second cell and is repeated until the entire flow path is covered. In this loop, the ordinary differential equations are solved by the Runge-Kutta method using the variables obtained in the previous step to calculate the solution and coolant temperatures and the concentration of the bulk solution. The non-linear equations are solved in each cell using the Newton-Raphson method to calculate the refrigerant mass transfer across the membrane, the absorption rate and interface temperature and the concentration of the solution. The Newton–Raphson iteration is repeated until the root is found and a minimal residual is left. The thermophysical properties of the working fluid mixtures are updated in each cell as a function of solution concentration and temperature. When the loop over the flow length is completed and all the variables are calculated in each cell then the output results are checked for consistency. As the coolant flows in a counter-flow direction, a guess value of coolant temperature in the first cell is taken for the calculations. If the coolant temperature predicted in the last cell is equal to the cooling water inlet temperature, then the solution terminates and results are displayed. Otherwise, the coolant initial guess value is updated and the calculations are repeated unless the exact cooling water inlet temperature is obtained in the last cell.

3.5. Thermophysical properties of the working fluid

In this study, a water-LiBr solution is used as a working fluid mixture. The thermophysical properties of the aqueous solution of lithium bromide are estimated as a function of the solution concentration in lithium bromide and temperature. The density and viscosity of the aqueous solution of lithium bromide are calculated using the correlations developed by Lee et al. [13]. The thermal conductivity of the water-LiBr mixture is calculated using the DiGuilio et al. [14] correlation. The specific heat capacity of the water-LiBr mixture is calculated using the correlation based on the Mc Neely data [15]. The diffusion coefficient of water in the aqueous lithium bromide solution is calculated from the Gierow and Jernqvist [16] experimental data which is determined at a constant temperature and different concentrations. However, at other temperatures the diffusion coefficient is estimated using the equation given below.

$$\frac{D_1 \mu_1}{T_1} = \frac{D_2 \mu_2}{T_2} \tag{20}$$

where D is the diffusion coefficient, μ is the dynamic viscosity and T is absolute temperature in Kelvin. State 1 refers to the values calculated at 25 °C whereas state 2 refers to the values calculated at any other temperature.

4. Model validation

The numerical model was validated by comparing the absorption rate predicted with the experimental data reported by Isfahani and Moghaddam [3]. In their experiment, they used a solution and cooling water channels measuring 1 mm and 4 mm in width respectively, and a channel length of 38 mm. They investigated two different heights for the solution channel, 0.1 mm and 0.16 mm, where the height of the cooling water channel was 0.4 mm. An important issue is that the correlations used in the present model remain valid in all the cases. A solution inlet velocity of 0.005 m/s, and an inlet solution concentration and temperature of 60% and 25 °C, respectively, were considered in their experiment. Further, they used a very high mass flow rate for the coolant channel and for this reason they did not observe a temperature change between the inlet and exit of the cooling channel. Therefore, in this study a constant cooling temperature is used to validate the numerical model for the given conditions. The absorption rate predicted by the model was compared to the absorption rate achieved in the experiments for both the 0.1 mm and 0.16 mm solution channels at different values of vapour pressure. Fig. 4 shows the comparison of predicted and experimental results which are well in agreement with a mean absolute percentage error of about 5.35%.

5. Results and discussion

Steady-state analysis is carried out over a 200 mm long and 200 mm wide solution channel with a solution inlet concentration and temperature of 60% and 40 °C, respectively. Coolant inlet temperature is set at 30 °C. A constant vapour temperature of 7 °C is assumed and a corresponding saturation pressure of 1 kPa is considered. These input variables are typical operating conditions of an absorption cooling system working with water-LiBr mixture. In this section, a parametric study is carried out to investigate the effect of membrane characteristics and operating conditions on the absorption performance of a plate-and-frame absorber.

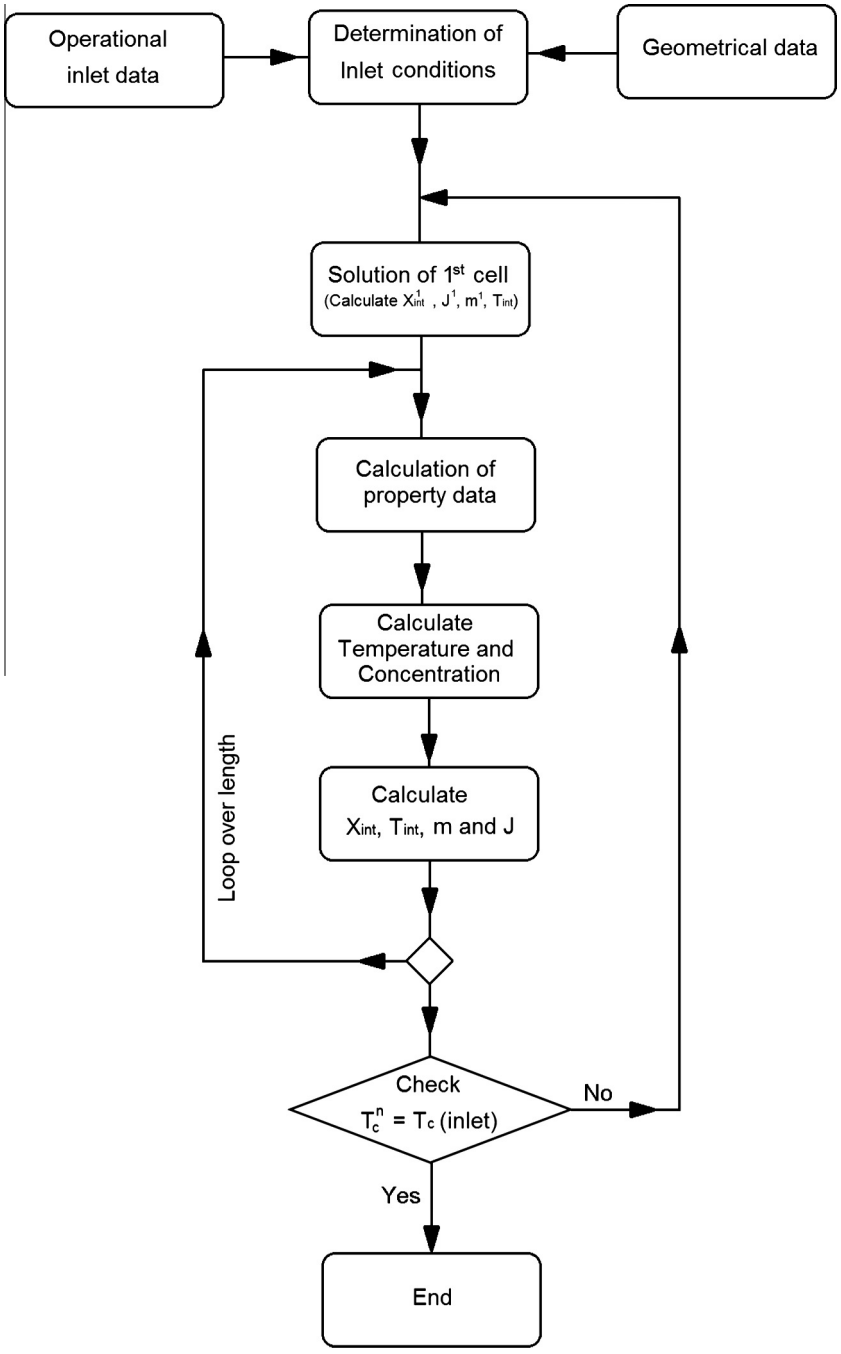

Fig. 3. Flowchart of the simulation code developed in the present work.

The obtained results provide sound information on the selection of the membrane characteristics and operating conditions in the case of different solution channel thicknesses.

5.1. Effect of membrane characteristics on the absorption process

In this study, a flat sheet membrane contactor made of polypropylene material is used. The membrane material characteristics considered for the parametric study are summarized in Table 1. The effect of membrane contactor mean pore size, porosity and thickness on the absorption rate is analysed in this section. Fig. 5 shows the effect of membrane pore size on the absorption rate. Results show that the absorption rate increases logarithmically with the increase in the membrane mean pore size. The increase in the absorption rate is more significant when the membrane mean pore diameter is increased from 0.25 μm to 1 μm because the effect of membrane mass transfer resistance is more dominant in membranes with small pore size and the mass transfer resistance decreases with an increase in the membrane mean pore diameter. However, further increasing the membrane pore diameter does not substantially affect the absorption rate because in membranes with larger pore diameter the diffusion resistance into the solution is a more dominant factor instead of the membrane mass transfer resistance. It can be seen from the results that at higher values of membrane pore diameter, the change in the absorption rate is negligible. Furthermore, it is evident from Fig. 5 that the increase in the absorption rate is lower in thicker solution channels when the membrane mean pore diameter is

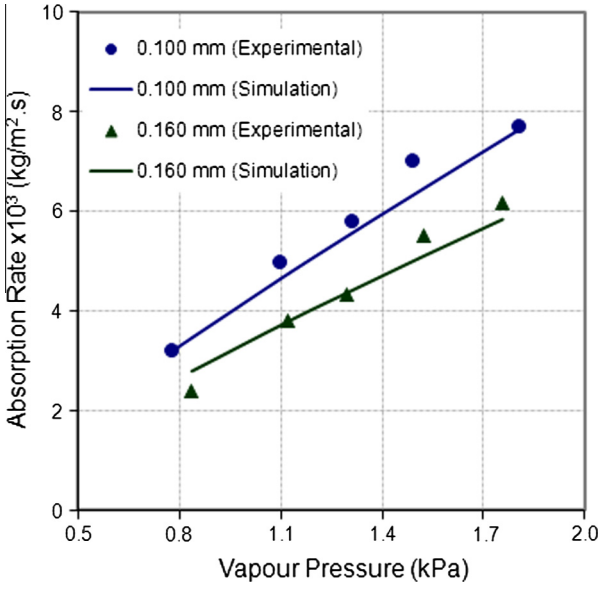

Fig. 4. Model validation using experimental data of Isfahani and Moghaddam [3].

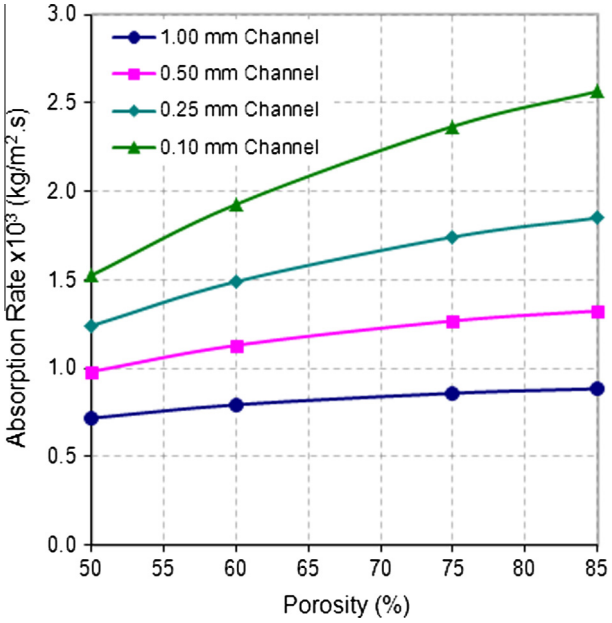

Fig. 6. Effect of membrane porosity on the absorption process.

Table 1
Membrane material characteristics.

Parameter	Base value	Range
Porosity, ε (%)	75	50–85
Tortuosity, $\tau\ (2-\varepsilon)^2/\varepsilon$	$(2-\varepsilon)^2/\varepsilon$	NA
Thickness, δm (μm)	40	20–100
Mean pore diameter, dp (μm)	1.0	0.25–3.00

increased. An increase of about 75%, 55%, 40% and 25% in the absorption rate is achievable when the membrane pore diameter is increased from 0.25 μm to 1 μm in the case of 0.1 mm, 0.25 mm, 0.5 mm and 1 mm solution channels, respectively. Moreover, further increasing the pore diameter from 1 μm to 5 μm results in an increase of about 22%, 16%, 11% and 7% in the absorption rate in the case of 0.1 mm, 0.25 mm, 0.5 mm and 1 mm solution channels, respectively. Increasing the membrane pore diameter reduces the resistance to the vapour transport through the pore which helps in enhancing the absorption rate, however, the mechanical strength of the membrane decreases with the increase in membrane pore size. Therefore, it is crucial to select a membrane with suitable pore diameter that will not only allow a higher absorption rate but will also augment the mechanical strength of the membrane.

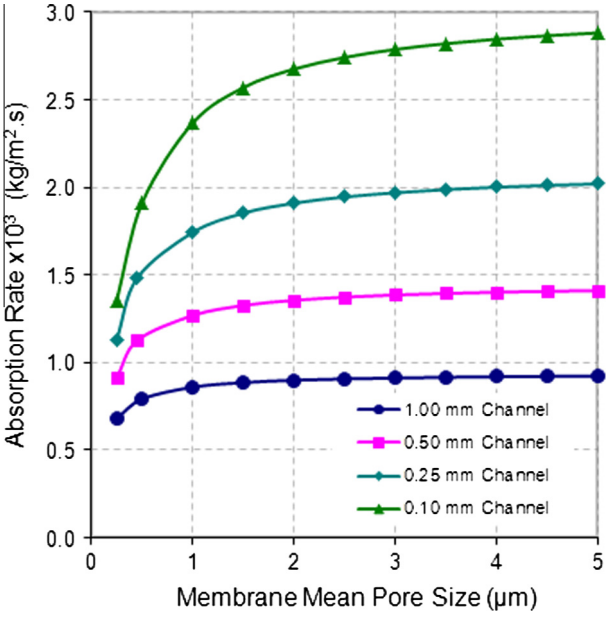

Fig. 5. Effect of mean membrane pore size on the absorption process.

Fig. 6 shows the effect of membrane contactor porosity on the absorption rate. Absorption rate increases almost linearly if the porosity of the membrane contactor is increased from 50% to 85%. Again, the increase in the absorption rate is lower in thicker solution channels when the membrane porosity is increased. An increase of about 68%, 49%, 35% and 23% in the absorption rate is achieved when the membrane porosity is increased from 50% to 85% μm in the case of 0.1 mm, 0.25 mm, 0.5 mm and 1 mm solution channels, respectively. Highly porous membranes exhibit less resistance to the mass transfer flux; however the mechanical strength of the membrane decreases with an increase in porosity.

Fig. 7 shows the effect of the membrane contactor thickness on the absorption rate. A linear decrease in the absorption rate is observed when the membrane contactor thickness is increased from 20 μm to 100 μm. It can be seen from the results that the decrease in the absorption rate is not significant in thicker solution channels when the membrane contactor thickness is increased. A decrease of about 35%, 28%, 21% and 15% in the absorption rate is observed when the membrane contactor thickness is increased from 20 μm to 100 μm in the case of 0.1 mm, 0.25 mm, 0.5 mm and 1 mm solution channels, respectively. Mass transfer resistance increases with an increase in the thickness of the membrane contactor which reduces the mass transfer across the membrane. However, the mechanical strength of the membrane contactor increases with an increase in thickness of the membrane.

In Fig. 8, the effect of the solution diffusivity on the mass transfer is evaluated by changing the diffusion coefficient. A higher value of the solution diffusion coefficient leads to a rapid transport of the refrigerant molecules within the solution. Results show that the change in the absorption rate is more significant in the case of thicker solution channels. The solution mass transfer resistance is more dominant in thicker solution channels and thus the diffusion

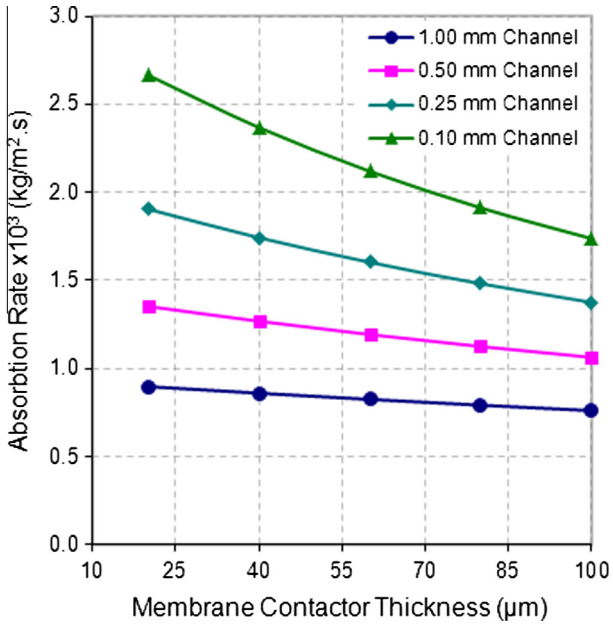

Fig. 7. Effect of membrane contactor thickness on the absorption process.

coefficient of the working fluid significantly affects the overall absorption rate. It is observed that if the diffusion coefficient of the solution is increased from 1.5×10^{-9} m^2/s to 3×10^{-9} m^2/s the overall absorption rate increases by approximately 29%, 25%, 20% and 13% in the case of 1 mm, 0.5 mm, 0.25 mm and 0.1 mm solution channels, respectively. These results show that an absorbent solution with a high diffusion coefficient can play an important role in the enhancement of the absorption rate.

The results obtained in this study clearly show that in the case of thicker solution channels, membrane contactor characteristics have a less prominent effect on the absorption rate and the solution resistance is the dominant resistance to the mass transfer of refrigerant molecules in the solution. Moreover, it can be concluded that the membrane mass transfer resistance is dominant only when the membrane contactor has a small pore diameter

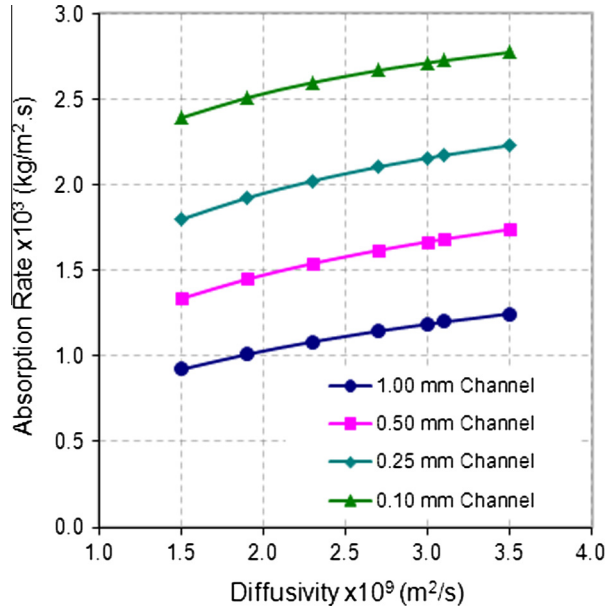

Fig. 8. Effect of solution mass diffusivity on the absorption process.

and the solution channel thickness is in the range of 0.1 mm. The thickness of the concentration and thermal boundary layers is smaller in thinner solution channels, which in turn reduces the solution mass transfer resistance. In addition, the heat is well dissipated to the coolant because of the decrease in thickness. Therefore, in this case the effect of the membrane mass transfer coefficient is more pronounced.

A membrane should have enough mechanical strength to withstand the absorption refrigeration system operating conditions. Therefore, a membrane contactor should be selected with a pore size and thickness of such that does not affect the mechanical strength of the membrane material. In this way, the use of an additional support layer of the membrane can be avoided, as it adds an additional resistance to the vapour mass transfer across the membrane contactor. The results obtained in this study urge that the selection of appropriate membrane characteristics should be made bearing in mind the solution channel thickness. It is worth noting that a solution channel thickness of the order 0.1 mm can allow a higher absorption rate. However, the higher pressure drop along the channel can hinder the performance of a membrane based absorber working under vacuum conditions. In a previous study, Asfand et al. [7] observed that the pressure drop increases exponentially when the solution channel thickness is reduced. They reported that a 50% decrease in the solution film thickness causes an increase in the accumulative pressure drop by a factor of approximately 7.5. They recommended the use of a solution channel thickness of 0.5 mm to avoid a higher pressure drop in the solution channel. From the present study, it is clear that the effect of membrane characteristics is low when the solution channel thickness is in the range of 0.5 mm. Thus, it will allow us to select membrane characteristics in a range that will enhance the mechanical strength of the membrane contactor without significantly affecting the absorption rate.

It is suggested that the membrane pore diameter should be in the range of 0.5–1 μm, the thickness in the range of 60–80 μm and the porosity in the range of 60–70% for a plate-and-frame membrane absorber with a solution channel thickness of 0.5 mm. This range achieves not only a high absorption rate, but also the mechanical strength of the membrane contactor can be enhanced. Further, it is important to select a membrane contactor with appropriate surface properties, such as the hydrophobicity of the material. This property limits the solution from passing through the pores which hinders the performance of a membrane based absorber.

5.2. Effect of operating conditions on the absorption process

A parametric study is carried out to evaluate the effect of operating conditions on the absorption performance of a plate-and-frame membrane absorber. Important parameters such as, solution mass flow rate, vapour pressure, solution inlet concentration and

Table 2
Operating conditions for the parametric study.

Parameter	Base value	Range
Absorber pressure (Pa)	1000	872.5–1500
Inlet solution concentration (% LiBr)	60	55–63
Solution mass flow rate (kg/h)	7.5	2–10
Solution inlet temperature (°C)	40	NA
Solution channel thickness (mm)	NA	0.1–1.0
Channel length (mm)	200	NA
Channel width (mm)	200	NA
Coolant inlet temperature (°C)	30	25–35
Coolant mass flow rate (kg/h)	36	NA
Coolant channel thickness, t (mm)	1	NA
Heat transfer wall thickness (mm)	0.5	NA

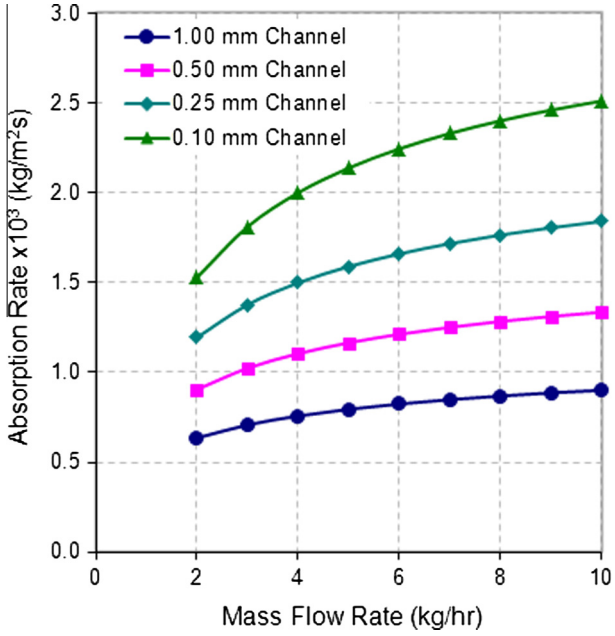

Fig. 9. Effect of solution mass flow rate on the absorption process.

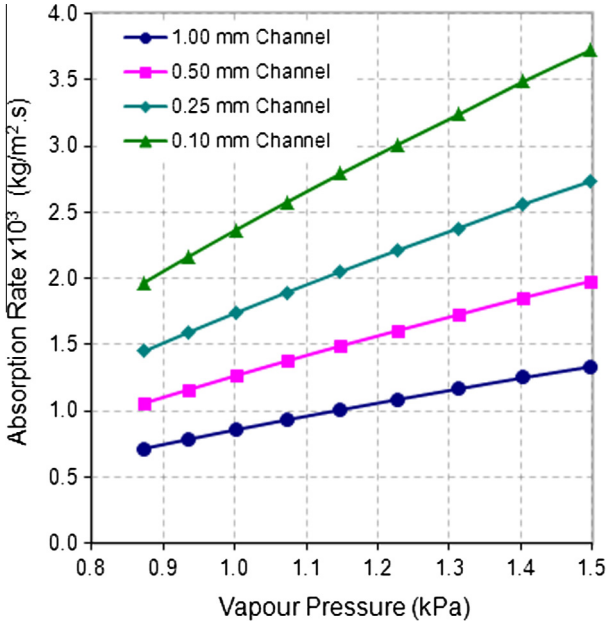

Fig. 10. Effect of vapour pressure on the absorption process.

coolant inlet temperature are varied according to typical operating conditions of the absorber in order to study the impact on the absorption rate. Table 2 summarizes the operating conditions considered for the parametric analysis.

Fig. 9 shows the effect of the solution mass flow rate on the absorption rate for different solution channels. The absorption rate increases with an increase in the solution mass flow rate. Increasing the solution velocity brings fresh layers of solution near the membrane interface, which in turn increases the absorption capacity. Further, it can be seen from Fig. 9 that the increase in absorption rate is more significant initially however, at higher solution flow rates, a further increase of the solution mass flow rate decreases the solution residence time and minimizes the diffusion of the water molecules across the solution. This causes a negative effect on the refrigerant mass transfer and therefore the increase in absorption rate is less pronounced. Increase in the absorption rate is more significant in the thinner solution channel. In the case of the 0.1 mm solution channel, increasing the solution mass flow rate from 2 kg/h to 10 kg/h causes an increase of about 65% in the absorption rate whereas as in the case of the 0.5 mm solution channel a 48% increase in the absorption rate is observed. It is also observed that about 50% increase in the absorption rate is achievable at the same operating conditions when the solution channel thickness is reduced by half from 1 mm to 0.5 mm. The thickness of the concentration and thermal boundary layers are reduced in the case of thinner solution channels and the heat of absorption at the interface is well dissipated by the coolant which lowers the partial pressure of water vapour in the solution and consequently increases the absorption capability of the solution.

Fig. 10 shows the effect of vapour pressure on the absorption performance. It can be seen that the absorption rate increases linearly with an increase in the vapour pressure. The absorption rate increases by approximately 10% when the vapour pressure is increased by 7% and the same mass flow rate is kept in each solution channel. However, at higher vapour pressure values, the increase in the absorption rate reduces gradually to about 7% when the vapour pressure is increased by 7%. Increasing the vapour pressure from 0.873 kPa to 1.498 kPa increases the absorption rate by 87% from 1.06 kg/m^2 s to 1.98 kg/m^2 s in the case of the 0.5 mm

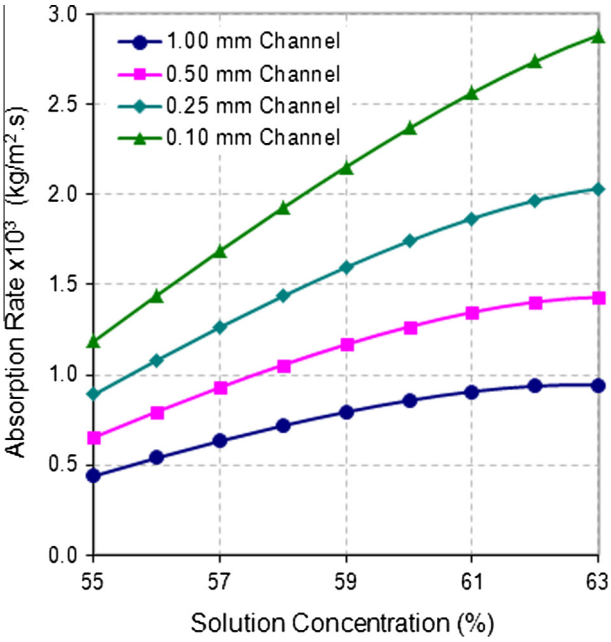

Fig. 11. Effect of solution inlet concentration on the absorption process.

solution channel, whereas in the 0.1 mm solution channel, the absorption rate increases by 89% from 1.97 kg/m^2 s to 3.72 kg/m^2 s. The higher absorption rate achieved in the case of the 0.1 mm solution channel is because of the thinner concentration and thermal boundary layers which lessens the solution mass transfer resistance at the interface. Fig. 11 shows the effect of the solution inlet concentration on the absorption rate. It can be seen that the absorption rate increases with an increase in the inlet concentration of the solution. The partial pressure of water vapour in the solution decreases at a higher solution concentration which in turn increases the absorption capacity. However, the increase in the absorption rate is less prominent at higher concentrations because at higher solution concentrations the mass diffusivity of water in the LiBr solution decreases and the solution mass transfer

resistance increases and limits the absorption rate. In addition, the increase in the absorption rate is lower in case of the thicker solution channels because the solution mass transfer resistance is more dominant in thicker solution channels. Increasing the inlet concentration from 55% to 63% mass fraction of LiBr increases the overall absorption rate from 0.66 kg/m^2 s to 1.43 kg/m^2 s in the case of the 0.5 mm solution channel whereas in the 0.1 mm solution channel the absorption rate increases from 1.19 kg/m^2 s to 2.98 kg/m^2 s. These results show that a higher absorption rate can be achieved if the solution inlet concentration is around 60%. In addition, at the given solution temperature and concentration, the aqueous solution of LiBr is not prone to crystallization according to the solubility chart of water/LiBr. Fig. 12 shows the effect of the cooling water temperature on the absorption performance of a plate-and-frame membrane based absorber. Increasing the cooling water temperature has a negative effect on the absorption performance because at higher cooling water temperatures the coolant is not well able to dissipate the heat of absorption and as a consequence the solution temperature increases. At higher solution temperatures, the partial pressure of water vapour in the solution increases and lessens the absorption capacity of the solution. Increasing the coolant water inlet temperature from 25 °C to 35 °C results in about a 35% decrease in the absorption rate. For instance, increasing the cooling water inlet temperature from 25 °C to 35 °C decreases the absorption rate from 1.61 kg/m^2 s to 1.07 kg/m^2 s in the case the of the 0.5 mm solution channel, whereas the absorption rate decreases from 3.02 kg/m^2 s to 1.98 kg/m^2 s when the solution channel thickness is 0.1 mm.

The operating conditions of an absorption cooling system are critically important for the efficient performance of the system. Therefore, the selection of appropriate operating conditions is essential when designing a membrane based absorber. It is concluded that for a water-LiBr absorption air-conditioning system utilizing membrane-based absorbers, a vapour pressure of about 1.3 kPa, a solution inlet concentration of 60% and a cooling water inlet temperature of 30 °C are recommended to achieve a higher efficiency. Although, the cooling water inlet temperature should be low for efficient performance, to eliminate the need of a cooling tower, a temperature in the range of 30 °C is selected. This will reduce both the size and cost of the system.

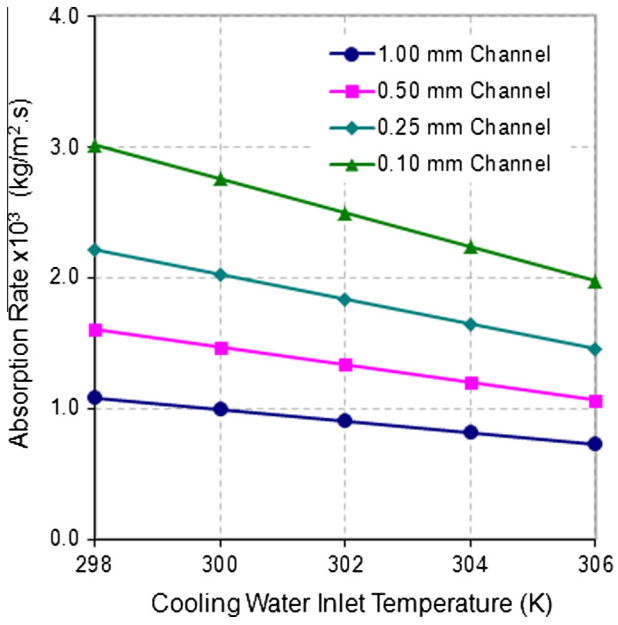

Fig. 12. Effect of cooling water temperature on the absorption process.

6. Conclusions

This study is focused on the impact of the solution channel thickness while investigating the effect of membrane contactor characteristics and operating conditions on the absorption process in water-LiBr membrane-based absorbers. The effect of the membrane mass transfer resistance is critically evaluated in the case of different solution channels with thickness in the range of 0.1–1.0 mm. It is observed from the results that the membrane characteristics have a less prominent effect on the absorption rate and the solution resistance is the dominant resistance in refrigerant mass transfer in the case of thicker solution channels. Furthermore, the membrane mass transfer resistance is considerable in the case of thinner solution channels. The membrane mass transfer resistance is more dominant in membranes with small pore size whereas the diffusion resistance into the solution is a more dominant factor in the case of membranes with larger pore diameter. The selection of appropriate membrane characteristics should be made keeping in mind the solution channel thickness. Although solution channel thickness of the order 0.1 mm can allow for a higher absorption rate, the higher pressure drop along the channel can hinder the performance of a membrane based absorber working under vacuum conditions. The pressure drop along the channel length increases exponentially when the solution channel thickness is reduced, therefore a solution channel thickness of about 0.5 mm is considered appropriate to avoid a higher pressure drop in the solution channel. Moreover, the analysis performed in this study shows that the effect of membrane characteristics is low when the solution channel thickness is in the range of 0.5 mm. Therefore, a membrane contactor with a pore size and a thickness that do not affect the mechanical strength of the membrane material is recommended. In this way, the additional support layer of the membrane can be avoided as it adds a resistance to the membrane mass transfer resistance. Further, emphasis should be placed on the selection of a membrane contactor with appropriate surface properties such as the hydrophobicity of the material as it is important to prevent the solution from passing through the pores which hinders the performance of a membrane based absorber. The selection of suitable operating conditions is important to achieve high absorption rates. The parametric study carried out to evaluate the effect of operating conditions shows that a high absorption rate is achievable in the case of thinner solution channels. Moreover, it is observed that the percentage change in the absorption rate remains almost the same when the vapour pressure, solution inlet concentration and coolant inlet temperature are varied in the case of different solution channel thicknesses.

Acknowledgement

This study is part of an R&D project funded by the Spanish Ministry of Economy and Competitiveness (DPI2012-38841-C02-02). Faisal Asfand gratefully acknowledges the Rovira i Virgili University for granting the Martí-Franquès research fellowship 2012 (2012BPURV-50) to pursue a doctorate degree.

References

[1] F. Asfand, M. Bourouis, A review of membrane contactors applied in absorption refrigeration systems, Renew. Sustain. Energy Rev. 45 (2015) 173–191.
[2] A.H.H. Ali, P. Schwerdt, Characteristics of the membrane utilized in a compact absorber for lithium bromide–water absorption chillers, Int. J. Refrig. 32 (2009) 1886–1896.
[3] R.N. Isfahani, S. Moghaddam, Absorption characteristics of lithium bromide (LiBr) solution constrained by superhydrophobic nanofibrous structures, Int. J. Heat Mass Transf. 63 (2013) 82–90.
[4] D. Yu, J. Chung, S. Moghaddam, Parametric study of water vapor absorption into a constrained thin film of lithium bromide solution, Int. J. Heat Mass Transf. 55 (2012) 5687–5695.

[5] R.N. Isfahani, K. Sampath, S. Moghaddam, Nanofibrous membrane-based absorption refrigeration system, Int. J. Refrig. 36 (2013) 2297–2307.
[6] S. Bigham, D. Yu, D. Chugh, S. Moghaddam, Moving beyond the limits of mass transport in liquid absorbent microfilms through the implementation of surface-induced vortices, Energy 65 (2014) 621–630.
[7] F. Asfand, Y. Stiriba, M. Bourouis, CFD simulation to investigate heat and mass transfer processes in a membrane-based absorber for water-LiBr absorption cooling systems, Energy 91 (2015) 517–530.
[8] M. Venegas, M. Vega, N. García-Hernando, U. Ruiz-Rivas, A simple model to predict the performance of a H_2O-LiBr absorber operating with a microporous membrane, Energy 96 (2016) 383–393.
[9] M. Venegas, M. Vega, N. García-Hernando, Parametric study of operating and design variables on the performance of a membrane-based absorber, Appl. Therm. Eng. 98 (2016) 409–419.
[10] L. Martınez, J.M. Rodrıguez-Maroto, On transport resistances in direct contact membrane distillation, J. Membr. Sci. 295 (2007) 28–39.
[11] T. Uemura, S. Hasaba, Studies on the lithium bromide-water absorption refrigeration machine, Technol. Rep. Kansai Univ. 6 (1964) 31–55.
[12] R.K. Shah, A.L. London, Laminar Flow Forced Convection in Ducts, a Source Book for Compact Heat Exchanger Analytical Data. Advances in Heat Transfer, Academic Press, New York, 1978. Suppl. 1.
[13] R.J. Lee, R.M. DiGuilio, S.M. Jeter, A.S. Teja, Properties of lithium bromide-water solutions at high temperatures and concentrations – II Density and viscosity, ASHRAE Trans. (1990) 709–714. Paper 3381. RP-527.
[14] R.M. DiGuilio, R.J. Lee, S.M. Jeter, A.S. Teja, Properties of lithium bromide-water solutions at high temperatures and concentrations – I Thermal conductivity, ASHRAE Trans. (1990) 702–708. Paper 3380. RP-527.
[15] N.A. McNeely, Thermodynamics properties of aqueous solutions of lithium bromide, ASHRAE Trans. 85 (1979) 413–434.
[16] M. Gierow, A. Jernqvist, Measurement of mass diffusivity with holographic interferometry for H_2O/NaOH and H_2O/LiBr working pairs, AES. Int. Abs. Heat Pump Conf., vol. 31, 1993, pp. 525–532.